Flue Gas Desulphurization using Natural Calcium Based Sorbents

BHAVESHNEE R. RAMSAROOP

University of KwaZulu-Natal
College of Agriculture, Engineering and Science
Howard College Campus

Examiner's Copy

This dissertation is submitted in fulfilment of the requirements for the Master of Science in the Chemical Engineering Degree, College of Engineering at the University of KwaZulu-Natal.

Supervisor: Prof. M. Carsky

Date of Submission: 14 December 2012

UNIVERSITY OF KWAZULU-NATAL
COLLEGE OF AGRICULTURE, ENGINEERING AND SCIENCE
DISCIPLINE OF CHEMICAL ENGINEERING

DECLARATION

I, Bhaveshnee Ramsaroop, declare that:

1. The research reported in this dissertation, except where otherwise indicated, is my original research.
2. This dissertation has not been submitted for any degree or examination at any other university.
3. This dissertation does not contain other persons' data, pictures, graphs or other information, unless specifically acknowledged as being sourced from other persons.
4. This dissertation does not contain other persons' writing, unless specifically acknowledged as being sourced from other researchers. Where other written sources have been quoted, then:
   a. Their words have been re-written but the general information attributed to them has been referenced
   b. Where their exact words have been used, then their writing has been placed in italics and inside quotation marks, and referenced.
5. This dissertation does not contain text, graphics or tables copied and pasted from the Internet, unless specifically acknowledged, and the source being detailed in the thesis and in the References sections.

Signed at Howard Campus on the 14th Day of December 2012

……..
B.R. Ramsaroop

As the candidate's supervisor, I Prof. M. Carsky, have approved this dissertation for submission.

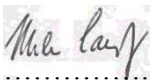

……..
Prof. M. Carsky

ACKNOWLEDGEMENTS

I would firstly like to thank the almighty for giving me good health, patience, strength and courage to successfully complete all the endeavours throughout my academic career.

I wish to express my sincere thanks to the following:

- My supervisor, Prof Milan Carsky for his continued guidance and assistance.
- ESKOM for the provision of the sorbents.
- The Senior Laboratory Technicians, Mr S. Naidoo, Mrs R. Maharaj and Mr D.C. Naidoo for their assistance in the ordering of lab equipment and essentials.
- The workshop staff for their continuous help and assistance in the repairing of equipment.
- The SEM unit of the Westville Campus for the provision of equipment for sorbent surface analysis.
- Mr Mzamo Shozi of the Westville campus who assisted with the undertaking of the physical property analysis.
- My colleagues and friends at the Howard Campus for their motivation and assistance.
- Finally I wish to express my most sincere gratitude to my parents for the values they have instilled in me and the support that they have given me through all walks of my life.

ABSTRACT

Power generation from coal combustion serves as a major source of energy however this process has detrimental environmental effects. SO_2 is a destructive pollutant and is oxidized with water vapour to form sulphuric acid which falls as acid rain causing corrosion to monuments, deforestation, soil erosion and destruction of the natural habitat. SO_2 emissions cause chronic respiratory diseases. The development and advancement in pollution control technologies is a pressing issue as environmental regulations become more stringent. The principal technology that is currently implemented is termed Flue Gas Desulphurization (FGD) and involves treating the flue gas before it is released into the atmosphere.

Industries are constantly welcoming new research and development that would reduce their SO_2 emissions. As a result most companies are turning to sorbents to solve the major environmental crisis.

In the work undertaken an effective test unit for sulphur dioxide capture was commissioned and recommended conditions for SO_2 removal were established. Four ESKOM sorbents were prepared and tested in the experimental set-up. These sorbents were then ranked according to their desulphurization efficiency. The effect of particle size on desulphurization efficiency was determined using four different size fractions and it was found that smaller particles have higher sulphur removal efficiency. The effect of the presence of CO_2 in the gas mixture was also determined by comparing the efficiencies obtained using two different flue gas mixtures. The chemical, physical and surface properties of each sorbent was also analysed and used to support the conclusions drawn from the ranking of the sorbents. A suitable model to represent the data set was also investigated and it was found that the simple shrinking core model best described the system investigated.

CONTENTS

Topic **Page**

LIST OF TABLES

LIST OF FIGURES

NOMENCLATURE AND ABBREVIATIONS

Nomenclature		
Variable	**Description**	**Units**
A,B	Modelling parameters	-
b	Stoichiometric coefficient	-
C_0	Initial Concentration	PPM
C_i	Bulk concentration of component i	mol/m^3
$C_{i.in}$	Inlet concentration of component i	PPM
$C_{i.out}$	Outlet concentration of component i	PPM
D_{eff}	Effective diffusivity	m^2/s
D_{kn}	Knudsen diffusion	m^2/s
D_{mol}	Molecular diffusion	m^2/s
D_{mol+kn}	Molecular and Knudsen diffusion	m^2/s
D_{pl}	Product layer diffusivity	m^2/s
D_{pore}	Pore diffusivity	m^2/s
f_{dif}	Function of conversion by diffusion	-
f_{kin}	Function of conversion by surface reaction	-
k_d	Deactivation rate constant	m/s
k_s	Surface reaction rate constant	m/s
M_i	Molar mass of component i	g/mol
P	Pressure	Pa, bar
r_{av}	Average pore radius	m
R_P	Particle radius	m
T	Temperature	°C, K
t	Time	s
V_i	Volume of i	m^3
V_i	Empirical constant of component i	-
$V_{mol,i}$	Molar volume of i	m^3/mol
X	Conversion	-
Z	Stoichiometric ratio of solid product and solid reaction phases	-
γ	Tortuosity	-
ε_0	Initial porosity	-
η	SO_2 removal efficiency	-
ρ_i	Density of component i	kg/m^3
$\rho_{mol.i}$	Molar density of component i	mol/m^3
τ	Surface time term	s
τ_{dif}	Surface time term for diffusion	s
τ_{kin}	Surface time term for surface reaction	s

ABBREVIATIONS	
Symbol	**Description**
BET	Brunauer-Emmett-Teller
CAA	Clean air act
$CaCO_3MgCO_3$	Dolomite
DSI	Duct sorbent injection
EDX	Energy dispersive x-ray
EPA	Environmental protection agency
ESKOM	Electricity supply commission
FBC	Fluidized bed combustion
FGD	Flue gas desulphurization
FSI	Furnace sorbent injection
HGI	Hardgrove grindability index
IGCC	Integrated gasification combined cycle
LOI	Loss of incineration
OPA	Oil palm ash
RH	Relative humidity
RHA	Rice husk ash
SEM	Scanning electron microscope
SO_2	Sulphur dioxide
SO_3	Sulphur trioxide
XRD	X-Ray diffraction
XRF	X-Ray fluorescence

CHAPTER 1: INTRODUCTION

1.1.General Introduction

Sulphur containing compounds such as coal have extensive use in various industrial processes that include the generation of electricity through the steam production process by utilizing the energy from fossil fuel combustion. This means of electricity generation remains the oldest and most frequently implemented process due to the large availability of coal, process simplicity and the economic benefits related to the process. However, the issues that arise from coal fired power plants have serious effects on the environment, architecture and human health. The occurrence of sulphur in the fossil fuels results in detrimental amounts of sulphur dioxide and other pollutants being released into the atmosphere daily.

The sulphur dioxide that is emitted from the coal combustion process combines with water droplets in the air to create sulphuric acid which is the principal cause of acid rain. This destroys architecture, monuments and buildings. The acid rain may also cause deforestation and soil erosion. It is the primary cause of the destruction of aquatic life by pH lowering of rivers and lakes by the addition of an acidic medium.

The devastating impacts of the various pollutants have resulted in the government imposing more stringent laws regarding the emission of the various pollutants particularly sulphur dioxide. These regulations are continuously revised and amended annually to determine if they are currently being met or are bypassing the standards that have been set.

Various methods have been implemented to decrease the sulphur dioxide emissions. This includes using an alternative fuel as a combustion fuel for coal power stations or using a fuel that has a decreased sulphur content formed by a blending process. Various flue gas desulphurization (FGD) processes have been implemented to decrease the sulphur dioxide emissions released into the atmosphere. Processes include wet, dry and semi-dry flue gas desulphurization techniques. These processes vary in terms of simplicity, cost, space requirements, the by-products produced and the removal efficiency.

Absorbents are used to remove or decrease the amounts of acid gas such as sulphur dioxide from flue gas emissions prior to their release. Various absorbents have been used since the development of flue gas desulphurization technologies however due to the cost related to sorbent material, the use of most

of these sorbents have declined. The use of a sorbent is selected based on the cost, abundance and sulphur removal capabilities. Limestone and dolomite are the most popular natural calcium based sorbents that are utilized in flue gas desulphurization. The use of hydrated lime sorbents express a definite advantage and is a growing popularity. Recently, various additives have been incorporated into the sorbent structure as it was found that these additives play the role of structural modifiers that improve the sulphur retaining abilities of the sorbent. This emerging development is continuously implemented in various FGD processes in coal-fired power plants.

1.2. Aims and Objectives

The investigation at hand involved testing the sulphur removal capabilities of various natural calcium-based sorbents that can be implemented at the ESKOM power station and hence conclude which of these sorbents is the most efficient in the flue gas desulphurization process.

- **Equipment Design**

Initially, it was required that a test unit be designed and developed for the sorbent testing process with a reactor configuration that allowed for sufficient contact between the solid sorbent and the sulphur dioxide gas. It was also found that the temperature gradients that were present in the test unit, which was operating at 850 ℃, affect the reaction between the sulphur dioxide and the sorbent hence creating uncertainties in the desulphurization efficiencies and sulphur removal capabilities. A temperature profile in the test oven was generated with the determination of hot-spots that were present in the oven. This established precisely the most suitable location of the sorbent in the reactor that allowed for maximum absorption.

- **Desulphurization Efficiency**

A ranking of the sorbents was performed to establish the best sorbent. A second gas mixture was then used to investigate the effects of the presence of CO_2 in the gas mixture on the desulphurization efficiency. The effect of particle size on desulphurization efficiency was also investigated using four different size fractions. The physical, chemical and surface properties of the different sorbents were analysed and this was then used to support the results obtained from the ranking process.

- **Modeling**

A suitable sulphation reaction model to represent the desulphurization process was then investigated and the appropriate parameters established via regression.

1.3. Methodological Approach

It was established that the initial step in successfully completing the task would be to develop a working experimental unit for the sorbent testing. This included developing a well thought off reactor design for the reaction between the sulphur dioxide and the absorbent. Familiarization with the test equipment and the use of the gas analyser was essential to successfully complete the experimental work. Calibration of the rotameters were also performed to set the required flowrate of the reactant and purge gas. Obtaining a temperature profile was important as this determined the placement of the sorbent within the reactor. Once these component tasks were completed, a successful test unit was developed for the appropriate and consistent measurement of ESKOM sorbent efficiencies and hence suitable recommendations made for sulphur dioxide capture.

The sorbents that were provided by ESKOM were processed into workable samples. A milling procedure including crushing and grinding the raw sorbent was performed for sorbent preparation. The sorbents were then sieved into four different size fractions and the effect of particle size on desulphurization efficiency was then determined.

A second gas mixture containing 2000 ppm SO_2, 10% CO_2, 11% O_2 and balance N_2 was then utilized to observe the influence of the presence of CO_2 on the desulphurization efficiency. The shrinking core model was implemented to represent the experimental results.

The chemical analysis involved determining the chemical composition of the sorbent. X-Ray diffraction technologies and Energy Dispersive X-Ray (EDX) were used to establish the composition. The surface properties were determined using the Scanning Electron Microscope (SEM) technique.
The physical properties of the sorbents such as the density, softness index, Brunauer-Emmett-Teller (BET) surface area, pore sizes, pore volume and the porosity were also investigated. The density was obtained using the liquid dispersion and pycnometer techniques. The softness index was determined using a method proposed by Carsky et al, 2006. The BET surface area, pore sizes, pore volume and porosity were determined using the Micrometrics TriStar Surface area and porosity analyser. These chemical, physical and surface properties were then used to support the results obtained from the investigation.

CHAPTER 2: LITERATURE SURVEY

2.1. Energy Demands and the Importance of Coal

The sources of energy used today around the world include nuclear power, hydro-electricity, wind and solar power as well as energy derived from fossil fuels. Fossil fuels have been used as the primary energy source since prehistoric times and the contribution of various factors make it unlikely for the alternative sources mentioned above to replace fossil fuels as the most dependent energy source (Chiang, 1995). Coal has supreme abundance, is least expensive and is the most widely distributed fossil fuel hence it is the most important source of energy throughout the world. The global production of steel also depends largely on the availability of the coal feedstock. Coal meets approximately 23% of the global energy requirements, generates 39 % of the world's electricity and supplies over 75% of South Africa's power demands (Rozpondek, 2009). South Africa processes over 260 million tons of coal yearly, of which over 25% is exported. This makes South Africa one of the major coal producing and exporting countries in the world.

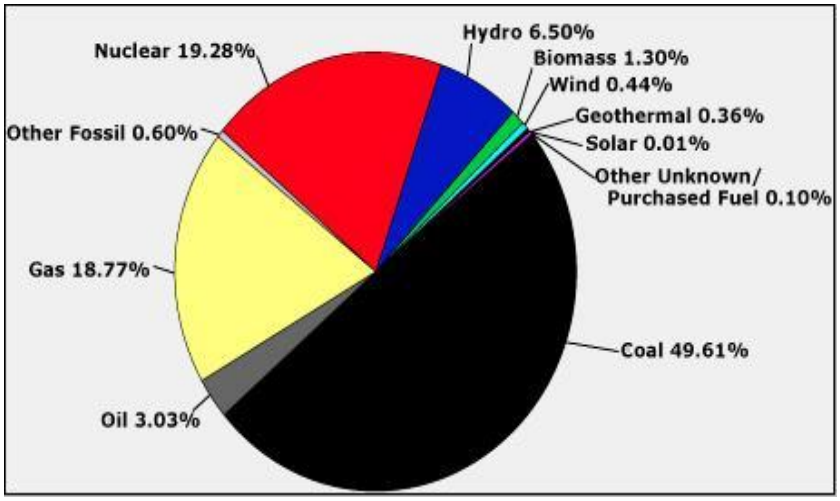

Figure 2-1: Global Contribution of Energy Sources for Electricity Generation (Vetter, 2012)

Since 1980, the demand for electricity in South Africa has been continuously increasing due to the continued development in the various industries including farming and agriculture, infrastructure and transport, import and export as well as the residential sector to compensate for the previously disadvantaged social groups evolving from the apartheid regime (Ogenga, 2009). Load shedding has become a major control measure for managing the electricity needs as the demand for electricity exceeded the possible supply capacity (Ogenga, 2009). ESKOM satisfies approximately 90% of South Africa's electricity needs and the availability of coal reserves in South Africa implies that such coal

fired power plants will remain the primary energy source for the future (Moodley, 2007). This plentiful and most reliable source of energy will continue to dominate the electricity supply sector not only in South Africa but also worldwide (Ogenga, 2009). A 43% increase in the utilization of coal for energy is expected by the year 2020.

2.2. Coal Composition and Combustion

Coal is a sedimentary rock that is brownish black and its chemical constituents include largely carbon, hydrogen, and oxygen with lesser amounts of nitrogen, sulphur and trace elements. Carbon is the primary constituent of coal forming approximately 50% of its weight and 70% of it volume. There are various classifications of coal including lignites, anthracite etc. that are ranked based on the heating value which depends on the carbon content of the coal. Sulphur is present in organic and inorganic forms (pyritic and sulphates). Coal contains 0.2-5 wt% sulphur on a dry basis (Zevenhoven and Kilpinen, 2001).

The combustion process of coal occurs only if oxygen is available and heat is added to the fossil fuel such that the temperature is increased to above the ignition point temperature (Ogenga, 2009). Combustion results in the breaking of the chemical bonds between the constituents of the fossil fuel. The heat that is generated from the combustion of coal is used to covert water to steam which in turn drives turbines that generate electricity.

As various impurities are present in coal, combustion results in the production and release of various hazardous and waste products. Some of the major environmental concerns that arise from coal combustion are the release of nitrogen oxides, sulphur dioxide, carbon dioxide, radioactive elements, heavy metals, ash and particulate matter that cause increased global warming and pollution related problems such as acid rain. Sulphur dioxide is the most destructive of the pollutants.

Table 2-1: Typical Flue Gas Composition (Adapted from Lee et al, 2007)

Components	Concentration
SO_2	350 ppm
NO_X	125 ppm
O_2	5.2 %
CO_2	13 %
H_2O	7.8 %
N_2	Balance

2.3. Effects of Sulphur Dioxide

The sulphur that is found in coal is oxidized during the combustion process in coal fired power plants to form approximately 95% sulphur dioxide. SO_2 is a non-flammable, colourless gas that has a strong odour. The amount of sulphur dioxide emissions depends directly on the type of coal that is being combusted hence coal that have a high sulphur content have a more detrimental effect on the environment. Sulphur dioxide that is released from power stations are oxidized with water vapour to form highly corrosive sulphuric acid which falls with hail, rain, snow, or fog as acid precipitation or acid rain.

The chemical reactions involved in the transformation of sulphur dioxide to acid rain are presented below.

Formation of sulphurous acid from sulphur dioxide and water:

$$SO_2(g) + H_2O(l) \leftrightarrow H_2SO_3(aq) \quad (2.1)$$

Oxidation of sulphur dioxide to sulphur trioxide:

$$SO_2(g) + O_2(g) \rightarrow SO_3(g) \quad (2.2)$$

Formation of sulphuric acid from water and sulphur trioxide:

$$SO_3(g) + H_2O(l) \rightarrow H_2SO_4(aq) \quad (2.3)$$

This causes deforestation that decreases the total atmospheric oxygen, resulting in soil erosion and a destruction of the natural habitat. Acid rain destroys the bark and results in the loss of leaves on plants and trees. This has very adverse effects on the natural forestation as it destroys the source of protection thus allowing for poor weather conditions, insects and diseases to cause harm to the trees. It also affects the natural growth of trees causing them to have stunted growth. Sulphur dioxide from the atmosphere and the sulphuric acid may also enter the trees through the openings that are found on the leaves called the stomata. Once these harmful emissions are inside, they cause total destruction of the chlorophyll, cell plasma, cell nucleus and the enzymes. This results in the destruction of the cells that open and close the stomata thus preventing the uptake of water by the plants which then causes the plants to dry up (Hasenberg, 2008).

Figure 2-2: The Effect of Acid rain on Forestry (Juriet, 2004)

Acid rain also destroys architecture by having a corrosive effect on monuments and buildings causing it to age more quickly. Statues and artwork that is limestone or sandstone based are destroyed by the reaction of these stones with the acid rain to form gypsum. Infrastructure such as bridges and railway tracks, modes of transportation such as cars and airplanes, are also affected by acid rain. SO_2 may also cause discoloration of paintings and artwork.

The figure below shows the effect of acid rain on a statue that was photographed in 1908 and again in 1968. This statue was built in the year 1708 and weather conditions had little effect on the statue however as the industrial revolution progressed, between the year 1908 and 1968, the statue goes almost unrecognized.

Figure 2-3: The Effect of Acid rain on Statues (Ophardt, 2003)

Sulphur dioxide disrupts the pH balance of rivers and lakes causing it to decrease below 5 or 6 causing many fish to die as they are unable to withstand the environmental change. This results in a break in the food chain as the food source for many birds becomes limited. Birds may also die due to the consumption of fish poisoned by the low acidity levels in the water.

Figure 2-4: The Effect of Acid rain on Aquatic Life (http://snowyoctomber.blogspot.com/)

Sulphur dioxide mists can also deteriorate the quality of cotton, linen and nylons and can also be corrosive to metals such as zinc, iron and steel. Corrosion is an electro chemical process and occurs due to the presence of moisture on metal surfaces which is accelerated if contacted with SO_2. Deterioration and corrosion are complex processes and can also occur simultaneously. Since 1970, the corrosion rates have decreased due to a decline in the SO_2 emissions.

Figure 2-5: The Effect of Sulphur Dioxide on Metal Surfaces
(http://www.freeimageslive.co.uk/free_stock_image/rustytank3974jpg)

Sulphur dioxide emissions also have a negative impact on human health as it causes chronic respiratory diseases. SO_2 causes nerve stimulation resulting in irritation of the nose and throat as well as allergic reactions. Short term exposure which is generally ranged between 5 minutes and a day is harmful to those suffering from asthma as it causes tightness of the chest and also reduces visibility. Brain damage, kidney malfunction and Alzheimer's disease are also caused by SO_2 emissions. Exposure to high SO_2 concentrations increases the susceptibility towards contracting bacterial infections (Treissman et al, 2003). Studies show that over 51 000 deaths and 200 000 pollution related illnesses are caused by sulphur dioxide annually. Between 1980 and 1990 the average SO_2 emissions were found to decrease by an average of 20% (Hecq, 1997). Because sulphur dioxide is such a destructive pollutant, methods for reducing these emissions are continuously investigated.

2.4. Air Pollution Legislature

The stigma attached to the industrial revolution, increased population growth and urbanization causes deterioration in the environment hence creating the need for analyzing the environmental air quality. Sulphur dioxide from coal-fired power stations represents a significant fraction of the total environmental emissions hence a subsequent understanding is important as this will enable the assessment of their contribution to local and global pollution. Various factors affect the amount of SO_2 that is present in flue gas namely the amount of sulphur in the coal, the amount of air present and the amount of sulphur present in the ash (Strauss, 1971). As the advancement in technology continues and the need for energy grows exponentially, the amount of pollutants in the atmosphere grows substantially. At least 90% of the sulphur present in fossil fuels enters the gas phase as sulphur dioxide during the combustion process (Austen, 2002). Plants' and animals' tolerance level for sulphur dioxide depends on the type of plant or animal and its condition or age, concentration of the pollutant as well as the exposure time (Strauss, 1971).

The maximum amount of SO_2 that can be released from any coal-firing power plant depends on a variety of contributing factors including the location, the size of the plant and the quality of the fossil fuel combusted. The maximum allowable concentration for an 8 hour work shift is 5 ppm, however longer exposures can cause death at lower concentrations. Legislation stipulates the amount of sulphur dioxide released into the atmosphere. The clean air act passed in 1977 was the pollution control legislature to be enacted and this act was revised in early 1990 (Mandlall, 1993). South African legislature (2007) permits 19 ppb of sulphur dioxide to be released into the atmosphere annually and current emission levels are over 30 ppb (Mohamed, 2008). Air quality monitors are used to measure the SO_2 concentrations in the atmosphere. The Environmental Protection Agency (EPA) establishes and reviews the SO_2 concentrations in order to maintain public health and a safe environment. In 2010, the EPA created a new standard of 75 ppb as a 99th percentile of 1-hour daily maximum

concentrations, averaged over 3 years (Cortley, 2010). The rapid increase in the quantities of sulphur dioxide emitted from coal-fired power plants have created a growing urgency to reduce the SO_2 emission levels as the environmental regulations become more stringent.

2.5. SO_2 Emission Control

The development and advancement in pollution control technologies that can be implemented in coal fired power stations is a pressing issue as the environmental regulations become more stringent. It is essential that the technologies be thoroughly analyzed and action be taken to put these developments into practice. Tall gas stacks were used to reduce the SO_2 emissions by dilution and dispersion of the pollutants into the atmosphere. Sulphur removal from fossil fuel is possible but difficult due to chemical bonding structure. Various processes have been suggested for decreasing sulphur dioxide emissions.

Clean coal technologies are used to address the environmental concerns arising from coal combustion. This includes pre-combustion, combustion and post combustion technologies. There are various limitations to these techniques including the extensive cost, reduced sulphur removal efficiency, operational experience that is required and the difficulty of disposing the waste products that are produced.

SO_2 removal efficiency is the most important limitation to any of the techniques and is defined as (Majeed et al, 1995):

$$\eta = \frac{C_{SO_2.in} - C_{SO_2.out}}{C_{SO_2.in}} \times 100\% \qquad (2.4)$$

$C_{SO_2.in}$ - SO_2 inlet concentration (ppm)

$C_{SO_2.out}$ - SO_2 outlet concentration (ppm)

2.5.1. Pre-combustion Techniques

Pre-combustion technologies include:

- Physical coal cleaning where the coal is crushed, washed and screened. This removes impurities and inorganic sulphur reducing the ash and sulphur dioxide emissions, increasing the plant efficiency but fails to remove the organic sulphur and is therefore not utilized as a stand-alone pollution control strategy. This method is relatively simple, cost effective and removes between 10-50% of the sulphur from coal.

- Coal selection, the type of coal that is being combusted has an influence on the amount of SO_2 released into the atmosphere. In general, coal that has a higher sulphur content is more likely to release a larger amount of pollutants. Changing the type of fuel that is being used is a relatively inexpensive method of controlling SO_2 emissions.

- A process of blending high and low sulphur coal to create a fuel that meets the environmental SO_2 regulations. Blending takes place when coal from different stockpiles are mixed together to form coal that when combusted, produces emission levels that are within the environmental regulations (Cheng et al, 2003). Various models have been developed to predict the blend ratio (Ogenga, 2009). It is essential that the blended coal still meets the boiler requirements as this affects efficiency and performance.

2.5.2. Combustion Techniques

Various technologies have made advancements in the removal of sulphur dioxide during the combustion process. Of these techniques only a few have been commercialized with applications in coal-fired power plants. The burner and boiler design does not affect the SO_2 emission levels hence the technologies that are used to reduce SO_2 emissions during the combustion process include Fluidized Bed Combustion (FBC) and the Integrated Gasification Combined Cycle (IGCC).

2.5.2.1. Fluidized Bed Combustion (FBC)

Fluidized bed combustion uses jets of air at high velocities through a distributor at the bottom of the bed to suspend the coal particles during the combustion process. This fluidized state allows for improved heat transfer and efficient steam generation which in turn drives the turbines to generate electricity. The high heat transfer efficiency allows for the system to be operated at lower temperatures. The SO_2 from the coal combustion reacts with a sorbent in the inert bed to form ash that is safely removed, reducing the SO_2 emissions by 90% (Air Pollution Control, 2010).
The disadvantages using fluidized bed combustion is that waste that requires proper disposal are produced and it proves to be expensive as the sorbent is required in large quantities

2.5.2.2. Integrated Gasification Combined Cycle (IGCC)

This technique utilizes a gasifier to turn coal into a gas before it is combusted. In the IGCC process, heat is utilized under high pressure to gasify the coal which is then used to drive turbines that are used to generate electricity. An important variable to be controlled is the amount of oxygen present as it is required that only a small quantity of the coal should be combusted completely. The sulphur that is

present in coal can be converted to hydrogen sulphide or sulphuric acid which is easily handled and sold can be sold as a by-product. The main disadvantage of this process is the extreme capital cost implication. Implementation of the IGCC process is proven to reduce sulphur dioxide emissions by approximately 99% (Air Pollution Control, 2010).

2.5.3. Post-combustion Techniques – Flue Gas Desulphurization (FGD)

The principal post combustion technology that is currently implemented to address the SO_2 emissions is termed Flue Gas Desulphurization (FGD). This involves treating the flue gas before it is released into the atmosphere via the stack.

2.5.3.1 History and Development of FGD

In 1930, the first FGD system was implemented at a power station in the United Kingdom. The FGD system in place had 95% sulphur removal efficiency (Satriana, 1981). This was followed by the installation of two wet FGD scrubbers at the coal-fired power plants near the vicinity of Thames River in England (Uno et al, 1971). Since then the need to reduce sulphur dioxide emissions have increased drastically and very few developments meet the requirements successfully. In 1967 it was established that coal fired power plants released approximately 6 million tons of sulphur dioxide into the atmosphere and it was approximated that these emission levels would increase to approximately 8 million tons by the year 1970 hence this created the need for immediate corrective measures to be put into place (Falkenberry and Slack, 1971). In 1968, an estimated $ 6,670,000 was set aside by the National Air Pollution Control Administration to undertake projects that were to improve the technologies available for reducing pollution emissions (Cortelyou, 1971). The regenerable dry FGD systems were first established and implemented in the 1980s. There was a substantial increase in the industrial applications of FGD systems between the year 1994 and 1998.

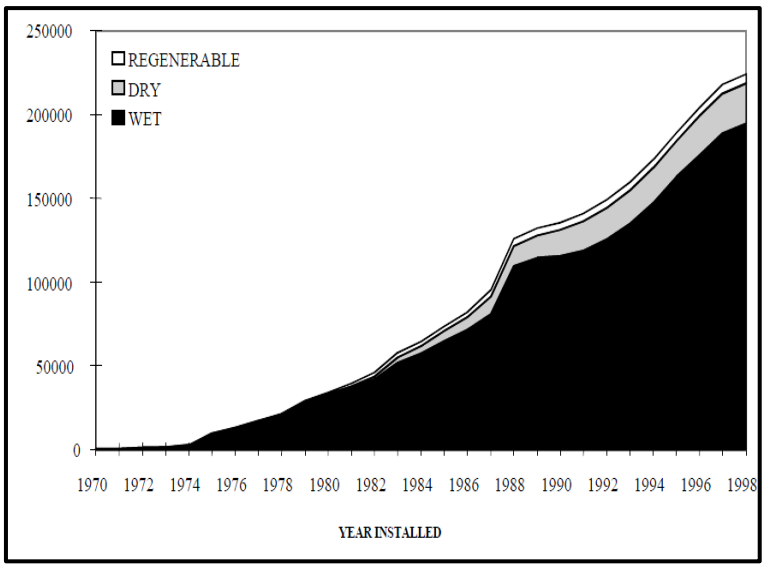

Figure 2-6: Development of FGD System around the World (Srivastava, 2000)

2.5.3.2. Classification of FGD

The major classifications of all FGD processes are either once-through or regenerable. In once through processes, the sorbent (limestone, dolomite) reacts with the SO_2 to form solid waste that must be properly disposed or it can generate useful by-products such as calcium sulphate. In the regenerable process, the sorbent is recycled after regeneration and the SO_2 that is released from the process can be used to form sulphuric acid or elemental sulphur (Srivastava, 2000). The regenerable sorbents used were homogenous alkali and alumina compounds. In 1987, Gavalas et al performed work with alkali-alumina sorbents i.e. an alumina sorbent with a thin layer of alkali support. It was found that by using alkali alumina sorbents, a faster and more complete reaction occurs as the alumina acts as a catalyst and a reactant. The cost of using such regenerable sorbents depends on the treatment process required for the off gas produced and the ability of the sorbent to resist attrition as it is continuously recycled between the sulphation and regeneration phases. 91% of all FGD applications are based on the once through process as this is much simpler and more feasible. These groups can be further classed as dry and wet processes. In dry FGD, the product produced is dry material and in the wet FGD process a slurry product is produced.

Some of the factors that affect the choice of FGD for applications include the amount of sulphur that needs to be removed, the cost of achieving the desired efficiency and the environmental and economic factors that affect the waste disposal technique (Ogenga, 2009).

The various processes for FGD are shown in the figure below (Srivastava, 2000)

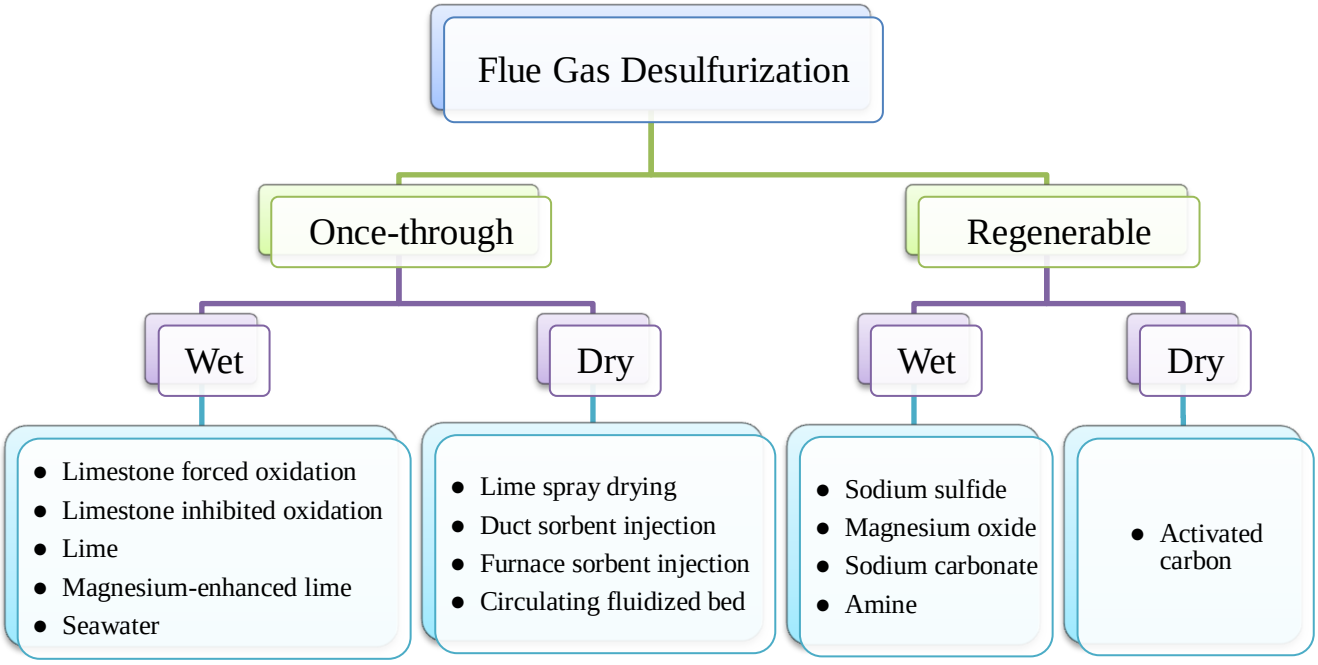

Figure 2-7: Various FGD Processes (Adapted from Srivastava, 2000)

2.5.3.3. The Basic Wet FGD Process

In the process below (Figure 2-8), the sorbent is first crushed into particles of smaller size and then mixed with water using an efficient ratio in a slurry tank resulting in the formation of limestone slurry. This slurry is then pumped to the upper section of an absorber where it passed through the relevant packing material, counter current to the direction of the flue gas flow. This allows for maximum contact hence optimal absorption of SO_2 by the sorbent. Any unfinished reactant that may be present is then passed to the reaction tank to allow for maximum conversion of the SO_2 to sulphates and sulphites. The slurry from the reaction tank has spent sorbent. Water from this stream is removed and then recycled to the slurry preparation tank. The remaining sorbent slurry or damp solid is safely disposed. The flue gas from the absorber is then passed to a stack before it is released into the atmosphere (Srivastava, 2000).

Various factors affect the SO_2 removal efficiency in the wet FGD systems. These include the pH of the slurry, the ratio of water to sorbent used in the slurry preparation, the temperature at which the slurry was prepared, the hydration time of the slurry preparation, the retention time in the absorber and reactor (Srivastava, 2000).

Wet FGD involves the use of slurries and was found to be more efficient in SO_2 removal than dry FGD and showed a higher sorbent utilization due to the increased interaction time between the sorbent used and the gases in aqueous form (Ogenga, 2009).

The SO_2 removal efficiency using the wet FGD system is usually over 90% (Ogenga, 2009) and the reaction rate very high. These systems enjoy widespread applications in industry as they are safe, mature and reliable.

In addition to the advantages there are many disadvantages as these systems have a high capital investment and operability cost. Wet FGD systems consume large amounts of energy and water. Much effort needs to put in to ensure that the sludge and waste produced are properly disposed of. The system is very complex and requires large land space. The process units are also much more susceptible to corrosion.

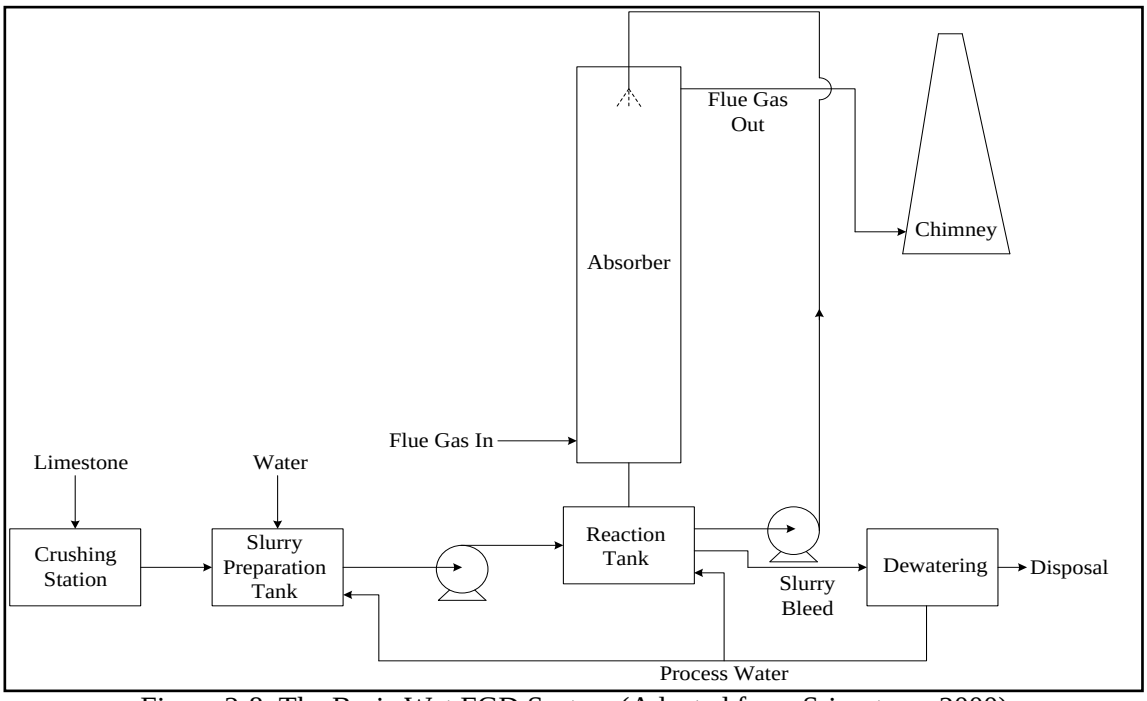

Figure 2-8: The Basic Wet FGD System (Adapted from Srivastava, 2000)

2.5.3.4. <u>The Dry FGD Process</u>

The principle operation of the dry FGD system is that a dry end product is produced. The flue gas comes into contact with the sorbent that can be in the form of slurry or a solid powder. The sorbent state then dictates whether the process is a dry-dry or dry-wet system.

The figure below (Figure 2-9) represents one of the dry FGD systems. The sorbent feed which can be in the form of a slurry or powder contacts the flue gas in a spray dryer. The sorbent absorbs the sulphur dioxide from the flue gas and the solid product that is produced is passed to a solid separator where the spent absorbent is removed as a solid waste and the flue gas is then sent to a tall gas stack before being released into the atmosphere.

Dry FGD systems are becoming more popular than the wet FGD systems as these systems are more environmentally friendly (DePriest et al, 2003). Dry FGD requires lower initial capital cost and the operating costs of these processes are also much lower due to the ease of dry waste handling. The waste that is produced has similar physical properties to that of fly ash hence waste disposal can be done simultaneously (Ogenga, 2009). The material of construction for the process units of dry FGD can be cheaper than that of wet processes due to the reduced susceptibility to corrosion (Ogenga, 2009). This system also has decreased space requirement and is easy to retrofit (Foo et al, 2011). The energy requirements and water consumption are much lower than that of the wet FGD process.

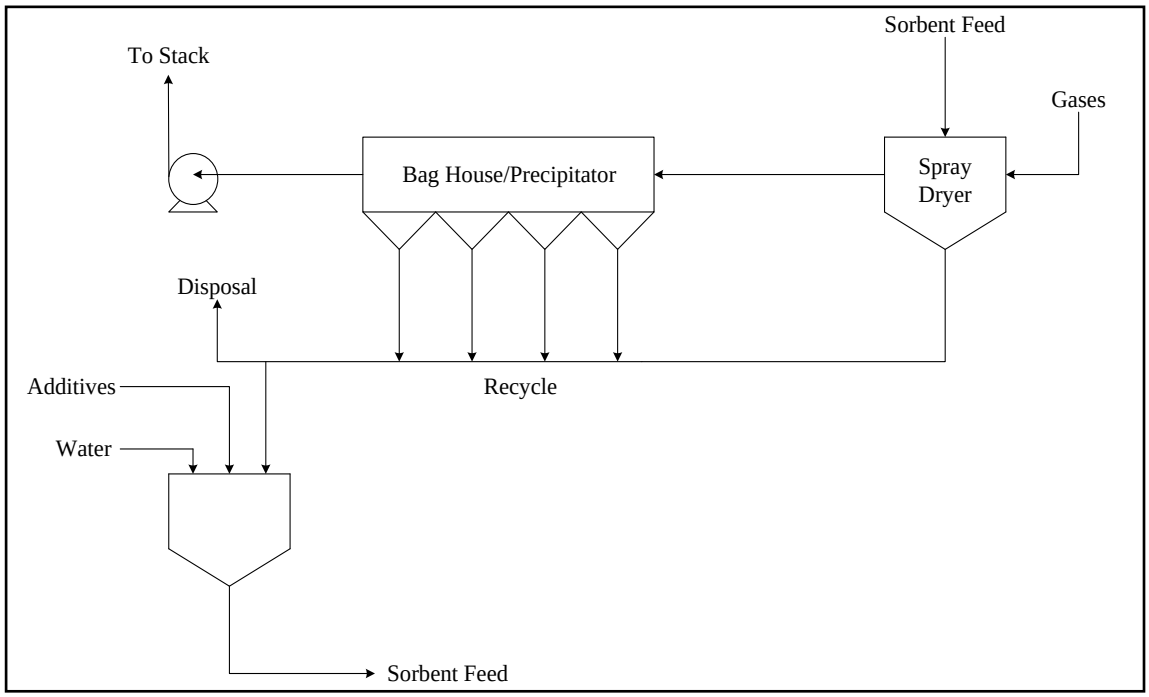

Figure 2-9: Basic Dry FGD System (Adapted from Mandlall, 1993)

2.5.3.5. Common FGD Systems

- **Duct Sorbent Injection (DSI)**

This system (Figure 2-10) operates at temperatures of about 450K (Ogenga, 2009). The sorbent in the form of a slurry or powder is injected into the duct work. This eliminates the need for an absorber hence reducing cost. Sorbent performance can be enhanced by adding water into the system either upstream or downstream. Reaction products are then sent to an electrostatic precipitator or fabric filter. SO_2 removal takes place in both the duct and the emission particulate control device (Ogenga, 2009). This process is simple, has reduced costs and is easy to construct however, there is poor utilization of the sorbent as it has a short residence time in the duct therefore having an efficiency of merely 40% (Ogenga, 2009).

The sulphur removal efficiency in sorbent injection systems is influenced by a variety of factors namely the sorbent injection rate, sorbent residence time, sorbent saturation and mixing with flue gas stream, particulate control device, flue gas temperature and the sorbent particle size (Patnaik, 2010).

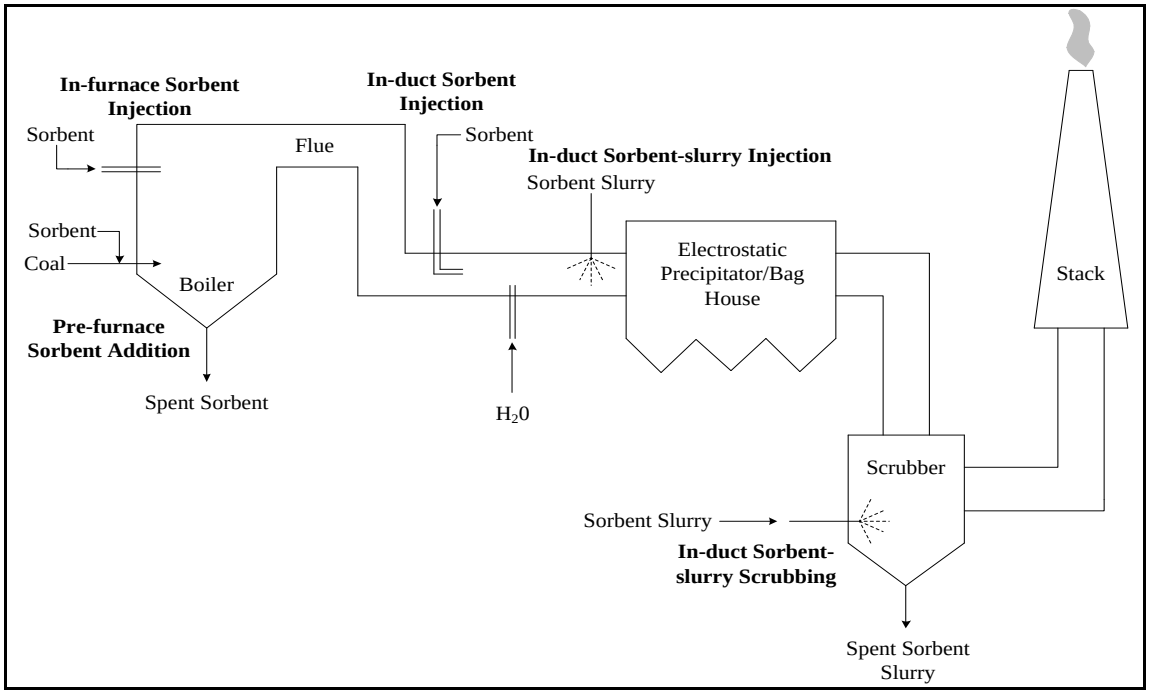

Figure 2-10: Duct and Sorbent Injection FGD Systems (Adapted from Chiang, 1995)

- **Furnace Sorbent Injection (FSI)**

This is a high temperature process and the furnace usually operates at temperatures of approximately 1000˚C (Srivastava, 2000). The sorbent can be in solid dry powder or hydrated form. This sorbent is injected above the flame in the furnace section of the boiler and is dispersed in the entire upper section. High temperature causes the decomposition of the sorbent resulting in a larger exposed surface area for reactions to occur. The reaction products, spent sorbent and flue gas then pass through the emission control device. This device allows ash and reaction products to be removed concurrently while the flue gas passes through a stack before being released into the atmosphere.

Case et al, 2006 performed work to establish the recommended conditions for sulphur capture using calcium containing sorbents by using a sorbent injection system. The negative impacts of using such a system such as fouling, reduced performance of the combustion chamber and the change in fly ash properties were also investigated. When the sorbent is injected into the furnace, it forms lime and reacts with oxygen and sulphur dioxide to form calcium sulphates/sulphites. The three essential processes that occur in this system are the sorbent activation, sulphur capture and regeneration. The sulphur capture occurs during the oxidizing and reducing conditions. It was found that in the oxidizing conditions, the most important parameter was the thermal environment. If the sorbent temperature surpasses a certain limit, the reactivity decreases due to dead-burning. This system is not very efficient as it has reduced reaction activity due to dead-burning and poor distribution of the sorbent. However, the system is simple, eliminates the need for large amounts of water consumption and has a removal efficiency of 40-80% (Ogenga, 2009).

- **Circulating Fluidized Bed**

These systems (Figure 2-11) can implement both dry and semi dry techniques. The sorbent that is present in the reactor can be hydrated or in the form of solid powder. Flue gases are passed through the bottom of the reactor at high velocities thus creating the fluidized state. There is intimate contact between the flue gas and the sorbent used due to recirculation thus allowing for maximum utilization of the sorbent. The product of the reaction is a dry solid and it is retained in the reacting vessel together with the spent sorbent and fly ash which are then sent to the disposal site (Srivastava, 2000). Some of the products enter the particulate matter control device together with the flue gas and are sent for disposal while the remaining flue gas passes through a stack before entering the atmosphere. This system is relatively inexpensive, requires less land space and has a high SO_2 removal efficiency.

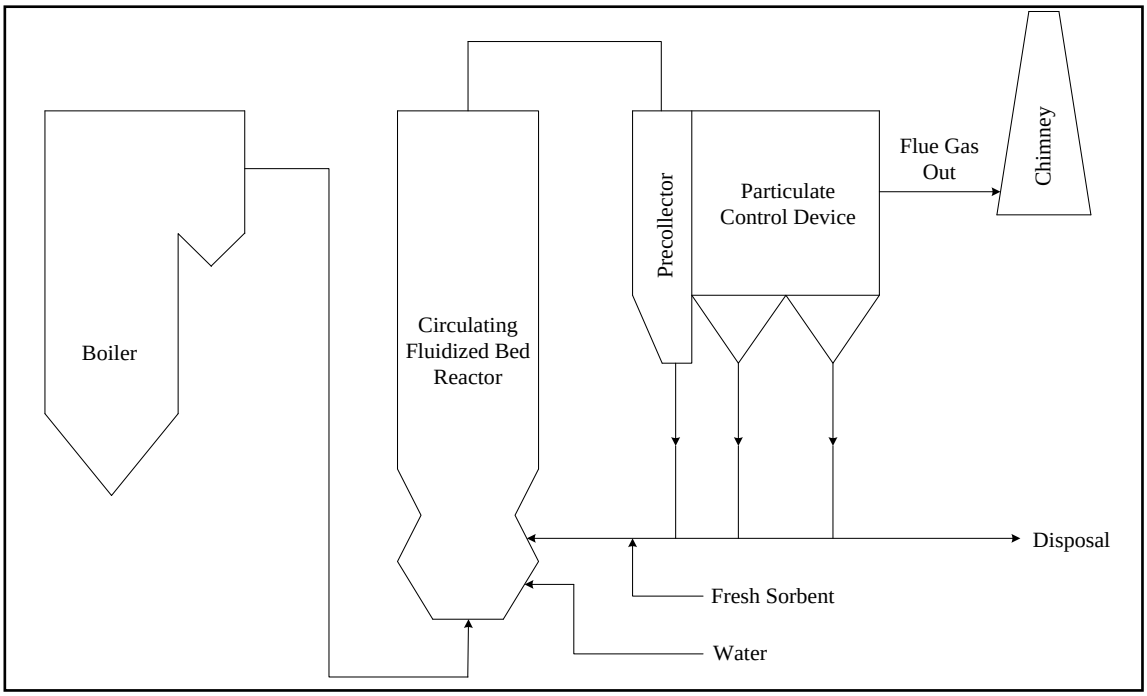

Figure 2-11: Circulating Fluidized Bed System (Adapted from Srivastava, 2000)

- **Spray Dry Process**

This is a semi dry system (Figure 2-12) that is chiefly implemented for processes that use high sulphur composition coal (Srivastava, 2000). The sorbent is prepared in a mill and water is added to form slurry. The slurry is then dispersed over the flue gas contained in the spray dryer. Simultaneous transfer of mass and heat occurs between the slurry and gas phase. The reaction and the evaporation of water from the slurry phase produces a powdered dry waste product. The flue gas enters a particulate control device namely a duct arrestor before it is released into the atmosphere via the stack. Increased utilization of the sorbent and increased SO_2 removal efficiency is achieved by recycling the bottoms of the dryer to the feed. This system is cost effective in terms of installation. However,

operating cost varies in relation to sorbent utilization which is lower than that of the circulating fluidized bed (Srivastava, 2000).

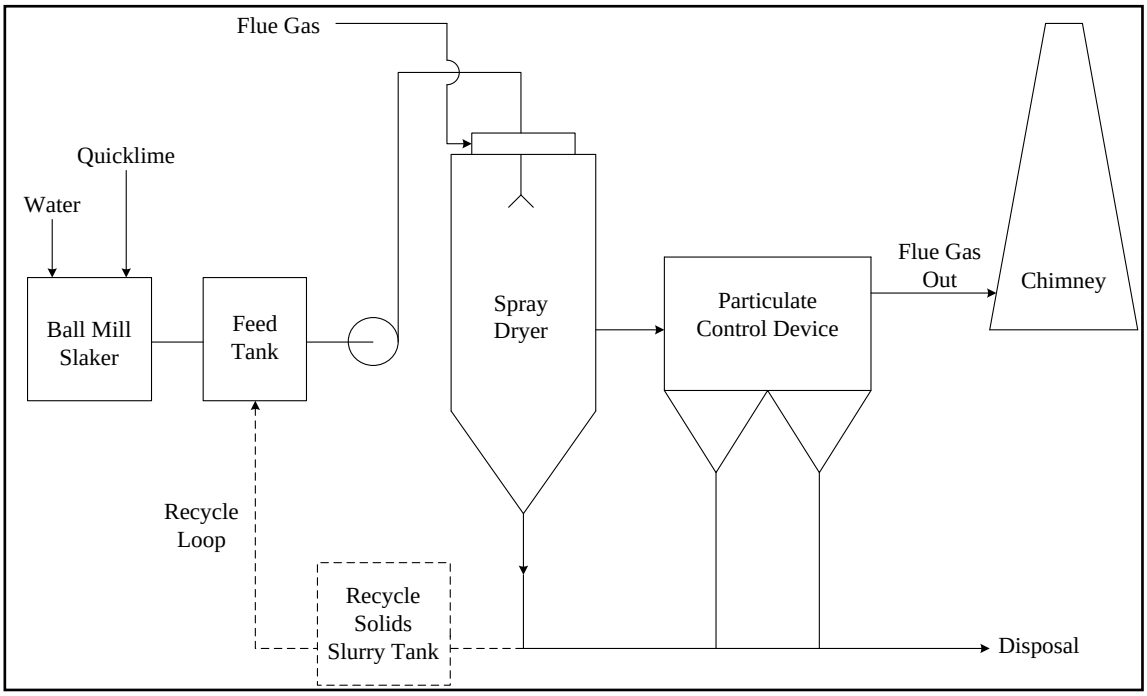

Figure 2-12: Spray Dryer System (Adapted from Srivastava, 2000)

- **Limestone/ Gypsum Process**

This process uses an alkaline sorbent that is readily available. In the limestone system, limestone slurry is formed by blending finely ground limestone with water. The flue gas that enters the limestone/gypsum process is initially passed through electrostatic precipitators to remove any dust or ash that may become problematic downstream. The flue gas then enters an absorber (Ogenga, 2009). The limestone slurry is then sprayed over the flue gas which reacts directly with the SO_2 to form a calcium sulphite slurry which is then oxidized in air to form calcium sulphate which can be safely removed. This process removes 90% of the sulphur dioxide from the flue gas and neutralizes it before it is released into the atmosphere via a stack (Air Pollution Control, 2010). Work undertaken by Özyuğuran et al in 2010 investigated the use hydrated lime or limestone slurries. The study showed that the desulphurization ability of the hydrated lime is superior to that of the limestone due to higher solubility, increased alkalinity, and better reactivity at low temperature.

However, hydrated lime used in the wet FGD proves to be very costly as calcination, transport and slaking need to be accounted for.

- **The Seawater Process**

Absorption of SO_2 using the seawater process makes use of the natural alkalinity of sea water to neutralize the flue gas. Untreated seawater contains calcium carbonate (Ogenga, 2009). The sea water and the flue gas flow counter current to each other in an absorption tower. The reaction between the calcium carbonate present in the seawater and the SO_2 present in the flue gas results in the formation of calcium sulphate and carbon dioxide (Ogenga, 2009). The seawater with the absorbed SO_2 is treated with more seawater to adjust the pH and the absorbed SO_2 is then oxidized with air to form sulphate removing 99% of the SO_2 (Air Pollution Control, 2010). After this water treatment process, the effluent is discharged into the sea. This process is simple and relatively inexpensive with no requirement for land disposal sites. However, it may cause pollution to seawater and it is only suitable for those power stations that are situated along the coastal regions.

- **The Wellman Lord Process**

This process has two distinct stages namely absorption and regeneration. The sorbent used in this system is sodium sulphite. Initially, the flue gas is scrubbed to remove HCl, HF, SO_3 and ash. The hot gas then passes through a cooler before it enters the absorption unit. The sorbent is then dispersed over the gas resulting in the formation of sodium bisulphate. This product is then sent to an evaporator for regeneration. This results in the decomposition of the sodium bisulphate and the formation of sodium sulphate which is then recycled to the initial flue gas absorption stage (Air Pollution Control, 2010). The remaining SO_2 is converted to valuable products such as sulphur and sulphuric acid which can be sold to other industries.

There is maximum utilization of the sorbent as it is continuously recycled and the process has a sulphur removal efficiency of 95% (Ogenga, 2009). However, the process is extremely complex and the reagent that is used is relatively expensive.

2.6. Sorbents

2.6.1. Different Types of Sorbents

Sorbents are a significant branch of the flue gas desulphurization process. The efficiency of the acid gas removal process is vastly dependent on the nature of the alkaline sorbent that is used as the composition of each sorbent varies. The type of flue gas desulphurization process that is implemented also affects the choice of sorbent. It is essential that the sulphation product that is formed is thermally stable at the furnace temperature as this also affects the sulphur removal efficiency (Cheng et al, 2003). The use of alkali earth metals as sorbents such as magnesium, calcium, barium, strontium etc. produces sulphates that are stable at high temperature. These elements have similar properties and

sulphur removal capabilities. Flue gas desulphurization commonly uses calcium, magnesium, sodium or potassium based sorbents as well as amine and seawater (Ogenga, 2009). The strontium based sorbents are much heavier than the calcium sorbents and are thus more expensive to use. The barium sulphates that are formed during desulphurization are more thermally stable than the strontium sulphates however, barium based sorbents are relatively expensive compared to the calcium based sorbents. Barium has better sulphur removal efficiencies hence a compromise between the cost and sulphur capture would be to blend the barium with calcium (Cheng et al, 2003). The sodium based sorbents have a high SO_2 removal efficiency (Ogenga, 2009). However, these sorbents are extremely expensive and they produce wastes that are hazardous and difficult to dispose. Work performed by Majeed et al, 1995 compared the capabilities and economics of $CaCO_3$ and NaOH slurry to absorb sulphur dioxide using an air lift reactor. A computer design program was implemented to optimize the SO_2 removal efficiency with the most important variable being gas velocity. As gas velocity is increased, the SO_2 removal efficiency decreases. From figure 2-13 it can be observed that the NaOH sorbent has an SO_2 removal efficiency that is 15 times greater than that of the calcium carbonate however the more commonly used sorbent is the latter due to the cost being approximately 6.5 times higher.

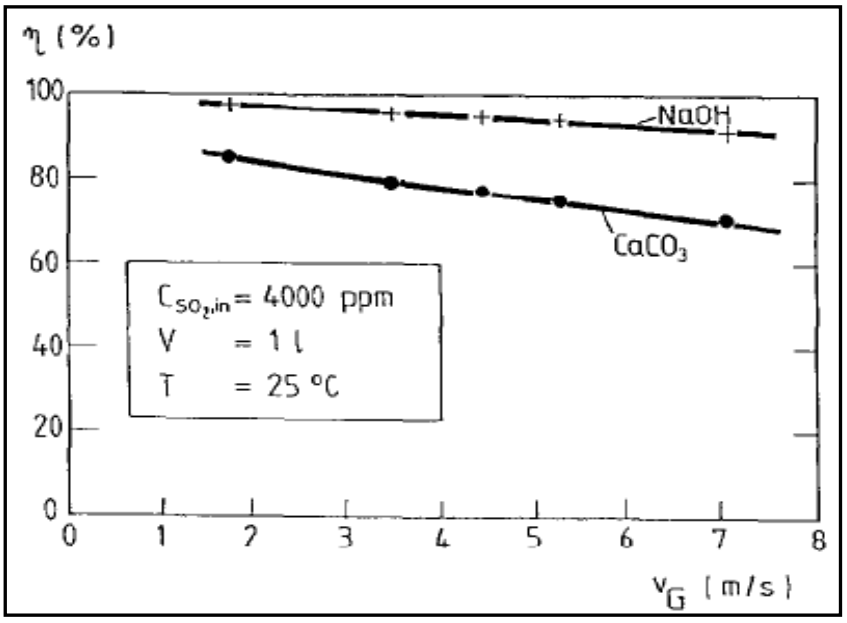

Figure 2-13: Comparison of NaOH and $CaCO_3$ Sorbent Slurries for SO_2 Removal Efficiency (Majeed et al, 1995)

The most commonly used calcium based sorbents for the FGD systems are lime (CaO), limestone ($CaCO_3$), hydrated lime ($Ca(OH)_2$) and dolomite ($CaCO_3MgCO_3$). Calcium based sorbents are most

commonly used as calcium is found abundantly and has no toxic effects. The spent sorbent from these processes is usually a solid waste that is easy to handle and environmentally safe to dispose.
The sorbent nature dictates the type of sulphite or sulphate produced after the chemical reaction with the sulphur dioxide occurs. Various process variables and sorbent properties may affect the chemical transformation process and the products that are produced including the operating temperature, the relative humidity of the flue gas, the initial SO_2 concentration of the flue gas, particle size, porosity, and surface area.

The most suitable sorbent should have the following combined characteristics (Chiang, 1995)

- Abundantly available and relatively cost effective.
- High SO_2 removal efficiency.
- React with the SO_2 to form by-products or waste that are environmentally safe, easily disposed or have some commercial market resale value.

2.6.2. Current Sorbents

The sorbents that enjoy widespread utilization in the flue gas desulphurization process is mainly limestone derived. Limestone or Calcium carbonate is a naturally occurring calcium based sorbent. It is a mineral that can be found abundantly in rocks in all parts of the world and it is a major constituent of the shells of marine animals. The composition of the limestone may vary depending on the area or location it was sourced from. Digenesis or the degree to which alterations occur due to time, temperature and pressure may also affect the formation of the sorbent. Geology and topography may result in limestone with similar compositions having different sulphur retention capabilities (Morrison, 2008). It was found by Dam-Johansen and Ostergaard in 1990 that young limestone has a higher capacity for the reaction with sulphur dioxide as compared to geologically older limestone. Limestone is comprised of different compounds including CaO, $CaCO_3$, $MgCO_3$, alumina, silica, iron, and other elements in very small proportions. Calcium and magnesium contribute 85-90% of the total limestone composition (Ogenga, 2009). Limestone can be calcium based or magnesium based (dolomite) depending on the quantity of these elements. Calcium based limestone is comprised of approximately 5% magnesium carbonate while dolomite comprises over 20% magnesium carbonate (Elert et al, 2002).

Limestones are crushed and mixed with water to create a slurry that is used in the limestone/gypsum wet FGD process removing over 90% of the SO_2. Lime, hydrated lime and dolomite sorbents are prepared with much ease from the limestone and are utilized in the dry and semi dry systems. (Ogenga, 2009).

Limestone has been used as the primary sorbent because it is inexpensive and abundantly available. Limestone is inert, it can be shipped without any possibilities of self-ignition due to resistance and agitation and it can be stored in an open environment (Majeed et al, 1995). A general conclusion drawn by Falkenberry and Slack, 1971 states that limestone that has a high calcium content is more reactive than dolomite sorbents. The magnesium has minimal participation in the reaction, however it increases the amount of the utilized calcium fraction in the sorbent. The limestone that reacts with the SO_2 forms sulphate, which can be easily disposed as waste or sold to the cement and cardboard manufacturing industry (Majeed et al, 1995). However, it has a low utilization rate and raw sorbent is constantly required (Mandlall, 1993). This has led to an increase in the use of hydrated lime as sorbent material.

Dolomite has good water retention capabilities and is commonly used in the construction industry (Elert et al, 2002). Recent work has shown that dolomite has a higher sulphur removal efficiency as compared to the calcium based limestone because it has a higher porosity. The dolomite is a better sorbent as it allows for greater utilization than the limestone based sorbents.

2.6.3. Calcination, hydration and Sulphation of Limestone

- **Calcination**

Calcination is a high temperature endothermic (Dam-Johansen and Ostergaard, 1990) process (between 925 and 1340℃) that is used to remove volatile components (Elert et al, 2002). The calcination of limestone takes place in the absence of air and it is used to form quicklime and remove the carbon dioxide from the carbonate mineral (Ogenga, 2009). Due to the large composition of calcium and magnesium in the limestone, calcination produces either calcium oxide (CaO) or magnesium oxide (MgO) depending on whether the limestone is calcium or magnesium based. The products formed during the calcination process have a larger surface area than the raw limestone reactants (Tullin et al, 1989).

The quality of the resultant quicklime that is produced from the thermal decomposition process is affected by a variety of factors (Ogenga, 2009):

- The nature of the limestone from which the quicklime is derived including the density, crystal structure, particle size and the presence of impurities.
- The temperature of the kiln in which calcination occurs.
- The residence time of the limestone in the kiln.

Limestone $CaCO_3\,(s) \longrightarrow CaO\,(s) + CO_2(g)$ T > 1030K (2.5)

Dolomite $CaCO_3.MgCO_3(s) \longrightarrow MgO.CaCO_3(s) + CO_2$ T > 890K (2.6)

$CaCO_3.MgCO_3(s) \longrightarrow MgO(s) + CaO(s) + CO_2(g)$ T > 1030K (2.7)

If hydrated lime is used as the sorbent, it is decomposed by the following reaction step to form the calcium lime powder with high surface area and porosity (Ghosh-Dastidar et al, 1996):

$$Ca(OH)_2(aq) \longrightarrow CaO(s) + H_2O\,(aq) \qquad (2.8)$$

The temperature at which the system operates is such that a stable product that can be easily removed is formed during sulphation (Zevenhoven and Kilpinen, 2001). The optimum temperature range for limestone is between 940-1400 ℃ and 65-93 ℃ less for dolomite. The length of time for the continued temperature exposure depends on how long it takes for the complete removal of the CO_2 from the limestone or the dolomite (Mandlall, 1993). The calcination parameters such as the temperature and the calcination time depends on the size of the limestone that is used. It was found that stones with a decreased size distribution had a larger heat transfer surface area and are more susceptible to calcination than the larger stones hence they require a decreased calcination time (Elert et al 2002). In contradiction to this it was established that the larger stones may have increased void space thus promoting the circulation of the flue gas resulting in uniform heat transfer (Elert et al, 2002).

It was found by Cheng et al, 2003 that the rate determining step was the chemical reaction for particle sizes between 9-15μm and the diffusion of carbon dioxide is the rate controlling step for particle size over 152 μm diameter at 1200℃.

Although natural calcium based sorbents such as the limestone is porous and contains some impurities, the calcium sulphate that is produced during the sulphation step will cause plugging and blockage of the pore structure (Zevenhoven and Kilpinen, 2001). Calcination of the limestone releases CO_2 and ensures that the pore structure is opened. This allows for pore diffusion to occur efficiently and reduces the possibility of plugging and pore blockage. The sorbent porosity may increase between 5 and 50 times during the process of calcination (Govender, 2006). MgO and CaO are more reactive with the SO_2 present in the flue gas as compared with limestone and dolomite hence this verifies the importance of calcination.

It can be concluded that the optimum parameters for calcination is determined by the structural and physical properties of the sorbent that is undergoing calcination (Elert et al, 2002).

- **Sulphation**

Sulphation is the exothermic (Dam-Johansen and Ostergaard, 1990) process that occurs after calcination and hydration. The calcined or hydrated lime reacts with the sulphur dioxide or sulphur trioxide that is contained in the flue gas to form sulphates, useful by-products or waste material that can be readily disposed. This process occurs in an atmosphere that has air present in excess (Tullin et al, 1989).

$$CaO(s) + SO_2(g) + \frac{1}{2}O_2(g) \longleftrightarrow CaSO_4(s) \quad (2.9)$$

$$CaO(s) + SO_3(g) \longleftrightarrow CaSO_4(s) \quad (2.10)$$

Desulphurization can also take place with the direct reaction with SO_x (Tullin et al, 1989).

$$CaCO_3(s) + SO_2(g) + \frac{1}{2}O_2(g) \longleftrightarrow CaSO_4(s) + CO_2 \quad (2.11)$$

$$CaCO_3(s) + SO_3(g) \longleftrightarrow CaSO_4(s) + CO_2 \quad (2.12)$$

The magnesium has no effect on the sulphation reaction as it does not form a stable product above a temperature of 760℃ and the system operates at a temperature greater than 800℃.

The operating temperature for the system is between 750 and 950℃. Flue gas contains about 15 % CO_2. At 860 C the equilibrium pressure was found to be 0.57 bar. Different CO_2 partial pressures will affect the bed temperature. Calcination takes place where the partial pressure of the CO_2 is low (Tullin et al, 1989).

The $CaSO_4$ that is formed creates a layer on the surface of the lime. This plugs and blocks the pores of the sorbent and prevents complete utilization of the sorbent that becomes hidden deep within the core (Govender, 2006). The calcination process that occurs prior to the sulphation assists in improving the pore diffusion capacity of the sorbent.

2.6.4. Chemical and Physical Properties of Sorbents

The effectiveness of a sorbent to capture sulphur dioxide is affected by both its chemical and physical properties. In previous studies, most of the investigations involved the effect of the physical properties and it was found that these properties as opposed to the chemical properties affect the desulphurization behaviour. However more recent studies have investigated the effect of chemical composition and have established that these properties also have a significant role in the desulphurization ability and are equally important in reducing the SO_2 emissions that are released into the atmosphere (Haji-Sulaiman et al, 1991).

These properties include:

2.6.4.1 Chemical Composition and Impurities

The chemical composition varies with the manner and the time period over which the source rock was formed. The compositional content of impurities that are present in the sorbent may vary from below 1% to approximately 20% (Haji-Sulaiman et al, 1991) and these may occur as quarts and clay or in trace quantities of copper, titanium or manganese. In early studies conducted by Dam Johansen and Ostergaard, 1990 it was concluded that there was a minimal relationship between the sulphur dioxide capture and the chemical composition and that ferric oxide had an adverse effect on the sulphur capture capacity however studies conducted in a later time frame indicate contradictory results.

Sorbents can be classified as limestone or dolomite. In the past it was believed that a sorbent with a high calcium carbonate composition improved the sulphur capture capacity, however in more recent studies by Pisupati et al, 1996 it was concluded that the calcium carbonate content had little effect on the sulphur capture efficiency. This result was also in agreement with the work performed by Carsky et al, 2006. Alvarez and Gonzale, 1999 found that dolomites have a more open porous structure and this allowed for maximum calcium utilization. Sorbents have a large amount of impurities, depending on where they were mined. Haji- Sulaiman, 1991 found that the presence of these impurities delay the pore closure that occurs during the sulphation process. This allows for better utilization of the sorbent.

Silica present in limestone as an impurity created undesirable effects. It causes fusion and forms a layer that reduces the reaction between the sorbent and sulphur dioxide (Falken and Slack, 1971).
Work undertaken by Spitsbergen et al, 1981 found that the chemical properties together with the microporous structure affect the sulphur retention capabilities. It was established that a sorbent with high Iron and Strontium content results in greater reactivity to sulphur capture as the iron initiates and promotes the reaction that occurs between the sorbent used and the SO_2. The sulphation capacity of CaO was measured at 850℃ by Yang et al, 1978 and was found that increasing the Fe_2O_3 % by a small amount caused the sulphation capacity to increase tremendously (Haji-Sulaiman et al 1991). Desai and Young, 1983 concluded that using a dolomite limestone coated with Fe_2O_3 both the sorption capacity and the sorbent utilization increased and these investigations established that the Fe_2O_3 acts as a catalyst for desulphurization (Haji-Sulaiman et al 1991).
Studies conducted by Özyuğuran et al, 2010 investigated the sulphation capacity of limestone and hydrated lime slurries.

Table 2-3 Composition of 12 Different Samples (Adapted from Özyuğuran et al, 2010)

Sample Code	% $CaCO_3$	Sample Code	% $CaCO_3$
L1	96.04	HL1	80.77
L2	93.16	HL2	79.87
L3	66.34	HL3	50.12
L4	97.29	HL4	88.27
L5	96.57	HL5	85.07
L6	89.13	HL6	61.02

Table 2-3 shows the chemical composition of 6 different samples of limestone and hydrated lime slurries. It was found that the sulphation capacities for the L1, L2, L4 and L5 were higher than that of the L3 and L6. Similarly, the hydrated lime samples with the higher calcium hydroxide content namely HL1, HL2, HL4 and HL5 also had higher sulphation capacity than the HL3 and HL6 samples. These results indicate that sorbents with an increased amount of Ca^{+2} ions have better sulphur removal efficiencies.

2.6.4.2 Particle Size and Surface Area

The particle size that is used has an effect on the SO_2 removal capacity and the sorbent utilization. Various resistances affect the reaction and these resistances determine which are the controlling steps in the modelling of the reaction. At high temperature it was found by Govender, 2006 that as the particle size increases, the diffusion through the $CaSO_4$ layer that is formed becomes the rate controlling step. When the particle size decreases, the rate determining step is pore diffusion and surface reaction.

Pisupati et al, 1996 established that using a larger sorbent particle size increases the amount of sorbent that is required. The smaller particles ensure that there is enhanced interaction between the solid and gas, hence improving the SO_2 removal efficiency.

Gosh- Dastidar et al, 1996 investigated the kinetics of sulphation at high temperatures. It was concluded that the particle size is one of the primary factors that affect the conversion of the Ca^{+} ions to $CaSO_4$. The results showed that the smaller particles have better SO_2 removal efficiency and this is because large particles have transport limitations that affect the reaction rates, rendering calcination and sulphation less efficient. Cheng et al, 2003 established also that small particle sizes result in improved sulphur removal efficiency and sorbent utilization. It was also established that the minimum size of 5 µm should be maintained to avoid extensive grinding cost and pore volume destruction. Fan et al, 1991 established that the most significant factor that affects the optimum particle size for circulating fluidized bed combustors is the separation characteristics. It was found that most technologies implementing these systems use a minimum particle size of 100 µm which results in a 99% operating efficiency.

The work performed by Chi et al, 1994 concluded that the larger particles resulted in the core being unreacted and thus decreased the extent of sulphation. In contrast to the above results, Chu et al, 2000 found that the larger particles spend a longer time in the combustion chamber and the attrition and abrasion breaks up the particles and increases the sulphation. A similar result was discovered by Morrison, 2008 who concluded that a layer of $CaSO_4$ forms on the outer surface of the smaller particle size fractions. This layer creates a resistance that reduces the penetration of SO_2 into the particle core. Large particles form thermally induced fractures on the boundaries that allow for the passage of the SO_2 into the core of the particle where it can be captured.

Ogenga et al, 2009 investigated the effect of sorbents prepared from fly ash and limestone on the SO_2 capture. It was found that these sorbents have a larger BET surface area as compared to the sorbent starting materials individually and this is due to the presence of calcium silicates. This results in improved SO_2 capture.

Work performed by Ho and Shih, 1992 investigated the reactivity of various sources of fly ash on SO_2 capture.

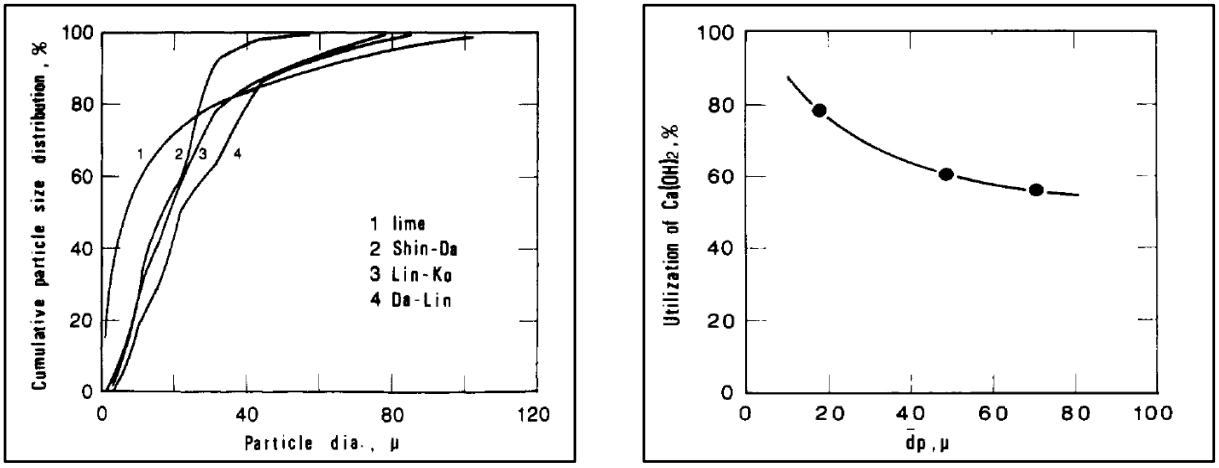

Figure 2-14 a) Particle Size Distribution for Fly ash Sorbent Prepared from Different Sources
b) Effect of Particle Diameter of Fly ash on the Sorbent Utilization (Ho and Shih, 1992)

From figure 2-15 below it is suggested that the fly ash used from the Shin- Da power plant has the greatest reactivity and it can be seen from figure 2-14.a that the Shin –Da fly ash has the smallest size distribution. The results conclude that the sorbent with the smaller particle size distribution is more reactive due to these particles having the largest exposed surface area for a reaction to occur.

Figure 2-14 b shows that as the particle size of the fly ash increases, the sorbent utilization decreases. Sorbent utilization may be larger due to the smaller fly ash particles having higher silica content.

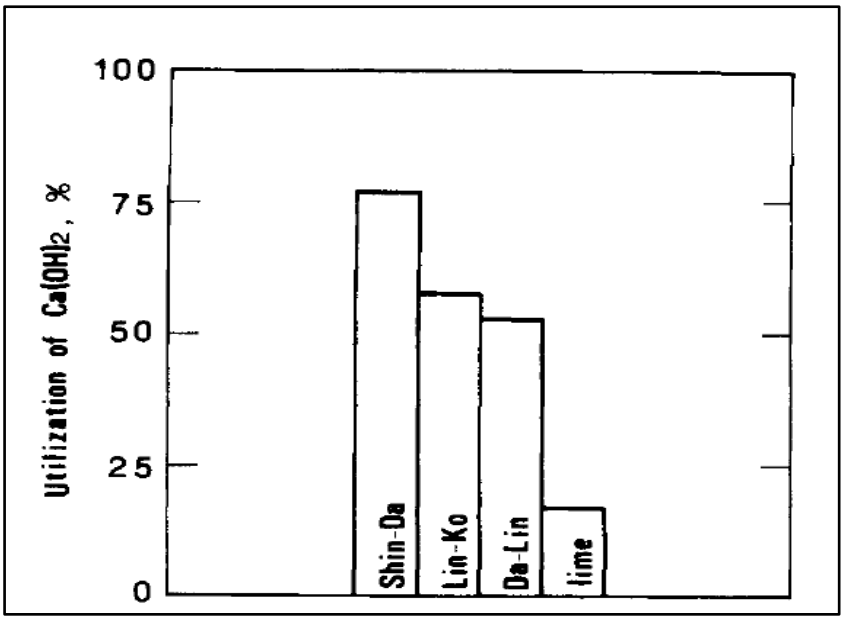

Figure 2-15: Effect of Source of Fly ash on Sorbent Reactivity
(Ho and Shih, 1992)

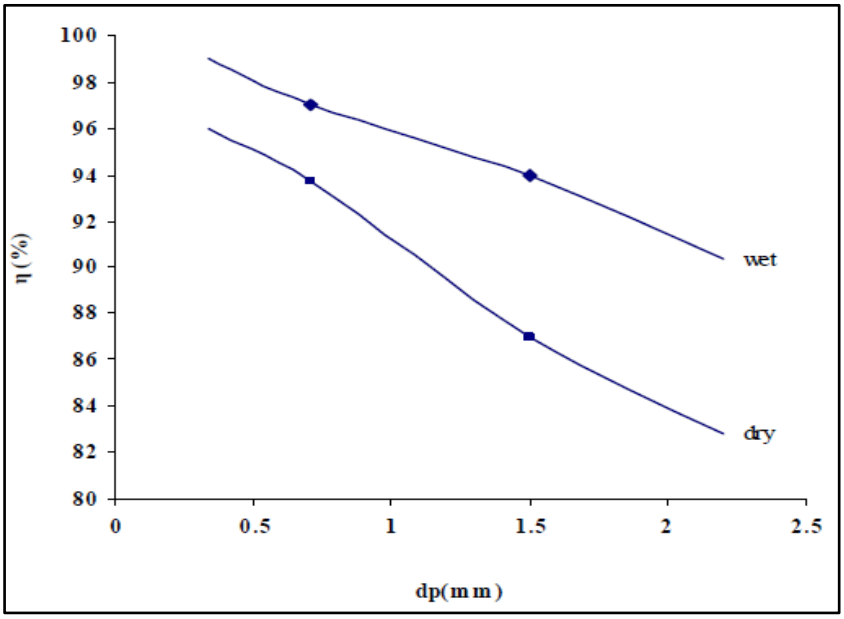

Figure 2-16: Effect of Particle size on SO_2 Removal Efficiency
(Ibrahim and Eliass, 2010)

Work performed by Ibrahim and Eliass, 2010 also supports the above idea. When the sorbent has a smaller particle size distribution, the area available for the reaction to occur is greater as the bed can accommodate a larger quantity of sorbent particles. The particles with larger diameters increase the SO_2 diffusion path and reduce the contact area between the solid-liquid and gas phases which decreases the rate of sulphation.

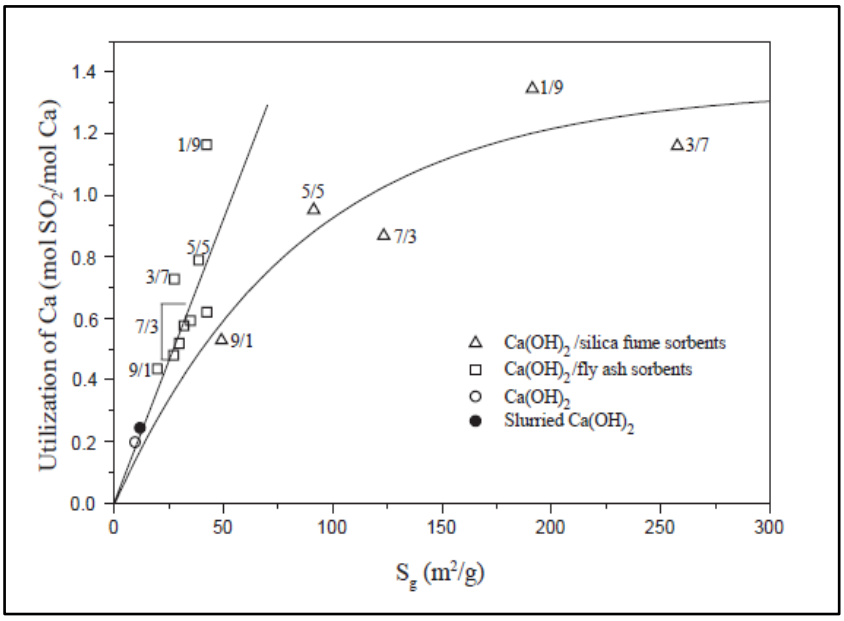

Figure 2-17: Effect of the Specific Area on the Sorbent Utilization
(Ren Bin et al, 2003)

Ren Bin et al, 2003 investigated the effect of specific surface area on the calcium utilization. The figure above was obtained at slurry conditions of 65℃ and 16 hour slurry period with water to solid ratio of 10:1. The sulphation conditions were 70% relative humidity, 60 ℃ with SO_2 concentration of 1000 ppm. The results show that increasing the specific area of the sorbent results in higher sorbent utilization. For the hydrated lime and fly ash sorbent, the sorbent utilization increases with the specific area almost linearly.

2.6.4.3 Porosity and Pore Volume

The pore volume is essential as it affects the amount of space available for the accommodation of the sulphation product which is larger than the raw sorbent. Haji-Sulaiman et al, 1991 established that during the calcination process, the pore volume changes from 34 to 17 cm^3mol^{-1}. This implies that the decomposition of one mole of $CaCO_3$ to CaO is accompanied by 20 cm^3 volume change. Studies conducted by Dam-Johansen and Ostergaard, 1990 concluded that a significant change in volume occurs during the progression of the desulphurization process. Calcium carbonate, calcium oxide and calcium sulphate were found to have molar volumes of 36.9, 16.9 and 46 cm^3mol^{-1} respectively.

Studies by Alvarez and Gonzalez, 1999 showed that if a sorbent has a more porous structure, it has maximum sorbent utilization and is highly reactive. Work performed by Davini, 2002 indicates that it is essential that the pore structure is large enough to allow molecules to penetrate to the inner part of the sorbent. It was found that pores with large diameters allow for higher regeneration and utilization

of the inner core. Work performed by Hartmen et al, 1976 concluded that sorbents with large pore volumes have a high SO_2 removal efficiency. This conclusion is in support of the work performed by Ren-Bin et al, 2003 who concluded that sorbents with hydrated lime and siliceous material were much more reactive than the homogenous sorbents due to increased pore volume and porous structure of the heterogeneous sorbent formed.

Studies conducted by Ghosh-Dastidar et al, 1996 investigating the sulphation kinetics showed that the CaO formed during calcination is subject to sintering depending on the initial sorbent and foreign ions present in the parent solid. Sintering is known as a deactivation phenomenon and it decreases the available surface area and sorbent porosity that is essential for the sulphation reaction. The pore size distribution of the CaO and its sintered form also affects the sulphation rate and the sorbent utilization. Previous work performed by Fan et al, 1991 showed that a pore size range (100-200Å) provides adequate surface area for sulphation. This avoids pore and mouth plugging which are foremost causes for early reaction termination. For pore sizes greater than 200 Å the ratio of surface area to pore volume decreases and the contribution to sulphation becomes insignificant. Best sorbents need to meet the requirements of small particle size, low sintering rate and favourable pore structure. Fan et al, 1991 also suggested that the most favourable reaction conditions are obtained by optimizing certain pore structure properties. This includes obtaining maximized surface area and surface area to pore volume ratios. These factors maximize overall sulphur capture capacity. Cheng et al, 2003 established that pore diameters of between 5-30 nm are recommended for a particle size distribution of 1-2 µm.

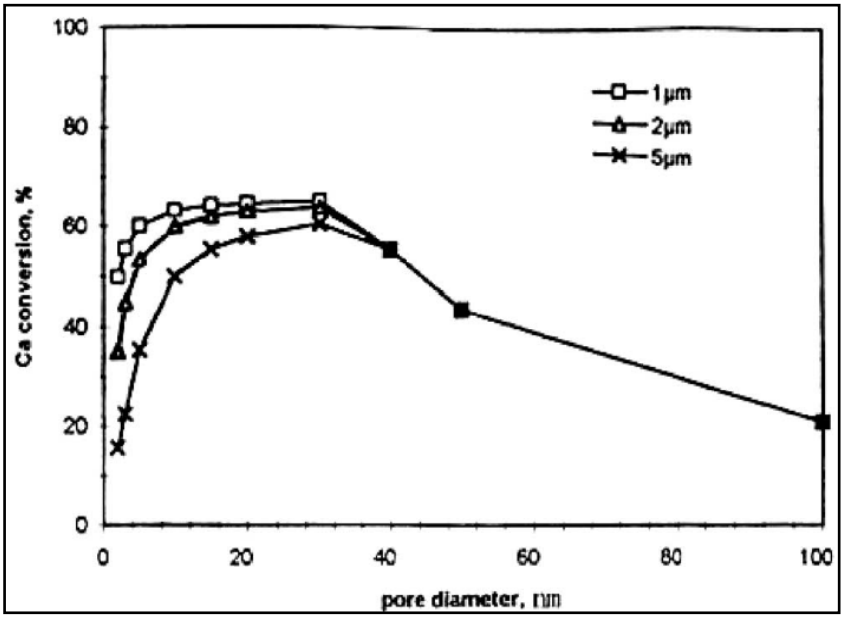

Figure 2-18: Effect of Pore Diameter on Sorbent Conversion for Different Size Particles (Cheng et al, 2003)

Work performed by Garea et al, 2005 also indicates that mesopores contribute significantly to the pore volume. It was concluded by Ortiz et al, 1993 and Garea et al, 2003 that the region with most mesopores on the sorbent structure is the region that has the optimum pore size distribution for effective desulphurization. Ogenga et al, 2009 indicated that the mesopore also increases the available surface area for sulphation to occur resulting in improved SO_2 capture. Ogenga et al, 2010 measured the pore volume using nitrogen adsorption-desorption and it was established that the pore volume increases as the surface area increases thus resulting in higher SO_2 capture and improved sorbent utilization.

2.6.4.4. Hardgrove Grindability Index (HGI)

This index indicates how hard or soft a sorbent is. It was found that the hardgrove grindability index presents no indication of the sulphur capturing tendencies of the sorbents. This conclusion is in support with the work undertaken by Pisupati et al, 1996 where it was found that there is no relationship between the HGI and the calcined products. HGI is however a good indication of the ease or difficulty experienced during the milling and grinding process. Good sorbents are neither hard nor soft but they are a balance of the two. If they are too soft, they are subject to excessive attrition and if the sorbent is too hard, it is difficult to obtain the required size distribution resulting in excessive cost. Sorbents with a high HGI produces the largest quantity of fine size distributions in the milling process (Pisupati et al, 1996).

2.6.4.5. Sorbent Modifiers and Additives

Additives represent structural modifiers. They act as catalysts and form CaO with different properties which in turn have an accumulative effect on the sulphation reaction.

Work performed by Dahlan et al, 2007 investigated the use of oil palm ash as an additive with limestone sorbents for SO_2 removal implementing the dry FGD process. Oil palm ash is a solid waste that is produced in the agricultural industry and it requires a large land area for safe disposal. Therefore using this waste to create a viable sorbent for SO_2 removal provides a beneficial solution to the environment. The use of the raw materials individually has a lower desulphurization capacity as compared to the sorbents prepared from both the raw materials. The amount of OPA and lime present are the most significant variables that affect the desulphurization efficiency. Figure 2-19 displays the effect of the two variables on the desulphurization activity at a constant hydration period of 10 hours. It can be shown that the higher the ratio of OPA to lime or the higher the amount of OPA present in the sorbent, the better the SO_2 removal efficiency.

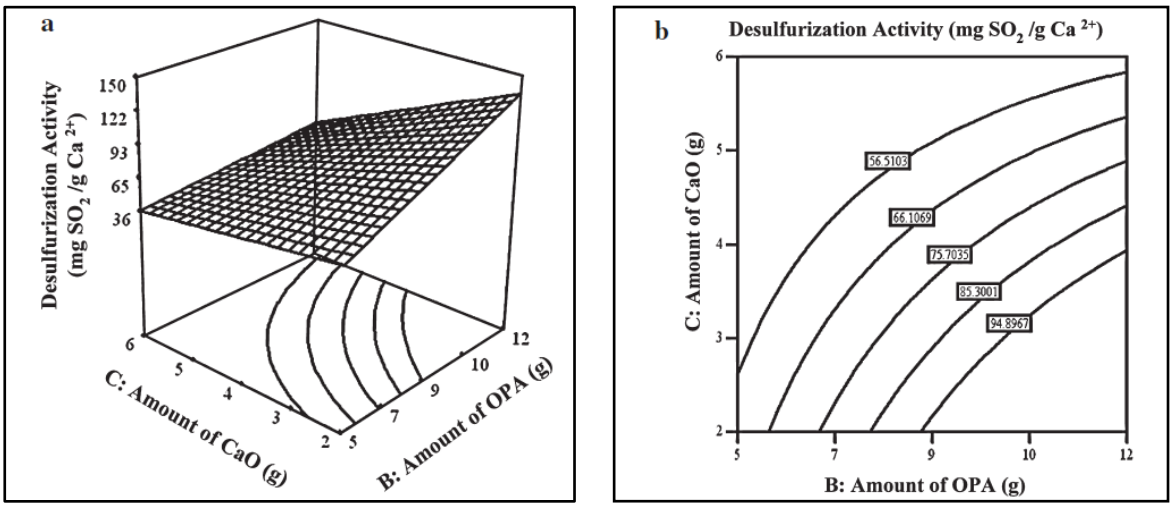

Figure 2-19: Effect of the Amount of Modifier and Limestone on the Desulphurization Capacity Surface and Contour Plots

Ho and Shih, 1992, investigated the reaction between $Ca(OH)_2$ / fly ash and SO_2 in a fixed bed reactor implementing the spray drying FGD system. The variables investigated were those involved in the sorbent preparation and the composition of the fly ash depending on the source. Fly ash contains alkali and alkali earth metals. It is possible to utilize fly ash to produce cost effective sorbents (Cheng et al, 2003). SiO_2, Al_2O_3, Fe_2O_3 and CaO are the main components of the fly ash. The addition of the fly ash to the hydrated lime sorbent creates a pozzolanic reaction due to the large quantities of silica and alumina that are present. This reaction results in highly reactive products that increase the sorbent utilization quantity. The resulting sorbent has a rough surface due to the precipitation of calcium silicates that modify the sorbent structure and increase the surface area for reactions to occur (Lee et al, 2003). The utilization of coal fly ash is beneficial as it is environmentally safe and it is cost

effective as it a product of coal power stations. The products that are produced after desulphurization using the coal fly ash are eco-friendly and can be used in the fertilizer industry.
This result is in agreement with work performed by Ogenga et al, 2010. The study involved the use of fly ash obtained from three different sources as shown in table 2. 4.

Table 2-4: Chemical Composition of Fly ash from Different Sources (Ho and Shih, 1992)

Source	% SiO_2	% Al_2O_3	% Fe_2O_3	% K_2O	% CaO	% Ign Loss
Shin-Da (boiler 3)	59.0	26.7	5.5	2.5	1.6	2.7
De-Lin (boiler 1)	49.6	24.4	8.4	1.6	2.1	9.8
Lin-Ko	51.7	24.0	11.2	2.5	2.1	6.7

The different sources produced fly ash with different compositions. Figure 2-15 shows that the fly ash sourced from the Shin-Da power plant had the greatest reactivity towards the SO_2 removal as it had the highest sorbent utilization. A possible reason for this is that the fly ash sourced from this plant has the highest composition of silica as seen in Table 2-4.

Hiroaki et al, 1996 investigated the effect of silica content as an additive on the SO_2 removal efficiency. The results show (figure 2-20) that as the silica content increases, the SO_2 removal efficiency increases. After a 30% silica content, the rate of SO_2 removal decreases as the specific surface area and accompanying pore volume of the silica decreases. This result is supported by Ogenga et al 2010.

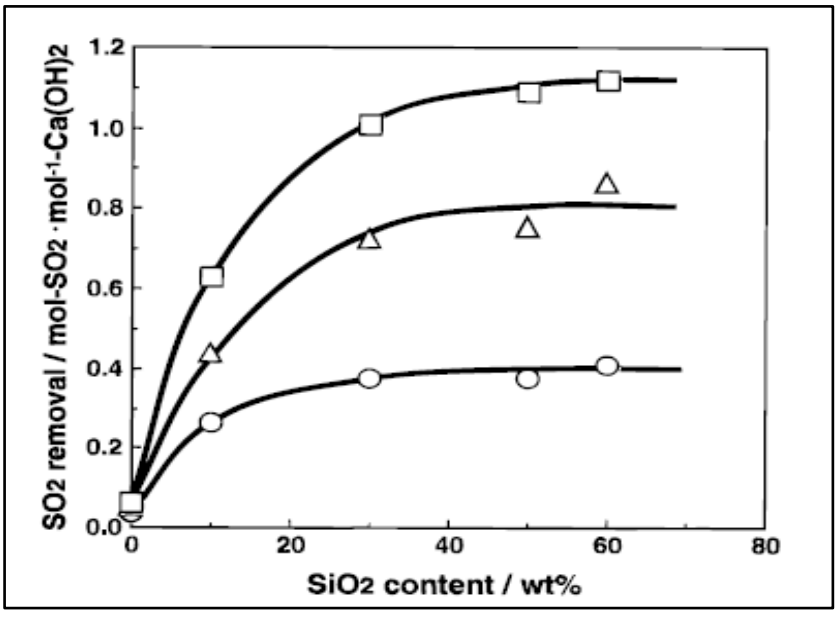

Figure 2-20: Effect of Silica Content on SO_2 Removal
(Hiroaki et al, 1996)

Ren-Bin et al, 2003 conducted studies on the use of silica enhanced sorbents. The raw materials used in the preparation of this sorbent were silica fume and hydrated lime. The reaction of this sorbent slurry with SO_2 was extremely fast due to the formation of the calcium silicate hydrates through the pozzolanic reaction that enhances the SO_2 capture ability. This result is also in agreement with the studies conducted by Ogenga et al, 2009.

From figure 2-21 it can be observed that as the silica fume composition in the sorbent increases, the sorbent utilization also increases. The SO_2 capture is also enhanced as the silica composition increases. SO_2 capture reaches a maximum value and thereafter any increase in the silica content results in a gradual decrease in SO_2 capture. The difference in the trends can be explained using the relationship between calcium utilization and SO_2 capture. It was established that the silica fume/$Ca(OH)_2$ sorbent has better SO_2 removal capabilities as compared to the fly ash/$Ca(OH)_2$ sorbent. The silica that is used in the sorbent preparation is an industrial waste product hence using the silica eliminates the need for disposal.

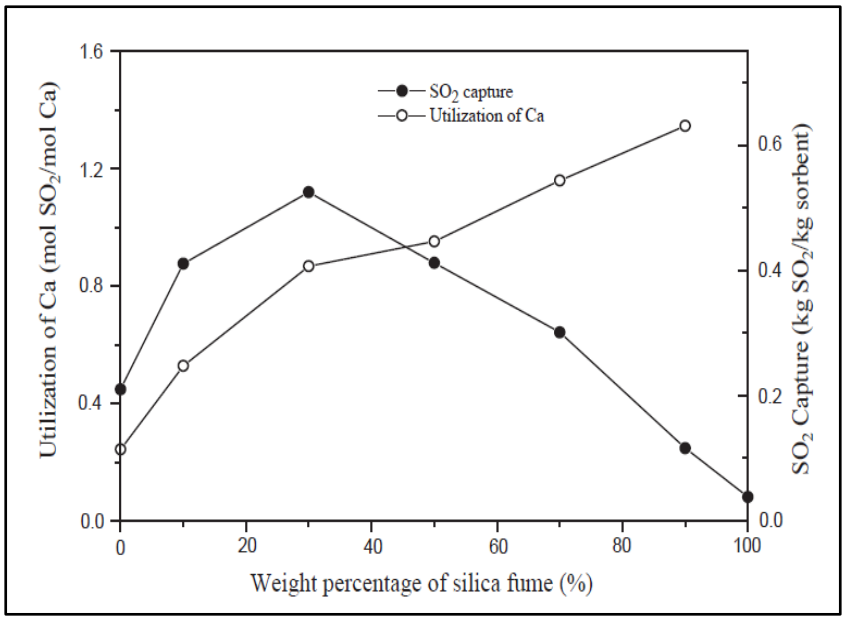

Figure 2-21: Effect of Silica Content on Calcium Utilization and SO_2 Capture (Ren-Bin et al, 2003)

Masias-Perez et al, 2006 studied the use of activated carbon as an additive to CaO sorbents. It was found that the activated carbon behaves as a dispersing agent and increases the CaO surface area available for reaction to occur thus improving the sulphur capture efficiency.

Work performed by Dahlan et al, 2007 investigated and compared the sorption capacities of three sorbents that were prepared from fly ash, rice husk ash, oil palm ash mixed with CaO. The removal of SO_2 was investigated using a stainless steel fixed bed reactor at 100℃. It was found that the rice husk ash sorbent had the highest SO_2 capture ability as it has the highest BET surface area based on break through curve analysis. This is also due to the higher silica composition of rice husk ash (RHA). These form various calcium silicate compounds which are pozzolanic products and are amorphous with higher surface areas.

In the work undertaken by Adanez et al, 2000 various sorbents were prepared by lime hydration with NaCl, KCl, lignosulphanate and water-ethanol solutions. These sorbents had high SO_2 removal abilities. It was found that the NaCl and the KCl contributed mostly to diffusion in the product layer. The best sorbent was the one prepared with the lignosulphanate and water ethanol solutions. The calcium hydroxide formed using the lignosulpanhate decreased the particle size by 5 times. The water ethanol solutions decreased the particle size and increased the porosity significantly. These effects contribute to the formation of favorable physical conditions for sorbents hence result in the maximum desulphurization abilities.

NO_x and SO_2 require separate capture equipment which proves to be very costly, so recently much work has been done to find ways for the simultaneous capture of SO_2 and NO_x (Han et al, 2011). In the work carried out by Han et al, the simultaneous absorption of SO_2 and NO_x were investigated using $KMnO_4$ and $NaClO_2$ additives and it was found that the use of these additives improve desulphurization and denitration significantly.

Studies conducted by Dahlan et al, 2007 investigated the simultaneous absorption of SO_2 and NO_x from flue gas. Flue gas comprises of a large fraction of SO_2 and NO_x and these pollutants together can have devastating effects. The siliceous material used was rice husk ash as this is an agricultural waste and is available abundantly. The RHA/CaO sorbent did not remove the NO gases simultaneously hence a wide range of metal/metal oxides and carbon activated supported metal oxides were implemented for the NO_x removal. The work at hand investigated the SO_2 and NO_x removal using RHA/CaO sorbents employing various metal oxides. The best metal oxide was found to be CeO_2 as it acts as a catalyst in the removal of SO_2 and NO_x forming sulphates and nitrates and seems to be promising for future commercial use.

Work carried out by Somoano et al, 2006 investigated the use of limestone, fly ash, kalotine (natural and industrial waste) and commercial sorbents (metal oxide mixtures and alumina) to remove trace elements including sulphur, nitrogen, particulate matter, alkali metals and halogens. The characteristics of the sorbents were analyzed and the efficiency and sorption capacity test were performed. It was found that the behaviour of the sorbent depends on the composition, type of element to be removed and the temperature.

2.6.5. Desulphurization Process Variables

Process variables are essential as these variables also affect the desulphurization efficiency. These process variables together with the chemical and physical properties influence the SO_2 removal efficiency of the sorbents. It is essential that these conditions are optimized so as to provide the best chemical and physical properties for maximum SO_2 removal and maximum sorbent utilization (Ogenga et al, 2010). For the use of limestone, dolomite and hydrated lime as the sorbent material, such variables include the following:

- **Temperature**

Work performed by Siagi et al, 2006 was performed in a low temperature isothermal fixed bed reactor using limestone and dolomite sorbents on silica support. The results showed that the temperature does not affect the SO_2 capture significantly. This is because increased temperature results in a higher reaction rate constant and decreases the water droplets available and the adsorption of the reaction gas simultaneously.

Studies show that there exists an optimal temperature range at which sulphation is maximum and this depends on the sorbent being used. Pisupati et al, 1996, tested the optimum temperature range for 3 different sorbents and found that optimum temperature was between 1650 and 1700°F. Haji-Sulaiman et al, 1990 found the optimal operating temperature that ensured maximum sulphur dioxide capture was between 800-900°C. This was supported by the work done by Adanez et al, 1994. Fan et al, 1991 concluded that the optimum temperature for calcium based sorbents for sulphur dioxide capture is 850°C.

It was also found that the physical characteristics of the sorbent used such as the particle size may also affect the sulphation process variables such as temperature. Haji-Sulaiman et al, 1990 reported that smaller size particles have a higher optimum temperature for sulphur capture than the larger particles.

For systems operating above the optimal conditions, Haji-Sulaiman et al, 1990 found that the rate of sulphation increased resulting in a product layer of $CaSO_4$ on the sorbent particles. High temperatures

cause the sintering of the CaO particles. When these sintering temperatures are reached it causes the lime to become dead-burned or hard-burned. This causes the limestone to shrink severely resulting in a decreased surface area which in turn reduces the sulphur removal efficiency through minimized chemical reaction (Elert et al, 2002, and Cheng et al, 2003).
Reduction in the surface area that is available for reaction to occur rapidly increases the amount of sorbent that is required. This work was also supported by Pisupati et al, 1996

Özyuğuran et al, 2010 investigated the sulphur capacities at two different temperatures using 6 different limestone and hydrated lime slurries in wet FGD systems.

Table 2-5 Sulphation Properties and Capacities (Adapted from Özyuğuran et al, 2010)

Sample Code	Sorbent Content of Slurry (weight %)	Sulphation Temperature			
		323 K		**298 K**	
		Sulphation Time (h)	**Total Sulphation Capacity** $\left(\frac{\text{mg } SO_3}{\text{ml slurry}}\right)$	**Sulphation Time (h)**	**Total Sulphation Capacity** $\left(\frac{\text{mg } SO_3}{\text{ml slurry}}\right)$
L1	1	4	17.3	4	21.1
	3	6	33.1	6	48.3
L2	1	4	17.3	-	-
	3	6	31.4	-	-
L3	1	4	14.0	4	17.4
	3	6	29.6	6	39.5
L4	1	4	17.3	4	20.9
	3	6	32.8	6	50.9
L5	1	4	17.0	-	-
	3	6	32.6	-	-
L6	1	4	15.1	4	17.3
	3	6	31.0	6	41.0
HL1	1	4	20.6	4	24.4
	3	6	38.3	6	53.5
HL2	1	4	21.3	-	-
	3	6	37.8	-	-
HL3	1	4	17.4	4	18.7
	3	6	32.9	6	48.4
HL4	1	4	21.3	4	25.6
	3	6	40.3	6	55.7
HL5	1	4	22.5	-	-
	3	6	40.4	-	-
HL6	1	4	18.9	4	22.3
	3	6	35.1	6	52.7

The results obtained indicate that the sulphation capacity is better at lower temperatures. In the wet FGD systems, the solubilities of the sorbents which are influenced by temperature affect the desulphurization capabilities of the sorbent. An increase in temperature results in the decrease of the SO_2 solubility. The sorbents used are almost insoluble and the solubility decreases with an increase in temperature. Similar results were obtained by Han et al, 2011 who researched the influence of temperature on the SO_2 capture using sorbents with $KMnO_4$ and $NaClO_2$ additives. The initial ionic reaction that occurs due to the water is very rapid. However temperature increase decreases the life span of the water droplets hence reducing the ionic dissolution. It was concluded that lower temperatures result in high SO_2 capture rates.

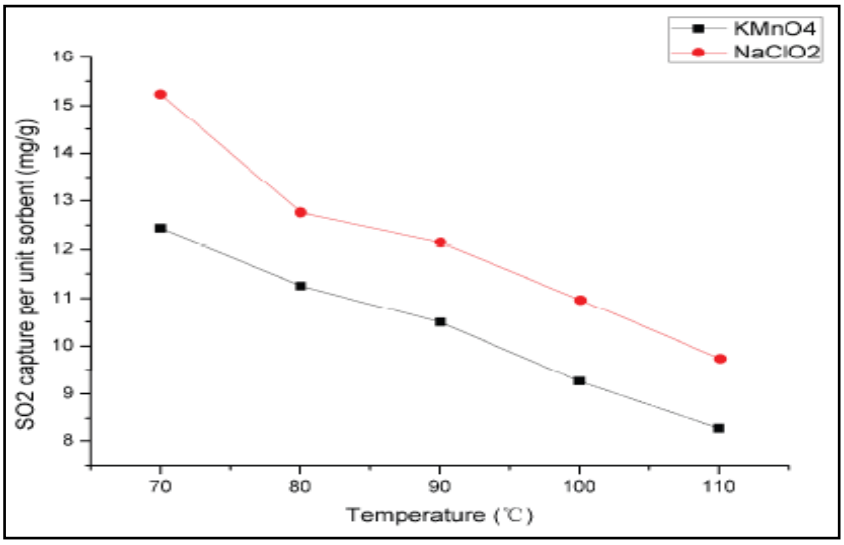

Figure 2-22: Effect of temperature on SO_2 capture

(Han et al, 2011)

Ibrahim and Eliass, 2010 investigated the effect of temperature by using fine activated carbon slurry in a fixed bed reactor. The sulphur removal efficiency tends to increase as the bed temperature increases.

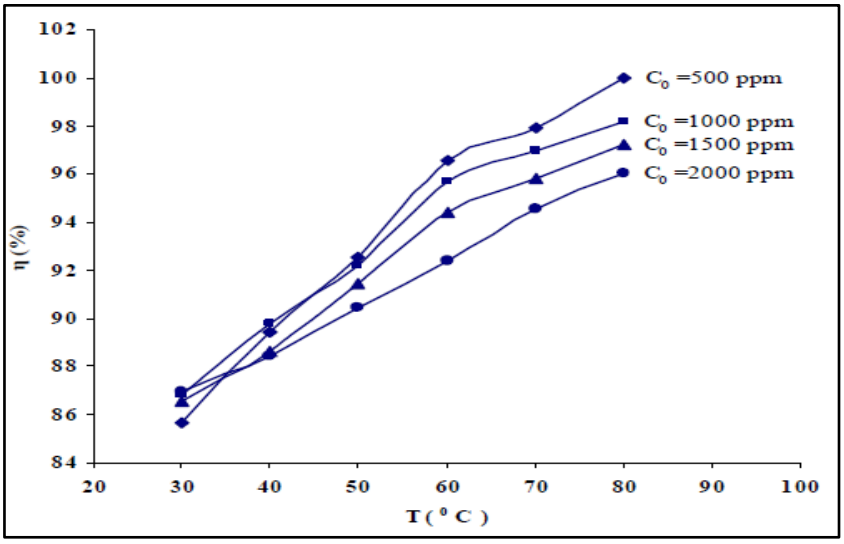

Figure Figure 2-23: Effect of temperature on SO_2 Removal Efficiency

(Ibrahim and Eliass, 2010)

- **Initial SO_2 Concentration**

Ibrahim and Eliass, 2010 found that higher initial concentration of the SO_2 gas decreases the removal efficiency. This is because the quantity of the sorbent remains the same while the SO_2 concentration increases. This result is depicted in figure 2-23 above.

Siagi et al, 2006 investigated the effect of the initial SO_2 concentration on the SO_2 capture using a fixed bed reactor operating as a batch-wise process. It was found that the time taken to reach maximum conversion decreases as the initial SO_2 concentration increases.

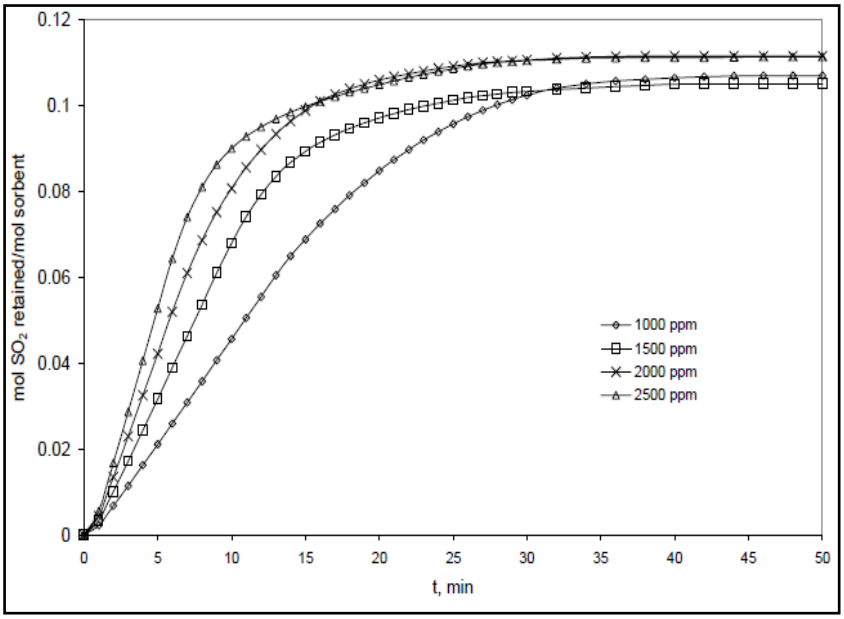

Figure 2-24: Effect of initial SO_2 Concentration on Sulphur Capture
(Siagi et al, 2006)

- **Ca/S ratio**

The calcium to sulphur ratio used in a desulphurization process depends on the sulphur removal efficiency required and the reactivity of the sorbent (Govender, 2006). It was found by Svoboda et al, 1988 that for large Ca/S ratios, the amount of sorbent that is required increases and the sulphur removal capacity is improved. However as the SO_2 removal efficiency increases, the sorbent utilization decreases (Govender, 2006). This study was conducted using four different sorbents and it was found that the sulphur removal capacity for the calcined limestone was better than the limestone.

Özyuğuran et al, 2010 performed work to investigate the sulphation properties of limestone and lime slurries using 6 different sorbents. It was found that an increase in the calcium content hence a larger ratio is essential for improved SO_2 removal. The conclusions established by Macias-Perez et al, 2006 and Lee et al, 2010 are also in support of the above results. It was found that the SO_2 retention depends on the amount of sorbent present hence the Ca/S ratio.

By increasing the amount of sorbent that is present, the reactive surface area available also increases resulting in improved sulphur retention. Fan et al, 1991 established that when coal with high sulphur content is used for electricity generation, the optimum Ca/S ratio is between 2-2.5 and this results in a 90% sulphur removal efficiency. There are also negative impacts for increasing the Ca/S ratio such as increased operating costs and increase of other pollutant emissions.

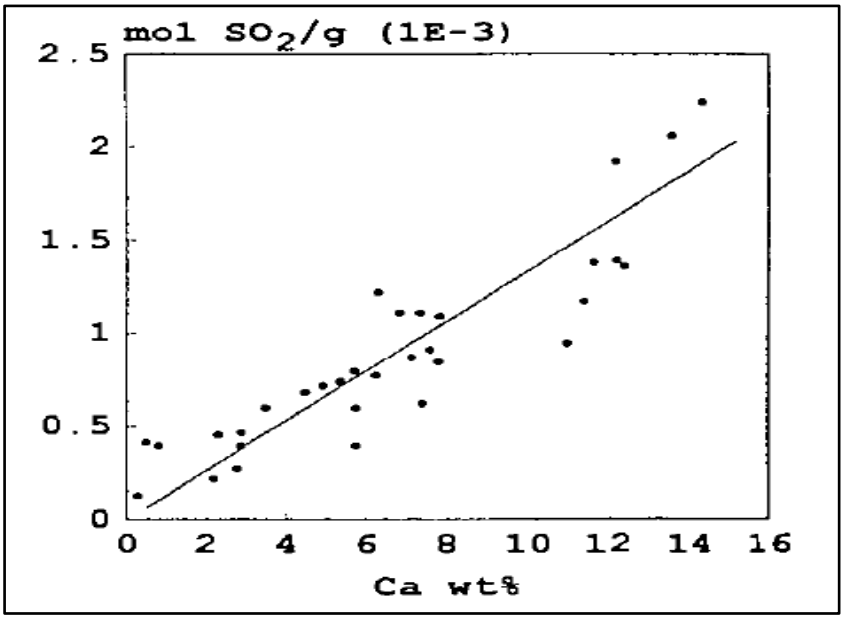

Figure2-25: Effect of Sorbent Content on Sulphur Retention Capacity
(Macias Perez et al, 2006)

- **Sorbent Particle Residence Time**

Lyngfelt and Leckner, 1999 concluded that the residence time of the sorbent in the reactor depends on the design and efficiency of the combustion chamber and the process. Haji-Sulaiman et al, 1990 reported that if the particles had a longer residence time, the desulphurization capabilities were much higher.

Falkenberry and Slack, 1971 supported the idea that short residence time reduced the desulphurization capacities. For maximum calcium utilization to occur the residence time of the sorbent particles need to be long enough to allow for the sulphur dioxide to be diffused into the internal sorbent structure.

However it was found that too long retention time results in a reaction product layer that develops on the surface of the sorbent which may cause the reaction to seize altogether (Lyngfelt and Leckner, 1999).

It was found that the combined effects of the particle size distribution and reactivity of the sorbent both affect the residence time of the sorbent. Particle size tends to decrease after exposure to

calcination conditions as this highly thermal process causes decomposition of the particles. Sulphation reduces the rate at which particle size tends to decrease due to the bed and wall resistances (Lyngfelt and Leckner, 1999).

Small particles are more reactive and have a smaller residence time in the combustion chamber. Large particles are prone to various resistances and are more likely to spend a large residence time in the combustion chamber resulting in larger sulphur capture (Lyngfelt and Leckner, 1999). Cheng et al, 2003 established also that particles with prolonged residence time, are subject to sintering when temperatures exceed 1000°C.

- **Hydration/Slurry Time**

The study undertaken by Lee et al, 2007 investigated the effect of slurry period on sulphation abilities. It was found that a longer hydration period provides adequate time required for the reactions to occur resulting in the formation of the highly porous material that is required to improve sulphation efficiencies.

The work performed by Ho and Shih 1992, investigated the effect of slurry time on the SO_2 removal capabilities.

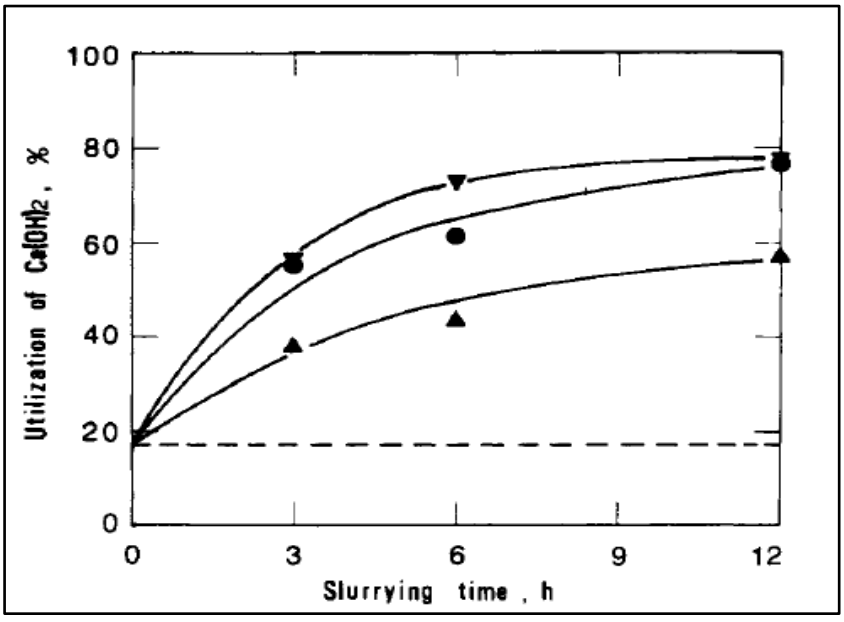

Figure 2-26: Effect of Slurrying Time on the Sorbent Utilization
(Ho and Shih, 1992)

This study was conducted for 3 time interval namely 3, 6 and 12 hour slurry time. The sulphation conditions for the results obtained were 60˚C, 50% relative humidity for a period of 1 hour, 1000 ppm SO_2. The slurring conditions were water/sorbent ratio 10:1 and fly ash/hydrated lime 16:1. Results for the study show that optimum sorbent utilization occurs for slurry time of 6 hours.

In general it can be seen that a longer slurry time results in greater reactivity and removal of SO_2. After a certain period of time, the slurry time tends to have little effect on the sorbent utilization and the SO_2 removal efficiency. Initially, the silica present in the fly ash and the hydrated lime dissolve to form the reactive specie that captures the SO_2 and after a certain time period, the rate of dissolution decreases resulting in the hydration time having little or no effect.

The work performed by Ogenga et al, 2009 also supports this idea by concluding that an increase in the hydration period together with the sorbent to additive ratio creates an increase in the available surface area for reactions to occur resulting in improved sulphur capture.

- **Hydration/Slurry Temperature**

Work performed by Ho and Shih, 1992 indicate that as the slurrying temperature increases, so does the sorbent utilization. The solubility of the hydrated lime decreases if the temperature is increased. However the reaction rate of the newly formed specie due to the dissolution of the silica and hydrated lime increases as the slurrying temperature increases. This observation becomes less profound at higher temperatures. Ogenga et al, 2008 concluded that higher slurry temperatures and longer mixing periods favour the sorbent conversion.

Work performed by Ogenga et al, 2009 uses a fixed bed reactor at constant temperature and relative humidity to test sorbent efficiency for capture. It was established that a longer hydration period and an increase in the temperature also increased the SO_2 absorption capability.

- **Sorbent / Water ratio**

The Work performed by Özyuğuran et al, 2010 investigated sulphation properties of lime slurries. It was found that as the amount of sorbent in the slurries increased, the SO_2 removal efficiency was greatly increased as more surface area is created for reactions to occur.

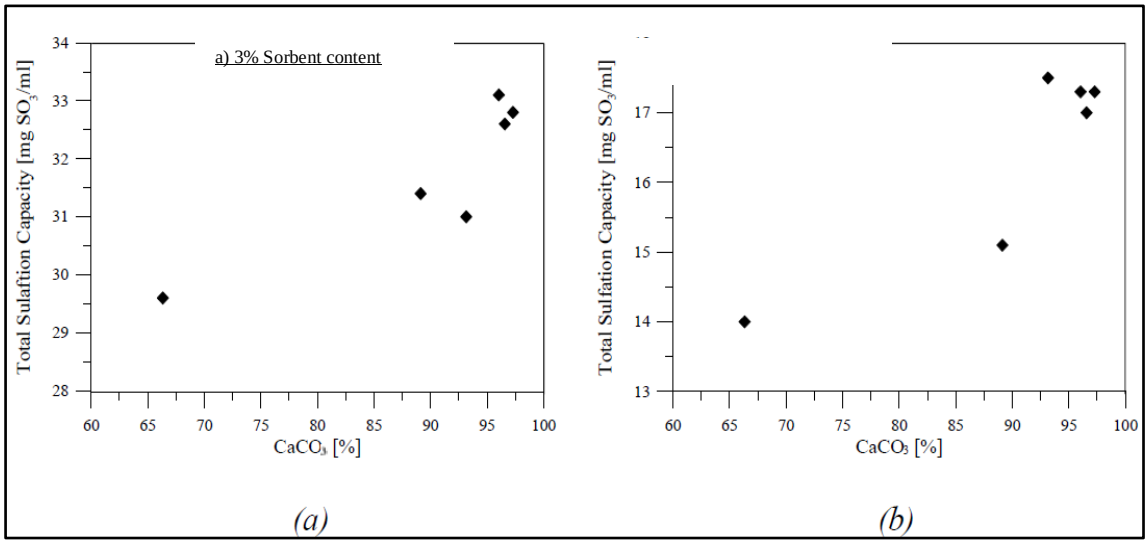

Figure 2-27: The Relationship between the $CaCO_3$ Content of Limestone and the Sulphation Capacity of Slurry (Özyuğuran et al, 2010)

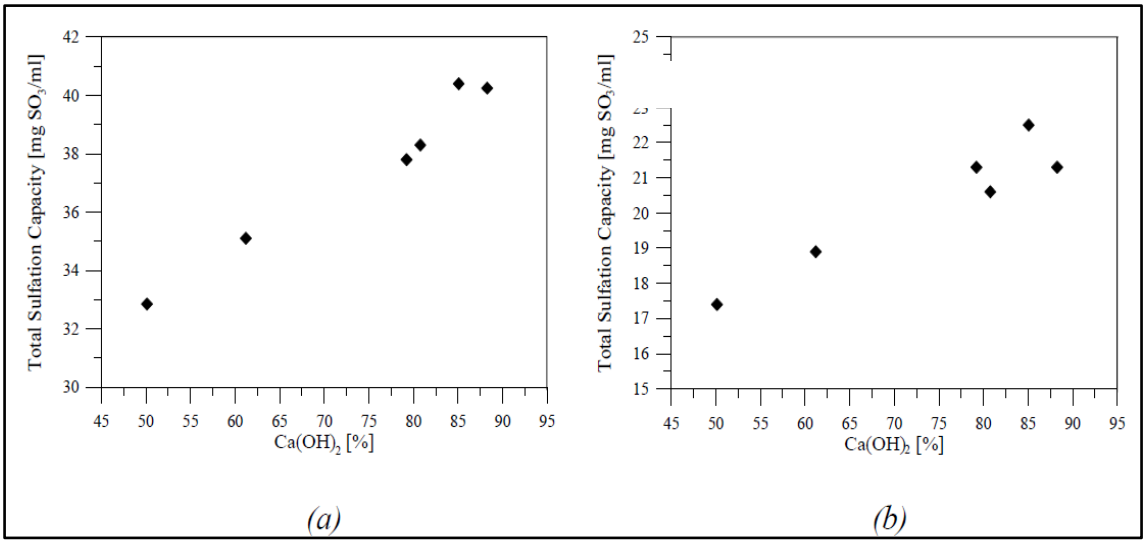

Figure 2-28 The Relationship between the $Ca(OH)_2$ Content of Hydrated lime and the Sulphation Capacity of Slurry (Özyuğuran et al, 2010)

The studies conducted by Özyuğuran et al, 2010 indicate that the sulphation capacity increases as the sorbent content of the slurry increases. The higher sorbent content implies that the Ca/S ratio at the inlet condition is increased. The increased Ca^{+2} ions result in better dissolution of the SO_2 and improved sulphur removal efficiency.

Han et al, 2011 conducted studies using sorbent additives to remove both SO_2 and NO_x concurrently. The influence of water content on the SO_2 removal was also investigated. The results obtained are in agreement with previous studies mentioned above. SO_2 capture increases linearly as the water content increases and reached 25%. An ionic reaction occurs in the liquid phase that improves the desulphurization efficiency due to reduced diffusion resistance.

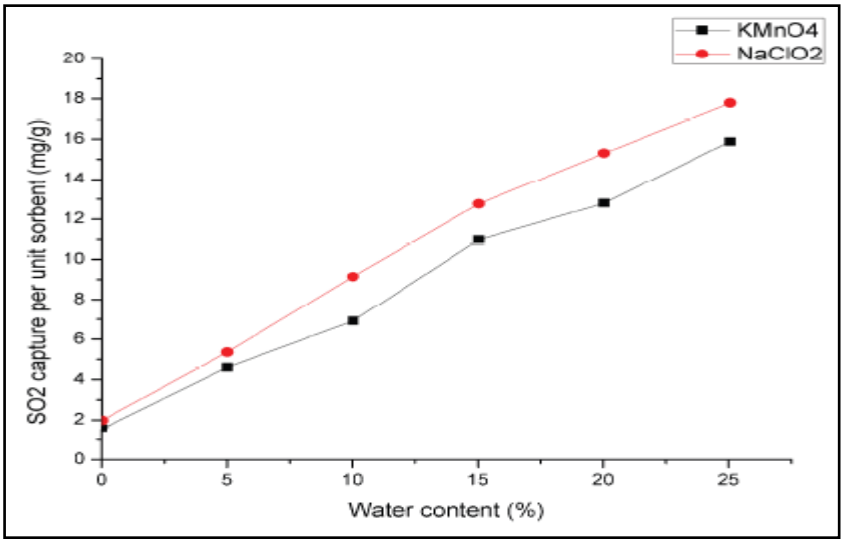

Figure 2-29: Effect of Water Content on SO_2 Capture (Han et al, 2011)

Ho and Shih, 1992 investigated the effect of adding siliceous material to hydrated lime in a spray drying system. The slurry conditions for preparing such a sorbent were also investigated. Water to solid ratios of 10:1 to 40:1 were used to determine the effect on the sulphur removal efficiency and the sorbent utilization.

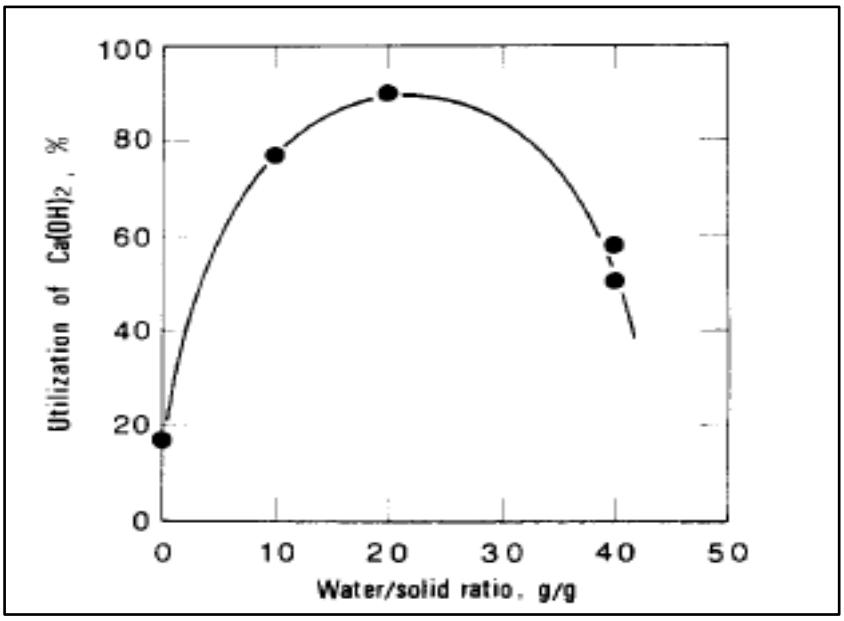

Figure 2-30: Effect of Water/solid ratio on Sorbent Utilization
(Ho and Shih, 1992)

The slurrying conditions for this study were fly ash/$Ca(OH)_2$ 16:1, temperature 65 ℃ and slurry time 12 hours. The sulphation conditions were 60℃, 50% relative humidity and sulphation period of 1 hour. The trend shows that as the ratio increases, initially there is an increase in sorbent utilization. The ratio reaches an optimum value after which the sorbent utilization decreases with increasing water to solid ratio. At low water to solid ratios, the total amount of solid dissolved is high therefore the solution is more alkaline and the dissolution rate of the calcium silicate hydrate that is formed is high. This results in an increase in sorbent utilization and improved SO_2 removal efficiency. When the water to solid ratio is high, the pH of the slurry is low resulting in decreased dissolution and reaction rates which accounts for the decrease in sorbent utilization and decline in SO_2 removal efficiency.

Work undertaken by Fernandez et al, 2006 determined the efficiency of SO_2 removal using the sorbents hydrated with sea water in different ratios and different slurry times. Sea water can be used as the hydrating medium as it proves to be inexpensive and abundantly available. However, it can only be easily supplied to coastal power stations. It was found that desulphurization using sea water was more efficient than using distillate water as the sorbents have higher specific surface area for reaction to occur.

- **Relative Humidity**

Ho and Shih, 1992 investigated the effect of relative humidity on sorbent conversion. It was found that an increase in humidity from 30 to 50% resulted in an increase in sorbent utilization. Any increase in relative humidity thereafter has little effect on the sorbent utilization.

Work undertaken by Garea et al, 2003 investigated the effects of relative humidity on sorbent utilization and sulphur capture. This strong relationship is due to the formation of a film of water on the outer surface of the sorbent. An increase in the relative humidity changes the appearance of the accumulation of reaction product by forming clusters that occupy less surface area resulting in easier access to the unreacted core hence improving sorbent utilization.

Table 2-6: Comparison of Desulphurization at Different Relative Humidity Levels (Garea et al, 2003)

RH (%)	From TG Analysis	From Gas Phase
20	0.309	0.275
40	0.607	0.565
45	0.731	0.667

A comparable result was obtained by Siagi et al, 2003. The investigation was carried out using a gas mixture containing 2000 ppm SO_2 at a temperature of 80℃. The Relative humidity was varied between 0 and 40 %.

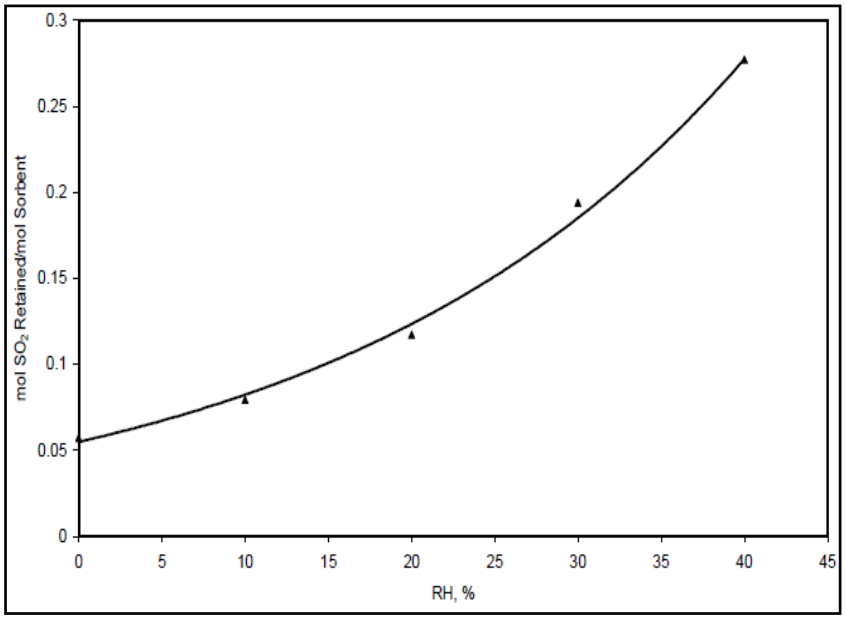

Figure 2-31: Effect of Relative Humidity on SO_2 Retention
(Siagi et al, 2003)

2.7. Techniques for Improving Sorbent Utilization

Studies conducted by Garea et al, 2003 evaluated the use of sorbent recycling to improve the sorbent utilization. The partially reacted sorbent was reused and the calcium utilization was compared to that of using fresh hydrated lime. The investigation was undertaken utilizing a fixed bed reactor, 230-1000 ppm SO_2 concentration and relative humidity between 20-45%. The results indicate that the reused sorbent has the best utilization between the 40-45% relative humidity range. The sorbent utilization in this range was $0.61\frac{\text{mol S}}{\text{mol Ca}}$ and $0.73\ \frac{\text{mol S}}{\text{mol Ca}}$ respectively. The study also concludes that the use of sorbent recycling is an effective means of sulphur capture and has improved sorbent utilization as compared to using fresh sorbent.

Davini, 2002 studied the properties and the effects of calcium based sorbents that have been regenerated. The sorbents that were used were partly regenerated using steam treatment. Regeneration allows for the total utilization of the sorbent to be increased. In addition the process of regeneration is simple and easy to implement.

2.8. Models used for Desulphurization Representation

Over the years, various gas-solid reaction models were proposed to adequately depict the desulphurization process. The aim of developing such models is to create a better understanding of the sulphation process. As a sulphate product layer develops on the outer surface of the sorbent, a change in the physical structure of the sorbent occurs and this changes the rate determining step hence creating the need for kinetic models (Lyngfelt and Leckner, 1999). Such models include the shrinking core model, the grain size model, single pore model and the random pore model. The implementation of these models is difficult due to the complexity of the calculation procedure. This gave rise to investigate simpler linear models such as the deactivation model (Dahlan et al, 2007).

Sulphur Dioxide retention in high pressure systems at temperatures between 850 and 950 ℃ can be modelled using the unreacted shrinking core model. Work performed by Zevenhoven et al, 1998 investigated the effect of particle structure on SO_2 capture by calculating the Thiele parameter and determining diffusivity and the reaction rate constant.

During desulphurization different stages can be rate determining:

1. Outer mass transfer, from the outer gas phase to the sorbent particle
2. Diffusion of gas to the sorbent
3. Pore diffusion –inside the sorbent
4. Chemical reaction

The study showed that for large particles, the layer of calcium sulphate that forms on the outer surface of the particle can retard desulphurization by pore plugging and can decrease the available surface area for reactions to occur. This layer also separates the solid and gas phase hence the rate determining step is the diffusion dependent. This model is efficient as an analysis of the sorbent after reaction shows that the inner core remains unreacted due to the product layer formation.

Studies conducted by Foo et al, 2011 involved determining a suitable model for desulphurization. The experimental work was that was conducted produced the kinetic parameters that were implemented in the kinetic model. The reaction was carried out at low temperatures using fly ash/ Ca- based sorbent. Various rate and volumetric expressions were used to formulate the most suitable model. A suitable computer program was used to evaluate the various parameters in the model. Reaction and diffusion were found to be the rate limiting steps at different times of the reaction span. By comparing the result of the experimental and eight model predictions and evaluating the root mean square error, it was established that a modified shrinking core model best describes the process with reaction step being rate controlling and an exponential expression for rate expression.

In the study conducted by Han et al, 2011 a grain reaction model was used to establish the kinetics of calcium based sorbents as it takes into account the effect of sintering. Similar investigations were conducted by Alvfors and Svedberg, 1986 and Haji-Sulaiman et al, 1991 who implemented the principle based on the grain theory to develop a mathematical model to describe sulphation. This model represents a gas-solid reaction that is non-catalytic. The rate determining steps are both pore and product layer diffusion. Initially, the chemical reaction stage is rate controlling and this occurs on the extended surface caused by the presence of grains in the solid sorbent. The product layer that forms on the grain surface then controls the rate of the reaction. As pore plugging is initiated, the reaction becomes pore diffusion controlled. The characteristics of the sorbents and their effect on the sulphation reaction were also determined. The particle microstructure and the pore structural properties of the sorbents were investigated.

Work undertaken by Dam-Johansen et al, 1991 implemented a modified grain model called the grain-micrograin model to describe desulphurization. This model was developed to account for the physical structure of the solids, implement the chemical composition of the sorbents and to minimize unknown parameters. In this model, the sorbent particle consists of grains and these grains are non-porous in the pre calcination state. The grains are further comprised of micrograins that are non-porous. Macropores and micropores are formed between the interstices of the grains and micrograins respectively. It was established that the mass transfer in the macro and micro pores takes place via molecular and knudsen diffusion. The reaction between SO_2 and the micrograins can be represented by the unreacted shrinking core mechanism and the reaction in the grains by the partially reacted core assumptions. In

order to prove the validity of the recommended model, the model predictions were compared to a large amount of experimental data and these were relatively similar hence reinforcing the validity.

Studies conducted by Adanez et al, 2000 investigated the desulphurization using sorbents with plate like and cylindrical pore geometries. The study implemented the furnace sorbent injection conditions and temperatures greater 950℃. The pore model was used to establish the kinetic parameters of limestone and natural calcium sorbents with the different geometries. This model accounts for sintering, calcination and sulphation simultaneously and is effective as the overall sorbent utilization depends on these three processes. It was found that the sorbents with the plate like geometries was more advantageous as compared to the cylindrical geometries due higher sorbent reactivity. The product layer that forms on the sorbent has a reduced thickness hence reducing the probability of pore plugging and this allows for improved $CaSO_4$ accommodation.

Garea et al, 2005 investigated the modelling of in duct desulphurization. This was carried out using an entrained flow reactor at low temperatures. $CaOH_2$ was used as the sorbent. Two models were used to represent the system, the shrinking core/grain model, and the non-ideal absorption kinetics in the mass balance. The variables input into the models were the sulphur to calcium molar ratio, the SO_2 inlet concentration, temperature, relative humidity, residence time and the presence of CO_2 in the inlet gas stream. It was found that the latter model gives a better prediction of the SO_2 concentration in the reactor.

Barletta et al, 2002 developed a dynamic model to describe the reaction between SO_2 and limestone under oxidizing and reducing conditions. This was carried out under atmospheric fluidized bed test conditions. This model can be used to make predictions for the initial sulphation period. The model has various assumptions which can be found in the work undertaken by Barletta et al, 2002 and these assumptions result in ordinary differential equations which can be solved rigorously by implementing the Runge-Kutta method and a suitable computer program. This model can be used to create sorbent and SO_2 concentration profiles within the particle.

Recent studies carried out by Dahlan et al, 2007 investigated the use of the simple deactivation model to illustrate desulphurization. This model is used for dry fixed bed desulphurization using rice husk ash, oil palm ash and coal ash as the silica based material mixed with CaO to prepare the sorbent. This is a first order model having a surface reaction rate constant and a deactivation rate constant. The model has many assumptions (Dahlan et al, 2007):

- A constant temperature is maintained in the system.
- External mass transfer is negligible.

- System is batch wise with constant plug flow.
- A pseudo steady state process is maintained.
- The deactivation of the sorbent is first order.

These assumptions result in the following equation to describe the deactivation model which can be plotted as a straight line (Dahlan et al, 2007):

$$\ln\left(\ln\left(\frac{C_0}{C}\right)\right) = \ln(k_s\tau) - k_d t \qquad (2.13)$$

C_o - initial SO_2 concentration

C- Outlet SO_2concentration

k_s – Surface reaction rate constant

k_d – deactivation rate constant

τ – Surface time term

The model predictions were then plotted together with the experimental data. It can be seen that the model predictions exhibit a good representation of the desulphurization process. The sorbents in order of best sorption capacity are rice husk ash, oil palm ash and coal fly ash. The values of k_s and k_d that are obtained from the model were also compared to those in literature.

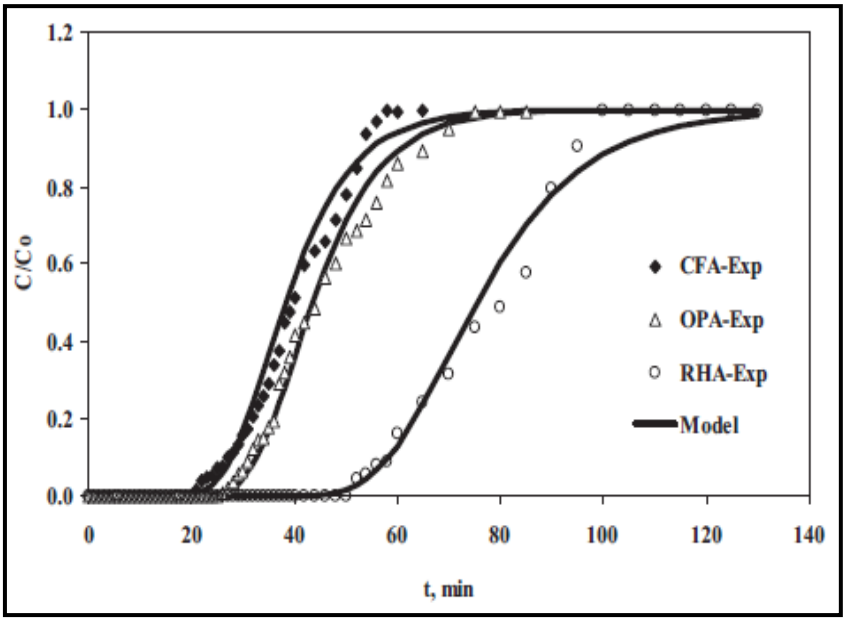

Figure 2-32: Model Predictions and Experimental results for Desulphurization using Deactivation Model (Dahlan et al, 2007)

2.9. Theory behind the Shrinking Core Model

The reaction between the sulphur dioxide and the sorbent is a heterogeneous reaction in which the gas contacts the solid, reacts with it and results in the formation of a product. The solid particles may shrink or remain unchanged in size depending on the amount of impurities present and the product that is formed. The various models come with a set of mathematical equations and a rate expression. If a model is a good representation of reality, then the rate expression will result in a good prediction of the reaction kinetics. The most suitable model is one that presents a good image of reality with minimal mathematical complexities (Levenspiel, 1972).

The shrinking core model stipulates that initially the reaction occurs at the outer surface of the sorbent particle and then progresses towards the core of the solid forming a sharp boundary. As the reaction progresses to completion, the outer surface is completely reacted while the inner core remains an inert solid that diminishes with reaction time (Levenspiel, 1972).

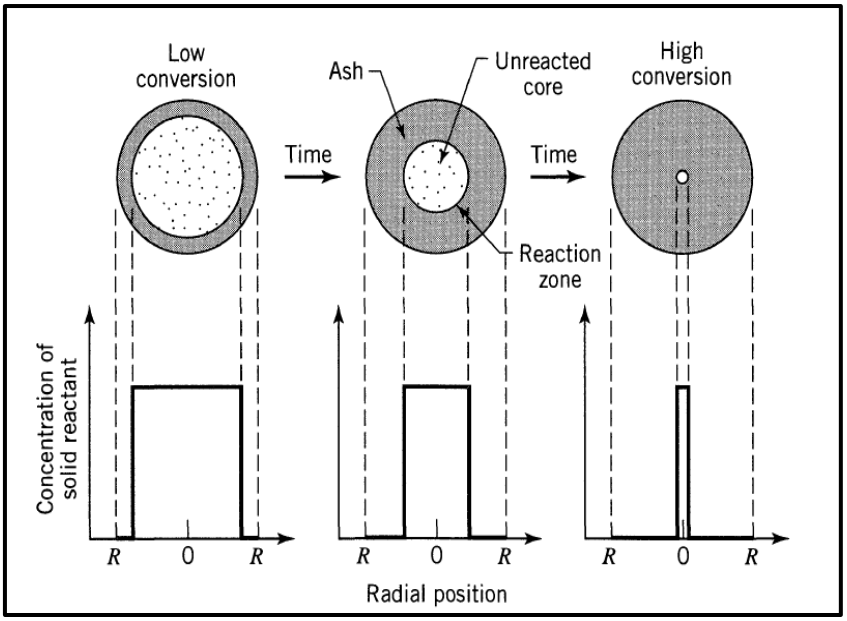

Figure 2-33: Graphical Representation of the Shrinking Core Model
(Adaped from Levenspiel, 1972)

The shrinking core model represents reality more closely than other models and it is used in a variety of situations such as burning coal, wood etc. This model was selected to represent the desulphurization process. The earliest development of the shrinking core model outlines five steps during the reaction (Levenspiel, 1972):

1. Diffusion of gas through the gas film to the surface of the sorbent particle.
2. Diffusion of the gas through the ash layer to the inner core.

3. Gas-solid reaction at the surface.
4. Diffusion of gas to the surface via the ash layer.
5. Diffusion of gas from the ash layer surface through the gas film back to the exterior surface of the particle.

Essentially there are only three reaction/diffusion processes that can be used to determine the reaction rate, steps 1, 2 and 3 mentioned above.

Rate Determining Step: Diffusion through the Gas Film

Gas diffuses through the gas film and immediately diffuses through the formed product layer and reacts. The gas velocity and properties as well as the particle size may affect the resistances in the gas film.

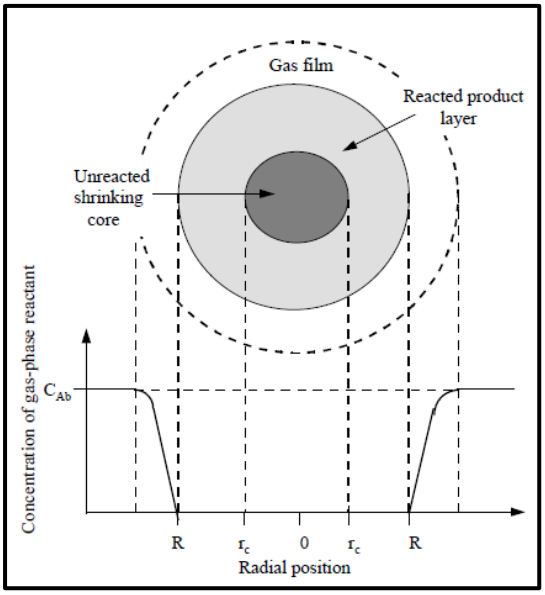

Figure 2-34: Concentration Profile with Diffusion through the Gas Film being Rate Controlling (Hepworth et al 1997)

A generalized gas-solid reaction is represented by the following:

$$A\,(g) + bB(s) = cC(g) + dD(s) \qquad (2.14)$$

The relationship between time and conversion for the rate controlling step being gas film diffusion is as follow (Hepworth et al, 1997):

$$t = \frac{\rho_B R}{3bk_g(C_{AB} - C_{Ae})} X \qquad (2.15)$$

$$X = 1 - \left(\frac{r_c}{R}\right)^3 \qquad (2.16)$$

Where kg mass transfer coefficient

ρ_B Molar density of B in the solid

X fractional conversion of a sphere

b stoichiometric coefficient

C_{AB} bulk concentration

C_{Ae} Equilibrium concentration =0

A straight line trend for a plot of conversion versus time indicates that the diffusion in the gas film is the rate controlling step and the mass transfer coefficient is determined from the slope of this plot.

Rate Determining Step: Diffusion through the Product Layer

The gas immediately diffuses through the gas film, then diffusion through the established product layer occurs followed by immediate reaction.

It is assumed that the concentration gradient of the reactant gas is at steady state in the ash layer.

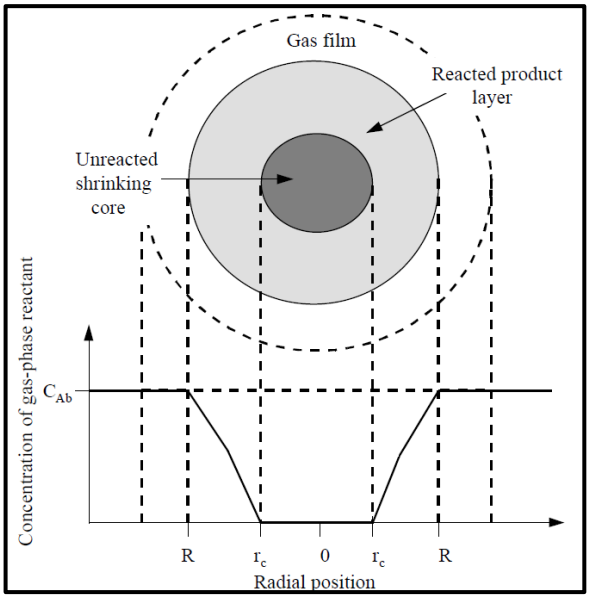

Figure 2-35: Concentration Profile with Diffusion through the Ash layer being Rate Controlling (Hepworth et al 1997)

The relationship between the reaction time and conversion for the rate controlling step being gas film diffusion is as follow (Hepworth et al, 1997):

$$t = \frac{\rho_B R^2}{6bD_e\,(C_{Ab} - C_{Ae})}\left[1 - 3(1-X)^{\frac{2}{3}} + 2(1-X)\right] \qquad (2.17)$$

A straight line trend for a plot of $\left[1-3(1-\mathrm{X})^{\frac{2}{3}}+2(1-\mathrm{X})\right]$ versus time indicates that the diffusion in the ash layer is the rate determining step and the diffusivity can be determined from the slope of this plot. It was also found that this is the dominant resistance in various applications.

Rate Determining Step: Chemical Reaction

If the chemical reaction is the rate determining step, it is implied that gas diffusion through the established product layer and gas film is much faster than the surface reaction.

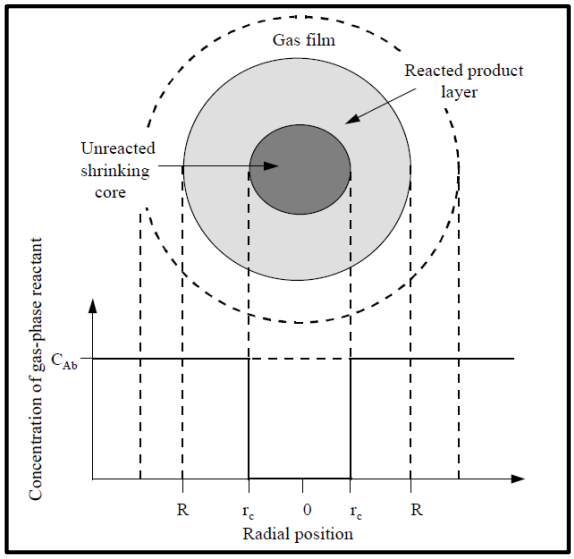

Figure 2-36: Concentration profile with chemical reaction being rate controlling (Hepworth et al 1997)

The relationship between the reaction time and conversion for the rate controlling step being gas film diffusion is as follow (Hepworth et al, 1997):

$$\mathrm{t}=\frac{\rho_{\mathrm{B}}\mathrm{R}}{\mathrm{bk}(\mathrm{C_{Ab}}-\mathrm{C_{Ae}})}\left[1-\ (1-\mathrm{X})^{\frac{1}{3}}\right] \qquad (2.18)$$

A straight line trend for a plot of $\left[1-\ (1-X)^{\frac{1}{3}}\right]$ and time indicates that the chemical reaction is the rate controlling step and the reaction rate constant can be determined from the slope of this plot.

Conversion-time equation for the combined resistances (Neeraj, 2001):

$$\mathrm{t_{total}}=\mathrm{t_{film}}+\mathrm{t_{product\ layer}}+\mathrm{t_{reaction}} \qquad (2.19)$$

$$\mathrm{t}=\frac{\rho_{\mathrm{B}}\mathrm{R}}{3\mathrm{bk_g(C_{A0})}}\mathrm{X}+\frac{\rho_{\mathrm{B}}\mathrm{R}^2}{6\mathrm{bD_e\ (C_{A0})}}\left[1-3(1-\mathrm{X})^{\frac{2}{3}}+2(1-\mathrm{X})\right]+\frac{\rho_{\mathrm{B}}\mathrm{R}}{\mathrm{bk(C_{A0})}}\left[1-\ (1-\mathrm{X})^{\frac{1}{3}}\right] \qquad (2.20)$$

CHAPTER 3: EXPERIMENTAL APPROACH

3.1. Experimental Objective

The main objective of the study conducted was to determine the most suitable sorbent for flue gas desulphurization process that can be implemented at ESKOM. This involved establishing an effective test unit with an effective reactor configuration. In order to complete the task successfully, a proper understanding of the operation of the various equipment within the laboratory experimental set-up was essential. The optimum operating conditions for the experimental set-up for sulphur dioxide removal was also considered as established from the literature review. After much consideration and controversy, an effective reactor design was established. The evaluation and comparison of the sorbent performance also involved investigating the effects of sorbent properties and reaction process variables on the desulphurization efficiency. The effects of other gases such as carbon dioxide present in the feed stream were also analysed.

3.2. Experimental Set- up and Equipment List

The initial phase of the task involved considering various reactor configurations and selecting the most suitable reactor design taking into account the constraints imposed by the established optimum operating conditions.

Figure 3-1 : The Testing unit developed for Desulphurization of flue gas

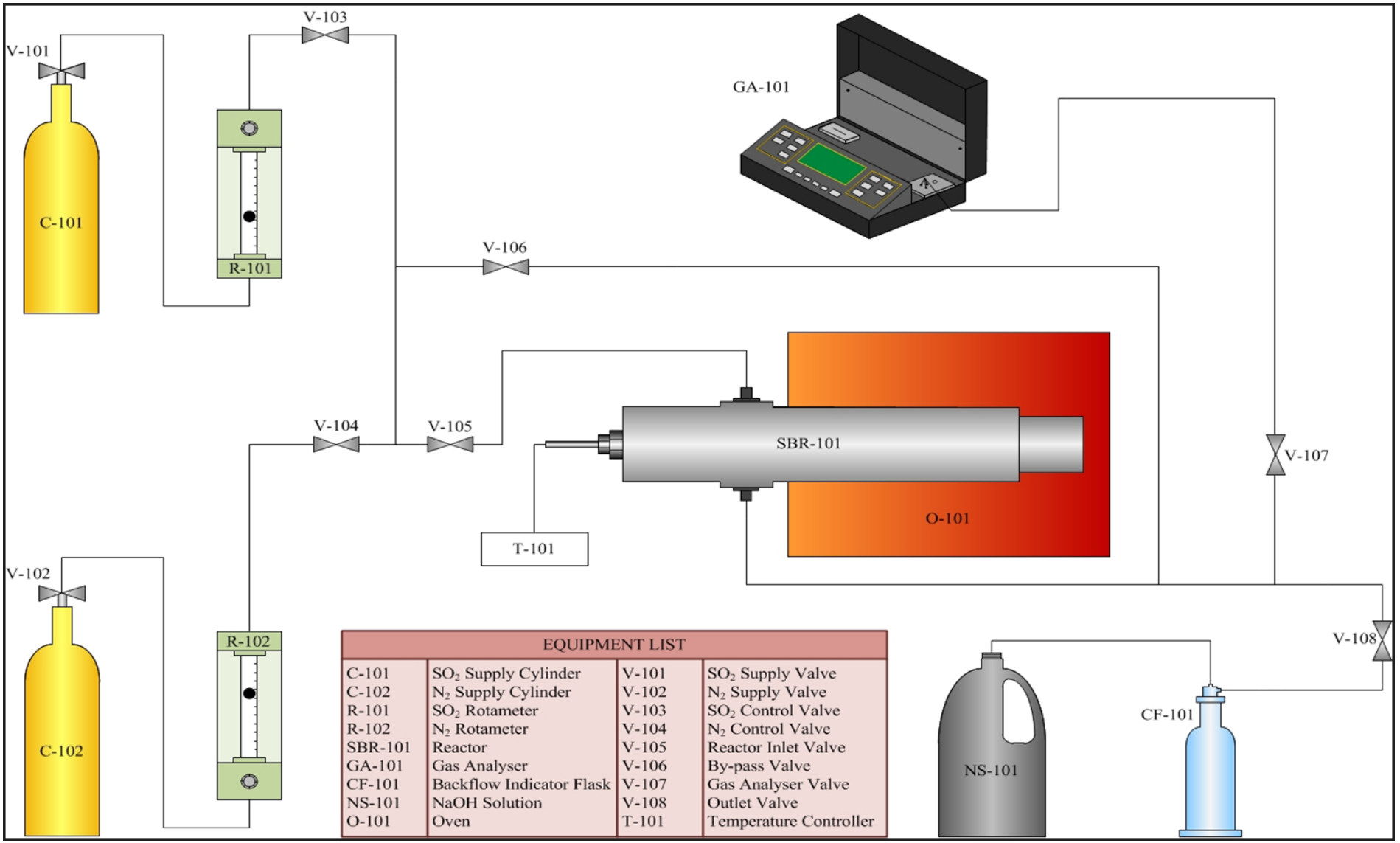

Figure 3-2: Process Flow Diagram (PFD) of the Experimental Set-up

3.3. Unit Description

The experimental test unit comprises of various apparatus each with its own relevance to the contribution of successful sorbent testing. Below is a description of each of these units and the function that the apparatus has in desulphurization investigation.

- **SO_2 and N_2 gas Cylinder (V101 and V102)**

The gas that is required for the experimental testing is supplied by these cylinders. The SO_2 cylinder provides typical concentration of flue gas that is released from the combustion of coal in coal-fired power plants. The typical concentration of the SO_2 provided by the gas cylinder is 2200 parts per million (ppm). Specifications also indicate that there is 20% oxygen concentration with the balance being nitrogen. The oxygen is essential for the oxidation of sulphites to sulphates. A second cylinder with 2000 ppm SO_2, 11% O_2, 10% CO_2 and balance nitrogen was also used to test the effect of the presence of CO_2.

The N_2 cylinder provides 99.99-100% inert N_2 with some impurities, oxygen and moisture content less than 3ppm as well as CO_2, CO and hydrocarbon content of less than 1ppm each. N_2 is essential as it is used in the initial rotameter calibrations and to test the system for any leakage. The nitrogen gas is also important as it is used to purge the system after each investigative run. This ensures that the results obtained from each run can be conclusive as it is unaffected by any impurities or excess gas from previous runs.

Figure 3-3: N_2 and SO_2 gas cylinders

Two pressure gages are situated on each of the gas cylinders mentioned above. These cylinders measure the static pressure of the cylinders which is a measure of the amount of gas actually present within each cylinder. The remaining pressure gages are situated over a valve alongside the fore

mentioned gages. These pressure gages measure the line pressure which controls the gas flow into the system. Controlling the valve opening determines the amount of gas entering the system by reflecting on the pressure gage. The gages measure the pressure in the units of kilo Pascal (kPa)

- **Rotameter (R101 and R102)**

There are two rotameters within the experimental unit. These rotameters are used to control and maintain the flow of the nitrogen and sulphur dioxide gas entering the testing unit. The rotameters each have a control valve that is used to establish the flowrate into the system. The flow can be set initially to the required flowrate by the bobbing ball position. An initial calibration of the rotameters was required prior to any experimental runs. The procedure for the calibration and the calibration chart will be discussed later on.

- **Needle Valves**

These valves are small with a needle shaped plunger and a thread. The turning of the screw can either increase or reduce the flow as it causes the gap between the plunger and the seat of the valve to increase or decrease. The retraction of the plunger makes it possible for precise flowrates to be maintained in the system. Needle valves are best suited for low calibrated flowrates that remain constant over a period of time thus rendering them suitable in this set up. This valve is used to control the flowrate of the SO_2 into the reactor and the flowrate of the purge gas into the system. These valves are commonly used as shut-off valves and are implemented as such during the purging of the system.

- **Ball valves**

These types of valves are versatile and have extensive use and they are durable due to their fabrication material. It comprises of a spherical disc that has a hole in the centre that controls the flow and a handle to close and open the valve. When the handle is parallel to the line, the valve is open. The hole is in line with the valve and flow is permitted. When the valve is closed, the handle is perpendicular to the line. This means that the hole is perpendicular to the line and the flow of gas into the system is restricted. These valves did not offer precise flow control but have excellent applications as shut off valves. These valves are used to control the sulphur dioxide flowrate into the gas analyser and to remove the unreacted sulphur dioxide from the system into a safe disposal solution of NaOH.

- **Oven (O-101)**

The oven was used to heat the reactor and the sorbent to approximately 850˚C, an optimum temperature determined from the literature survey. The oven is fabricated from stainless steel material in order to withstand the high exposure temperatures. The depth, length and breadth of the oven were

505, 570 and 465mm respectively. A hole was cut on the oven frontier such that the reactor could be suspended inside the oven.

Figure 3-4: The oven with the temperature controller and thermocouple

- **Thermocouple**

The Thermocouple is a type of sensor that is used to detect the temperature. The thermocouple comprises of two different metals that coupled together at the ends. Heating the oven causes a voltage to be produced at the junction which can be expressed as temperature by using the relevant sensor conversions. The temperature probe is situated on one end that is placed inside the reactor close to the sorbent to ensure that the reaction occurs at the desired temperature. The other end is connected to the temperature controller that displays the actual oven environment temperature.

- **Temperature Controller (T-101)**

The Process Integrator and Differentiator controller is built into the experimental set-up and is located towards the bottom of the oven. After the oven is switched on, the desired temperature can be set on the controller and this is displayed in red on the controller screen. This temperature is known as the set-point. The temperature displayed in green is the temperature of the reactor that is transmitted using the thermocouple. Deviations from the set-point may occur and the correct controller action is taken to regulate the temperature so that it remains as close to the set-point as possible.

- **Fixed Bed Reactor (SBR-101)**

The fixed bed reactor is a cylindrical pipe that is fabricated from stainless steel to withstand the high oven temperatures and the corrosiveness of the sulphur dioxide. It has a diameter and length of 33mm and 330mm respectively. Attached to the reactor is the thermocouple and the gas inlet and outlet pipes.

Figure 3-5: Fixed Bed Reactor

The front half of the reactor has a diameter that is less than the latter half and is easily detachable due to the threading present. This set-up allows for the placement of the sorbent sample that is packed between two horizontally placed sieves each with a diameter of 22mm. The sieves have a 0.5cm hole to allow for the passage of the gas pipe and a mesh size of 0.5mm allowing for the diffusion of sulphur dioxide through the sorbent.

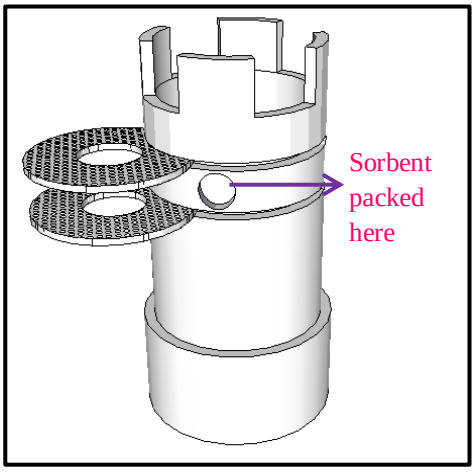

Figure 3-6: Three Dimensional Reactor View

The gas is released towards the closed end of the reactor, diffuses through the bed of sorbent where reaction occurs before it moves out through the gas outlet pipe. A description of the reaction process is shown in the figure below. The location of the sieves and the sorbent within the reactor was determined by investigating the temperature profile within the reactor to establish the location of the hot-spots. In order to allow for easy filling and emptying of the sorbent within the sieve, a hole was drilled on the cylindrical pipe between the sieves.

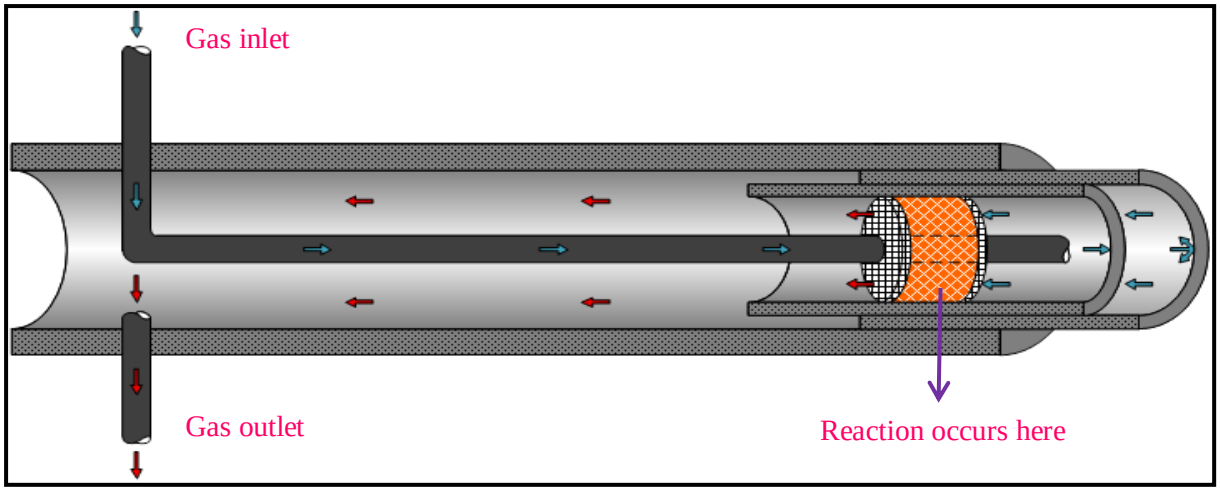

Figure 3-7: Axial Cross-sectional view of the reaction process within the reactor

- **Nickel Paste**

Nickel paste is light grey anti-seize compound. This smooth paste is smeared over the threading at the various joints in the stainless steel reactor. It was developed to prevent the metal components of the reactor from seizing due to prolonged exposure to high temperatures. The maximum exposure temperature of the paste is approximately 1315 ℃ and it is well suited as the reactor temperature is approximately 850℃. This paste also reduces the friction and wear of the equipment parts. In industry this paste has various other uses such as protection against high temperatures, corrosive chemicals, and it prevents the reduction of material strengths due to mechanical vibrations.

- **NaOH Solution (NS-101)**

The NaOH solution was prepared using the NaOH pellets as described later on. This solution is essential as it is used to absorb the sulphur dioxide gas that exits the reactor. The sulphur dioxide gas is taken from a sampling point in the set-up where the exit gas line is split into two separate lines. One line goes to the gas analyser while the other enters the NaOH solution. The presence of bubbles in the solution indicates that the gas is being absorbed safely. If the sulphur dioxide gas is released into the atmosphere, it can be hazardous and have detrimental effects on human health thus a safe means of the gas disposal is required.

The reaction between the sulphur dioxide gas and the NaOH solution is as follows:

$$SO_{2\,(g)} + NaOH_{\,(aq)} \longrightarrow NaHSO_{3\,(aq)}$$

- **Gas Analyzer (GA-101)**

A portable electronic gas analyzer was used to determine the inlet and outlet reactor concentrations of sulphur dioxide in ppm. This device is auto-calibrated and has a chemical sensor for the gas that is being detected. The outlet pipe from the reactor is connected to the sensor probe to capture sulphur dioxide concentrations. This analyzer may also be used to determine the concentrations of other gases such and CO and N_2. Three input streams are required by the analyzer, exit lines (gas stack), pressure and temperature. It is essential that these lines are connected correctly to avoid the encounter of operational problems. The data is logged onto the analyzer system memory and is transferrable to a pc via a DB9 connector. It is essential to ensure that the backflow of liquid NaOH into the gas analyzer is prevented as this causes malfunction of the equipment.

Figure 3-8: Portable Gas Analyzer

- **Flask collector (CF-101)**

A glass backflow indicator flask is connected between the gas analyzer and the NaOH solution. This additional apparatus serves as an analyzer protective measure. The flask is fitted with a liquid and air tight stopper that has two connections on either side, a longer liquid line from the NaOH solution and a shorter gas line that connects to the analyser. This ensures that if there is any backflow of liquid from the NaOH bath, it will collect in the flask and remain there thus preventing any suction or backflow of the liquid to the gas line that connects to the gas analyser.

- **Sorbents**

Four types of sorbents have been used in the experimental investigation. These sorbents were prepared and then placed between the sieves inside the reactor.

Figure 3-9: Sorbent A

Figure 3-10: Sorbent B

Figure 3-11: Sorbent C

Figure 3-12: Sorbent D

3.4. Experimental Approach and Procedures

The sorbent testing process involved a series of experimental work. Prior to the actual desulphurization process, various pre-experimental work was conducted to ensure that the system was safe to use and produced accurate results.

3.4.1. Leakage Evaluation

- The system was analyzed for any leaks as this may result in sulphur dioxide being released into the laboratory environment.
- Nitrogen was used as the test gas as it is inert and safe.
- The nitrogen gas cylinder was opened and the rotameter adjusted to allow a flow of gas into the system.
- Soapy water was poured over the various connection and junction points of the system.
- The formation of bubbles at these points would indicate system leakage.
- This was performed prior to experimental runs to ensure that no SO_2 escaped from the system and that the working environment was safe.

3.4.2. NaOH Preparation

- The sodium hydroxide solution was used to absorb the unreacted sulphur dioxide that exits the reactor.
- The release of sulphur dioxide is hazardous and release into the atmosphere would pose a threat to human health.
- Five litres of a 1 molar solution of NaOH was prepared using the sodium hydroxide pellets.
- Approximately 200g of the pellets are weighed using a mass balance.
- These pellets were then dissolved in 5 litres of distilled water using the magnetic stirrers.
- The solution is prepared in a fume cupboard in order to contain the hazardous fumes that may be released during the dissolution process.

Figure 3-13: NaOH Pellets

3.4.3. Rotameter Calibration

- A calibration chart was required for the SO_2 rotameter in order to obtain an accurate estimate of flowrate in ml/s from the actual rotameter reading.
- The rotameter was removed from the experimental set-up and gas flow tubing was connected to the rotameter to provide the gas flowrate required for the calibration.
- A tank was filled with water and placed close to the rotameter.
- A 1000 ml cylinder was filled with water and the open end was sealed using the experimenter's hand.
- The cylinder was then inverted and lowered into the water bath before removing the hand seal from the open end.
- The valve on the nitrogen gas cylinder was opened and the rotameter reading was set to 10ml/s
- The gas tubing then created bubbles in the water bath which indicated the presence of nitrogen gas.
- The inverted cylinder was suspended a few centimetres from the bottom of the water bath and the gas tube was then inserted into the open end of the cylinder.
- The volume of water displaced and the time taken to create the displacement was recorded so as to provide flowrate in ml/sec.
- The rotameter reading was then changed at regular intervals and the same procedure was followed to generate a series of values.
- A series of three such experimental runs were carried out for repeatability analysis and performed in different directions to account for hysteresis.
- An average of the results obtained was used to generate the calibration chart with the flowrate versus rotameter reading which can be found in Appendix A, Figure A-1.

3.4.4. Temperature Profile

- It was required that a temperature profile be obtained in order to determine the temperature gradients within the reactor.
- This allows for the determination of hotspots and establishes the best sample location point within the reactor.
- The thermocouple was inserted into the reactor at full length and the reactor was then placed into the oven.
- The oven was then switched on and set to a temperature of 850℃.
- It was then allowed to heat for approximately three hours.
- Once the temperature of the reactor stabilized at 850℃, a reference point was marked on the thermocouple before taking gradient values.

- The thermocouple was then pulled back by 10mm and temperature was recorded after two minutes. This was repeated at increments of 10mm until the thermocouple was displaced by 100mm from the original reference point.
- A graph of temperature versus distance was then plotted as this represented the temperature profile within the reactor (Appendix B, Figure B-1).

3.4.5. Sample Preparation

The raw sorbent materials that were used in the experimental testing unit were obtained from ESKOM. Four different natural calcium based sorbents were used to test desulphurization abilities. The raw samples that were brought in were in the form of large stones which needed further processing before it could be used in the test unit.

Figure 3-14: Roller Crusher

- The sorbent first needed to be crushed into smaller sizes
- This was performed using a roller crusher.
- The distance between the two rollers were adjusted by turning the handle at the side of each crusher.
- By adjusting the distance, desired particle sizes could be obtained.
- Careful consideration was taken when performing the adjustments to ensure that the sample didn't crush to fine powder.
- The crusher was switched on and sample was raw sample was inserted through the caged opening at the top of the crusher.
- A tray was placed at the bottom of the crusher for processed sample to be collected.

Figure 3-15: Mortar and Pestle

- The processed sample from the roller crusher were approximately 10mm in diameter.
- These samples needed to milled further and grouped into various size fractions.
- The grinding was performed manually using a mortar and pestle.
- It was then sieved using tray size of 125, 250, 500, 710, 850 and 1000 microns.
- The different size fractioned samples were then marked and placed into separate sample packets.
- For each run, two grams of sample was filled in the sample location space between the two sieves.

3.4.5. Desulphurization Test Experiment

- Initially the system was tested for leaks as explained earlier.
- The oven was then switched on and set at the required temperature.
- The reactor was then disconnected from the set-up in order to accommodate for the filling of the sample.
- The sieves were carefully inserted to ensure that the gas line passed through.
- Two grams of sample was then weighed and filled into the hole on the reactor such that it would lie between the two sieves creating a type of packing.
- This was done with great care to minimize the loss of sample.
- Nickel paste was then applied to the threads and the reactor was then sealed using a screw cap made of the stainless steel reactor material.
- The nickel paste minimizes the effect of the seizing of the two stainless steel reactor parts that occurs at high exposure temperatures.
- Once the sample is filled, the reactor is carefully placed into the oven and is allowed to heat for three hours.

- The gas analyzer and the backflow indicator flask were then connected to the experimental set-up.
- Once the reactor temperature reached 850℃, the initial SO_2 concentration was required.
- This was obtained by opening the SO_2 gas cylinder valve and setting the rotameter reading to 14ml/sec.
- The SO_2 bypass valve was then opened while all other valves remained closed and the gas analyzer was turned on.
- Data was logged onto the analyzer internal memory every 15 seconds for approximately 1 hour.
- The SO_2 flowed through the bypass line into the analyzer which logged the initial SO_2 concentration and was then absorbed by the NaOH solution.
- Thereafter, the bypass line was closed and the reactor inlet valve was opened allowing SO_2 to enter the system.
- The sulphur dioxide reacted with the calcium based sorbent allowing for desulphurization to take place.
- The SO_2 concentration was then logged using the analyzer for approximately an hour or until the SO_2 concentration stabilized.
- After the data logging process, the SO_2 valve was closed and the analyzer was switched off.
- Nitrogen was then passed through the system via the bypass valve in order to purge the system and remove any impurities before the next run.
- The reactor was then removed from the system and allowed to cool before the sample was removed. Fire-proof asbestos gloves were used to remove the reactor from the oven as a safety precaution due to the high temperatures.
- This process was repeated for the different sorbents using the different size fractions specified.

3.5. Sorbent Physical Property Analysis

Physical property analysis is essential as it was concluded from the literature survey that these properties have an effect on the ability of the sorbent to absorb sulphur dioxide. These properties include the particle sizes, density, porosity etc.

3.5.1. Particle Size

The particle sizes were obtained from the sorbent preparation process. The various sieve trays that were used to separate the crushed particles into various size fractions give average particle diameter estimations.

3.5.2. Density Analysis

Water Displacement Technique

- The density of the various sorbents was estimated using a displacement test method.
- A cylinder was filled with a known volume of water.
- A random sample was taken and then weighed.
- It was then placed in the cylinder in water and the water displacement was taken.
- The displacement represents the volume of the sample and using the known mass, density can be estimated.

Pycnometer Apparatus

A pycnometer is a standard glass vessel with a precise volume and it is used to accurately determine density of substances in the gas, solid and liquid phases. It has a glass fitting called a stopper with a channel through it.

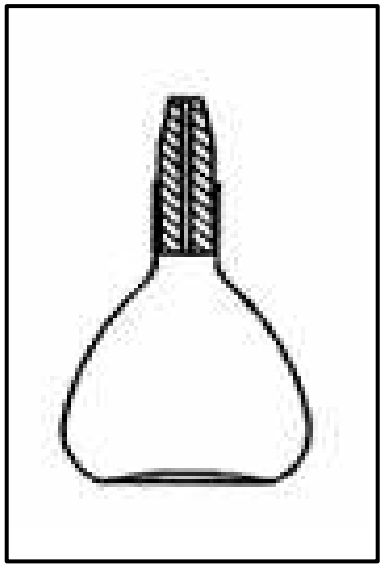

Figure 3-16: Pycnometer Apparatus

This lab scale apparatus is known as a density measuring device however it can only be utilized to measure volume. Density can then be determined by using mass and volume. The mass can be determined very precisely using a mass balance. The density of the solid sorbent can be determined by placing it together with a liquid in the pycnometer. The major advantage of using the pycnometer apparatus for density determination is that this method ensures a high accuracy of measurements.

Procedure

- Accurate density determination using this method requires that the mass and volume measurements are precise.
- The mass of an empty pycnometer m_1 was determined.
- The pycnometer and the capillary hole were then filled with water and any water droplets over the side were dried off.
- The temperature of the water was also obtained using a thermometer in order to use the precise liquid density measurement.
- The mass of the pycnometer and water, m_2 was them determined.
- The pycnometer was then dried and sorbent particles were added.
- The mass of the pycnometer and particles, m_3 was then determined.
- Water was then added to the pycnometer with the particles and the mass, m_4 was then determined

Density of the solid was then calculated based on the following:

- Volume of Pycnometer $= \frac{m_2 - m_1}{\rho_{water}}$
- Mass of particles $= m_3 - m_1$
- Mass of water added $= m_4 - m_3$
- Volume of water added $= \frac{m_4 - m_3}{\rho_{water}}$
- Volume of Particles $=$ Volume of Pycnometer $-$ Volume of water added
- $\rho_{particles} = \frac{m_3 - m_1}{\text{Volume of Particles}}$

3.5.3. Softness Index

The Hardgrove Grindability Index (HGI) was not determined due to the unavailability of specialized equipment and in place of this an alternate test was developed to determine the softness index of the particles (Carsky et al, 2006).

- The sorbent was prepared to a standard size of 850-1000 µm using crushing techniques.
- 40 grams of the sorbent particles was placed into a tumbling mill of approximately 150mm length and 80mm diameter.
- The mill was half filled with steel balls of approximately 20mm diameter.
- The particles were milled for approximately 20 seconds.
- It was then sieved and the softness index is approximated by the mass percentage that passed through the 425 µm sieve.

3.5.4. Porosity, Surface Area, Pore Sizes and Pore Volume

These properties are essential in order to understand the structure of materials and how these properties affect the quality of materials. The physical property analysis of the sorbents were undertaken at the University of KwaZulu Natal, Westville Campus.

The samples were prepared by weighing out and degassing overnight at 200 ℃ under constant flow of Nitrogen.

The instrumentation used to undertake the analysis was a Micrometrics TriStar II Surface Area and Porosity Analyser using TriStar II 3020 v1.03 software. This instrument allows for over a thousand data points to be obtained. The software allows for the analysing and storing of the data.

3.6. Sorbent Chemical Composition Analysis

3.6.1. X-Ray Fluorescence (XRF)

The chemical Composition of the samples A, B, C and D were verified using the X -Ray Fluorescence analysis. It is highly specialised for the acquisition of chemical and elemental analysis. This highly specialized equipment was used to identify all of the mineral compounds present in each of the sorbents.

The XRF determination is undertaken by bombarding the sorbent under analysis with gamma rays and then observing the secondary emission of x-rays. Sufficient energy is created to expel inner electrons from the orbital structure. These results in an unstable orbital structure and electrons fill vacancies to create a stable structure. This process emits characteristic x-rays with a specific energy. The secondary fluorescence rays that are emitted from the sorbent material are directed to a solid material such as a crystal and it produces a continuous energy dispersion pulse. An X-Ray Fluorescence energy spectrum is built up with a number of peaks and intensities. The number of pulses is counted. This analysis was determined at ESKOM.

3.6.2. Energy Dispersive X-Ray Analysis (EDX)

This is an analytical x-ray technique and was used to identify the major elements present in each of the sorbents. The analysis relies on the atomic structure of the elements that comprise the sorbents which determine the peaks present on the spectrum. In the ground state all atoms present in the sorbent will have electrons bound to their nucleus. When an x-ray beam is projected onto the sorbent, the atom enters an ‘excited’ state that causes the electrons from the low energy levels to be displaced leaving behind an empty shell. An electron from a higher energy level will then fill the shell. The x-ray peaks present on the spectrum are determined from the difference between the higher and lower energy shells. This energy is specific to all elements and hence determines the elements that are present.

The analysis was conducted for the fresh and spent sorbent at the University of Kwa-Zulu Natal, Westville Campus.

3.6.3. Lab Scale Test for Calcium Carbonate and Magnesium content

The amount of calcium carbonate present in each of the sorbents was also determined using a laboratory scale method as follows:

- 10 grams of sorbent was weighed and placed in a beaker.
- This beaker was then placed in a larger beaker due to the chemical reactivity expected.

- 12 ml of a 32% hydrochloric acid solution was then added to the sorbent in the beaker and the contents were continuously stirred using a glass rod. This was performed in a fume cupboard.
- The reaction was highly exothermic and resulted in froth formation and overflow.
- After the sorbent was completely dissolved and the froth stabilized, the contents were filtered under suction to retain any impurities.
- The filter paper and the impurities were then placed in an oven for approximately 2 hours to remove the water content.
- The contents were then weighed using the mass balance and the amount of calcium carbonate present in each sample was then calculated.
- In order to reduce uncertainties, this procedure was repeated a number of times and the average results were presented.

3.7. Sorbent Surface Analysis

3.7.1. Scanning Electron Microscopy (SEM)

The Scanning Electron Microscope present at the University of Kwa-Zulu Natal was used to produce high magnification images of the various sorbents. Scanning electron miscrscopes have various components such as an electron source, lenses, specimen chamber, signal detectors, data output devices, and power supply. It is essential that the SEM analysis is undertaken in a work space that is free of magnetic and electric fields.

This specialized piece of equipment scans the surface of the sample or sorbent with a beam of electrons in a predetermined pattern. These electrons come into contact with the atoms present in the sample and create certain signals that help to describe the surface of the sample and its composition. It also reveals information about the crystalline structure of the sample. The atoms may be present at or close to the surface of the sample. The sample is prepared such that it is of appropriate size and has easy access to the specimen chamber. This high resolution equipment presents effective images of the sorbent surfaces and assists in identifying various elements that may be present on each of the surfaces that may affect the desulphurization capacity of the sorbents. SEM images are typically three dimensional images and they assist in helping to understand the surface structure of the sample. The analysis for the surface characteristics of the sorbents were determined at the University of Kwa-Zulu Natal- Westville Campus.

3.8. Operating Conditions Summary

Table 3-1: Operating Conditions Summary

Operating Parameter	Condition	
Oven Temperature	850˚C	
Pressure	1 atm	
Approximate mass of sorbent	2 gram	
Sulphur Dioxide Flowrate	3L/min	
Nitrogen flowrate	3L/min	
Sulphur Dioxide Concentration	2200 ppm	
Oxygen concentration	20%	3 Gas Mixture
Nitrogen	Balance	
CO_2	10%	
SO_2	2000 ppm	4 Gas Mixture
Oxygen	11%	
Nitrogen	Balance	

CHAPTER 4: RESULTS AND DISCUSSION

4.1. Experimental Design Layout

The initial phase of the work undertaken involved designing and developing an effective experimental test unit for flue gas desulphurization. Various configurations together with process and design parameters were considered to decide on the best design layout. It was decided that a static bed reactor would be implemented in place of a fluidized bed reactor. Fluidized bed reactors were found to have a limestone conversion between 30% - 40% (Montagnaro and Salatino, 2002). Sorbent particle attrition is also a concern that arises from fluidized bed combustion as this affects the combustor efficiency and the pollutant emission levels. During fluidized bed combustion, sorbent particles are susceptible to wear and attrition due to the impact caused by loading. This reduces the mechanical efficiency of the sorbent and results in poor sorbent performance (Montagnaro and Salatino, 2002).

Developing the experimental test unit also involved designing and implementing a reactor configuration that proves to work efficiently (figure 3-7). This reactor configuration allows for sorbent to be packed between two sieve-plates with gas passing through.

The test unit was used to investigate dry flue gas desulphurization which involved packing sorbent in a fixed reactor inside a furnace. On an industrial scale, this process is cost effective, requires less operation space and is easier to retrofit hence it was decided to represent this process on a lab-scale for analysis (Ho and Shih, 1992). Dry FGD also produces a solid product that is much easier to handle and dispose. The fully developed testing unit is presented in figure 3-1 and figure 3-2.

The test unit was designed to investigate high temperature desulphurization as it was concluded that this type of process has been attracting attention due to its increased desulphurization efficiency and diminished capital costs (Chang et al, 1998). The oven was set at a temperature of 850˚C based on previous studies that were conducted on calcium based sorbents. Experiments were undertaken using a typical flue gas composition of 2000 ppm SO_2 for a reaction period of one hr. For each run, approximately 2 grams of sorbent was used with a gas flowrate of 3L/min.

4.2. Sorbent Chemical Analysis

4.2.1. X-Ray Fluorescence (XRF)

The four unreacted sorbent samples that were provided by ESKOM were analyzed using the X-Ray Fluorescence technique. This test procedure provides a chemical composition analysis for the various sorbents by successfully identifying the solid species of which the sorbent is comprised. The XRF analysis involved the emission and measurement of characteristic X-Rays from the sample by bombarding with high-energy gamma rays. Refer to Appendix C for a detailed calculation explaining the relationship between ESKOM purity and lab scale purity.

Table 4-1: Chemical Composition of the Various Sorbents

Component	Sorbent			
	A	**B**	**C**	**D**
SiO_2	0.09	0.24	0.64	0.59
Al_2O_3	0.06	0.10	0.21	0.22
CaO	44.50	52.20	53.49	51.60
MgO	8.60	2.21	0.62	0.61
Fe_2O_3	1.07	0.32	0.26	0.14
K_2O	0.09	0.11	<0.01	0.13
MnO	0.23	0.16	0.668	0.52
Na_2O	<0.05	<0.05	<0.01	<0.05
P_2O_5	<0.01	<0.01	0.002	<0.01
TiO_2	0.02	0.05	-	0.01
Cr_2O_3	0.02	<0.01	0.002	<0.01
V_2O_5	<0.01	<0.01	-	<0.01
LOI	44.83	43.67	42.95	43.13
Total	99.5	99.1	98.77	96.9

The above analysis was undertaken at the ESKOM power station and the results accompanied the arrival of the sorbents

4.2. 2. Lab-Scale Purity Test

A laboratory scale test as described in the previous chapter was undertaken to determine the percentage purity (CaO) of the different sorbents. These results were then compared to the percentage purities obtained from the XRF analysis that was undertaken at ESKOM.

Table 4-2: Comparison between the Lab Scale and XRF Percentage Purity of the Various Sorbents

Sorbent	XRF % Purity	Lab Scale % Purity
A	94.82	94.51
B	97.16	96.83
C	96.62	96.71
D	93.23	96.69

4.2.3. Energy Dispersive X-Ray Analysis (EDX)

This technique was used to identify the major elements present in each of the sorbents. The analysis was conducted for the fresh and spent sorbents at the University of Kwa-Zulu Natal, Westville Campus. The results indicate that the major elements present were mostly calcium and magnesium as can be seen in the table below.

Table 4-3: EDX Analysis of Fresh and Spent Sorbent

Component (Wt. %)	Sorbent				
	A	**B**	**C**	**D**	**Spent A**
Ca	86.00	97.20	94.42	93.02	65.84
Mg	12.74	2.80	0.79	4.51	10.89
Fe	1.26	-	0.66	-	1.22
Al	-		0.59	-	-
Si	-	-	1.90	0.95	-
Mn	-	-	1.64	1.52	-
S	-	-	-		22.05

It can be seen from the above analysis that the spent sorbent has a significant amount of sulphur. This is due to the sulphates of Calcium that formed due to the sulphation reaction.

4.3. Sorbent Physical Property Analysis

4.3.1. Density

The densities of the solid sorbents were initially determined using the water displacement technique as outlined in the experimental section. This technique may prove to be inaccurate due to the incorrect volume readings as volume cannot be measured precisely. The use of the lab scale apparatus known as a Pycnometer provides a more rigorous and reliable technique for density determination as it involves the measurement of mass which can be accurately determined using a sensitive mass balance. Sorbent A was found to be the most dense with a value of 2.86 g/ml followed by Sorbents B, D and then C.

4.3.2. Softness Index

HGI indicates how hard or soft sorbents are. Previous studies indicate that the HGI has no effect on the desulphurization efficiency however it indicates how easily sorbents can be milled. A good sorbent is neither too hard nor too soft. If it is too hard, it will have extensive milling costs and if too soft it will easily break when used under fluidized bed conditions. The HGI could not be determined due to the unavailability of the specialized equipment that was needed hence a softness index test was developed to indicate how hard or soft the sorbent particles are.

The softness index was determined using the milling procedure outlined in Chapter 3. The procedure results in a loss of mass due to the fine dust-like particles being lost due to transference. It was found that Sorbent C had the highest softness index.

4.3.3. BET Surface Area, Porosity, Pore size and Pore volume

Analysis was done on a Micrometrics TriStar II Surface Area and Porosity Analyser using TriStar II 3020 v1.03 software. This process produces absorption and desorption isotherms. The properties were determined by the nitrogen adsorption data and the Brunauer-Emmett-Teller (BET) method.
Sorbent C has the largest porosity, BET surface area and pore volume and it has the smallest average pore size. Sorbent B has the lowest porosity, smallest surface area and pore volume.

Table 4-4: Summary of Sorbent Physical Property Analysis

Property	Sorbent			
	A	**B**	**C**	**D**
Density - Water Displacement (g/ml)	2.83	2.72	2.43	2.60
Density – Pycnometer (g/ml)	2.86	2.73	2.55	2.57
Softness Index (%)	2.24	3.40	4.31	3.57
Porosity (ε)	0.0045	0.0030	0.0068	0.0061
BET Surface Area (m^2/g)	0.48	0.35	0.91	0.80
Pore Size(Å)	132	123	117	121
Pore Volume (cm^3/g)	0.0016	0.0011	0.0027	0.0024

4.4. Sorbent Surface Analysis and Desulphurization

4.4.1. Scanning Electron Microscopy (SEM)

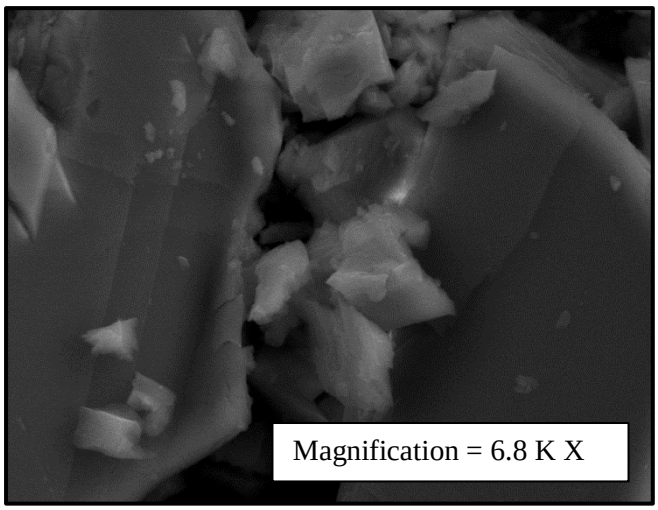

Figure 4-1: SEM Image for Sorbent A

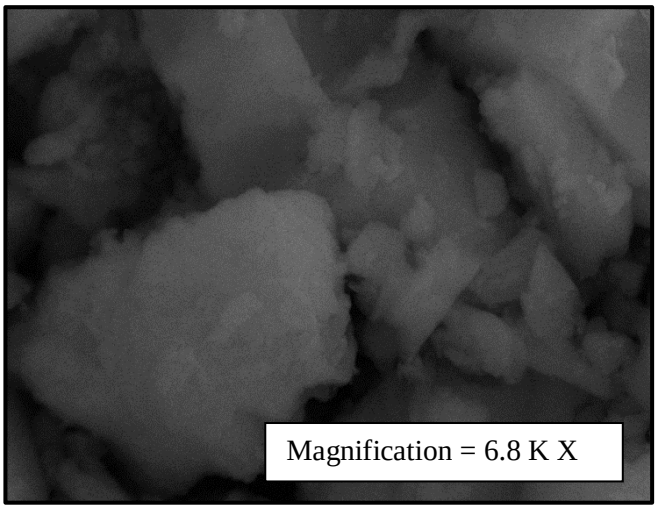

Figure 4-2: SEM Image for Sorbent B

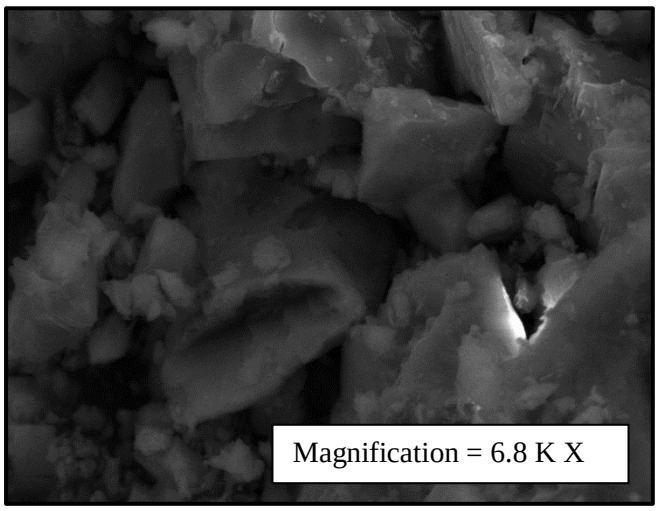

Figure 4-3: SEM Image for Sorbent C

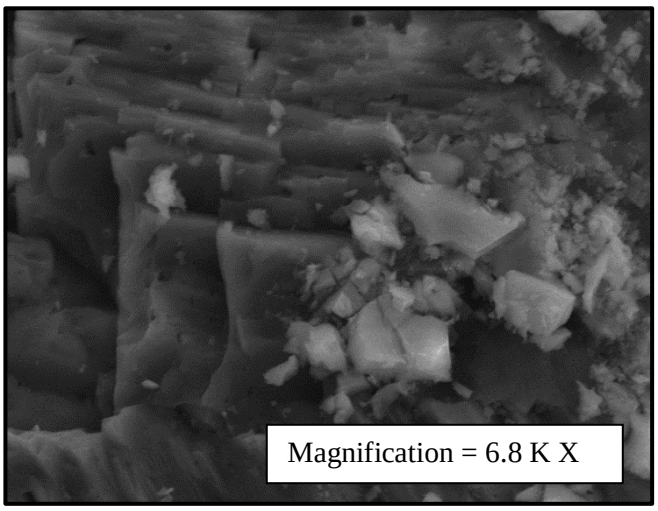

Figure 4-4: SEM Image for Sorbent D

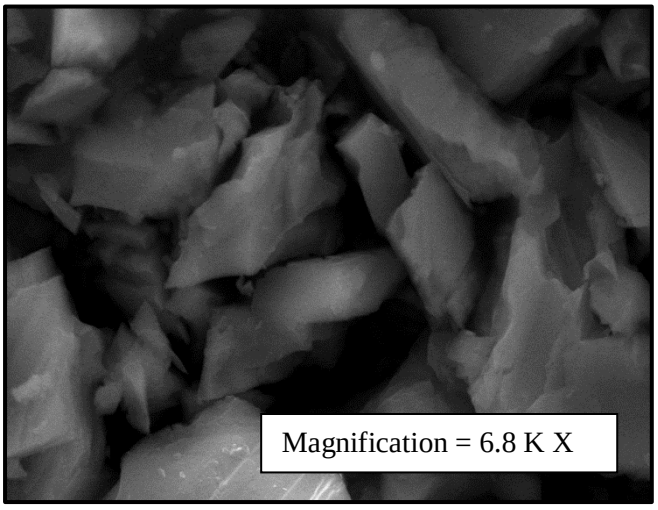

Figure 4-5: Sorbent A before Reaction

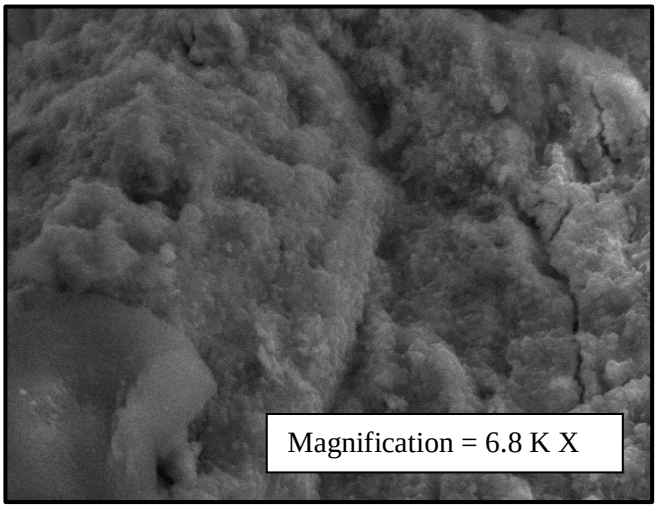

Figure 4-6: Sorbent A after Reaction

SEM images were taken at the University of Kwa-Zulu Natal, Westville Campus. The apparatus was used to produce a high magnification image of the surface that is seen. A three dimensional image is produced and different contrast is used to indicate the different surface regions. These images were taken of the fresh and spent sorbents and are showed in the figure 4-1 to figure 4-6 above. These images can be used to investigate the surface properties of the sorbents.

It can be seen that the surface of Sorbent A is relatively smooth compared to the other sorbents. The white spots on the surface are an indication of the presence of calcium. Sorbent A appears to have decreased amounts of calcium as compared to the other sorbents. The darker shades that are present on this sorbent are due to the presence of impurities that include silicates and iron oxides. This is in agreement with the XRF and EDX analysis which indicates that this sorbent has the least amount of calcium. All of the images indicate that the sorbent surfaces are fairly irregularly shaped. The sorbents consist of asymmetrical shape particles with uneven texture and various structural porosities.

The surface morphologies of the calcium based limestone before and after reaction were also observed and compared using SEM. The SEM of the spent sorbent was taken after the sorbent reacted for approximately an hour at 850 ℃ at atmospheric pressures with the gas composition of 2000 ppm SO_2, 20% O_2 and balance nitrogen. The SEM image of Sorbent A after reaction indicates that the sorbent becomes covered with a layer of calcium sulphate which is the main product of the sulphation reaction. This layer is very rough and porous and consists of fragments of calcium sulphate that is of lighter shade of grey to white.

The porous surface is due to the release of carbon dioxide during the calcination process (Carsky et al, 2006). Fresh sorbents have surface morphologies that are free from fractures whereas there is a clear indication of fractures on the spent sorbent. These cracks that can be observed are due to the difference in the molecular volumes of CaO and $CaSO_4$. Previous studies indicate that the more rough surfaces produce more rough layers of calcium sulphate which improves the desulphurization ability and result in better utilization of the calcium layer underneath the surface. Smooth surfaces result in a smooth layer of calcium sulphate that is compact and prevents the diffusion of SO_2 to the sorbent core (Carsky et al, 2006). The desulphurization analysis that was undertaken indicates that Sorbent C has the highest desulphurization efficiency. The high porosity and high BET lead to good adsorptive characteristics; these manifest as a more porous and rough structure as seen in the SEM images for sorbent C. It is also seen from the conversion vs. time plot (figure 4-17) that Sorbent C has the highest conversion. This is because the rough surface enables the formation of a rough product layer. This layer allows for the SO_2 to penetrate deep into the sorbent structure enabling increased amounts of sorbent utilization hence resulting in higher conversions (Carsky et al, 2006). Sorbent A with a

smooth surface results in the formation of a more compact product layer that limits mass transfer hence resulting in lower efficiencies and conversion.

4.5. Analysis of Desulphurization Test Results

4.5.1. Interpretation of Graphical Representation

The desulphurization tests were conducted as explained in the experimental procedure in Chapter 3. The data obtained from the desulphurization tests are represented graphically in Appendix F. An example of such a plot is seen below in figure 4-7. This graph represents the desulphurization test data for Sorbent A at 850 ℃ for the particle size fraction of 250-500 μm. It shows an initial SO_2 concentration of approximately 2100 ppm as established in the bypass line, before the gas flow is interchanged between the bypass and the reactor inlet line. The remaining data points represent the outlet concentration of sulphur dioxide after the reaction occurs at a particular instant in time.

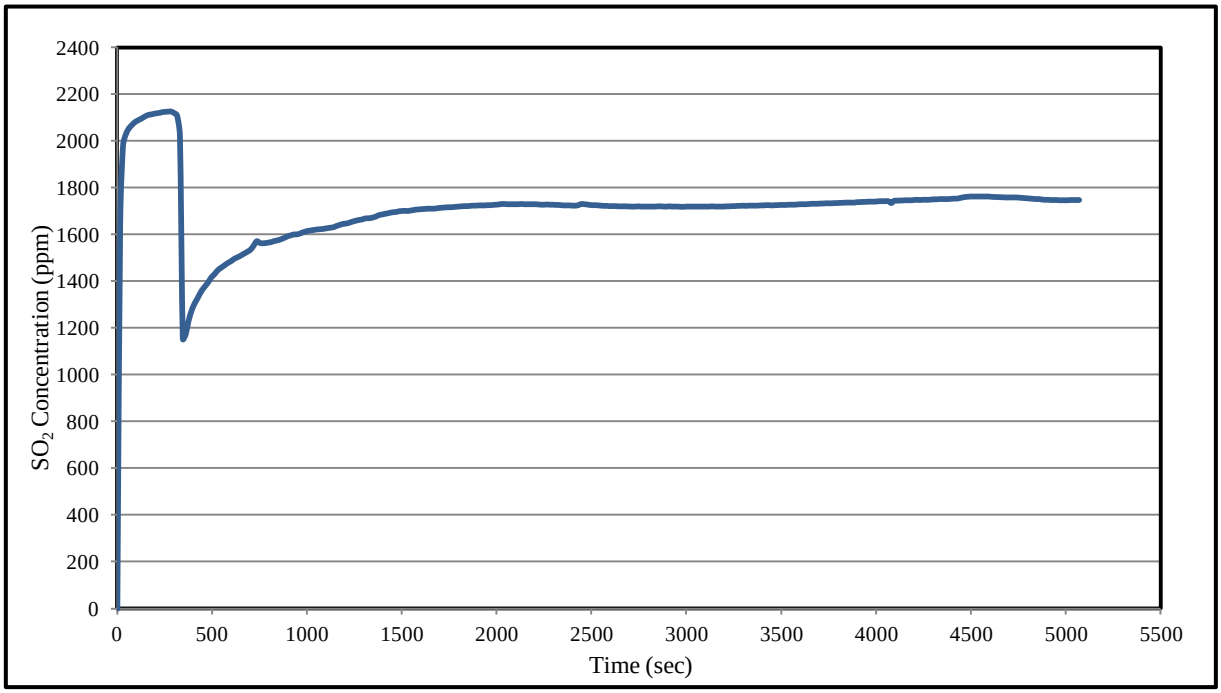

Figure 4-7: SO_2 Concentration vs. Time for Sorbent A using Size Fraction 250-500μm at 850℃

It can be seen from the curve presented above that after the initial SO_2 concentration is established through flow in the bypass line, the SO_2 concentration rapidly decreases as the reaction is initiated. The minimum outlet gas concentration is established which determines an estimate for the maximum sulphur retention capacity of the sorbent. SO_2 concentration thereafter increases very slowly in an attempt to reach initial SO_2 levels. This indicates a gradual saturation of the sorbent.

This trend indicates that the reaction rate for the sulphation reaction is very high at the beginning of the reaction as is found by Renedo et al, 2000. Maximum desulphurization occurs in the first 0.3 seconds of the process (Cheng et al, 2003). Studies conducted by Ye and Bjerle, 1996 investigated the high temperature reaction between natural calcium based sorbents and SO_2 and found a similar trend. It was further explained in this work that the possible reason for the initial rapid reaction rate can be attributed to the initial reaction phase being controlled by the surface reaction. This is further enhanced by the high concentration of the reactants that are present initially. As the reaction proceeds, the reactants become depleted and the successive reaction stage is controlled by product layer diffusion hence resulting in a reduced reaction rate.

After analyzing the results for Sorbent A, it was found that the initial concentration of approximately 2100 ppm could not be attained even after a long period of time. The trend for the outlet SO_2 concentration appears to stabilize at approximately 1700 ppm. A possible reason for the above result was sought by conducting further experiments of which the results are presented below.

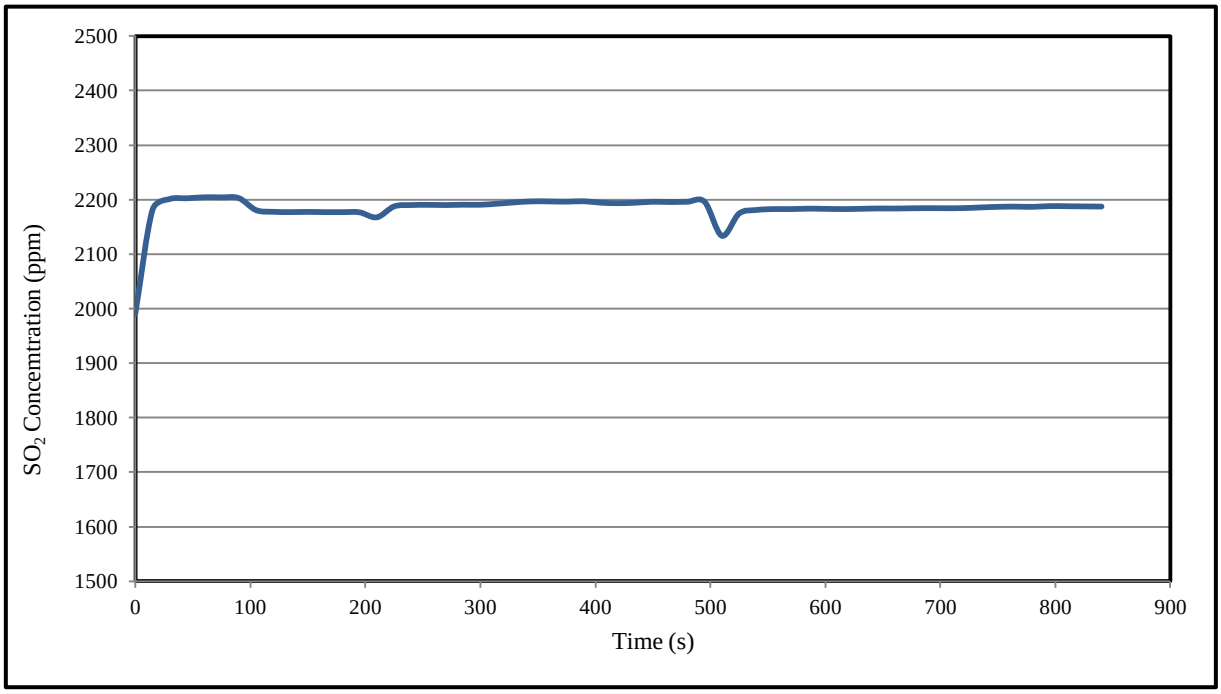

Figure 4-8: SO_2 Concentration vs. Time at 25 ℃ without Sorbent

Figure 4-8 shows the SO_2 concentration at 25℃ without any sorbent present in the fixed bed reactor. The peaks at times 100, 200 and 500 seconds are due to the interchanging of gas flow between the bypass and reactor inlet lines. This graph clearly indicates that the outlet SO_2 concentration reaches the initial SO_2 concentration value.

The peaks found in figure 4-9 after 3000 seconds is again due to the interchanging of flow between bypass and the reactor inlet. It can be seen the concentration levels reach values of 1700 ppm and 2100 ppm alternately. It can be seen that the SO_2 outlet concentration does not reach the initial concentration and this can be explained by accounting for the possible formation of sulphur trioxide via the oxidation of sulphur dioxide as described by Montagnaro and Salatino, 2002.

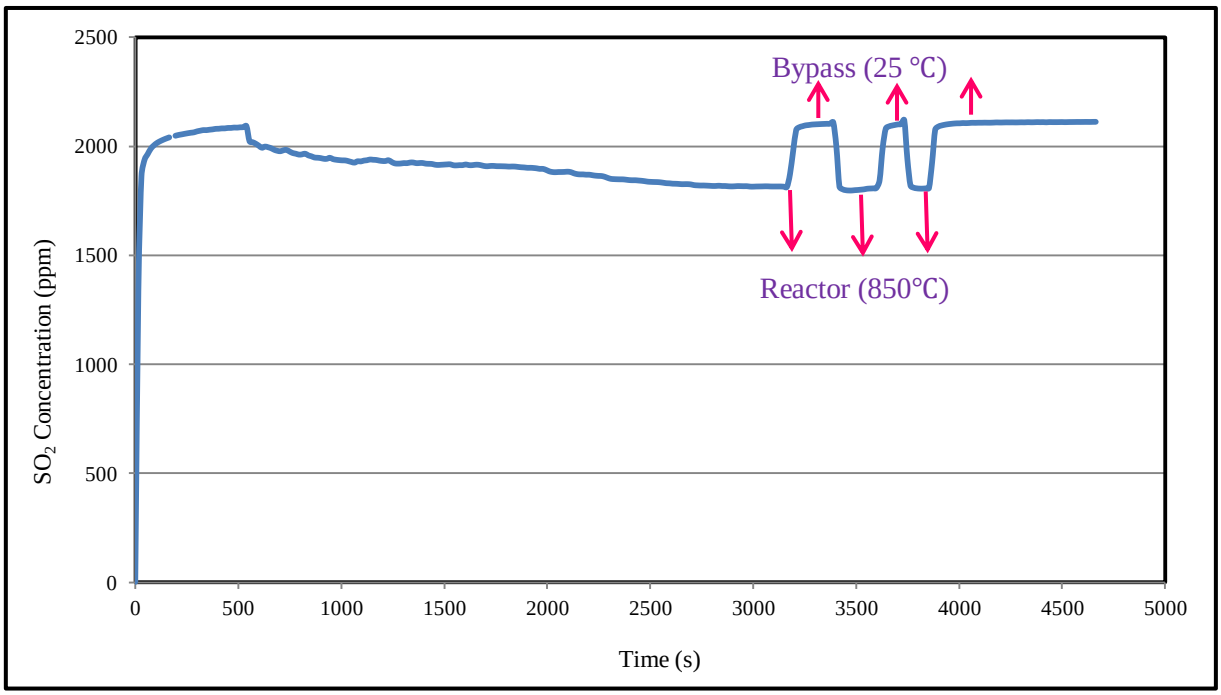

Figure 4-9: SO_2 Concentration vs. Time at Typical Reaction Conditions (850 ℃) without Sorbent

The reaction between sulphur dioxide and oxygen can be described by equation 2.2

$SO_2(g) + O_2(g) \leftrightarrow SO_3(g)$ (Flagan and Seinfeld, 1988):

The equilibrium constant K_p is given by $K_p = 1.53 \times 10^{-5} e^{11\,760/T} atm^{-1/2}$ (4.1)

The above reaction is one of the most significant industrial reactions pertaining to sulphur dioxide. It occurs primarily in the gas phase and only at elevated temperatures (Hasenberg, 2008). This equilibrium reaction was studied by Cullis et al, 1966. It was found that at temperatures above 500℃, the right hand-side of the reaction is favoured and a large quantity of sulphur trioxide is produced. For temperatures well above 1000℃, the equilibrium shifts and the reverse reaction is favoured resulting in minimal production of sulphur trioxide. This idea of thermodynamic equilibrium is also supported by Hasenberg, 2008 and it was found that for temperatures above 1200 ℃ the equilibrium lies completely on the side of SO_2 and for temperatures above 400℃, it lies on the side of SO_3.

It was found that various factors affect the reaction kinetics and can contribute to the formation of SO_3 (Hasenberg, 2008):

- The amount of oxygen present
- The flue gas temperature
- The residence time at a specific temperature

The equilibrium reaction is temperature sensitive and it can be predicted using the equations above that a decrease in the temperature would cause the equilibrium yield of SO_3 to increase (Flagan and Seinfeld, 1988).

It was also found that the above reaction occurs rapidly for temperatures below 900℃ in the presence of certain catalysts. These catalysts include vanadium pentoxide, iron, nickel and alkali earth metals (Hasenberg, 2008). This indicates that the anti-seize nickel paste that is smeared over the stainless steel reactor surface to prevent locking of the reactor parts at high temperatures may appear to be a possible catalyst for the reaction. The formation of SO_3 may also be catalyzed by the hot stainless steel reactor (Hamer, 2009).

Various other researchers also indicated that the initial SO_2 concentration is not reached due to the oxidation of SO_2. Such work was presented by Hansen et al, 1993 were SO_3 was taken into consideration but no experimental measurement of the SO_3 present was undertaken. The SO_3 that is formed is undesired as it may be problematic. It can combine with the water vapour that is present in the flue gas to produce sulphuric acid. This can cause corrosion and fouling of the process equipment and it may also condense thus increasing the probability of aerosol emissions (Glarborg, 2006).

4.5.2. Desulphurization Efficiency and Average Sorbent Ranking

The experimental trials were based on two gram of sorbent to ensure appropriate comparison of sorbent efficiencies. The test data obtained represents the SO_2 outlet concentration. The data was used to calculate the minimum and maximum sorbent efficiency. Various lines were constructed to clearly demarcate areas to enable the calculation of the desulphurization efficiency. Area 1 represents the total amount of SO_2 present in the system. Area 2 represents the amount of SO_3 formed. Area 3 represents the total area of SO_2 and SO_3. The shaded region represents the amount of SO_2 removed.

$$\text{Maximum Desulphurization Efficiency (\%)} = \frac{A_1 - A_{\text{Under Curve}} + A_2}{A_3} \qquad (4.2)$$

The maximum efficiency includes the formation of SO_3 and it assumes that all the SO_3 is absorbed by the sorbent as no measurement of SO_3 was taken during the experiments. However a significant amount of the SO_3 exits unreacted thus the maximum efficiency value is overstated. This is justified by the fact that the final SO_2 concentration is well below the feed concentration which implies that

SO_3 is exiting the reactor after the sorbent is spent. This suggests that the SO_3 may also be exiting the reactor in some proportion to the unreacted SO_2 before the sorbent is spent.

$$\text{Minimum Desulphurization Efficiency (\%)} = \frac{A_1 - A_{\text{Under Curve}}}{A_3} \quad (4.3)$$

The minimum desulphurization efficiency does not take into account the amount of SO_3 that has reacted with the sorbent and hence this value most probably understates the actual efficiency. As it is unclear of the exact amount of SO_3 absorbed by the sorbent, the actual desulphurization efficiency lies between the minimum and maximum value. Validity of eq. 4.2 and 4.3 is correct only if concentration of the outlet SO_2 reaches a constant value. The results presented are the average of two obtained data sets for four natural calcium based sorbents at four different size fractions.

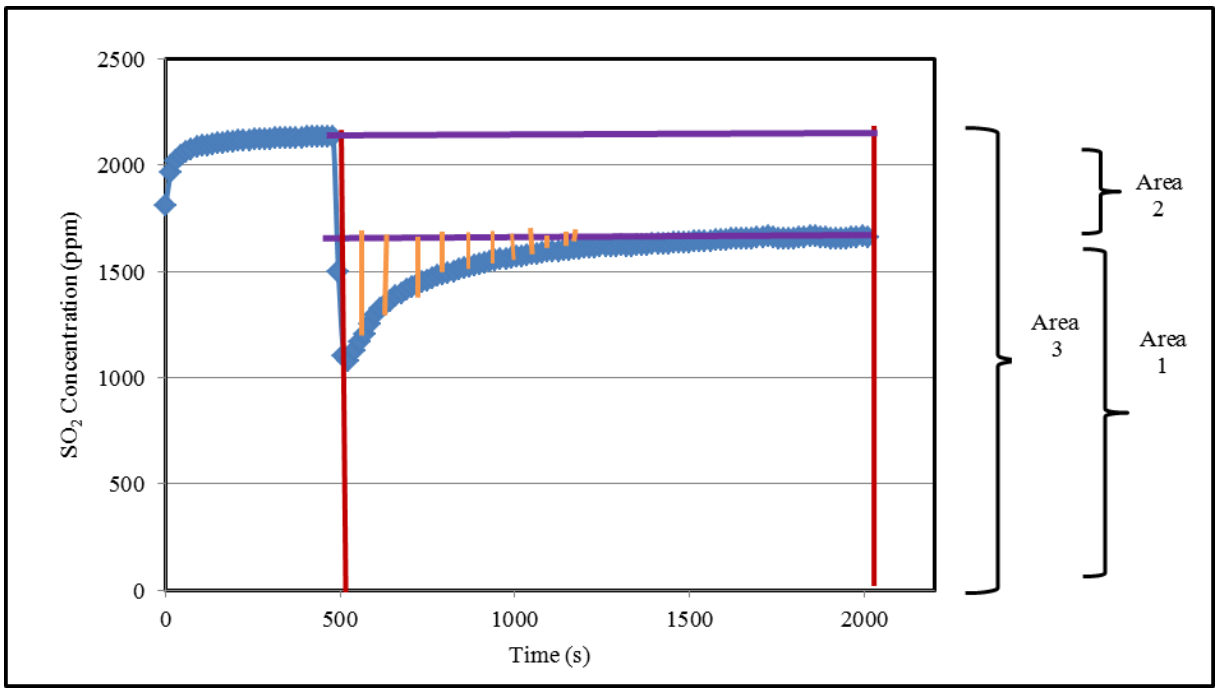

Figure 4-10: Desulphurization Test Graph Showing the Areas used for the Determination of Desulphurization Efficiency for the 850-1000 µm Particle Size

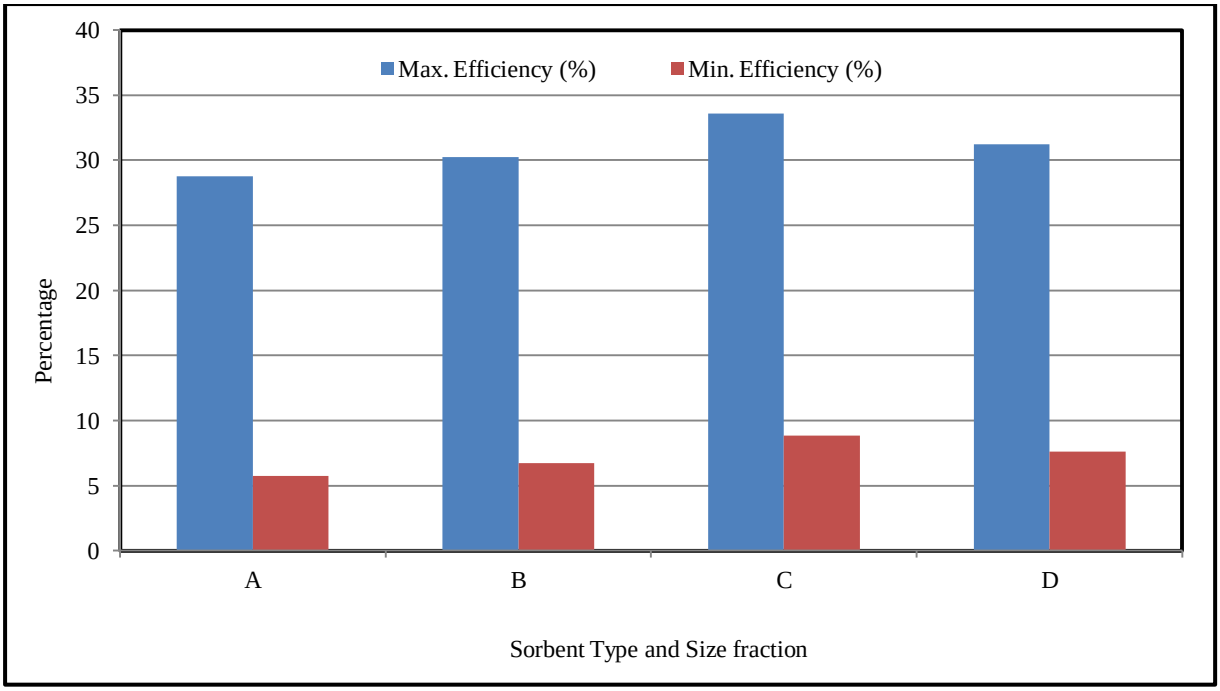

Figure 4-11: Graphical Representation of the Maximum & Minimum Desulphurization Efficiency of the different Sorbents at 850 ℃ using the Three Gas Mixture

Table 4-5: The Ranking of the Sorbents based on the Desulphurization Efficiency.

Sorbent	Max. Efficiency (%)	Min. Efficiency (%)	Rank
A	28.78	5.76	4(Worst)
B	30.23	6.72	3
C	33.57	8.85	1(Best)
D	31.21	7.63	2

From table 4-5 and figure 4-11, it can be observed that Sorbent C has the highest desulphurization efficiencies while Sorbent A has the lowest desulphurization efficiencies. The maximum efficiencies found range between 28.78% and 33.57%. The work undertaken by Cheng et al, 2004 investigated the desulphurization efficiencies of three different limestone with a gas mixture containing 2200 ppm SO_2 in air at temperatures ranging from 800℃ to 950℃. At 850℃, the desulphurization efficiencies ranged between 25% and 40%. The desulphurization efficiency results that are found in the present work are in agreement with this finding.

4.6. The Effect of Process Variables on Desulphurization Efficiency

The different process variables that can be manipulated to enhance desulphurization efficiency include operating temperature, pressure, mass of sorbent, sulphur dioxide concentration and the ratio of sorbent to sulphur dioxide. In the work undertaken these process variables were kept constant at the recommended value as established in the literature review. Two synthetic flue gas mixtures were used to determine the effect of the presence of carbon dioxide on desulphurization efficiency. The first was a three gas mixture comprising 2000 ppm SO_2, 20% O_2 and balance N_2. The four gas mixture comprised of 2000 ppm SO_2, 11% O_2, 10% CO_2 and balance N_2.

4.6.1 The Effect of the Presence of Carbon dioxide in the Flue Gas Mixture

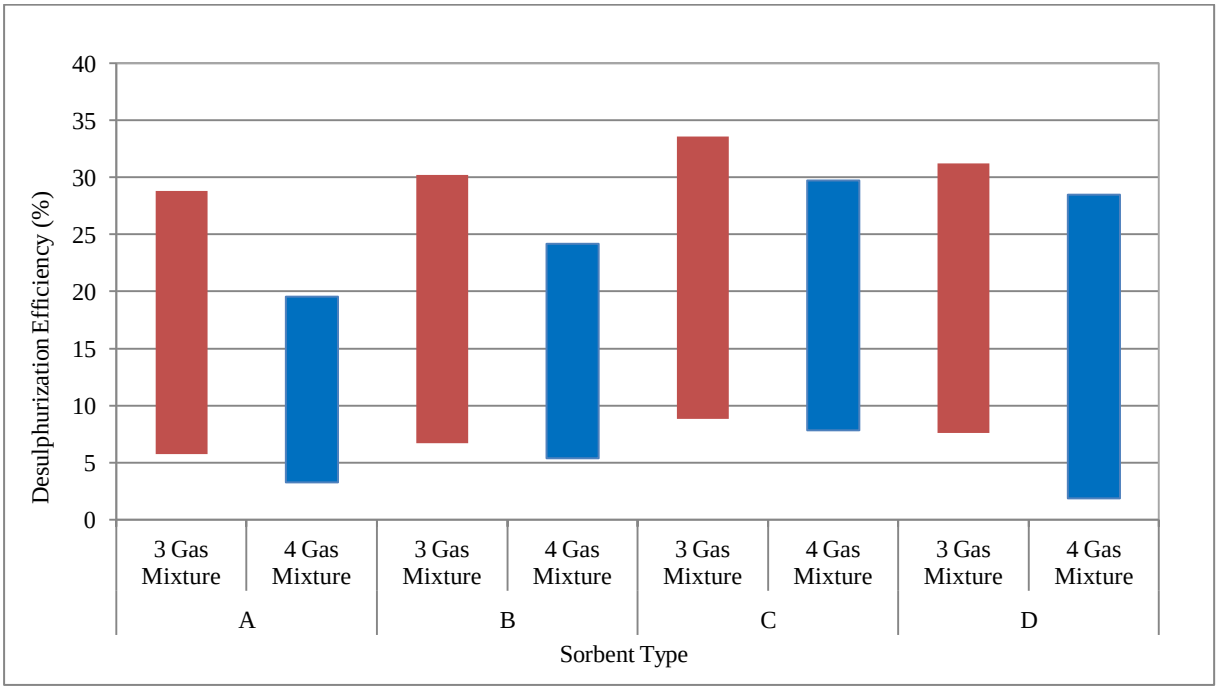

Figure 4-12: Desulphurization Efficiencies for the Different Sorbents using the Two Different Gas Mixtures at 850 ℃

The relationship between the different sorbent type and desulphurization efficiency for the two gas mixtures is represented in figure 4-12. The bars represent a range for the desulphurization efficiencies clearly indicating the minimum and maximum efficiencies. It can be clearly seen that the range for the desulphurization efficiencies for the different sorbents decrease with the presence of CO_2 in the flue gas. Sorbent C has the highest desulphurization efficiency range using both gas mixtures while Sorbent A has the lowest desulphurization efficiency range. The sorbents have the same ranking

pattern using both gas mixtures however the efficiencies using the 4 gas mixture is significantly lower than the 3 gas mixture.
An attempt was then made to explain the decreased efficiencies obtained in the presence of CO_2.

It was found that between the operating temperatures of 800-900 ℃ the formation of sulphates via the direct sulphation reaction (equation 2.11) was so slow that it was negligible.

$$CaCO_3 + SO_2 + \frac{1}{2} O_2 = CaSO_4 + CO_2$$ Direct sulphation

This process is usually comprised of two steps with the initial being an endothermic calcination step which decomposes the $CaCO_3$, producing CO_2 and CaO. The release of the carbon dioxide results in a more porous surface with a larger exposed surface area that allows for maximum sulphation to occur. The second step is exothermic sulphation where the CaO absorbs sulphur dioxide to form a relatively stable sulphate product. The calcination and sulphation is described by equations 2.5 and 2.9 respectively.

$$CaCO_3 = CaO + CO_2 - 183\ KJ/gmol$$ Calcination

$$CaO + SO_2 + \frac{1}{2}O_2 = CaSO_4 + 486KJ/gmol$$ Sulphation

The SO_3 that is formed through the oxidation of SO_2 at high temperatures can also react with the $CaCO_3$ to produce the sulphates (Sellakumar and Conn, 1999) as described by equation 2.12.

$$CaCO_3(s) + SO_3(g) = CaSO_4(s) + CO_2(g)$$

The occurrence of CO_2 in the gas mixture can enhance or reduce the desulphurization efficiency. This is governed by the partial pressure of the CO_2 in the flue gas mixture. The process occurs through the two step calcination and sulphation when the partial pressure of the CO_2 in the gas mixture is less than the equilibrium pressure (Basu, 2006).

The equilibrium pressure P_e is represented by the following equation (Basu, 2006):

$$P_e = 1.2 \times 10^7 \exp\left(\frac{-E}{RT}\right) \quad (4.4)$$

Where $P_e -$ Equilibrium Pressure (bar)

$E -$ Activation Energy $(159000 \frac{KJ}{mol})$

$R -$ Universal Gas Constant $(8.314 \frac{KJ}{mol}. K)$

At the operating temperature of the system which is 850℃ the equilibrium pressure was calculated as 0.48 bar. The partial pressure of the carbon dioxide in the gas mixture depends on the total system pressure and the volume % of CO_2. The synthetic flue gas mixture used, containing 10% by volume CO_2, has a partial pressure of 0.1 bar at the operating system conditions. Since this partial pressure is less than the equilibrium pressure of the system and the operating temperature is 850 ℃ desulphurization occurs via the two step calcination and sulphation stages.

Previous studies indicate that the BET surface area and pore volume of calcined CaO is significantly decreased if the $CaCO_3$ is calcined in an atmosphere that contains CO_2. The presence of CO_2 in the flue gas mixture influences the phenomenon of sintering (Cheng et al, 2003). Sintering is a deactivation phenomenon that reduces the surface area, shifts the pore size distribution to favour larger pores and it reduces the porosity. The rate of sintering depends largely on the type of sorbent and the chemical composition. The sintering phenomenon produces crystal structures that are very compact. This reduces the conversion of the CaO particles resulting in decreased sulphation capacity and hence reducing the desulphurization efficiency (Ghosh-Dastidar et al, 1996 and Ye and Bjerle, 1996).

Wang et al, 2009 conducted studies between the CO_2 and O_2 atmospheres at 900℃. It was found that the efficiencies were lower when CO_2 was present. It was found to be 23.1% and 26.9% in an O_2 atmosphere for 30 and 40 minutes respectively and 9.6% and 16.5% in the presence of CO_2.

Hu et al, 2007 studied the effect of the CO_2 concentration in the reacting gas mixture on the levels of conversion. It was found that by increasing the amount of CO_2 present, the conversion of the limestone sorbent decreased significantly. CO_2 affects the solid-state diffusion of calcite. It changes the crystal lattice structure of the calcite by reducing the number of extrinsic carbonate vacancies that are present. A minimized number of CO_3^{2-} ions will have reduced probability to form bonds with the SO_3^{2-} ions hence reducing the sulphation capacity.

The results in the studies mentioned above are in agreement with the results obtained in the current investigation which depict that the CO_2 presence reduces the desulphurization efficiency.

4.7. The Effect of Physical Properties on Desulphurization Ability

4.7.1. Effect of Particle Size on Desulphurization Ability

The Effect of particle size on desulphurization efficiency was determined by testing four size fractions of the four sorbents. The four size fractions tested were 850-1000µm, 710-850µm, 500-710µm, and 250-500µm. The tests were performed using both the gas mixtures and the results are presented below.

Table 4-6: The Ranking of Sorbents Based on the Desulphurization Efficiency at 850 ℃ Using the Three Gas Mixture

Sorbent	Particle Size (µm)							
	850-1000		710-850		500-710		250-500	
	Min Eff. (%)	Max Eff. (%)	Min Eff. (%)	Max Eff. (%)	Min Eff. (%)	Max Eff. (%)	Min Eff. (%)	Max Eff. (%)
A	4.83	24.64	5.52	29.23	5.85	30.44	6.85	30.84
B	6.12	26.93	6.38	29.98	7.05	31.73	7.34	32.31
C	7.11	27.74	8.35	32.97	9.81	36.30	10.08	37.30
D	6.47	25.87	7.25	30.46	7.82	32.05	8.90	36.47

Table 4-7: The Ranking of Sorbents based on the Desulphurization Efficiency at 850℃ using the Four Gas Mixture

Sorbent	Particle Size (µm)							
	850-1000		710-850		500-710		250-500	
	Min Eff. (%)	Max Eff. (%)	Min Eff. (%)	Max Eff. (%)	Min Eff. (%)	Max Eff. (%)	Min Eff. (%)	Max Eff. (%)
A	3.06	18.06	3.10	19.23	3.21	20.09	3.65	20.79
B	5.05	21.88	5.12	23.56	5.38	25.27	5.91	26.01
C	7.11	27.03	7.44	29.76	7.94	30.17	8.78	31.97
D	6.26	26.29	6.87	28.18	7.19	29.47	7.32	30.01

Table 4-6 and table 4-7 indicate the minimum and maximum desulphurization efficiency of the four different sorbents at the different size fractions. Due to the difficulty of observing the relationships between the parameters the results were then represented graphically.

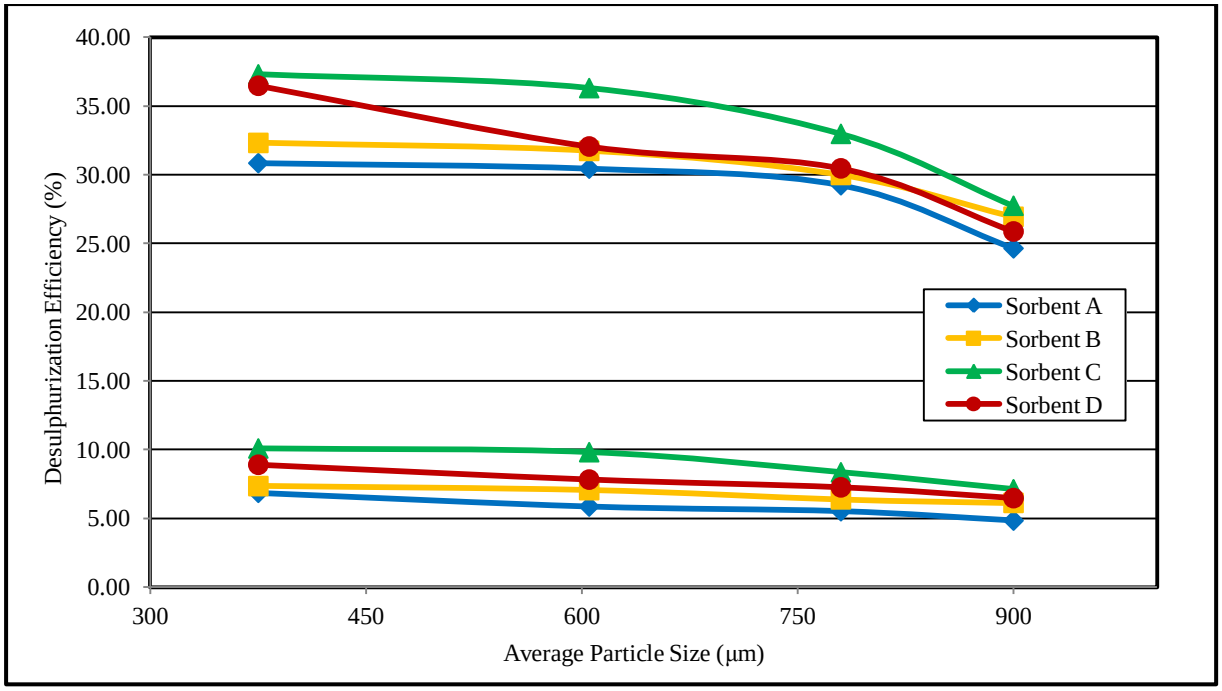

Figure 4-13: Effect of Particle Size on Desulphurization Efficiency Using the Three Gas Mixture

Figure 4-13 and figure 4-14 represents the relationship between the particle size and desulphurization efficiency. It can be observed that the desulphurization efficiency increases for smaller particle size and decreases as the particle size gets larger. This is evident for both the maximum and minimum values attained. The four gas mixture results in reduced efficiencies as compared to the three gas mixture. The maximum desulphurization efficiency was 37. 30% for the 250-500 µm size fractions of the three gas mixture. A similar pattern is found for all of the tested sorbents.

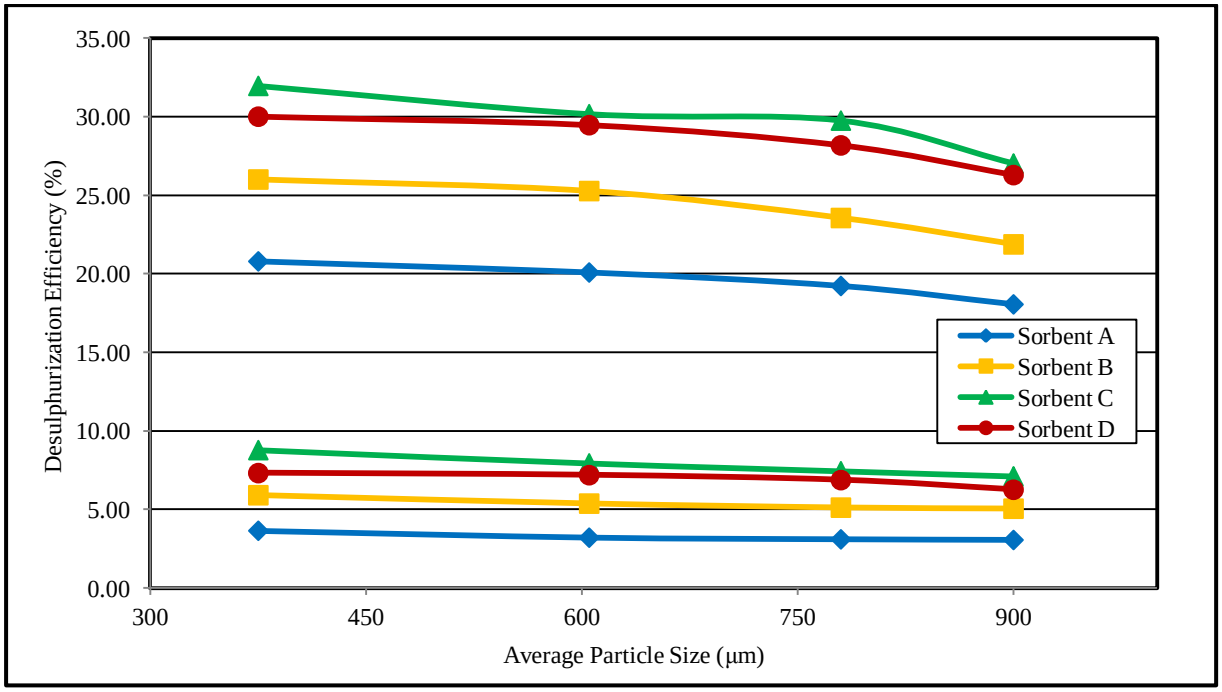

Figure 4-14: Effect of Particle size on Desulphurization Efficiency using the Four Gas Mixture

It is clearly indicated by the results above that the particle size distribution has an immediate effect on the desulphurization efficiency. The results found are in agreement with the work conducted by Pisupati et al, 1996 and Cheng et al, 2003. Smaller particles have a larger exposed surface area hence the contact between the sorbent and the SO_2 is greatly improved which results in maximum sulphur removal efficiency. Gosh - Dastidar et al, 1996 also explained that small particle size results in better conversion of the sorbent as they have reduced mass transfer limitations. Particles that have large diameters have an increased SO_2 diffusion path which in turn reduces the contact area between the solid and gas phase hence resulting in decreased sulphation. Larger particles exhibit transport limitations that affect the reaction rates thus decreasing the calcination and sulphation efficiencies. Larger particles also result in a larger unreacted core which decreases the extent of sulphation resulting in reduced sorbent utilization and reduced desulphurization efficiencies (Chi et al, 1994). Smaller size distribution particles also have a greater exposed surface area as it allows for a greater volume of sorbent particles to be packed between the sieve plates which allows for maximum desulphurization efficiency.

A similar trend is found for all the size fractions tested using both the gas mixtures. However, the desulphurization efficiencies that were found using the four gas mixture were significantly lower due to the phenomenon of sintering which increases the particle size thus having a diminishing effect on the desulphurization efficiency.

4.8. Overall Sorbent Efficiency Ranking

The overall sorbent ranking from the best to the worst is in the order C > D >B >A.

The Softness Index of the Sorbents were found to increase in relation to the ranking of the sorbents. The SEM image of the spent sorbent indicates that at the operating temperatures of the system cracks and fractures are present on the $CaSO_4$ product layer that is formed. This is due to the evolution of CO_2 during the calcination stage which leads to thermal stresses and internal overpressure (Scala et al, 2011). The particles with the higher softness index are susceptible to develop cracks more easily hence allowing for the unreacted inner core to be exposed. This will allow for greater SO_2 capture.

The physical property analysis revealed that the surface area, porosity and pore volume of Sorbent C exceed that of the other sorbents. The sulphur capturing capacity and reactivity of the limestone is increased if the BET surface area is large (Ogenga, 2010, Ho and Shih, 1992 and Ren Bin et al, 2003). It was found that a larger surface area results in better utilization of the sorbent hence improved desulphurization capacities (Lee et al, 2005). The large surface area is usually due to the presence of the impurities that modify the sorbent structure (Lee et al, 2007) such as the presence of the silica component (Hiroaki et al, 1996).

Sorbent C with the highest pore volume of approximately 0.0027m^3/g has the highest average desulphurization efficiency of nearly 34% and 29% for the three and four gas mixtures respectively. Sorbent D with an approximate pore volume of about 0.0024m^3/g has desulphurization efficiency exceeding 31% and 28% for the three and four gas mixtures respectively. The pore volume increases if the surface area is increased and largest pore volume has the highest desulphurization efficiency (Ogenga et al, 2010, Redeno et al, 2000). Cheng et al, 2004 tested limestone sorbents that had pore volumes between 0.002m^3/g and 0.005m^3/g. The desulphurization efficiencies for these sorbents were ranged between 25% - 40% which is in agreement with the results found in the current study.

Sorbent C with the highest desulphurization efficiency has the smallest average pore size while sorbent A with the lowest desulphurization efficiency has the largest average pore size. The results found are in agreement with Haji-Sulaiman and Scaroni, 1991. The small pores are not blocked as easily as the large pores hence they have a higher desulphurization efficiency. These results are also in support of the work undertaken by Han et al, 2005 where it was suggested that if the pores are too large, the surface area is reduced and the ratio of the surface area to pore volume decreases and this results in a negligible effect on sulphation.

Sorbent C with the largest porosity has the highest desulphurization efficiency which is then followed by sorbent D. Haji-Sulaiman and Scaroni, 1991, Ye and Bjerle, 1996 found that higher porosities result in greater desulphurization efficiency because sorbents with higher porosities are able to accommodate the calcium sulphate product, which has a higher molar volume as compared to the reactants, with more ease as compared to sorbents with a lower porosity. It was suggested that the sorbents with the higher porosities have improved desulphurization efficiencies as elevated porosity prevents plugging of the pores.

The Chemical composition of the sorbents was determined using the XRF and EDX analysis as described earlier. The major compounds detected in relatively substantial amounts were CaO, MgO, SiO_2, Al_2O_3 and Fe_2O_3.

Sorbent A with a CaO content of 44.5% has the lowest desulphurization efficiency for all of the size fractions tested. The highest desulphurization efficiency is found for the sorbent C with the highest CaO content of 53.49%. These results follow the general perception that the higher the CaO content, the better the desulphurization efficiency (Siagi et al, 2006 and Ogenga et al, 2010). Calcium has a significant role in the sulphur removal efficiencies because the product, $CaSO_4$ is stable at the operating temperatures (850-900℃) while the products of the other minor elements are not (Cheng et al, 2003).

In the results obtained Sorbent A with the largest MgO quantity has the lowest desulphurization efficiency. Sorbents C and D which have approximately 0.6% MgO have higher desulphurization efficiencies.This is because a large quantity of MgO can form a type of coagulative glue which reduces the pore sizes. This then prevents the easy access of SO_2 to the CaO as it causes a blockage and restricted diffusion hence reducing the desulphurization capacity of the sorbent (Carsky et al, 2006 and Chang et al, 1998).

Sorbent C with the highest silica content has the highest desulphurisation efficiency and this result may be due to the fact that the silica is a harder material than the $CaSO_4$ layer that is formed. The outer $CaSO_4$ layer is cracked as the reaction proceeds, and this leaves behind a greater exposed unreacted CaO surface that has silica present. This allows for improved reaction to occur and increases the desulphurization efficiency (Carsky et al, 2006). Hiroaki et al, 1996, Haji Sulaiman and Scaroni, 1991 found that the silica content modifies the sorbent structure and can improve desulphurization efficiency by up to 40%. The silicates bind to the $CaSO_4$ product that is formed and improves the stability of the product at the operating system temperature (Cheng et al, 2003). The presence of impurities such as silica results in delayed pore closures which enable improved desulphurization efficiencies and sorbent utilization.

Alumina is known as an additive that is present to enhance the desulphurization efficiency by modifying the sorbent physical structure. The presence of alumina assists in maintaining a more open porous structure during sulphation. Maintenance of the pore network within the sorbent structure allows for increased desulphurization efficiency and increased sorbent utilization. Gavalas et al, 1987 suggested that the alumina improves the desulphurization ability as it acts as a catalyst.

The ranking of the sorbents indicate that sorbents A and B have lower desulphurization efficiencies and sorbents C and D have higher efficiencies. According to previous studies, there exists a range of Fe_2O_3 content for which the desulphurization efficiency increases, after which Fe_2O_3 content has a negative effect on the desulphurization efficiency. The investigation performed by Cheng et al, 2004 tested limestone with Fe_2O_3 content of 0.008-0.3%. It was found that in this range the Fe_2O_3 enhanced the desulphurization efficiencies. This finding supports the ranking of Sorbents D and C with an Fe_2O_3 range between 0.14 – 0.26% having the higher efficiencies.

Dam- Johansen and Ostergaard, 1990 concluded that the presence of ferric oxide has very adverse effects on sulphation capacity. The results obtained for the ranking of Sorbents A and B with higher Fe_2O_3 are in agreement with the work undertaken by Koval, 1982. It was found that the presence of impurities such as Fe_2O_3 has a significant effect on the progression of sintering. Fe_2O_3 increases the rate of sintering in limestone and dolomite sorbents. Sintering reduces the surface area and increases the pore sizes which results in reduced desulphurization and conversion. The research conducted by

Koval, 1982 established that the rate of sintering is significantly increases at the addition of approximately 0.4% Fe_2O_3 which explains the results obtained.

The work conducted by Haji Sulaiman and Scaroni, 1991 indicated that a 1% presence of Fe_2O_3 is substantial to promote sintering during calcination. The range found from literature then explains why the Fe_2O_3 presence decreases the sulphation capacity between 0.40% - 1%.

In recent years it is becoming a well-established trend to modify the sorbent structure through the addition of the above mentioned additives. These additives enhance the sorbent performance and improve the desulphurization capacity substantially.

4.9. Sorbent Conversion

The conversion of the different size fractions of the four sorbents were calculated using the outlet SO_2 concentration and time data points that were obtained from the SO_2 analyser.
The algorithm to generate the conversion curve is illustrated below.

Point Area which is defined as the area representing the SO_2 present at an instant in time. (P_i)

$$P_i = \frac{C_{SO_2(i+1)} + C_{SO_2(i)}}{2} \times (t_{i+1} - t_i) \quad (4.5)$$

Where C_{SO_2} and t represents the concentration and time data that is logged by the analyser.
Area of the concentration vs. time curve seen in figure 4-10 at each point in time is defined as A.

$$A_i = P_i + A_{i-1} \quad (4.6)$$

The concentration of $S0_3$ present at each instant in time is defined as:

$$C_{SO_3(i)} = \left(C_{SO_2(initial)} - C_{SO_2(final)}\right) \times t_{i+1} \quad (4.7)$$

Where the initial SO_2 concentration is the value logged when the gas flows through the bypass line and the final concentration is the value where the data remains stable after the reaction has occurred and t_{final} is the time at which the final concentration data is logged.

$$C_{SO_2(present\ at\ i)} = C_{SO_2(final)} \times t_{i+1} \quad (4.8)$$

$$C_{SO_2(removed\ at\ i)} = C_{SO_2(present\ at\ i)} - A_i + C_{SO_3(i)} \quad (4.9)$$

The conversion at an instant in time is represented below.

$$X_i = \frac{C_{SO_2(removed\ at\ i)}}{C_{SO_2(initial)} \times t_{final}} \quad (4.10)$$

X_i is calculated at each time the data is logged, and this is then used the generate the conversion plot.

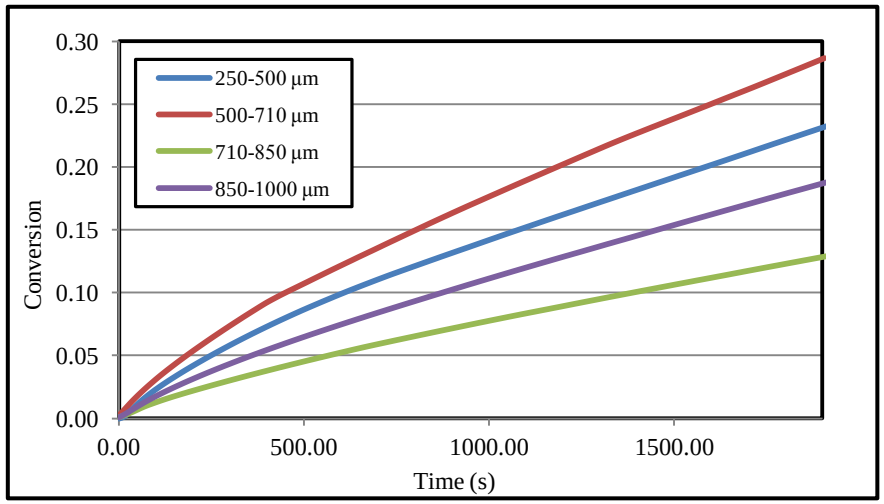

Figure 4-15: Conversion vs. time (Sorbent A)

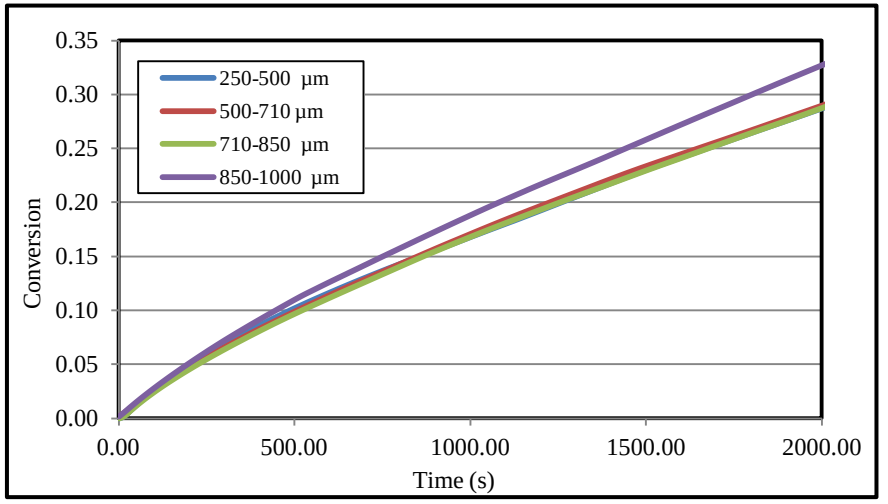

Figure 4-16: Conversion vs. time (Sorbent B)

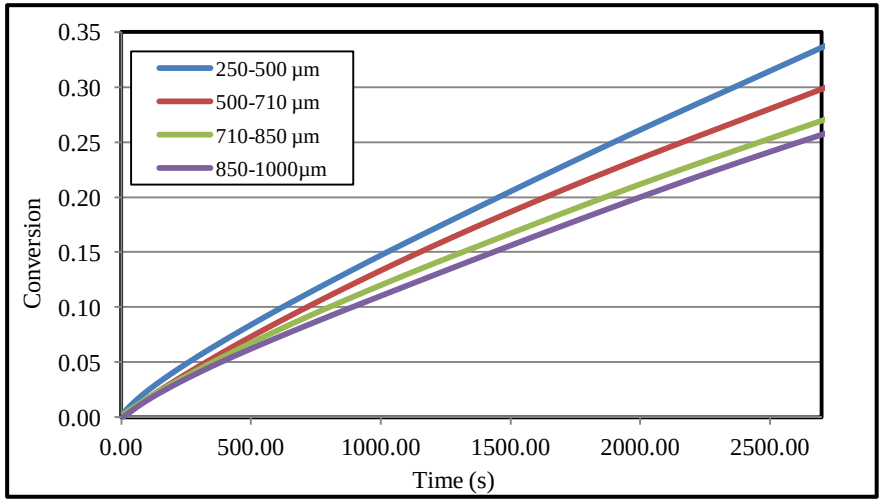

Figure 4-17: Conversion vs. time (Sorbent C)

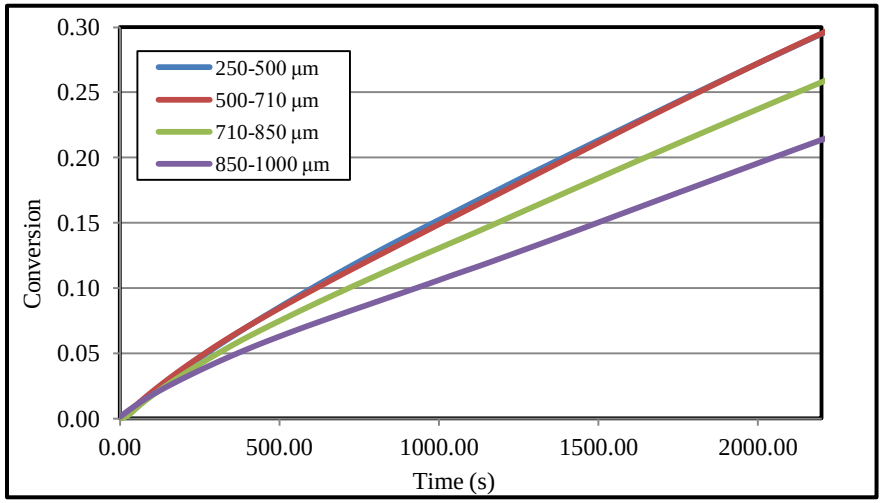

Figure 4-18: Conversion vs. time (Sorbent D)

Plots of Conversion vs. time for the Different Size Fractions and Sorbents Tested using the Three Gas Mixture

The plots above of conversion vs. time for each of the sorbents at different size fractions are represented above. A comparison can be made between the conversions of different sized particles for any sorbent at any instant in time. It can be seen for sorbent A that in general the smaller size fractions have a higher conversion at any instant in time. However this is not true for comparison between the 250 μm and 500 μm size fraction as well as the 710 μm and 850 μm particle size. This may be due to the manner in which particles break during the milling procedures. The impurities such as the silica that is present is usually harder and difficult to mill and may remain intact on the larger size fractions enhancing the sorbent physical structure thus enabling higher conversion. An increase in particle size resulting in increased conversion can be explained with the conclusion obtained from the work performed by Chu et al, 2000. It was suggested that larger particles have decreased surface area which results in a decrease in the product layer formation and plugging of the surface pores that in turn results in a reduction in the diffusion limitation. This then allows for higher conversion levels to be achieved.

For Sorbent B, a comparison of conversion at 500 seconds indicates that the highest conversion is for the 850-1000 μm sample. However all other size fraction show increasing conversion as the particle sizes are reduced. Sorbent C and D clearly indicate the general perception that smaller size fractions have increased level of conversion. This result is due to the improvement of the gas-solid contact and reaction efficiency that is attained with the use of smaller size distributions. This is in agreement with Chi et al, 1994 who concluded that larger particles result in unsulphated cores and reduced conversion levels. Smaller particle diameters result in improved conversion for constant mass of sample used as a greater reaction surface is generated due to the existence of an increased number of sorbent particles in the reactor (Ibrahim and Eliass, 2010). Larger particles may also have mass transfer limitations due to deeper lying pores and thicker gas films hence higher conversion may not be achieved (Ye and Bjerle, 1996).

Cheng et al, 2003 found that the use of particles between 5-100 μm would allow for approximately 50% conversion and desulphurization efficiency of sorbent particles. This explains why the maximum conversion obtained is below 40% as the smallest particles used are between 250-500 μm. Chang et al, 1998 concluded that conversion levels are below 30% which is in support of the herein work conducted.

The conversion levels attained in the experimental work is in agreement with that obtained by Mattison and Lyngfelt, 1998 and Montagnaro et al, 2010. It was found that at atmospheric conditions, conversion levels do not exceed 30-40%. This is due to the formation of a $CaSO_4$ product layer on the shell of the particle which induces diffusional resistances. This diminishes the rate of sulphation and prevents any further reaction from occurring.

The conversion levels attained are also in agreement with the work conducted by Montagnaro et al, 2002. Particles used in the experiments were between 425-600 μm at conditions of 850 ℃ over a reaction period of three hours. The conversion levels attained were between 23.7% and 37.5 % which is fairly similar to the results obtained. The low conversion levels that are obtained in the current work can also be explained using the pore plugging phenomenon. The molar volume of CaO, $CaCO_3$ and $CaSO_4$ is 16.9 cm^3/mol, 36.9 cm^3/mol and 52.2 cm^3/mol respectively. The stoichiometric relationship between $CaCO_3$ and $CaSO_4$ indicates that a mole of $CaCO_3$ results in the formation of one mole of $CaSO_4$ however the volume that is occupied by the $CaSO_4$ is much greater than that which is occupied by $CaCO_3$. This larger volume of solid products can then plug the pores and the pore entrances of the sorbent which prevents the inner surface of the sorbent from reacting thus resulting in poor sorbent utilization which results in low overall sorbent conversion.

4.10. Modelling of the Desulphurization Process

Various models that can be used to represent the desulphurization process. Such models include the shrinking core model, the grain size model, single pore model and the random pore model as discussed in the literature review. In the work presented, the shrinking core model (SCM) was implemented to represent the experimental data. A study into the other models indicated that this was the most suitable model due to the low sorbent porosities. The grain model could not be used to represent the system as it sufficiently describes sorbents with porosities greater than 0.4 and the sorbents under study had a maximum porosity of only 0.006 (Neeraj, 2001).

4.10.1. The Objective of Modelling

It is essential to note that although two grams of sample were placed within the reactor bed for each test run, sample still remains unreacted. The conversion of CaO to $CaSO_4$ is represented by equation 2.9.

$$CaO(s) + SO_2(g) + \frac{1}{2}O_2(g) \leftrightarrow CaSO_4(s)$$

A solid layer of calcium sulphate forms on the outer surface of the sorbent. This layer separates the sorbent from the gas phase hence resulting in reduced conversion. It reduces heat and mass transfer to the core thus is a major limitation to conversion. Analysis of the spent sorbent steered the modelling procedure to be based on the shrinking core model with negligible diffusion resistance in the gas film and rate determining steps being product layer diffusion and surface reaction. The use of this model (SCM) enables one to achieve an improved understanding of the rate controlling mechanisms and to

determine the various parameters such a reaction rate constants and diffusivities (Zevenhoven et al, 1996).

4.10.2. The Experimental Results to be Modelled

It was decided that the sulphation test results that were obtained for the various size fractions of sorbents A, B, C, and D using the gas mixture comprised of 2000 ppm SO_2, 20% O_2 and balance N_2 would be modelled. This allowed for the comparison of results for the different size fractions of the different sorbents. The experimental data obtained for Sorbent C using the four gas mixture, was also modelled in order to establish the influence of the presence of CO_2.

4.10.3. Shrinking Core Model Equations

The simple Shrinking core model that was implemented incorporates the chemical reaction and product layer diffusion controlling steps. The equation then becomes (Mchabe, 2011):

$$t = t_{kin}A(X) + t_{dif}B(X) \quad (4.11)$$

This equation is a representative of the overall reaction time that includes both the steps mentioned above.

The kinetic and diffusion parameters are t_{kin} and t_{dif} respectively.

$$t_{kin} = \frac{\rho_{mol,CaO}R_P}{bk_sC_{SO_2}} \quad (4.12)$$

$$t_{dif} = \frac{\rho_{mol,CaO}{R_p}^2}{6bD_{dif}C_{SO_2}} \quad (4.13)$$

Where: $\rho_{mol,\,CaO}$ − molar density (mol/m^3)

R_P − average particle size (m)

C_{SO_2} − Bulk concentration (mol/m^3)

k_s − Reaction rate constant (m/s)

D_{dif} − Diffusivity constant (m^2/s)

b − Stoichiometric coefficient

A(X) and B(X) account for the size reduction of the core as conversion proceed in the reactor stipulated by the Shrinking Core Model.

$$A(X) = 1 - (1 - X)^{\frac{1}{3}} \quad (4.14)$$

$$B(X) = 1 - 3(1 - X)^{\frac{2}{3}} + 2(1 - X) \quad (4.15)$$

4.10.4. Rate Determining Mechanisms

The rate determining step can be obtained using the (t, X) data set by plotting F(X) vs. t/τ. The F(X) is represented by either A(X) or B(X) as reaction controlled or diffusion controlled respectively. The time scale τ follows directly from the slope of this line and represents t_{kin} or t_{dif} . The plot of A(X) has a greater slope than the B(X). This indicates that the surface reaction is a slower mechanism than the gas diffusion and this mechanism contributes more to the overall resistance than the gas diffusion.

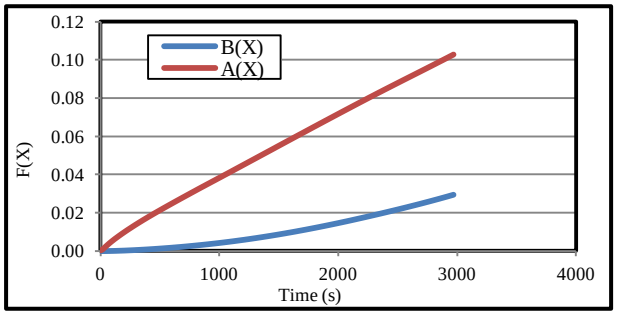

Figure 4-19: 3 Gas Mixture (850-1000 µm)

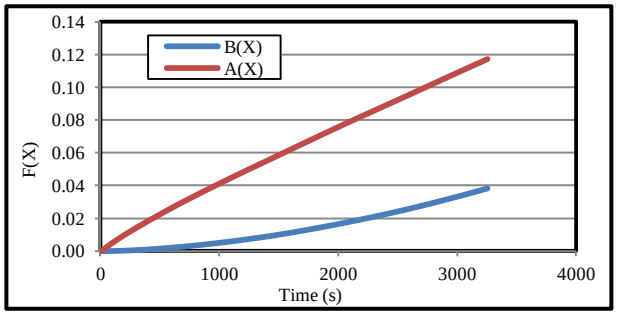

Figure 4-20: 3 Gas Mixture (710-850 µm)

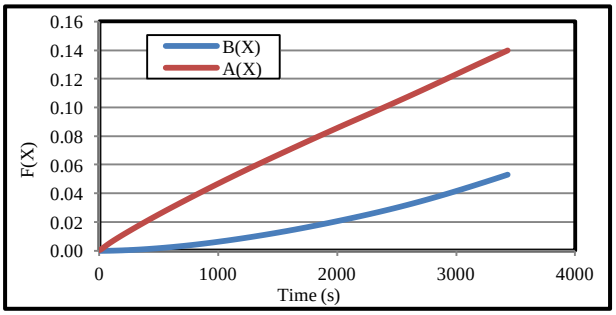

Figure 4-21: 3 Gas Mixture (500-710 µm)

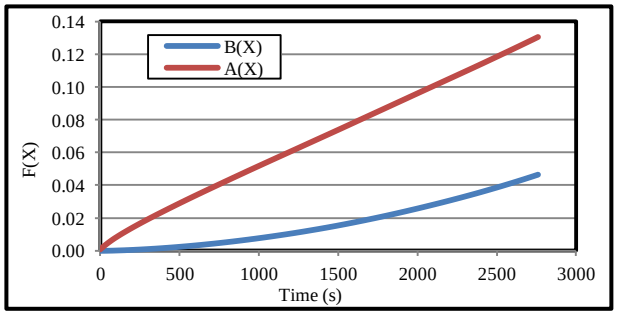

Figure 4-22: 3 Gas Mixture (250-500 µm)

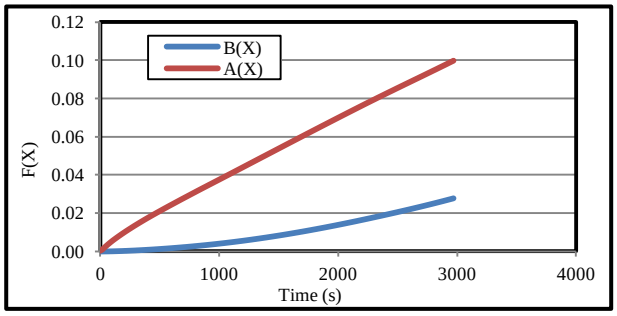

Figure 4-23: 4 Gas Mixture (850-1000 µm)

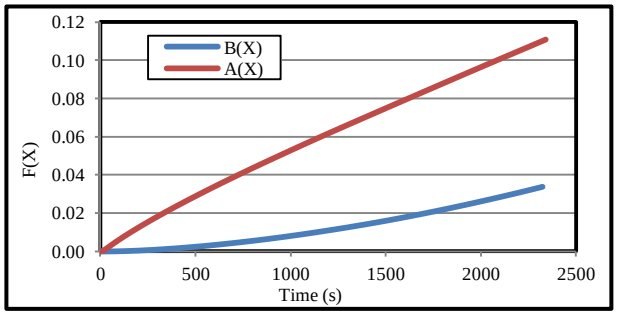

Figure 4-24: 4 Gas Mixture (710-850 µm)

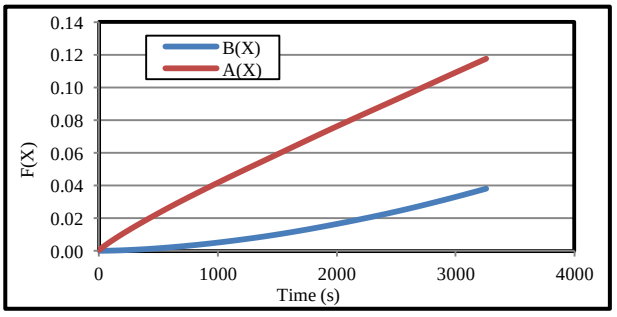

Figure 4-25: 4 Gas Mixture (500-710 µm)

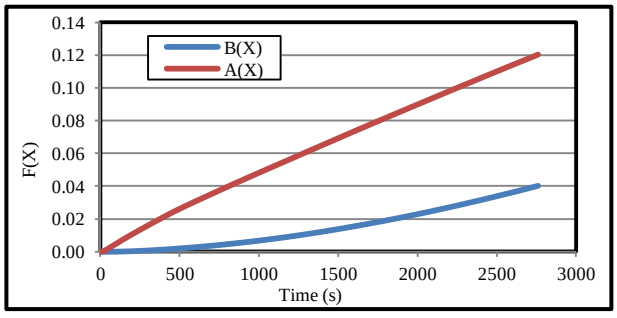

Figure 4-26: 4 Gas Mixture (250-500 µm)

Graphical Representation of the Rate Determining Mechanisms for the different size fractions of Sorbent C using the Different Gas Mixtures

4.10.5. Variable Effective Diffusivity Approach

The simple unreacted shrinking core model as described has various limitations. This model does not account for the conversion differences between sorbents that are chemically similar but physically different (Zevenhoven et al, 1998). The unreacted shrinking core model with variable effective diffusivity (USC-VED) takes into account the various parameters that are derived from the physical texture of the sorbent such as the density, porosity, particle sizes and average pore sizes. This model modification approach was first incorporated in the work conducted by Krishnan and Sotirchos, 1993. Work performed by Rahmani and Sobrabi, 2006 also used the variable diffusivity approach to represent the kinetics of the system.

4.10.6. Kinetic Modelling (USC-VED)

Chemical Kinetics

Using the assumption that the reaction is first order with respect to SO_2

$$\tau_{kin} = \frac{\rho_{mol,CaO} R_P}{b k_s C_{SO_2}} \quad (4.16)$$

$$f_{kin}(X) = 1 - (1 - X)^{\frac{1}{3}} \quad (4.17)$$

$$\rho_{mol,CaO} = \frac{\rho_{sorbent} x_{CaO}}{M_{CaO}} \quad (4.18)$$

Intra-Particle Diffusion

$$\tau_{dif} = \frac{\rho_{mol,CaO} {R_p}^2}{6 b D_{dif} C_{SO_2}} \quad (4.19)$$

$$f_{dif}(X) = 3\left[\frac{Z - \left(Z + (1-Z)(1-X)\right)^{\frac{2}{3}}}{Z-1} - (1 - X)^{\frac{2}{3}}\right] \quad \text{if } Z \neq 1 \quad (4.20)$$

$$Z = \frac{V_{mol\ product}}{V_{mol\ reactant}} \quad (4.21)$$

Z is the stoichiometric ratio of the solid product and the solid reactant phases (Krishnan and Stroitchos 1993). Z was found to have a value of 2.71.

When both these mechanisms are rate controlling, the total time is the sum of the various mechanisms and is expressed as the following:

$$t = \tau_{kin} f_{kin}(X) + \tau_{dif} f_{dif}(X) \quad (4.22)$$

Effective diffusivity accounts for pore and product layer diffusion. The assumption made is that these processes occur in series. This is based on the temperature and the physical structural properties of the

sorbent. Combining the porous and product layer results in effective diffusivity (D_{eff}) which is based on volume fractions that change as the reaction proceeds.

$$\frac{V_{pore}+V_{pl}}{D_{eff}} = \frac{V_{pl}}{D_{pl}} + \frac{V_{pore}}{D_{pore}} \quad (4.23)$$

$$V_{pl} = (1-\epsilon_0)XZ \quad (4.24$$

$$V_{pore} = \epsilon_0 - (1-\epsilon_0)(Z-1)X \quad (4.25)$$

Gas diffusion within a porous solid with porosity (ε) and tortuosity(γ) is a function of molecular and Knudsen diffusion. The tortuosity is assumed to be 3 as based on the work undertaken by previous researchers. (Zevenhoven et al, Mukondiwa, 2007):

$$D_{pore} = D_{mol+kn}\frac{\varepsilon}{\gamma} \quad (4.26)$$

D_{mol+kn} represents the combination of molecular and Knudsen diffusion that occurs in the gas phase with the porous solid. Values with a magnitude of $10^{-6}m^2/s$ were calculated for the combined molecular and Knudsen diffusion.

$$\frac{1}{D_{mol+kn}} = \frac{1}{D_{mol}} + \frac{1}{D_{kn}} \quad (4.27)$$

The Knudsen diffusivity is expressed as a function of the average pore size of the particles.

$$D_{kn} = 97\, r_{av}\sqrt{\frac{T}{M_{SO_2}}} \quad (4.28)$$

The molecular diffusivity is based on the mixture of gases and is determined from a correlation proposed by Fuller, Schettler and Giddings (Perry et al, 2008):

$$D_{mol} = \frac{10^{-3}T^{1.75}\left[\frac{1}{M_A}+\frac{1}{M_B}\right]^{\frac{1}{2}}}{P\left[(V_{N_2})^{\frac{1}{3}}+(V_{SO_2})^{\frac{1}{3}}\right]^2} \quad (4.29)$$

Combining the equations results in a relationship between effective diffusivity and conversion:

$$D_{dif}(X) = \frac{\epsilon_0+(1-\epsilon_0)X}{\frac{3}{D_{mol+kn}}+\frac{Z(1-\epsilon_0)X}{D_{pl}}} \quad (4.30)$$

To obtain a simple expression for variable diffusivity, parameters A and B are introduced, where A is depends on the initial porosity and B is ontained from time-conversion data set.

$$A = \frac{1-\epsilon_0}{\epsilon_0} \quad (4.31)$$

$$B = \frac{Z(1-\epsilon_0)D_{mol+kn}}{3\,D_{pl}} = \frac{AZD_{dif,0}}{D_{pl}} \quad (4.32)$$

$$D_{dif} = D_{dif,0}\frac{1+AX}{1+BX} \quad (4.33)$$

$$D_{dif,0} = D_{pore,0} = D_{mol+kn}\frac{\varepsilon_0}{\gamma} \quad (4.34)$$

The ε_0 is the initial porosity of the sorbent that is determined experimentally and the tortuosity factor γ is estimated as 3 from previous studies conducted by Dam-Johansen et al, 1991.

The USC-VED can be simplified and generalized to yield the following basic modelling equation:

$$t = \tau_{kin}f_{kin}(X) + \tau_{dif,0}\frac{1+BX}{1+AX}f_{dif}(X) \quad (4.35)$$

4.10.7. Numerical and Regression Procedure

MATLAB™

The experimental conversion was calculated using the SO_2 concentration profile. A plot of experimental conversion vs. time was then generated. The experimental conversion was then used to calculate the predicted time of the overall model equation with initial guesses for the kinetic (t_{kin}) and diffusion parameters (t_{dif}) when using the simple shrinking core model.

When the variable effective diffusivity model was implemented, using equation 4.35, there were two unknown parameters that required initial guesses, τ_{kin} and B. The parameter A was calculated using equation 4.31. $\tau_{dif,0}$ is the initial time scale prior to diffusion and is estimated using equation 4.19 with $D_{dif,0}$ calculated using equation 4.34.

The sum of square errors between the calculated and experimental time was then minimized using the in-house fminsearch function and the regression procedure allowed for the determination of the kinetic (t_{kin}) and diffusion parameters (t_{dif}) as well as parameter B and the kinetic time scale (τ_{kin}). MATLAB™ implements a rigorous non-linear regression technique that converges at the global minimum allowing for accurate model fitting and reliable parameter estimation. The procedure outlined above was implemented using different forms of the overall shrinking core model equations namely diffusion controlled, kinetic controlled and a combination of the two as well as the USC-VED model.

MICROSOFT EXCEL™

A similar mathematical approach was adopted in EXCEL however due to the sensitivity of the results on initial guesses for kinetic and diffusion parameters, the regressed MATLAB™ results were used as initial guesses. The sum of square errors between the calculated and experimental time was then minimized using solver and the regression procedure allowed for the determination of the kinetic and diffusion parameters. This procedure was implemented using different forms of the overall shrinking core model equations namely diffusion controlled, kinetic controlled and a combination of the two.

4.10.8. Shrinking Core Model Results and Verification

The various forms of the simple shrinking core model predictions namely diffusion controlled, reaction controlled and a combination of the two as well as the modified shrinking core model with variable effective diffusivity were compared to the experimental data in the form of conversion vs. time profiles.

Results clearly indicate that the simple shrinking core model with combined effects of the reaction and diffusion best describes the data set. This simple model is described by equations 4.11 – 4.15. Individual reaction kinetics being the rate controlling step was also a good model prediction of the observed data as compared to the model being diffusion controlled. This is be verified by the larger slope of A(X) illustrated in figures 4-34 to 4-41 which indicate that this mechanism contributes more towards the rate of reaction.

The shrinking core model with variable effective diffusivity model, does not provide a suitable fit for experimental data as can be seen in the figures presented below and is therefore omitted from numerical results going forward.

Modelling Results

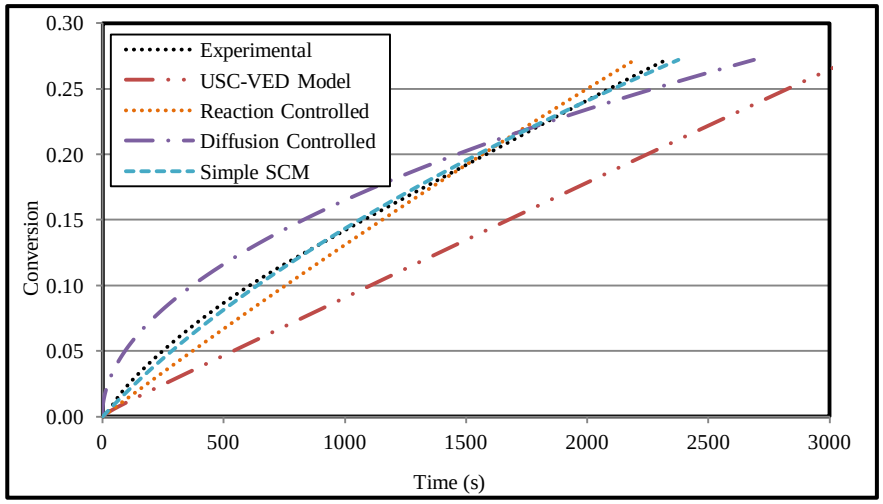

Figure 4-27: Conversion vs. time (250-500 µm)

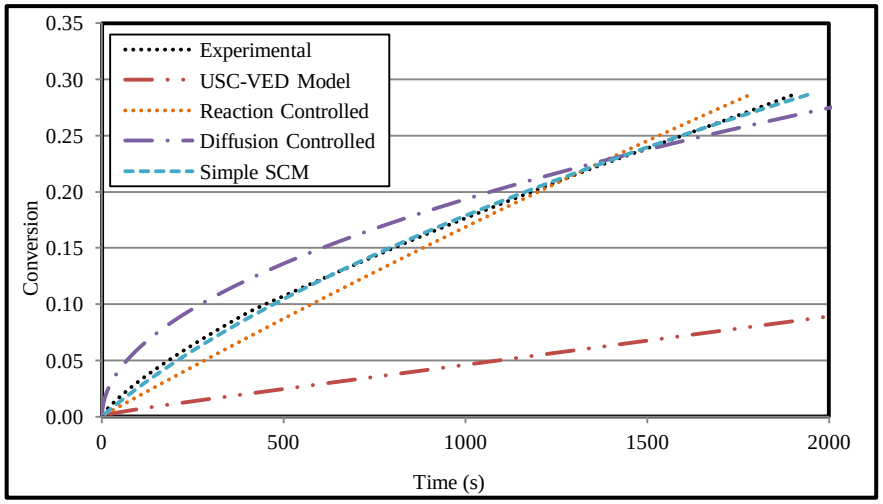

Figure 4-28: Conversion vs. time (500-710 µm)

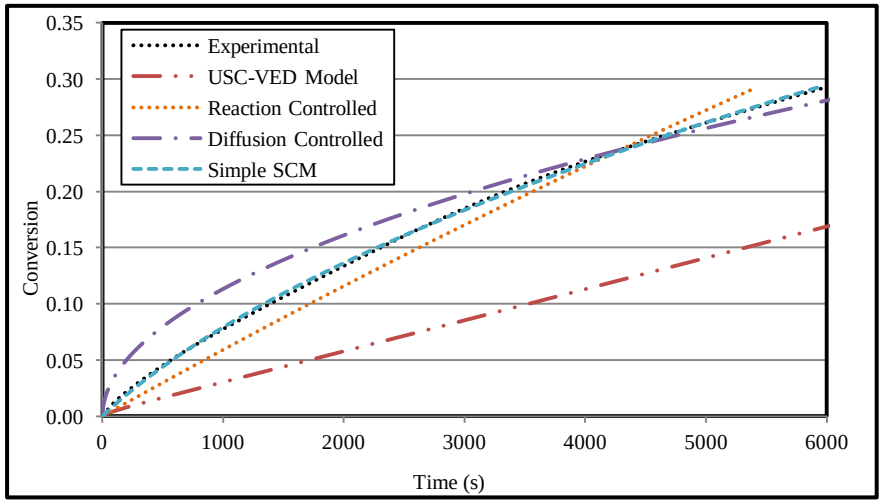

Figure 4-29: Conversion vs. time (710-850 µm)

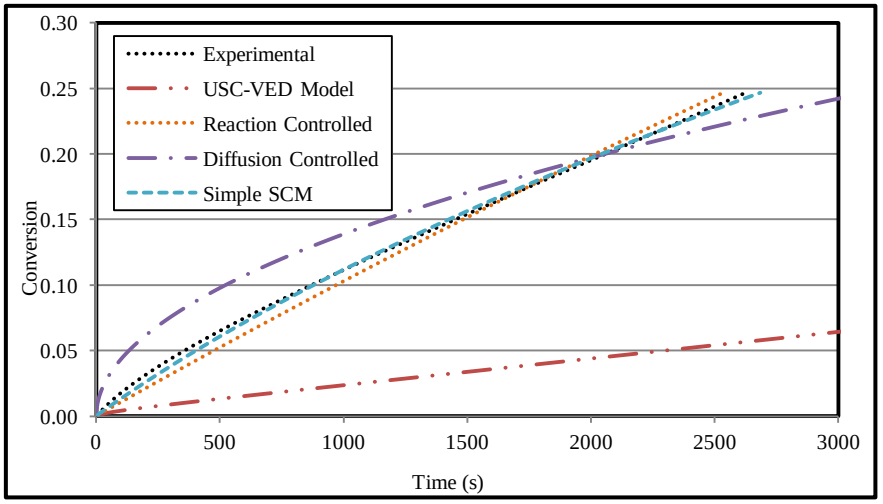

Figure 4-30: Conversion vs. time (850-1000 µm)

Graphical Representation of Experimental and Calculated Conversion over a Period for the different size fractions of Sorbent A

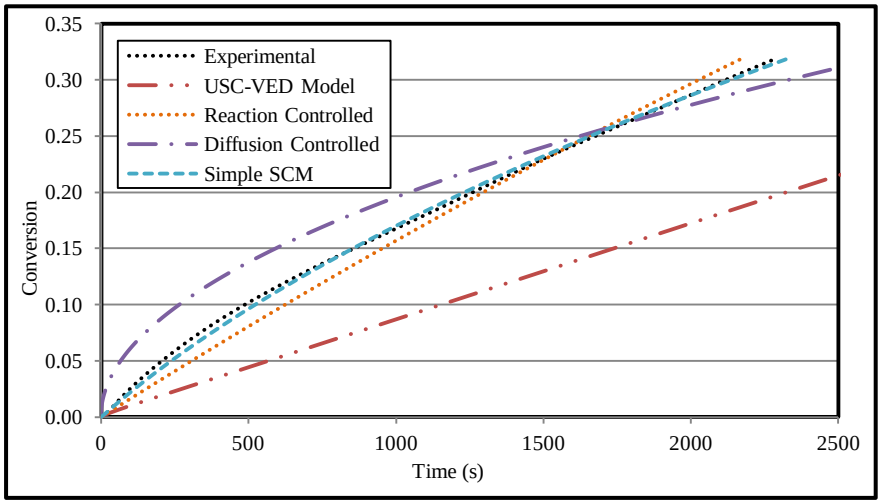

Figure 4-31: Conversion vs. time (250-500 µm)

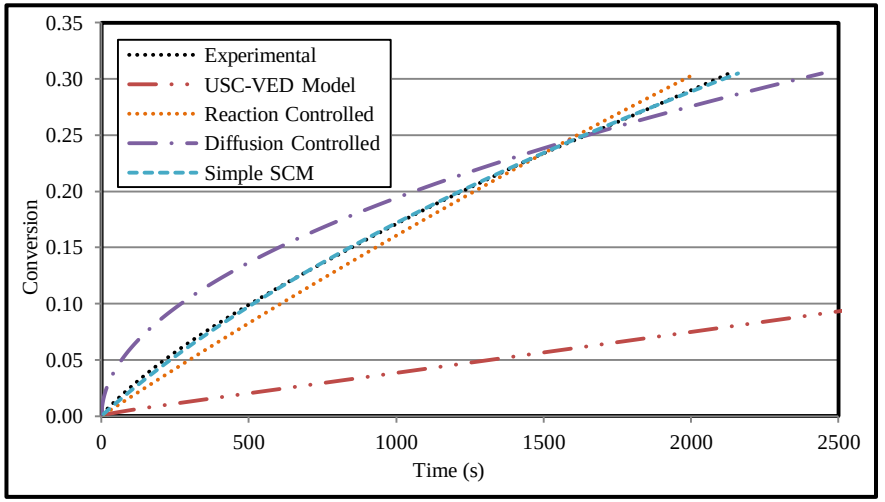

Figure 4-32: Conversion vs. time (500-710 µm)

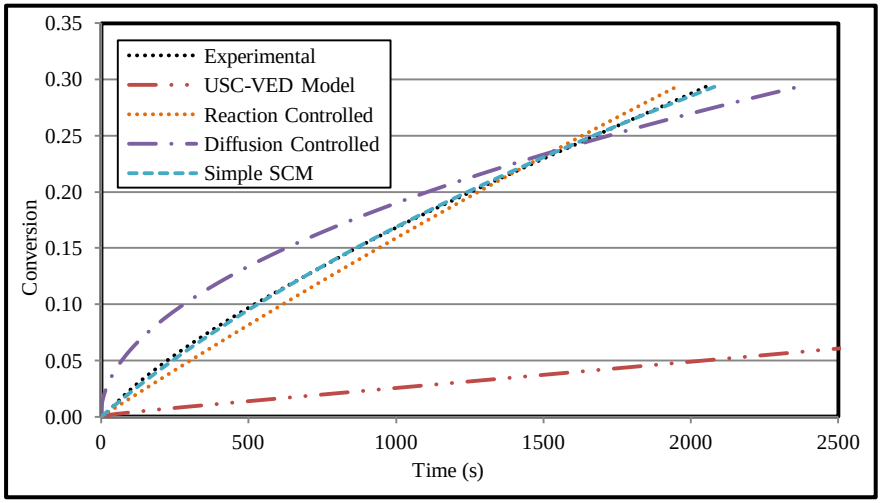

Figure 4-33: Conversion vs. time (710-850 µm)

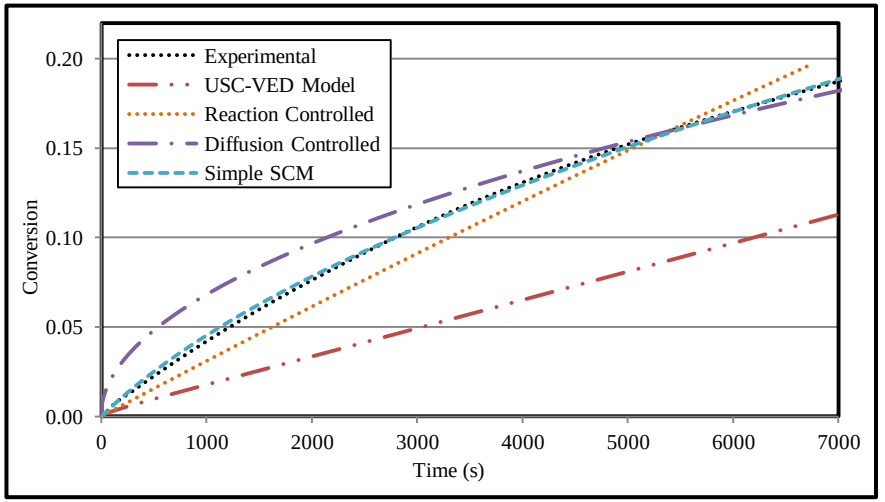

Figure 4-34: Conversion vs. time (850-1000 µm)

Graphical Representation of Experimental and Calculated Conversion over a Period for the different size fractions of Sorbent B

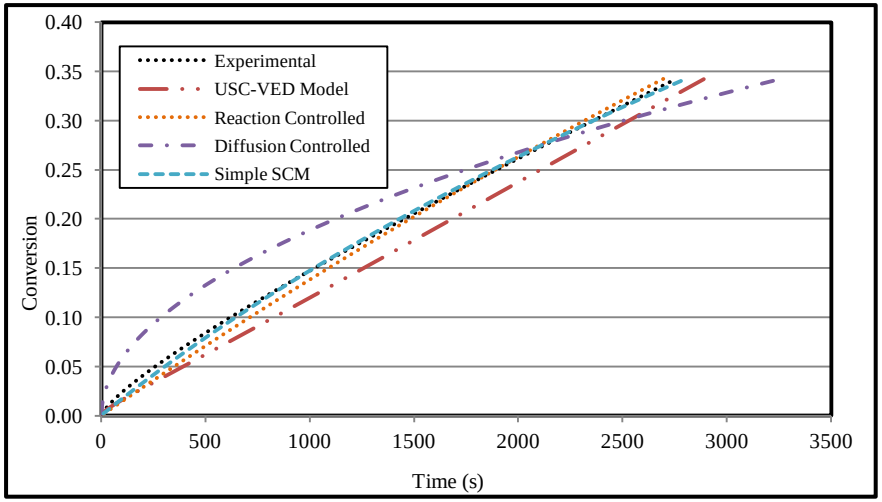

Figure 4-35: Conversion vs. time (250-500 µm)

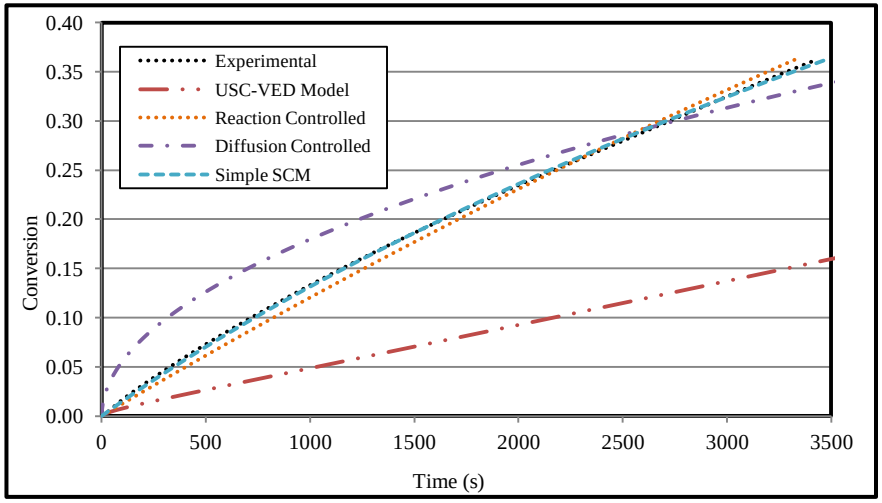

Figure 4-36: Conversion vs. time (500-710 µm)

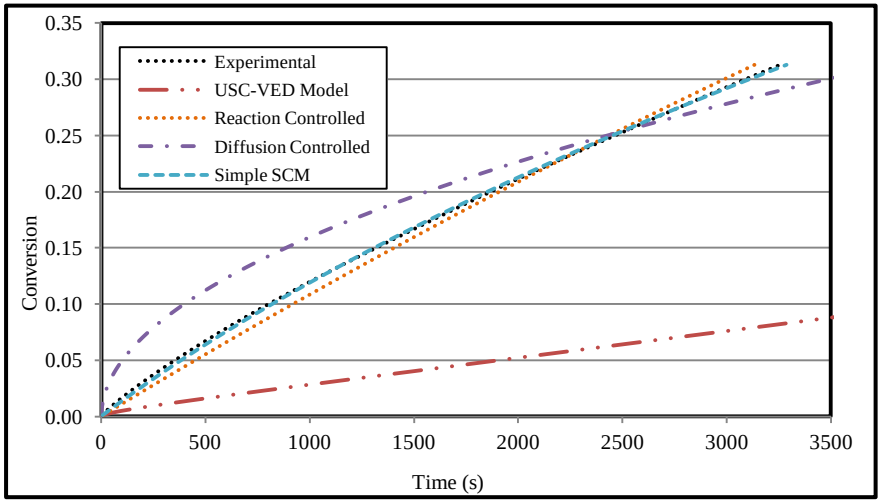

Figure 4-37: Conversion vs. time (710-850 µm)

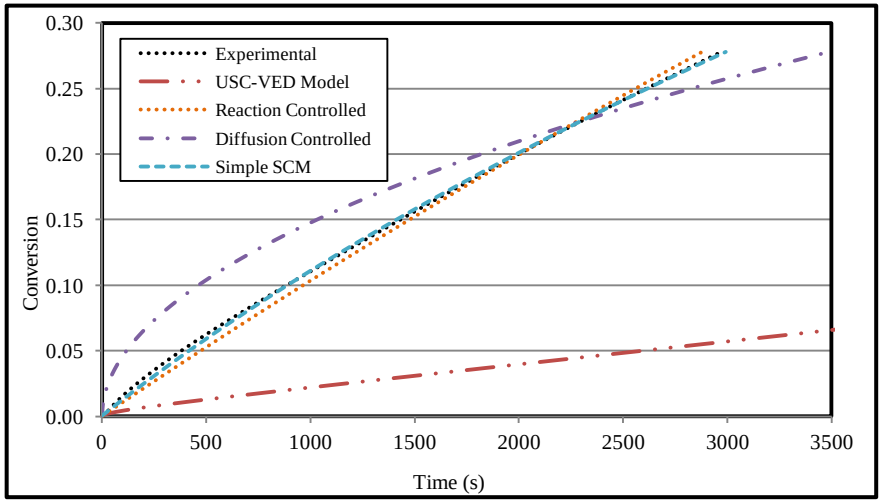

Figure 4-38: Conversion vs. time (850-1000 µm)

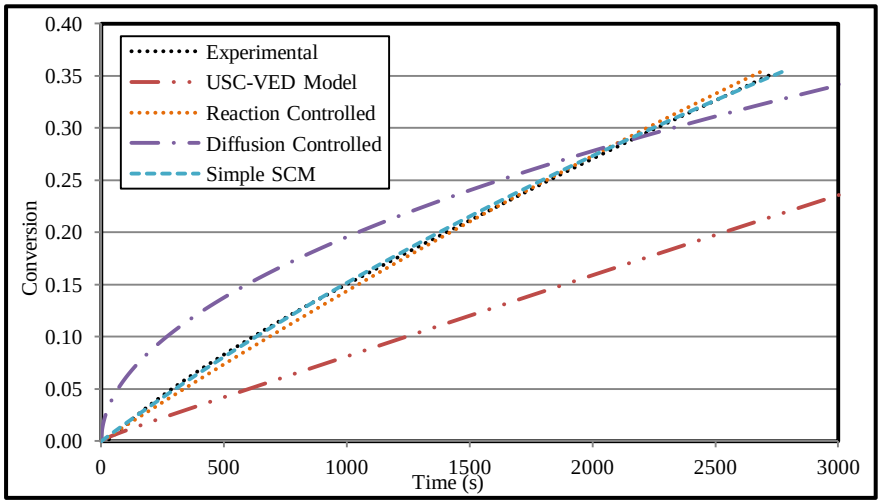

Figure 4-39: Conversion vs. time (250-500 µm)

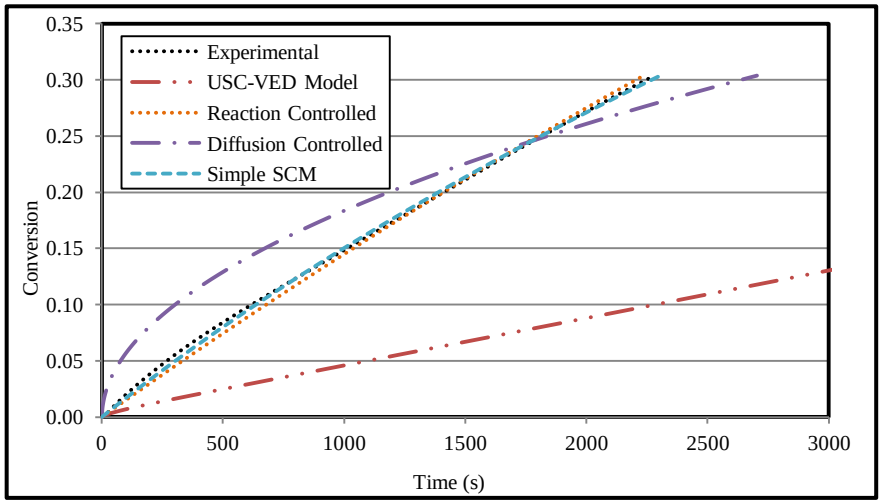

Figure 4-40: Conversion vs. time (500-710 µm)

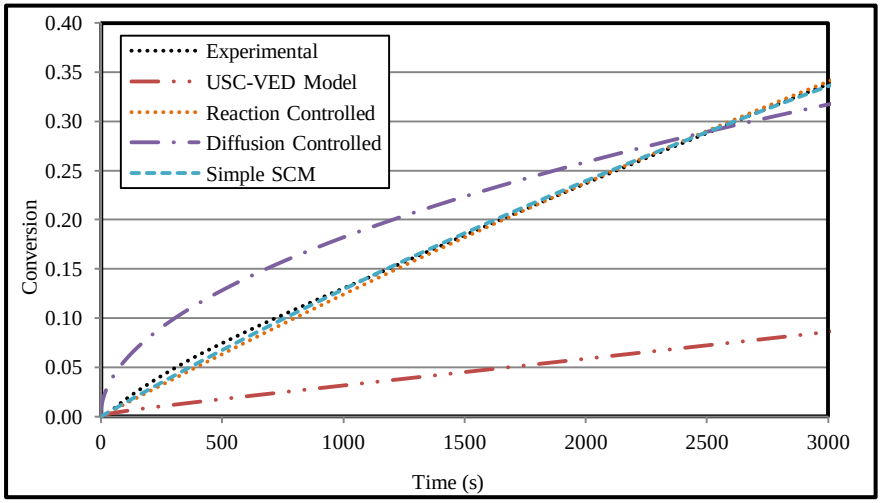

Figure 4-41: Conversion vs. time (710-850 µm)

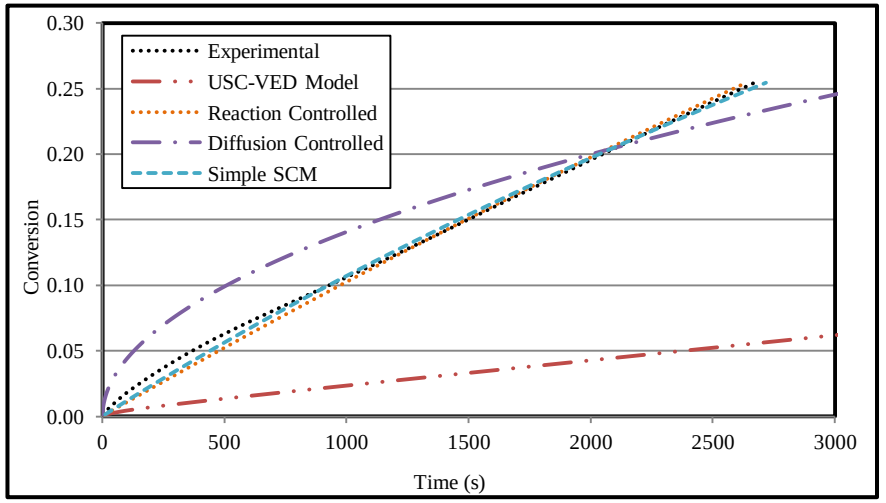

Figure 4-42: Conversion vs. time (850-1000 µm)

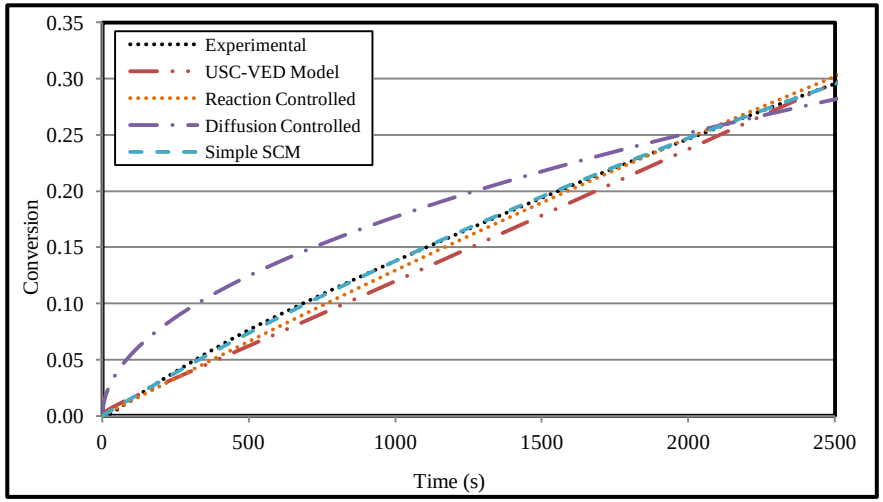

Figure 4-43: Conversion vs. time (250-500 µm)

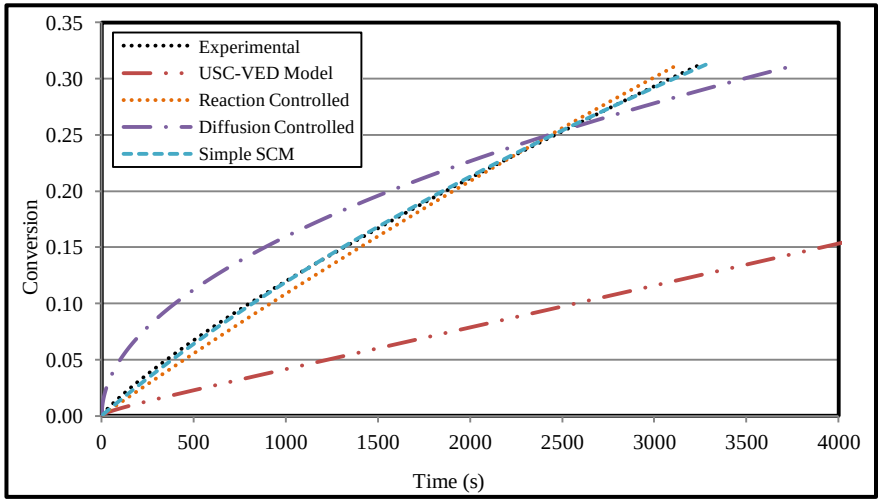

Figure 4-44: Conversion vs. time (500-710 µm)

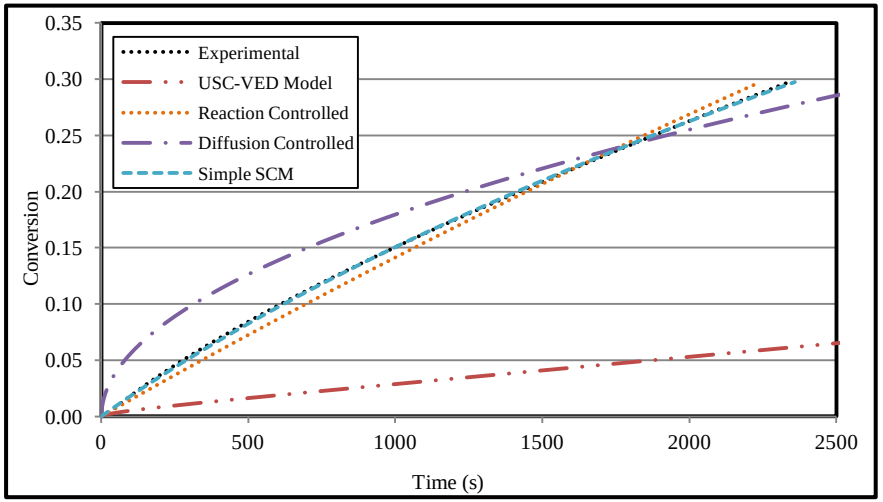

Figure 4-45: Conversion vs. time (710-850 µm)

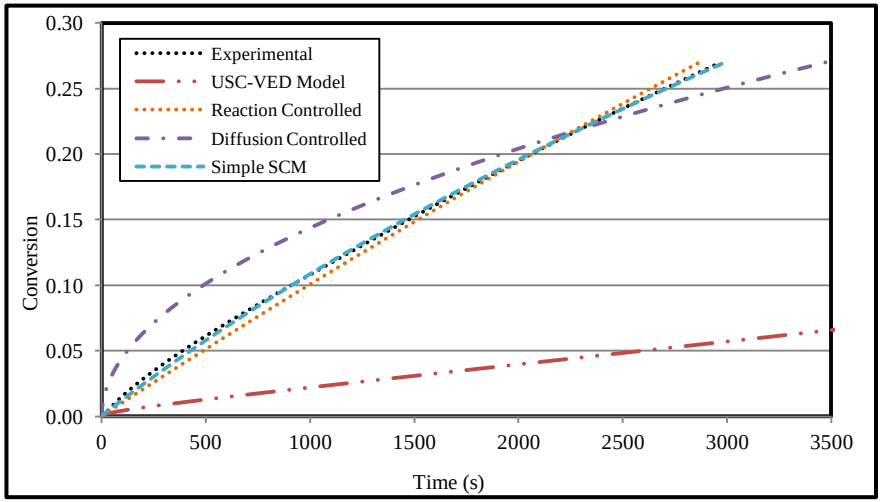

Figure 4-46: Conversion vs. time (850-1000 µm)

Table 4-12: Constants and Regression Parameters for the SCM: Individual Reaction and Diffusion controlling Mechanisms

Individual Reaction and Diffusion Controlling Mechanism					
	Size Fractions (μm)	t_{kin}	k_s	t_{dif}	D_{dif} (× 10^{-7} m^2/s)
Sorbent A (3 Gas Mixture)	250-500	21871.75	0.009	42178.17	1.473
	500-710	16753.23	0.019	30781.05	5.252
	710-850	49723.43	0.008	88341.71	3.042
	850-1000	28160.60	0.017	59344.20	6.369
Sorbent B (3 Gas Mixture)	250-500	18067.72	0.012	30109.04	2.312
	500-710	17667.71	0.022	30638.20	5.914
	710-850	17851.40	0.026	31996.28	9.413
	850-1000	95567.92	0.006	242467.22	1.747
Sorbent C (3 Gas Mixture)	250-500	20675.97	0.010	32415.72	2.057
	500-710	23856.30	0.014	35484.74	4.890
	710-850	26622.24	0.017	44989.75	6.411
	850-1000	27994.88	0.019	52510.00	7.724
Sorbent D (3 Gas Mixture)	250-500	19792.87	0.010	30017.06	2.157
	500-710	19647.35	0.017	34055.46	4.948
	710-850	23154.75	0.019	34703.69	8.071
	850-1000	28293.83	0.018	57740.62	6.822
Sorbent C (4 Gas Mixture)	250-500	22150.25	0.010	36634.56	1.820
	500-710	26622.24	0.013	44989.75	3.857
	710-850	20203.20	0.024	35685.08	8.082
	850-1000	28778.05	0.018	55316.63	7.332

Table 4-13: Constants and Regression Parameters for the SCM: Combined Reaction and Diffusion Controlling Mechanisms

Combined Reaction and Diffusion Controlling Mechanisms					
	Size Fractions (μm)	t_{kin}	k_s	t_{dif}	D_{dif} (× 10^{-7} m^2/s)
Sorbent A (3 Gas Mixture)	250-500	15008.76	0.013	13652.29	4.550
	500-710	10867.37	0.030	11121.21	0.145
	710-850	29241.53	0.014	37220.15	7.220
	850-1000	22150.00	0.022	13157.39	0.287
Sorbent B (3 Gas Mixture)	250-500	12819.02	0.017	901.34	7.719
	500-710	12654.48	0.028	8962.47	0.202
	710-850	13142.81	0.035	8714.26	0.346
	850-1000	51424.87	0.011	114413.30	3.702
Sorbent C (3 Gas Mixture)	250-500	17387.87	0.012	5353.47	0.125
	500-710	19560.98	0.018	6614.54	0.262
	710-850	21447.07	0.021	9062.80	0.318
	850-1000	23735.02	0.022	8313.91	0.488
Sorbent D (3 Gas Mixture)	250-500	17165.53	0.012	4140.23	0.156
	500-710	17336.00	0.019	4177.484	0.403
	710-850	21165.33	0.020	3108.77	0.901
	850-1000	25204.19	0.020	6603.39	0.596
Sorbent C (4 Gas Mixture)	250-500	18686.17	0.011	5946.04	0.112
	500-710	21447.07	0.016	9062.80	0.191
	710-850	16044.86	0.028	7606.00	0.379
	850-1000	24060.53	0.022	9430.47	0.430

The shrinking core model with a combination of chemical kinetics and diffusion being rate controlling best described the system. The reaction rate constants are between values of 0.011 - 0.035 m/s which differs from the constants found in previous studies which range between 0.0243-0.03 cm/s (Steady, 2007). The values for the diffusivities that were obtained were of the magnitude 10^{-7} m^2/s and is similar to the values found by McCabe, 2011 which was of magnitude 10^{-8} m^2/s.
Using the pre exponential factor of 4.3 cm/s (Zevenhoven et al, 1997), and the rate constants found in the work at hand, the average Arrenhius type activation energies found is 10 KJ/mol which is similar to the apparent activation energy found for sorbents investigated by Zevenhoven et al,1997 which were in the range of 6.6- 10.8 KJ/mol.

The shrinking core model with only the diffusion as the rate controlling mechanism assumed constant diffusivity and did not predict the data set very well. As the process time increases, a $CaSO_4$ product layer develops hence the diffusion through the product layer eventually becomes rate determining. However this is not seen in the results possibly due to the short allowed reaction time. The development of the product layer decreases the sulphation rate and the rate then becomes proportional to the square of the available surface area (Ghosh Dastidar et al, 1996 and Bruce et al, 1989).
The pore sizes and porosity also decreases due to the phenomena of pore filling and mouth plugging as the $CaSO_4$ product has a larger molar volume and this then results in reduced available surface area.

The product later thickness is calculated from the following equation (Krishnan and Sotirchos, 1993):

$$d = a_0 \left[\left(Z + (1 - Z)(1 - X)\right)^{1/3} - (1 - X)^{1/3}\right] \quad (4\text{-}30)$$

Where $a_0 -$ initial particle size

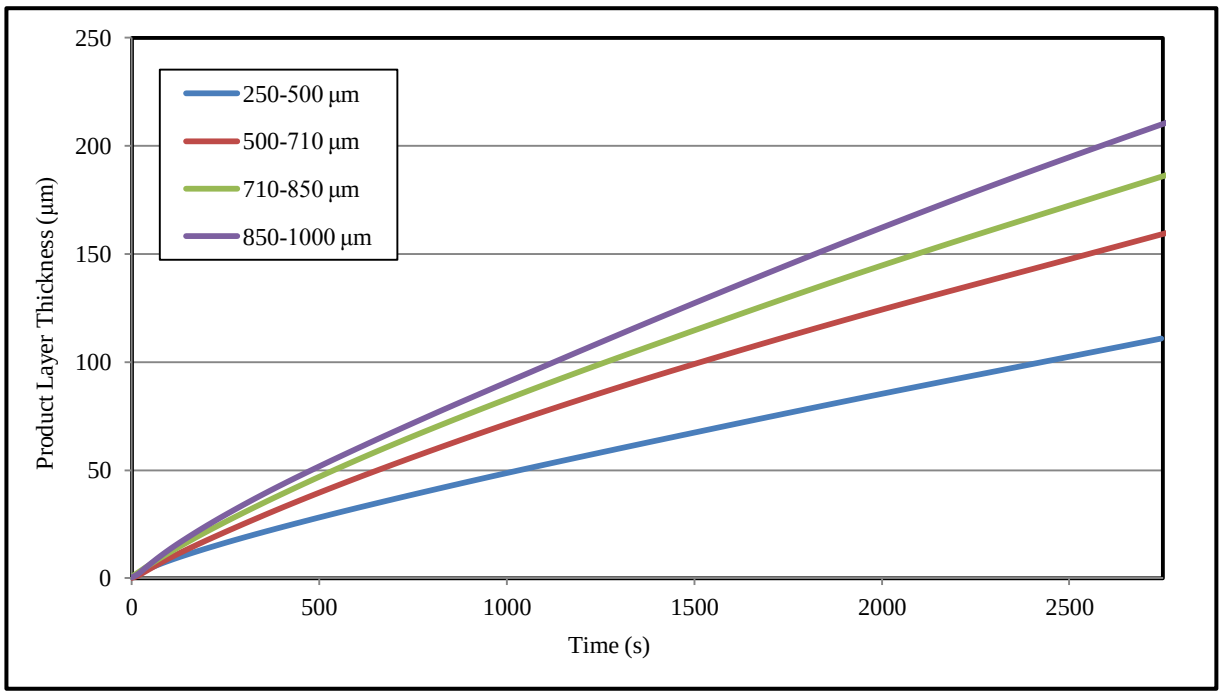

Figure 4-47: The Development of the Product Layer Thickness with Time for the Different Size Fractions for Sorbent C at 850℃.

With the molar volumes of CaO and $CaSO_4$ being 16.946 $\frac{mol}{m^3}$ and 46 $\frac{mol}{m^3}$ respectively, the $CaSO_4$ layer that is formed on the surface occupies over 170 % more space that the reactant. It can be seen from the plot of product layer development that as time progresses, the product layer thickness increases. Smaller size fractions have a smaller product layer thickness, hence a reduced resistance to diffusion which results in higher overall conversion. As the conversion increases so does the layer of the thickness and hence the resistance to diffusion. This explains why a simple shrinking core model with constant diffusivity in the product layer would not result in good reproduction of experimental behavior (Krishnan and Sotirchos, 1993). This then brings the need to use a model with variable effective diffusivity to replicate experimental data.

The SCM-VED was found to deviate the most from the experimental data. This model is essentially used for porous solid-gas reactions and it accounts for the internal structure of the particle such as porosity, pore sizes and BET surface area. The effective diffusivity model accounts for the pore diffusivity and product layer diffusion. Initially the gas must diffuse through the pores of the particle and the product layer before it reacts with the sorbent. However because the porosity and pore sizes of the sorbent particles are so small, this prevents the penetration of the sulphur dioxide gas to the core of the particle hence having negligible diffusion effects. The concept of effective diffusivity and the USC-VED model becomes almost negligible (Zevenhoven et al, 1996).

CHAPTER 5: CONCLUSIONS

5.1 Conclusions

The conclusions that can be made from the investigation work at hand are presented below:

- The control of power plant emissions such as sulphur dioxide will continue to be a major concern in the near future as the government legislature becomes more stringent.
- Sorbent selection based on the physical properties only will result in inadequate SO_2 capture therefore it is essential that there is a balance between optimum chemical and physical characteristics to produce the expected sorbent performance.
- A fully working experimental testing with a reactor design configuration has been designed, developed and implemented. The test unit proves to be working effectively.
- The general perception obtained is that smaller size fractions of sorbent have an improved desulphurization efficiency and higher conversion.
- The presence of CO_2 in the gas mixture decreases the desulphurization efficiency as it initiates the phenomenon of sintering.
- SEM images indicate that sorbents with a more rough surface morphology have higher desulphurization efficiencies and conversions due to improved penetration of SO_2 within the sorbent.
- The desulphurization efficiency depends on a combination of the physical, chemical and surface properties of the sorbents.
- The simple shrinking core model presents the closest agreement with the experimental data obtained.

CHAPTER 6: RECOMMENDATIONS

6.1.Recommendations

The current investigation tested the desulphurization capacities of four different ESKOM sorbents and four size fractions at atmospheric conditions. In order to establish an improved understanding of the desulphurization process the following is recommended to future researchers that who may want to further the investigation:

- Increase the number of sorbents that are tested.
- The presence of SO_3 was calculated using the equilibrium constant, it is recommended that a means for testing the presence of SO_3 be investigated in the future.
- The investigation should be carried out under pressurized conditions to replicate the flue gas conditions.
- The CO_2 concentration in the flue gas mixture should be increased such that the partial pressure of the CO_2 is greater than the equilibrium pressure. The effect on the desulphurization efficiency should then be determined in verify the expected increase due to direct sulphation.
- Investigate a suitable model to represent the desulphurization under the pressurized system conditions.
- Compare the results obtained on a laboratory scale with that obtained at actual power plants.

REFERENCES

Adanez, J., Fierro,V., Garcia-Labiano, F., and Palacios, J.M., 1997, Fuel, *Study of Modified Calcium Hydroxides for enhancing SO_2 Removal during Sorbent Injection in Pulverized Coal Boilers*, Elsevier Science LTD, Vol. 76(3), Page 257-265

Adanez, J., GarcmHa-Labiano, K., and Fierro,V., 2000, Chemical Engineering Science, *Modelling for the High-temperature Sulphation of Calcium-Based Sorbents with Cylindrical and Plate-like Pore Geometries*,Pergamon, Vol. 55, Page 3665-3683

Air Pollution Control, 2010, *Industrial Emission Control: Sulphur Dioxide*

Alvarez, E., and Gonzalez, J.F., 1999, Fuel, *High Pressure Thermogravimetric analysis of the direct Sulphation of Spanish Calcium-based Sorbents*, Vol. 78, Page 341-348

Austen.J., Brimblecombe,P., Styrges, W., 2002, *Air Pollution Science for the 21st Century*, Elsevier, Morwich, United Kingdom

Barletta,D., Marzocchella, A., and Salatino,P., 2002, Chemical Engineering Science, *Modelling the SO_2–limestone Reaction Under Periodically Changing Oxidizing/Reducing Conditions: The Influence of Cycle Time on Reaction Rate*, Pergamon, Vol. 57, Page 631 – 641

Basu, P., 2006, *Combustion and Gasification in Fluidized Beds*, Taylor and Francis Group, Canada

Bowen, B.H, Irwin, M.W., 2007, *Sulfur Dioxide Control Technologies In Electric Power Plants*, Indiana Centre for coal Technology Research, Purdue University

Boynton, R.S., 1980, *Chemistry and Technology of Lime*, John Wiley and Sons, New York.

Bruce, K. R., Gullet, B. K., and Beach, L. O., 1989, AIChE J, *Comparative SO_2 Reactivity of CaO Derived from $CaCO_3$ and $Ca(OH)_2$*, Vol. 35 (1), Page 37-41

Carsky, M., Dunlevey, J.N., Baitchu, S., Ralebakeng, T.B., and Ramohamane, N.J., 2006, *Study of Natural Sorbents, suitable for Desulphurization of Flue gas during in-bed Fluidized bed Combustion of Coal*, SACEC, Durban, South Africa

Case, P.L. and Heap, P.M., 2006, *The Capture and Retention of Sulphur Species by Calcium Compounds during the combustion of Pulverized Coal*, California, Page 1-9

Chang, L., Zhu, S., Xie, K., and Bao, W., 1998, Journal of Environmental Sciences, *Effect of Impurities on Desulphurization Properties of Limestone during Coal Gasification*, China, Vol. 10 (4), Page 485-490

Cheng, J., Zhou, J., Liu, J., Zhou, Z., Huang, Z., Cao, X., Zhao, X., and Cen, K., 2003, Progress in Energy and Combustion Science, *Sulfur removal at High Temperature during Coal Combustion in Furnaces: A Review*, Pergamon, Zhejiang University, China, Vol. 29, Page 381–405

Cheng, L., Chen, B., Liu, N., Luo, Z., and Cen, K., 2004, Fuel, *Effect of Characteristic of Sorbents on their Sulfur Capture Capability at a Fluidized Bed Condition*, Elsevier, Zhejiang, China, Vol. 83, Page 925-932

Chi,Y., Basu,P., and Cen, K., Fuel, 1994, *A simplified technique for measurement of sorbent reactivity for use in circulating fluidized bed combustors*, Vol. 73 (1), Page 117-122

Chiang, R.K., 1995, *Calcium Based Sorbents for Flue Gas Desulphurization*, PHD Thesis, Case Western Reserve University

Chu, C.Y., Hseuh, K.W., and Hwang, S.J., 2000, Journal of Hazardous Materials, *Sulphation and Attrition of Calcium Sorbent in* a *Bubbling Fluidised Bed*, Vol. 80, Page 119-133

Control Technologies and Abatement Costs for the Mexican Electricity Sector, Final Report, Mexico

Cortelyou, C.G., 1971, Sulphur and SO_2 Developments, *Commercial Processes for SO_2 Removal*, American Institute of Chemical Engineers, New York, Page 52-60

Cortley, J., 2010, Revision *to the Primary National Ambient Air Quality Standard, Monitoring Network, and Data Reporting Requirements for Sulphur Dioxide*, Fact Sheet, EPA Headquarters, Washington DC

Cullis, C.F., Henson, R.M., and Trimm, D.L., 1966, Mathematical and Physical Sciences, *The Kinetics of the Homogenous Gaseous Oxidation of Sulphur Dioxide*, the Royal Society, Vol. 295 (1440), Page 72-83

Dahlan, I., Mei, G.M., Kumaruddin, A.H., Mohamed, A.R., and Lee, K.T, 2008, Journal of Engineering Science and Technology, *Removal Of SO_2 And NO Over Rice Husk Ash (RHA)/CaO-Supported Metal Oxides*, School of Engineering, Taylor's University College, Malaysia, Vol. 3(2), Page 109 -116

Dahlan, I., Mei, G.M., Kumaruddin, A.H., Mohamed, A.R., and Lee, K.T., 2007, Chemical Engineering Technology, *Dry SO_2 Removal Process Using Calcium/Siliceous-Based Sorbents: Deactivation Kinetics Based on Breakthrough Curves*, Wilet Interscience, Vol. 30(5) , Page 663–666

Dahlan,I, Chiew Li,T, Lee, K.T, Kamaruddin, A.H, and Mohamed, A.R., 2007, Environmental Engineering Science, *Flue Gas Desulfurization Using Sorbent Synthesized from Lime (CaO) and Oil Palm Ash (OPA) Derived from Empty Fruit Bunches (EFB): Statistical Design Approach*, School of Chemical Engineering, Pulau Pinang, Malaysia, Vol. 24(6), Page 760-777

Dam Johansen, K., and Ostergaard, K., 1990, Chemical Engineering Science, *High Temperature Reaction between Sulphur Dioxide and Limestone- Comparision of limestones in Two Laboratory Reactors and a Pilot Plant*, Pergamon, Denmark, Vol. 46 (3), Page 827-837

Dam-Johansen, K., Hansen, P.F.B., and Ostergaard, K., 1990, Chemical Engineering Science, *High Temperature Reaction Between Sulphur Dioxide and Limestone-III. A grain and Micrgrain Model and its Verification*, Pergamon, Denmark, Vol. 46 (3), Page 847-853

Davini, P., 2002, Fuel, *Properties and Reactivity of Reactivated Calcium Based Sorbents*, Elsevier, Vol. 81, Page 763-770

DePriest, W., and Gaikwand, P.R., 2003, *Economics of Lime and Limestone for Control of Sulfur Dioxide*, Chicago

Desai, J.J., and Young, R.T., 1983, Ind. Chem. Eng. Process Des. Dev., Vol. 17, Page 411

Diaz-Somoano, M., Lopez-Anton, M.A., and Martinez-Tarazona, M.R., 2006, Global Nest Journal, *Trace Element Removal from Hot Gasification Flue Gases using Solid Sorbents*, Spain, Vol. 8(2), Page 137-145

Elert, K., Rodriguez-Navarro,C., Pardo, E.S., Hansen, E., and Cazalla, O., 2002, Studies in Conservation , *Lime Mortars for the Conservation of Historic Buildings*, Vol. 47(1), Page 62-75

Falkenberry, H.L., and Slack, A.V., 1971, Sulphur and SO_2 Developments, *SO_2 Removal by Limestone Injection,* American Institute of Chemical Engineers, New York, Page 67-72

Fan, L.S., Jiang, P., Agnihotri., S.K., Mahuli, S.K., Zhang, J., Chaul,S., and Ghosh- Dastidar, A., 1999, Chemical Engineering Science, *Dispersion and ultra-fast reaction of Calcium-based Sorbent Powders for SO2 and their toxic removal in coal Combustion* , Pergamon, Elsevier Science LTD, Vol. 54, Page 5585-5597

Ferna´ndez,J, Rico, J.L, Garcı´a,H, and Renedo, M.J, 2006, *Ind. Eng. Chem. Res, Development of Sorbents for SO_2 Capture Prepared by Hydration of Fly Ash and Hydrated Lime in Seawater*, Spain, Vol. 45, Page 856-862

Flagan, R.C., and Seinfeld, J.H, 1988, *Fundamentals of Air Pollution Engineering*, Carlifornia Institute of Technology, Prentice Hall, Englewood Cliffs, New Jersey

Foo, H., Teong, K.T., Fernando, N., and Mohamed, A.R., 2011, Journal of Advanced Chemical Engineering, *Flue Gas Desulphurization at Low Temperatures Using Coal Fly Ash/Ca-Based Sorbent: Determination of Rate Limiting Step*, Ashdin Publishing, Malaysia, Vol. 1, Page 1-10

Garea, A., Marqués, J.A., Irabien, A. , Kavouras, A. ,and Krammer, G., 2003, Thermochimica Acta, *Sorbent Behavior in Urban Waste Incineration: Acid Gas Removal and Thermogravimetric Characterization*, Spain, Vol. 397 , Page 227–236

Garea,A., Marques, J.A., Irabien A., 2005, Chemical Engineering Journal, *Modelling of In-duct Desulfurization Reactors*, Elsevier, Vol. 107, Page 119–125

Gavalas, G.R, Edelstein,S, Flytzani-Stephanopoulos,M., 1987, AIChE Journal, *Alkali-Alumina Sorbents for High-Temperature Removal of SO_2*, California Institute of Technology, Vol 33.(2), Page 258-266

Ghosh-Dastidar, A., Mahuli, S.K., Agnihotri, R., and Fan, L.S., 1996, Ind. Eng. Chem. Res., *Investigation of High-Reactivity Calcium Carbonate Sorbent for Enhanced SO_2 Capture*, Department of Chemical Engineering, The Ohio State University, Columbus, Ohio Vol. 35,Page 598-606

Gibbins, J., 2008, *Science for Environment Policy* – Issue 3, Euorope

Glarborg, P., 2006, *Hidden Interactions-Trace Species governing Combustion and Emissions*, The Combustion Institute, Elsevier, Lyngby, Denmark

Govender, K., 2006, *Systematic Study of Selected Sorbents available in South Africa for Desulphurization of Flue Gas during In-Bed Fluidized Bed Combustion of Coal*, MSc Thesis-Chemical Engineering, University of KwaZulu-Natal

Haji-Sulaiman, M.Z., and Sacroni,A.W., 1991, Fuel, *The Calcination and Sulphation Behaviour of Sorbents in Fluidized Bed Combustion*, Butterwoth-Heinemann Ltd, Vol. 70, Page 169-176

Hamer, C.A., 2009, Energy, *Evaluation of SO_2 Sorbents in a Fluidized Bed Reactor*, Canada, Page 458-507

Han, B., Zhong, Y., Zhang, Y., Gao, X., Luo, Z., Ni, M., and Cen, K., 2011, *Simultaneous Removal of SO_2 and NO from Coal Flue Gas with $NaClO_2$/ $KMnO_4$ Enhanced Ca-based Sorbent*, Zhejiang University, China, Page 5448- 5452

Han, K., Chunmei, L., Cheng, S., Zhao, G., Wang, Y., Zhao, J., 2005, Fuel, *Effect of Characteristics of Calcium-Based Sorbents on the Sulfation Kinetics*, Elsevier,Vol. 84, Page 1933–1939

Hansen, P.F.B., Dam-Johansen, K., and Ostergaard, K., 1993, Chemical Engineering Science, *High Temperature Reaction between Sulphur Dioxide and Limestone-V. The Effect of Periodically Changing Oxidising and Reducing Conditions*, Pergamon Press Ltd, University of Denmark, Vol. 48(7), Page 1325-1341

Hare, S, Cresswell, L, Twigg, R, Buchdahl, J., 2002, Air Pollution & Acid Rain Fact Sheets Series: KS4 & A, *Industrial Emission Controls: Sulphur Dioxide*

Hartman, M., and Coughlin, R.W., 1976, AIChE Journal, *Reaction of Sulfur Dioxide with Limestone and the Grain Model*, Vol. 22(3), Page 490-498

Hasenberg, L., 2008, *Corrosion Handbook: Sulphur Dioxide*, Dechema,

Hassibi,M., 1999, *An Overview Of Lime Slaking And Factors That Affect The Process*

Hecq,P., 1997, *SO_2 Position Paper*, European Commission, Europe

Hepworth, M.T, Berns, J.J, Sadecki, K.A., 1997, *Kinetics of Mn-based sorbents for Hot Coal Gas Desulphurization*, Final Technical Report, University of Minnesota, Minneapollis

Hiroaki,T, Ishizuka,T, Nakamura, H, Ueno, T, and Hattori, H., 1996, Ind. Eng. Chem. Res, *Study of Flue Gas Desulfurization Absorbent Prepared from Coal Fly Ash: Effects of the Composition of the Absorbent on the Activity*, Japan, Vol. 35, Page 2322-2326

Ho, C.S. and Shih, S.M.,1992, American Chemical Society, *$Ca(OH)_2$/Fly Ash Sorbents for SO_2 Removal*, Taiwan, Vol. 31(4), Page 1130-1135

http://snowyoctomber.blogspot.com/ Author: Unknown, Date accessed: 16 May 2012

http://www.britannica.com/EBchecked/media/106953/Many-trees-in-the-Great-Smoky-Mountains-such-as-those , Date accessed: 16 May 2012, Author: Juriet, R.,

http://www.elmhurst.edu/~chm/vchembook/196buildings.html., Date accessed : 23 April 2012, Author: Ophardt, C., 2003

http://www.freeimageslive.co.uk/free_stock_image/rustytank3974jpg , Author : Unknown, Date accessed 16 May 2012

http://www.motherearthnews.com/uploadedImages/Blogs/Craig_Vetter/9-pie-chart-3.jpg., Date accessed: 3 March 2012, Author: Vetter, C.

Hudson, J.L., and Rochelle, G.T., 1981, Flue Gas Desulphurization, American Chemical Society, Washington D.C

Ibrahim, M.K and Eliass, A.I., 2010, Engineering and Technology Journal, *Modelling and Simulation of Flue Gas Desulfurization Using Slurry of Fine Activated Carbon Particles*, Baghdad, Vol. 28 (12), Page 2294 – 2298

Lee, K.T., Bhatia, S., Mohamed, A.R., J,2003, Mater Cycles Waste Management, *Preparation and Characterization of Sorbents Prepared from Ash (waste material) for Sulfur dioxide (SO_2) Removal*, Vol.7, Page 16-23

Koval, E.J., 1982, MSc Thesis, The Pennsylvania State University, USA

Krsihnan, S.V., and Sotirchos, S.V., 1993, The Canadian Journal of Chemical Engineering, *A Variable Diffusivity Shrinking Core Model and its Application to the direct Sulphation of Limestone*, New York, USA, Vol. 71, Page 734-745

Lee, K.T., Bhatia, S., and Mohamed, A.R., 2007, Energy Sources, *Preparation and Characterization of CaO/$CaSO_4$/Coal Fly Ash Sorbent for Sulfur Dioxide (SO_2) Removal: Part I*, Taylor and Francis Group, Malaysia, Vol. 28, Page 1241–1249

Levenspiel, O., 1972, *Chemical Reaction Engineering*, John Wiley and Sons, 3rd Edition, New York

Lyngfelt, A., and Leckner, B., 1999, Chemical Engineering Science, *Sulphur Capture in Circulating Fluidized-bed Boilers: Can the efficiency be predicted*, *Pergamon*, Elsevier Science LTD, Vol. 54, Page 5573-5584

Macias-Parez, M.C., Salinas-Martinez de Lecea, C., Muiloz-Guillena, M.J. , and Linares-Solano, A., 2006, Fuel Gas Clean-up, *Low Temperature SO_2 Capture by Calcium Bases Sorbents: Characterization of the Active Calcium*, Spain, Page 422-426

Majeed, J.G., Korda, B., and BhkBssy-Molntir, E., 1995, Gas Separation and Purification, *Comparison of the Efficiencies of Sulfur Dioxide Absorption using Calcium Carbonate Slurry and Sodium Hydroxide Solution in an ALT Reactor*, Technical University of Budapest, Department of Chemical Engineering, Hungary, Vol. 9(2), Page 111 -120

Mandlall, D.K., 1993, *Production of Improved Calcium-Based Sorbents for Sulphur Dioxide Capture*, MSc Thesis, Ohio University

Mattisson, T., and Lyngfelt, A., 1998, Can. J. Chem. Eng , *A method of evaluating limestone reactivity with SO_2 under fluidized bed combustion conditions*, Vol. 76, Page 762.

Mattson, B., and Saunders, E., 2003, *Microscale Gas Chemistry*, A chemistry laboratory Experiment, Chem13 News, 131, Part 24

Mchabe, D., 2011, MSc Thesis, *Sulphur Self Retention and Sulphur Dioxide Capture with Active Calcium Minerals in Mineral Rich Coal*, University of Johannesburg, South Africa

Miller, P.J., 2004, *Power Plant Air Emissions*, Commission for Environmental Co-operation, North America

Mitra, D, Basak ,R, and Paliwal , D., 2010, International Journal of Engineering Science and Technology, *A note on Prevention and Control of Sulpur Oxide Pollution*, Vol. 2(8), Page 3926-3928

Mohamed, W., 2008. *Desulphurisation of South African Coal using Low Power Microwave Energy*, MSc Thesis, University of Witwatersrand, Page 10

Montagnaro, F., and Salatino, P., 2002, Combustion Science and Technology, *The Influence Of Sorbent Properties and Reaction temperature on Sorbent attrition, Sulphur uptake, and Particle sulphation Pattern during fluidized bed desulphurization*, Taylor and Francis, Vol. 175(11 and 12), Page 151-169

Montagnaro, F., Salatino, P., and Scala, F., 2010, Experimental Thermal and Fluid Science, *The influence of Temperature on limestone sulphation and Attrition under Fluidized Bed Combustion Conditions*, Elsevier, Italy, Vol. 34, Page 352-358

Moodley, L., 2007, *The Evaluation of the Fluidized Bed Combustion Performance of South African Coal in the Presence of Sorbents*, Msc Thesis, University of KwaZulu-Natal

Morrison, J., 2008, Project Fact Sheet, *Sorbent Performance in Fluidized-Bed Combustors*, College of Earth & Mineral Sciences, Pennsylvania State University

Morrison, J.L., Lui, Y., Pisupati, S.V., Sacroni, A.W., and Romans, E.D., 1996, *Sorbent Behaviour in Circulating Fluidised bed Combustor*, Fuel, Vol. 57(6), Page 759-768

National Energy Foundation, 2001, *Coal and the Environment*

Neeraj, P., 2001, MSc Thesis, *Numerical Modeling of Cold Flow and Hot Gas Desulfurization in a Circulating Fluidized bed*, West Virginia University

Nolan, P.S., 1996, *Emission Control Technologies for Coal-Fired Power Plants*, Balbcock and Wilcox, Ohio, USA

Ogenga, D.O., 2009, *Performance of South African Calcium/Siliceous–Based Materials as Sorbents for SO_2 Removal from Flue Gas*, M.Tech Mechanical Engineering, Tshwane University of Technology, Page 35

Ogenga, D.O., Mbarawa, M.M., Lee, K.T., Mohamed, A.R., Dahlan, I., 2010, Fuel, *Sulphur dioxide removal using South African limestone/siliceous materials*, Elsevier LTD Vol. 89 , Page 2549–2555

Ogenga,D.O., Siagil Z. O., Onyango, M.S., and Mbarowo, M., 2008, R & D Journal, *An Overview of the Use of Ca(OH)/Fly Ash in Flue Gas Desulphurization*, South African Institution of Mechanical Engineering, Vol.24(3), Page 4-9

Ogenga,D.O., Lee, K. L., Mbarawa, M., 2009, Engineering Letters, *Sulphur Dioxide Abetment Using Synthesized South African Limestone/Siliceous Sorbents*, South Africa

Ortiz, M.I., Garea, F., Cortabitarte, F., and Irabien, A., 1993, Powder Technology, Vol. 75, Page 167

Özyuğuran, A and Ersoy-Meriçboyu,A.,2010, *Flue Gas Desulfurization by Limestone and Hydrated Lime Slurries*, Istanbul Technical University, Maslak-Istanbul-Turkey

Patnaik, T., Brown, W., 2010, *Increasing SO_X Removal Efficiencies in Dry Sorbent Injection Systems*, Hosokawa Micron Powder Systems, New Jersey

Perry, R.H., and Green, D.W., 2008, *Perry's Chemical Engineers' Handbook*, 8th Edition, McGraw-Hill, New York

Pisupati, S.V., Wasco, R.S., Morrison, J.L., Scaroni, A.W., 1996, Fuel, *Sorbent Behaviour in Circulating Fluidized Bed combustors*, Elsevier Science Ltd, Britain, Vol. 75 (6), Page 759-768

Ragnunathan, K.., and Gullett, B.K., 1994, Energy and Fuels, *Reduction of Coal-Based Metal Emissions by Furnace Sorbent Injection*, Research Triangle Park, North Carolina, Vol. 8, Page 1068-1076

Rahmani, M., and Sohrabi, M., 2006, Chem. Eng. Tech, *Direct Sulphation of Calcium Carbonate using the Variable Diffusivity Approach*, Amirkabir University of Technology, Iran, Vol. 29 (12), Page 1496-1501

Reh, L., 1999, Chemical Engineering Science, *Challenges of Circulating Fluid-bed Reactors in Energy and Raw Materials Industries*, Pergamon, Switzerland, Vol.54, Page 5359- 5368

Ren-Bin, L, Shin-Min, S, Chiung-Fang, L., 2003, Chemical Engineering Science, *Characteristics and Reactivities of Ca (OH)2/silica fume sorbents for Low-Temperature Flue Gas Desulfurization*, Department of Chemical Engineering, National Taiwan University, Taiwan, Vol. 58, Page 3659 – 3668

Renedo, M.J., Fernandez, J., Garea, A., and Irabien, J.A., 2000, Chemical Engineering Communications, *The Influence of Particle Size and Structural Properties of Sorbent Prepared from Fly-ash and $Ca(OH)_2$ on the SO_2 Removal ability*, Taylor and Francis, Vol. 182, Page 69-80

Rentz. O., Dorn, R., Holschumacher, R., Padberg, C., 1993, *Advanced Emission Controls for Power Plants*, OECD Documents, Paris

Rozpondek ,M., and Siudek, M., 2009, *Pollution Control Technologies applied to Coal Fired Power*, Plant Operation, Poland, Page 156-160

Satriana, M., 1981, *New Developments in Flue Gas Desulphurization technology*, Noyes Data Corporation, New Jersey, USA

Scala, F., Chirone, R., Meloni, P., Carcangiu, G., Manca, M., Mulas, G., and Mulas, A., 2011, MCS, *Enhanced Fluidized Bed Desulphurization by Pre-treated Limestone Particles*, Italy, Vol. 7

Sellakumar, K.M., and Conn, R., 1999, A Comparison Study of AFBC and PFBC Ash Characteristics, Livingston, USA

Siagi, Z.O., Mbarawa, M., Mohamed, A.R., Lee, K.T., and Dahlan, I., 2006, *Removal of Sulphur Dioxide by Calcium-Based Materials from Different Sources in South Africa*, 8thAsia-Pacific International Symposium on Combustion and Energy Utilization, Sochi, Russian Federation

Smith, S.J.,van Aardenne, J., Klimont, Z., Andres, R.J., Volke, A., and Arias, D.S., 2011, Atmospheric Chemistry and Physics, *Anthropogenic sulfur dioxide emissions*: 1850–2005, USA, Page 1101- 1116,

Spitsbergen, U., Vincent, C,J., Longe, T.A., 1981, Journal of the Institute of Energy, *Comparison of Selected European Limestones for Desulphurization of Gases from atmospheric Fluidized bed combustion*, London, Vol. 53-55, Page 94-100

Srivastava, R.K., 2000, *Controlling SO_2 Emissions: A Review of Technologies*, Washington, Page 35,6,17

Strauss, W., 1971, Environmental Science and Technology, *Air Pollution Control*, Jonh Wiley and Sons, Victoria, Australia

Treissman, D., Guigard, S., Kindzierski, W., Schulz, J., Guigard E., 2003, *Sulphur Dioxide: Environmental effects, Fate and Behaviour*, WBK and Associates, Alberta

Tullin,C., and Ljungstrom, E., 1989, Energy and Fuels, *Reaction between Calcium Carbonate and Sulfur Dioxide*, Goteborg, Sweden, Vol. 3, Page 284-287

Twalton, 2009, *Proposed SO_2 RIA*, Chapter 1, Page 11-16

U.S Department of Energy., 2000, *Integrated Dry NO_X/SO_2 Emissions Control System A DOE Assessment*, United States

U.S Department of Energy, 1999, *Advanced Technologies for the Control of Sulfur Dioxide Emissions from Coal-Fired Boilers*, Topical Report 12, United States

Uno, T., Fukui, S., Atsukawa, M., Higashi, M., Yamada, H., Kamei, K., 1971, Sulphur and SO_2 Developments, *Scale-up of an SO_2 Process* , American Institute of Chemical Engineers, New York, Page 73-77

Van der Zwaan, B., 2005, *Will Coal Depart or will it Continue to Dominate Global Power Production during the 21st Century*, Climate Policy, Amsterdam, Netherlands

Van Greunen, L.M., 2006, Selection *of Air Pollution Control Technologies for Power Plants, Gasification and Refining Process*, University of Pretoria

Wang, H., Xu, H., Zheng, C., and Qiu, J., 2009, Springer, *Temperature Dependence of the reaction of $CaCO_3$ in O_2/ CO_2 Coal Combustion,* Huazhong University of Science and Technology, China, Vol. 16, Page 845-850

Witlow, J., 2002, *Flue Gas Desulphurization Systems-Lesson 9*

World Bank Group., 1998, Pollution Prevention and Abatement Handbook, *Sulphur Oxides : Prevention and Control*, Washington

Yang, R.T., Shen, M.S., and Steingberg, M., 1978, Environmenal Science Technology, Vol. 12, Page 411

Ye, Z., and Bjerle, I., 1996, Air and Waste Management Association, *Technical Paper On the Intrinsic High Temperature Calcium Oxide-Sulfur Dioxide Reaction Using the Vacuum Thermogravimetric Analysis Technique*, Sweden, Vol. 46, Page 734-741

Zevenhoven and Kilpinen., 2001, *Sulphur*, New York

Zevenhoven and Kilpinen., 2004, *Chapter 3 - Sulphur*, New York

Zevenhoven, R., Yrjas, P., and Hupa, M., 1998, Fuel, *Sulfur dioxide Capture under PFBC Conditions: The Influence of Sorbent Particle Structure*, Abe Akademi University, Finland, Vol. 77(4), Page 285-292

Zevenhoven, R., Yrjas, P., and Hupa, M., 1996, Ind Eng. Chem. Res, *Hydrogen Sulphide Capture by Limestone and Dolomite at elevated Pressure.2 Sorbent Particle Conversion Modelling*, Abe Akademi University, Finland, Vol 35(), Page 943-949

Zitholele Consulting ., 2009, *Kusile Railway Project: Draft Scoping Report*, Eskom

APPENDIX A: CALIBRATION CHARTS

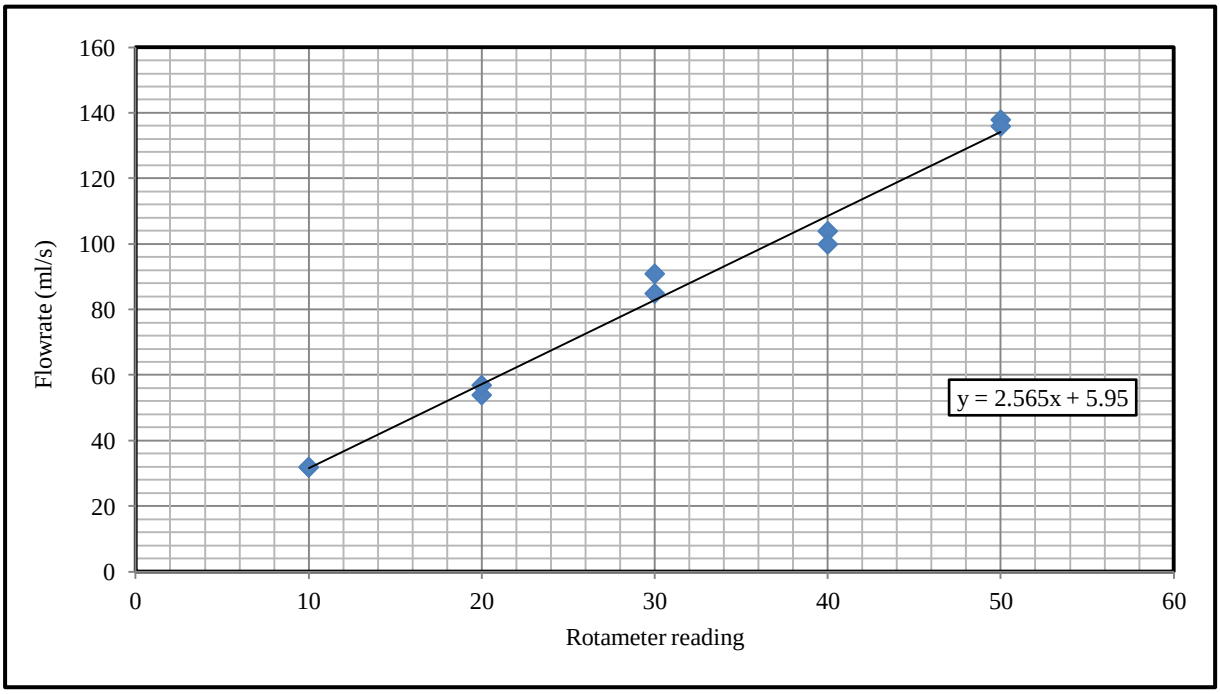

Figure A-1 Rotameter Calibration Chart

The calibration chart was generated using two data sets as shown below.

Table A-1 SO_2 Rotameter Calibration Data

Rotameter reading (l/sec)	Time (sec)	Initial Volume (ml)	Final Volume(ml)	Volume Change (ml)	Flowrate (ml/sec)
10	5	110	270	160	32
20	5	270	540	270	54
30	5	105	530	425	85
40	5	170	690	520	104
50	5	120	810	690	138
10	5	100	260	160	32
20	5	260	545	285	57
30	5	165	620	455	91
40	5	135	635	500	100
50	5	130	810	680	136

Run 1 - Rotameter Reading 10

$$\text{Flowrate} = \frac{\text{Final Volume} - \text{Initial Volume}}{\text{Time}}$$

$$= \frac{270-110}{5} = 32 \text{ ml/sec}$$

APPENDIX B: TEMPERATURE PROFILE

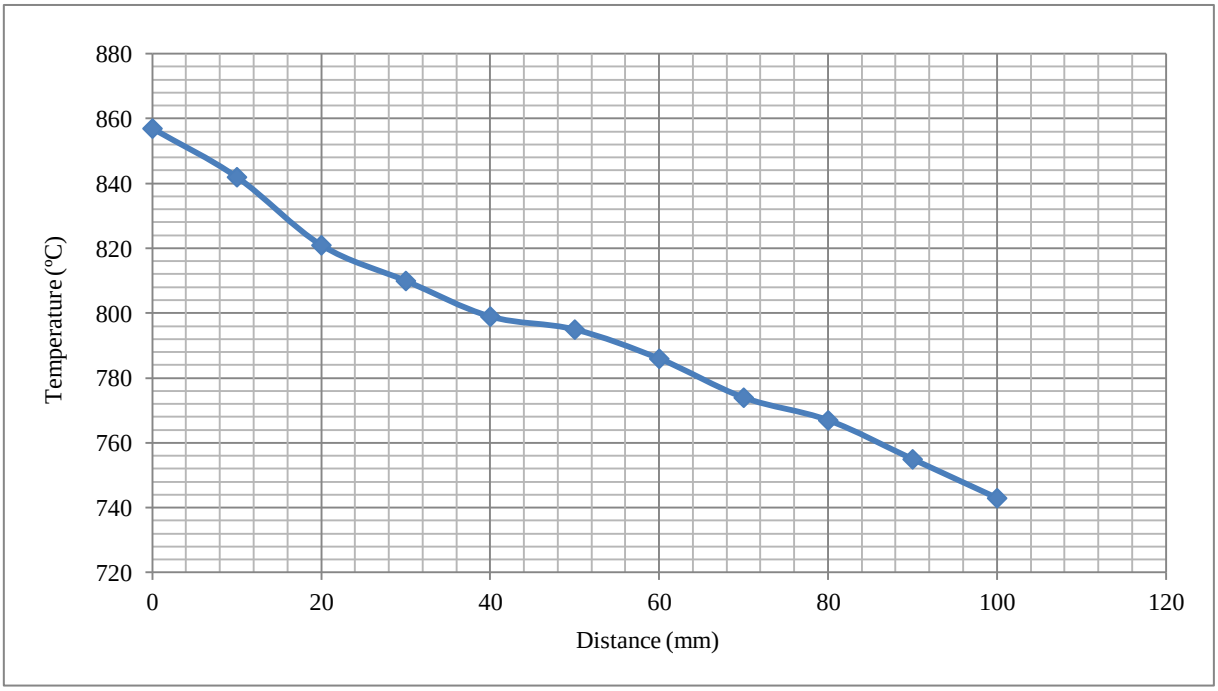

Figure B-1: Graph of temperature at different locations in the reactor

A temperature profile within the reactor was obtained by recording the temperature at incremental distances from the centre of the oven. The zero distance marks the reference point at the centre of the oven which was found to be the optimum location. The reactor was then placed at this location in the oven. It can be clearly seen that as the distance from the centre to the outer skirts of the oven increases, the temperature decreases.

APPENDIX C: SAMPLE CALCULATIONS

C.1. Purity Analysis

- **Determination of amount of HCl required for dissolving of impurities**

The chemical reaction that occurs between hydrochloric acid and calcium carbonate is as follows (Mattson and Saunders, 2003):

$$2HCl\ (aq) + CaCO_3\ (s) \longrightarrow CaCl_2\ (aq) + CO_2\ (g) + H_2O\ (l)$$

Mass of sorbent A = 10g

Molar mass (MM) of $CaCO_3$ = 100.09 g/mol

Molar mass (MM) of HCl = 36.5 g/mol

$$n_{CaCO_3} = \frac{m}{MM_{CaCO_3}} = \frac{10}{100.09} = 0.1 \text{ mols}$$

$$n_{HCl} = 0.2 \text{ mols}$$

$$m_{HCl} = n_{HCl} \times MM_{HCl}$$

$$= 0.2 \times 36.5$$

$$= 7.3 \text{ g}$$

$$= 7.3 \times 10^{-3} \text{ kg}$$

Density of 32% HCl = 1.159 kg/L (Perry and Green, 1984)

$$V_{HCl} = \frac{7.3 \times 10^{-3}}{1.159} = 6.29 \times 10^{-3} \text{ L}$$

$$= 6.29 \text{ mL}$$

Therefore, 12 mL of HCl was used to ensure that all the $CaCO_3$ was converted into $CaCl_2$.

- **Determination of percentage purity of sorbent A**

The percentage purity for sample A is shown below:

Mass of sorbent = 10.333 g

Mass of impurities = Mass of impurities and filter paper – Mass of filter paper

= 0.869 – 0.414

= 0.455 g

$$\% \text{ Purity} = \frac{\text{Mass of sorbent} - \text{Mass of impurities}}{\text{Mass of sorbent}} \times 100$$

$$= \frac{10.333 - 0.455}{10.333} \times 100$$

= 96.60 %

Similarly, the percentage purity for test 2 and test 3 were found and the average percentage purity was calculated.

$$\text{Average \% purity} = \frac{95.59 + 93.45}{2}$$

= 94.52 %

- **Determination of Eskom purity analysis compared to lab scale purity for Sample A**

CaO content = 44.5 %

MgO content = 8.6 %

Therefore, the total purity of CaO of sorbent A is shown below:

Molar mass (MM) of CaO = 56 g/mol

$$\% \text{ Purity CaO} = (44.5 + 8.6) \times \frac{100}{56}$$

= 94.82 %

C.2. Density Evaluation

The following calculations are based on the measurements obtained for sample A.

- **Pycnometer Technique**

Table C-1: Various Masses used in the Pycnometer Technique

M_1 (mass of empty pycnometer)	**25.8171g**
M_2 (mass of pycnometer + water)	76.3843g
M_3 (mass of pycnometer + dry particles)	27.6533g
M_4 (mass pycnometer + particles +water)	77.5789g

Density of water at 19 ˚C is 0.998405g/ml

mass of water (g) $= m_2 - m_1$

= 50.5762g

Volume of Pycnometer $= \frac{m_2 - m_1}{\rho_{water}}$

Volume of Pycnometer $= \frac{76.3843 - 25.8171}{0.9984}$ = 50.6479ml

Mass of particles $= m_3 - m_1$ = 1.8362g

Mass of water added $= m_4 - m_3$ = 49.9256g

Volume of water added $= \frac{m_4 - m_3}{\rho_{water}}$ = 50.0053

Volume of Particles $=$ Volume of Pycnometer $-$ Volume of water added = 0.6426ml

$\rho_{particles} = \frac{m_3 - m_1}{\text{Volume of Particles}}$ = 2.86g/ml

- **Water Displacement Technique**

Mass of sorbent = 9.26g

Initial volume = 10ml

Final volume = 13ml

$\rho_{particles} = \frac{\text{mass}}{\text{volume change}} = \frac{9.26}{3}$ = 3.08g/ml

C.3. Softness Index

Table C-2 Data obtained for the Softness Index Test

Sorbent	A	B	C	D
Initial Mass(g)	40.0002	40.0005	38.8849	40.0005
Mass through 425 µm sieve	0.8961	1.3621	1.6764	1.4300
% Passed through Sieve	2.24023	3.40520	4.3111	3.5749

Sorbent A

$$\text{Softness Index} = \frac{40.0002 - 0.8961}{40.0002} \times 100$$

$$= 2.24\%$$

C.4. Area Calculation and Desulphurization Efficiency

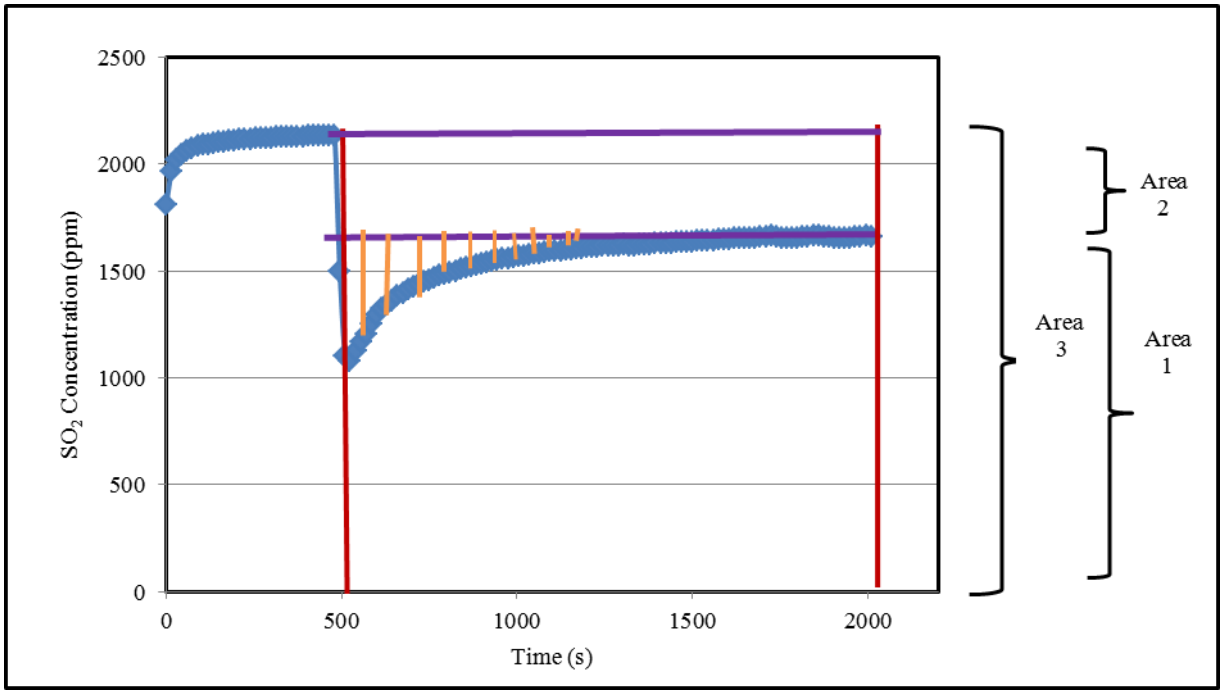

Figure C-1: Typical Concentration vs. Time Plot

The figure above is a representation of the SO_2 concentration over a period of time for Sorbent A, size fraction 850-1000µm. Various lines were constructed to clearly demarcate areas to enable the calculation of the total SO_2 removed by the sorbent and hence calculate the desulphurization efficiency. Area 1 represented the total amount of SO_2 present in the system. Area 2 represented the amount of SO_3 removed from the system. Area 3 represented the total area of SO_2 and SO_3. The shaded region represents the amount of SO_2 removed.

The area under the curve was calculated using an integration method in Microsoft Excel where random intervals were chosen. The formula used is shown below where A represents the SO_2 concentration and B represents the time. The initial concentration was taken as the concentration after the bypass and the final concentration was the concentration at which the curve remained uniform for a long period of time.

Area a = $\frac{(B2-B1)\times(A2+A1)}{2} = \frac{(225-135)\times(1026.39+2186.96)}{2}$ = 144600.8 units^2

Area b = $\frac{(B3-B2)\times(A3+A2)}{2} = \frac{(300-225)\times(1103.89+1026.39)}{2}$ = 79885.5 units^2

Etc…

Total area under the curve = $\sum$(Area a + Area b + ⋯ + Area final)

= $\sum(144600.8 + 79885.5 + \cdots + 394346.4)$

= 4244902.5 units^2

Calculation of concentration of SO_3

Initial concentration of SO_2 = 2134 ppm

Final concentration SO_2 = 1663 ppm

Concentration of SO_3 = Initial concentration of SO_2 – Final concentration of SO_2

= 2134 – 1663

= 471 ppm

Calculation of Area 1

Initial time = 480 s

Final time = 3210 s

Area 1 = (Final concentration of SO_2) × (Final Time – Initial Time)

= (1663ppm) × (3120-480)

= 4390320 units^2

Calculation of Area 2

Initial time = 3120 s

Final time = 480 s

Area 2 = (Concentration of SO_3) × (Final Time – Initial Time)

= (471 ppm) × (3120– 480)

= 1243440 units^2

Calculation of Total Area 3

Total Area 3 = Area 1 + Area 2

= 5633760 units^2

$$\text{Desulphurization Efficiency}(\%) = \frac{A_1 - A_{\text{Under Curve}} + A_2}{A_3}$$

$$= \frac{4390320 - 4244902.5 + 1243440}{5633760}$$

= 24.6%

C.5. <u>Calculation of the Equilibrium molar fraction of SO_3</u>

The calculation of equilibrium molar fraction of SO_3 was determined from the equilibrium constant for pressure.

$K_p = \frac{[SO_3]}{[SO_2][O_2]^{0.5}}$

Rearranging: $[SO_3] = K_p \times [SO_2] \times [O_2]^{0.5}$

Where $[SO_2]$ = (Initial concentration of SO_2) ppm × (10^{-6}) = 2134 ×10^{-6}

$[O_2] = \frac{20}{100} = 0.2$

$K_p = 1.53 \times 10^{-5} \times e^{\frac{11760}{T}}$

Where T = 850 +273.15 = 1123.15 K

$K_p = 1.53 \times 10^{-5} \times e^{\frac{11760}{1123.15}}$

= 0.54

Therefore, $[SO_3] = 0.54 \times 2134 \times 10^{-6} \times (0.2)^{0.5} = 5.15 \times 10^{-4}$

APPENDIX D - XRF ANALYSIS

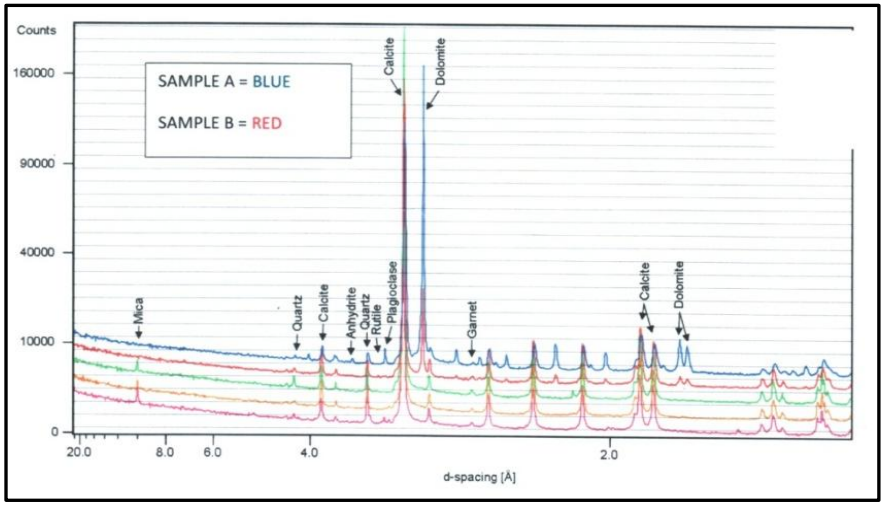

Figure D-1: X-Ray Fluorescence Patterns for Sorbents A and B

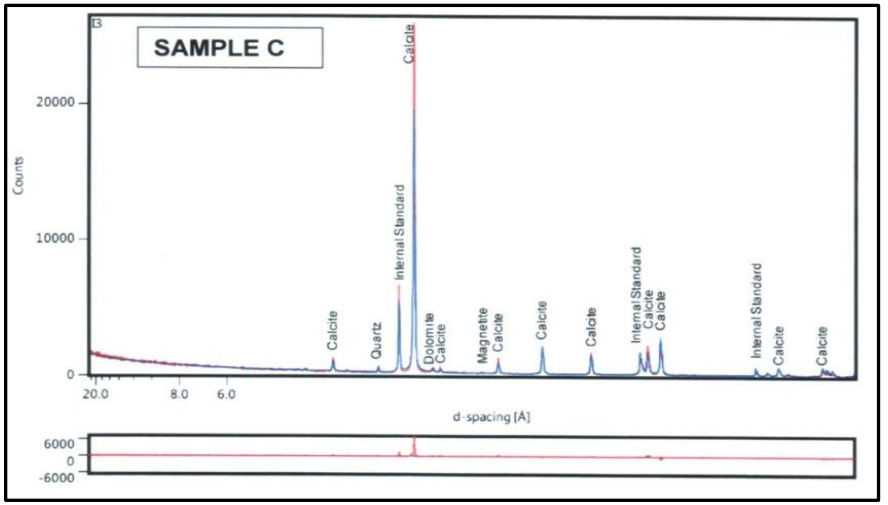

Figure D-2: X-Ray Fluorescence Pattern for Sorbent C

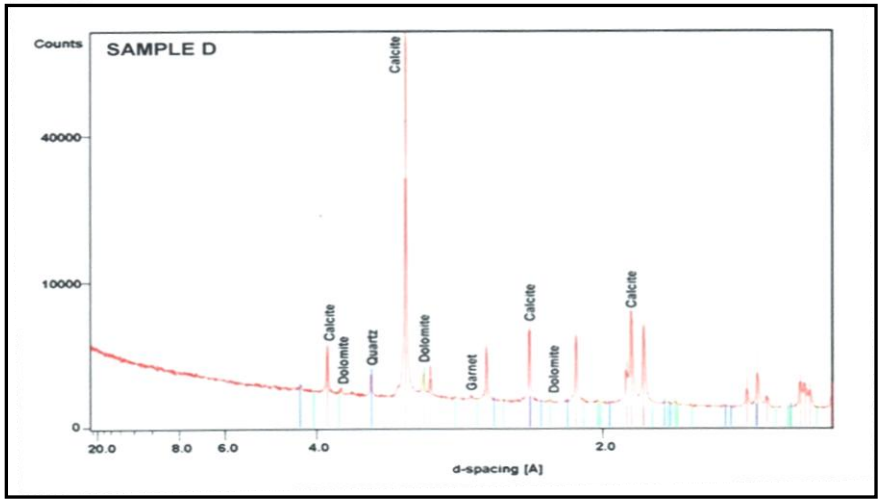

Figure D-3: X-Ray Fluorescence for Sorbent D

APPENDIX E - EDX ANALYSIS

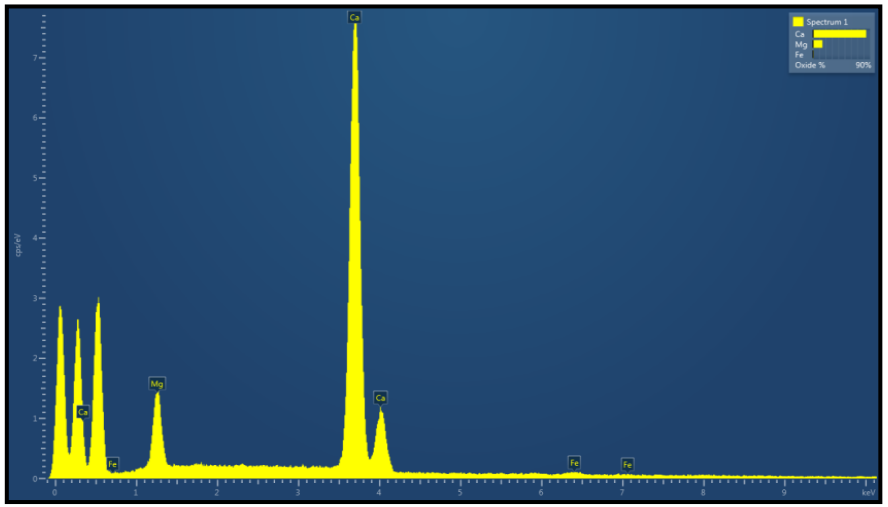

Figure E-1: EDX Analysis for Sorbent A

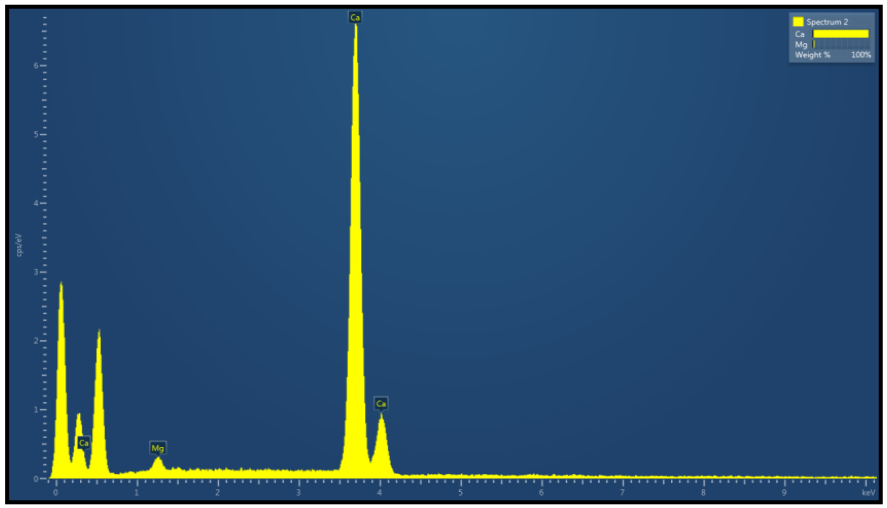

Figure E-2: EDX Analysis for Sorbent B

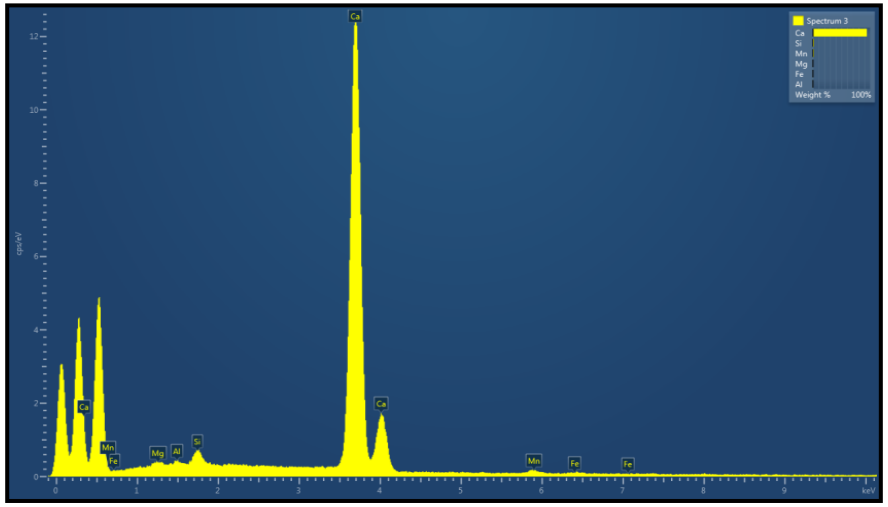

Figure E-3: EDX Analysis for Sorbent C

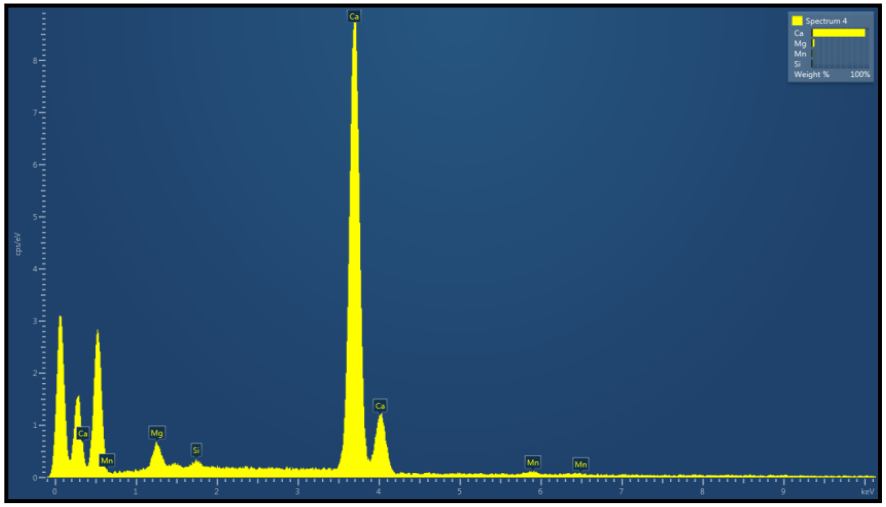

Figure E-4: EDX Analysis for Sorbent D

APPENDIX F- RAW DATA

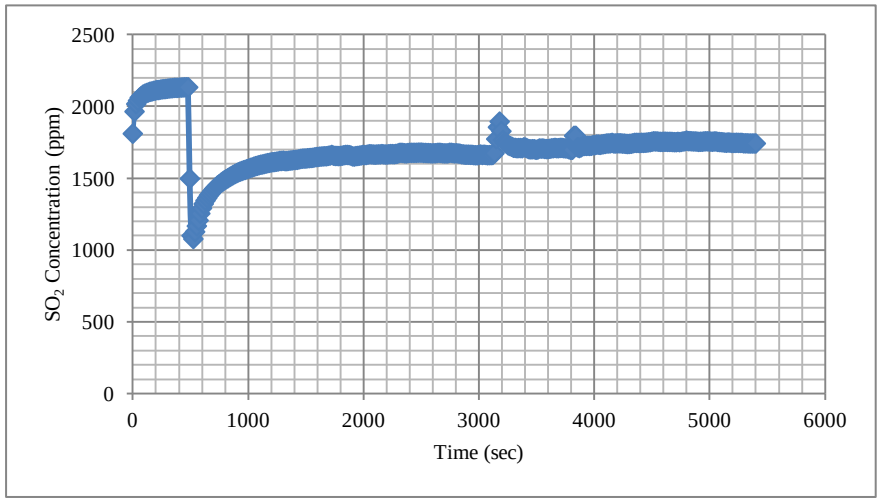

Figure F-1: Sorbent A, 850-1000 µm

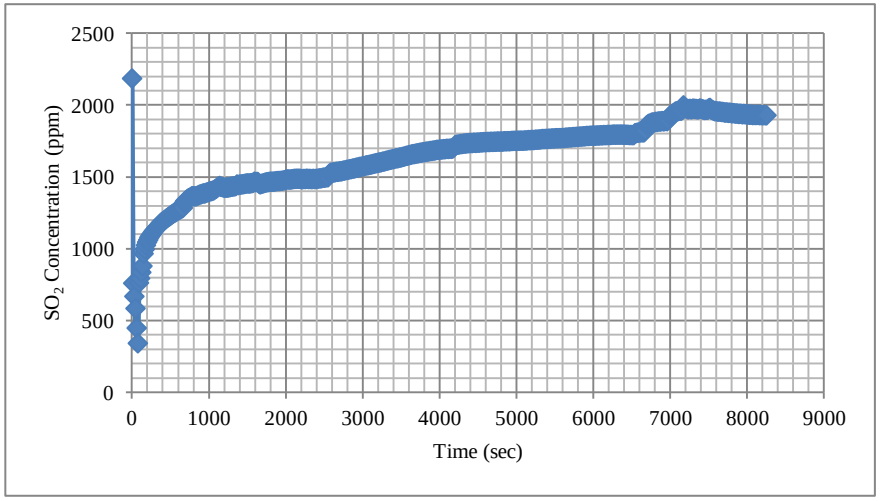

Figure F-2: Sorbent A, 710-850 µm

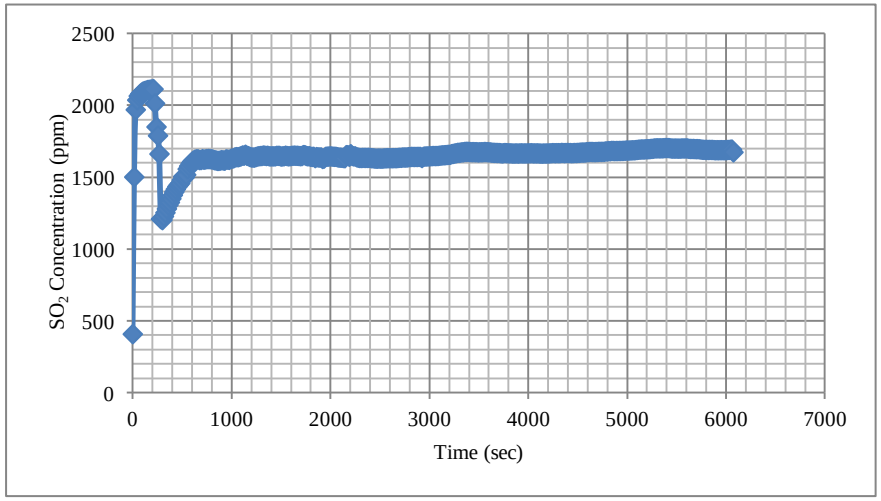

Figure F-3: Sorbent A, 500-710 µm

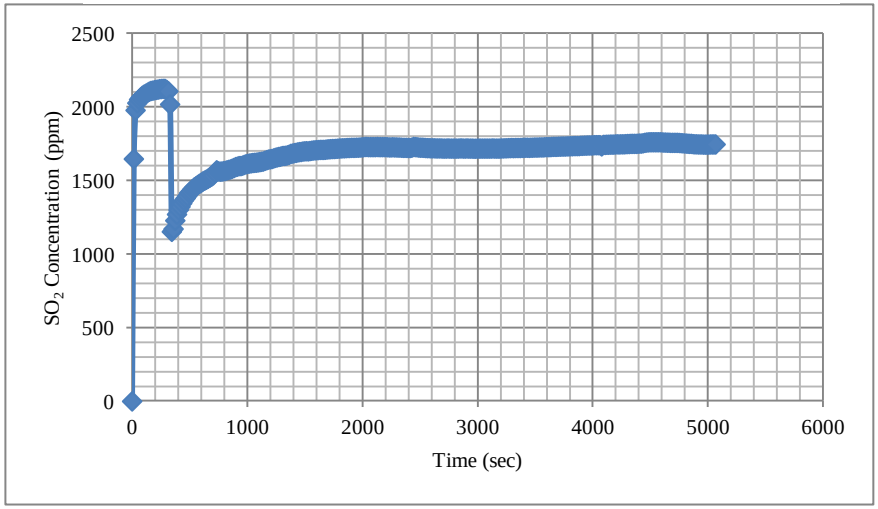

Figure F-4: Sorbent A, 250-500 µm

Graph of SO_2 Concentration vs. Time (Data Set, Sorbent A: 850°C, 2200 ppm SO_2, 21 % O_2, Balance N_2)

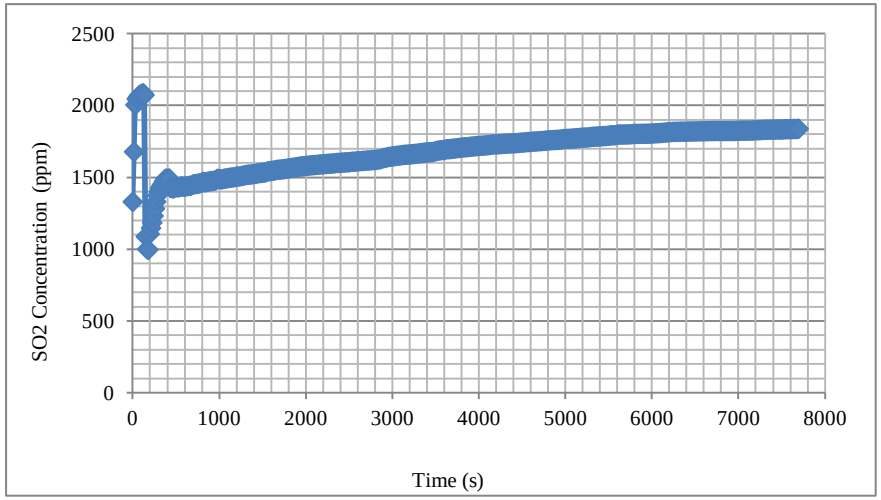

Figure F-5: Sorbent B, 850-1000 µm

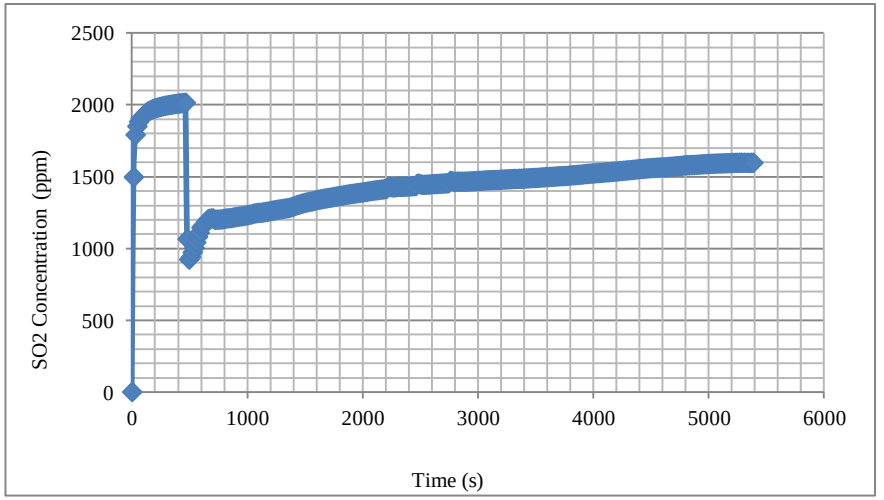

Figure F-6: Sorbent B, 710-850 µm

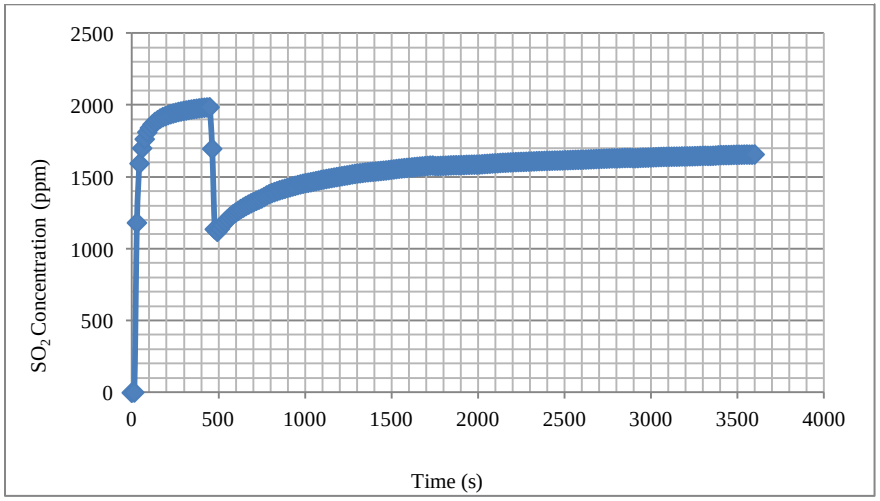

Figure F-7: Sorbent B, 500-710 µm

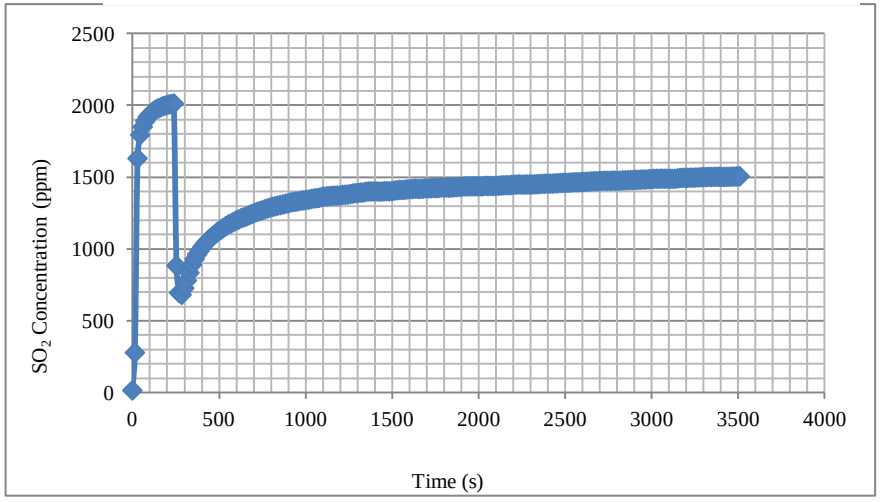

Figure F-8: Sorbent B, 250-500 µm

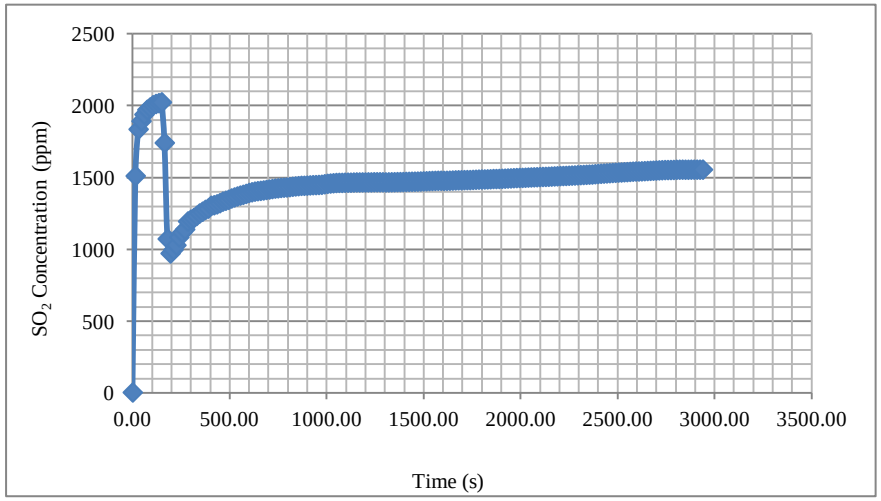

Figure F-9: Sorbent C, 850-1000 µm

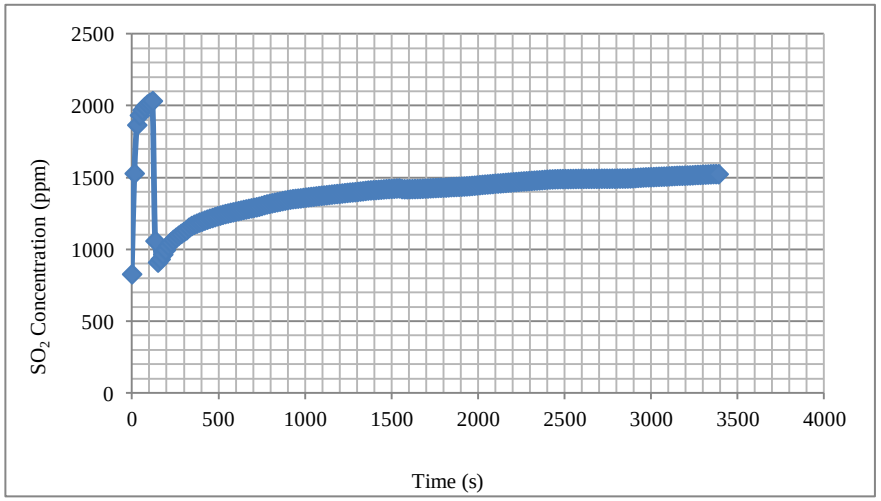

Figure F-10: Sorbent C, 710-850 µm

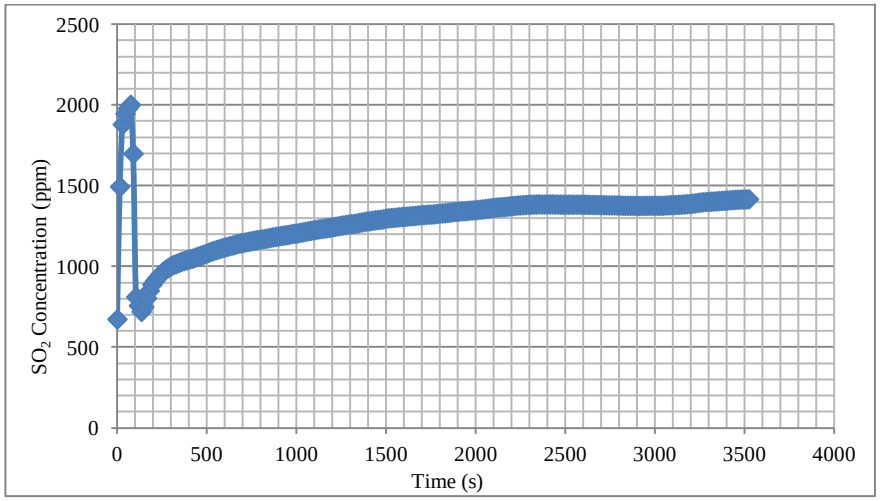

Figure F-11: Sorbent C, 500-710 µm

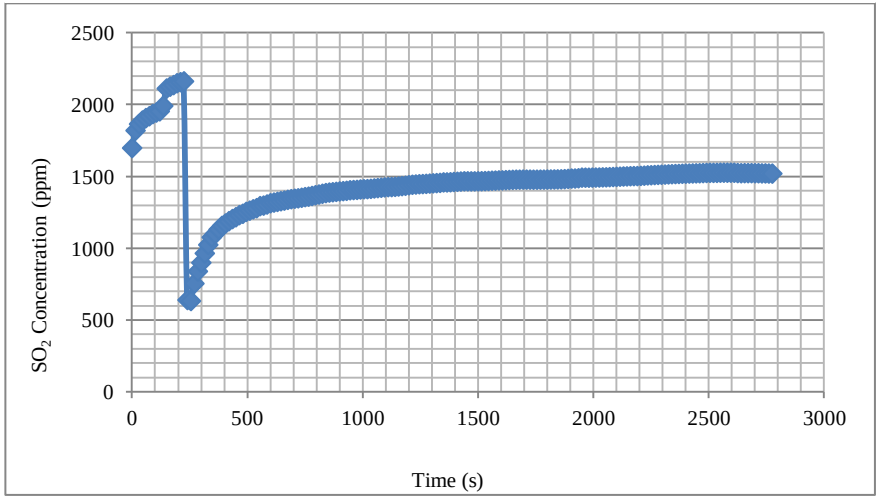

Figure F-12: Sorbent C, 250-500 µm

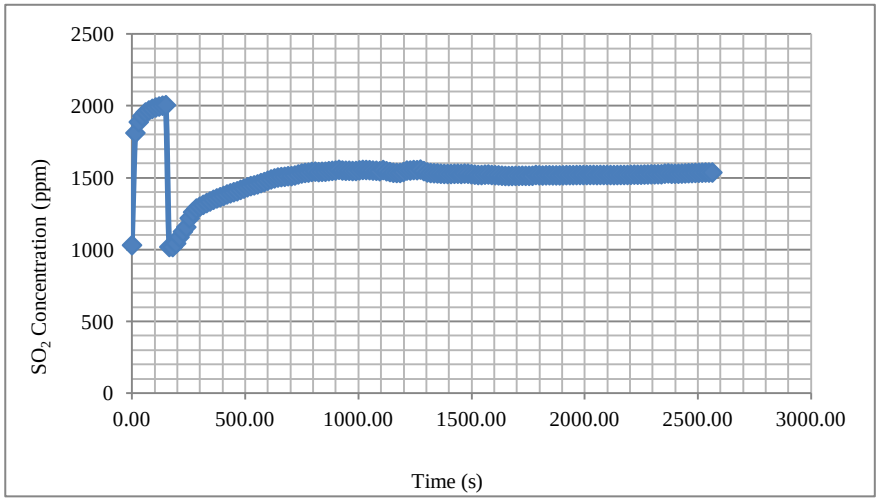

Figure F-13: Sorbent D, 850-1000 µm

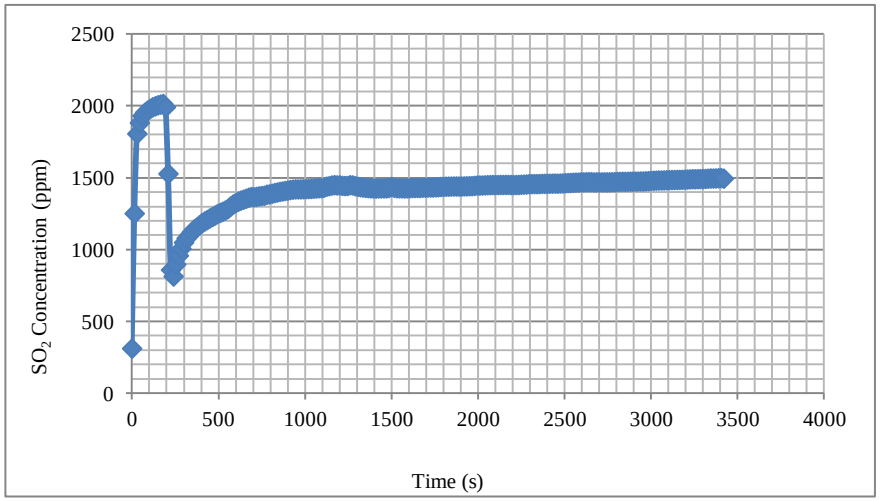

Figure F-14: Sorbent D, 710-850 µm

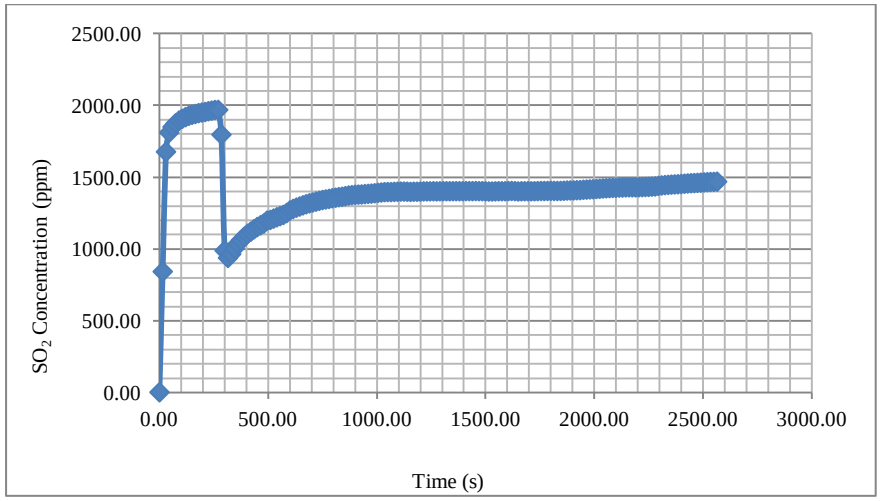

Figure F-15: Sorbent D, 500-710 µm

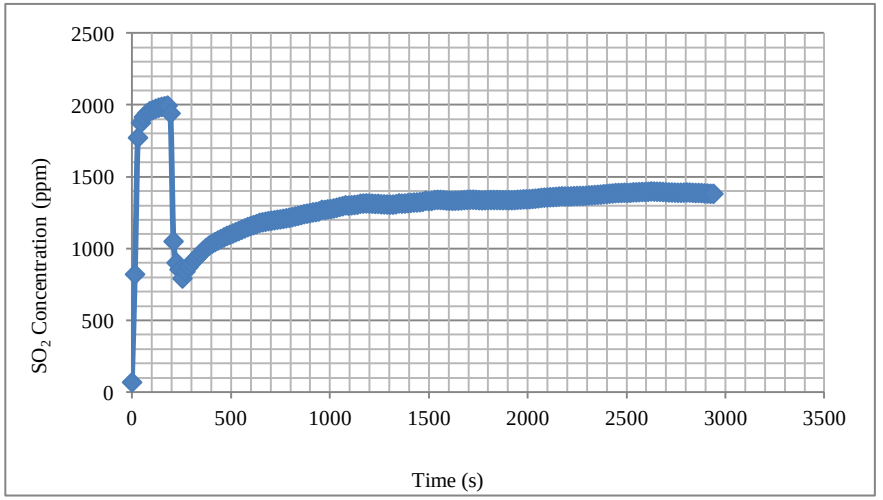

Figure F-16: Sorbent D, 250-500 µm

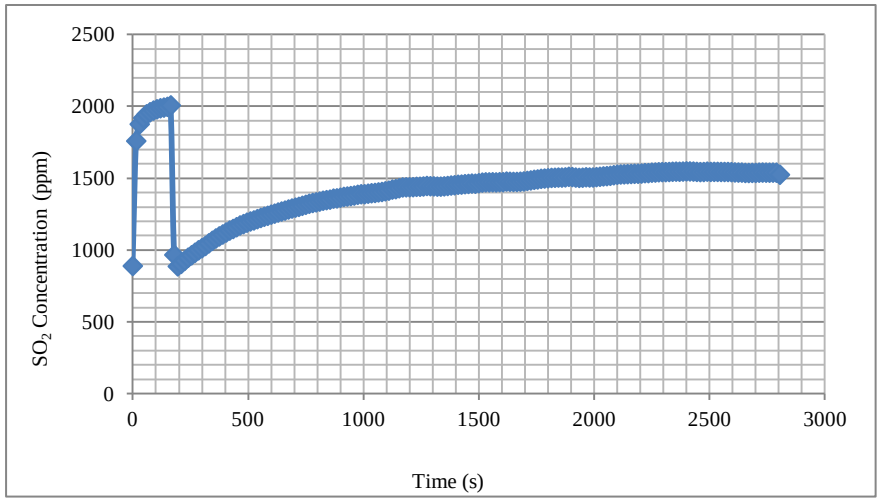

Figure F-17: Sorbent A, 850-1000 µm

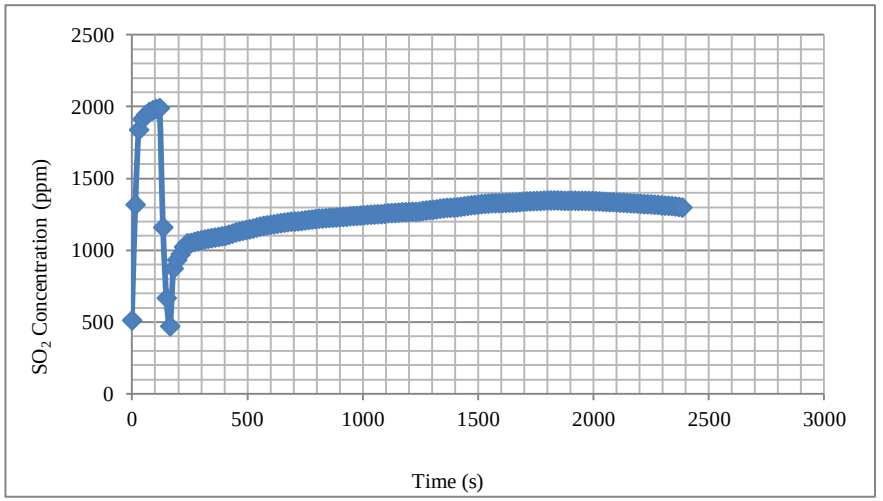

Figure F-18: Sorbent A, 710-850 µm

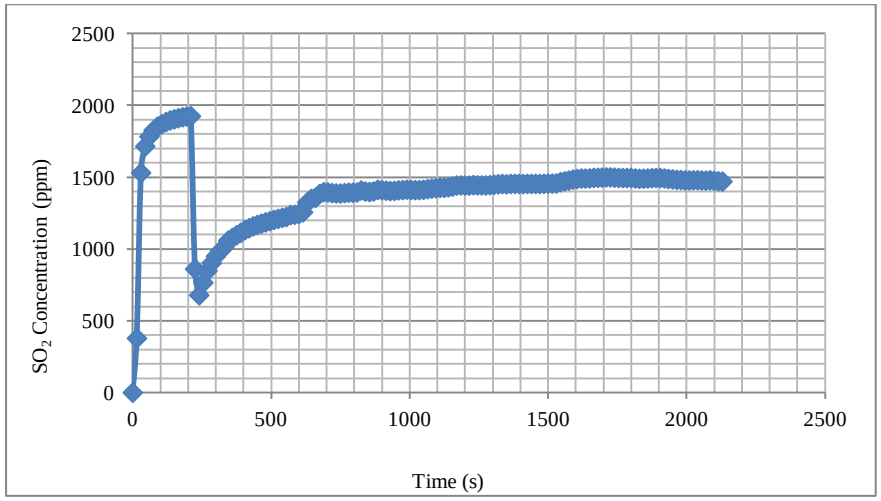

Figure F-19: Sorbent A, 500-710 µm

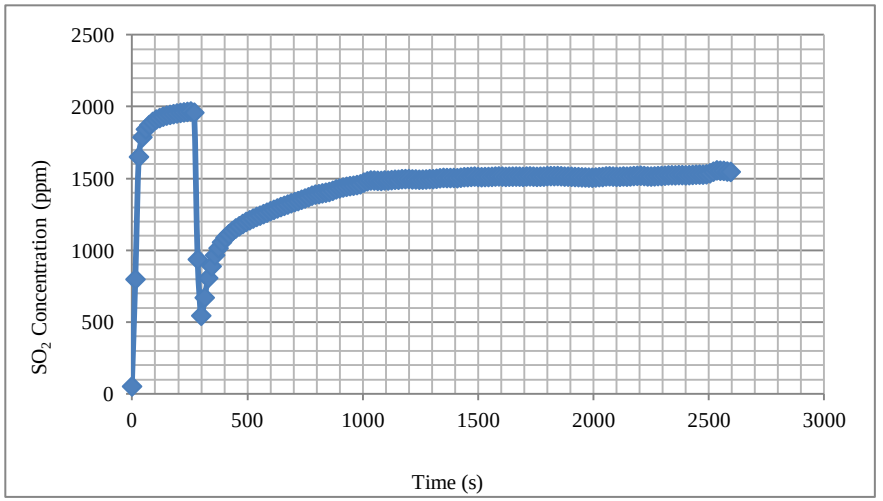

Figure F-20: Sorbent A, 250-500 µm

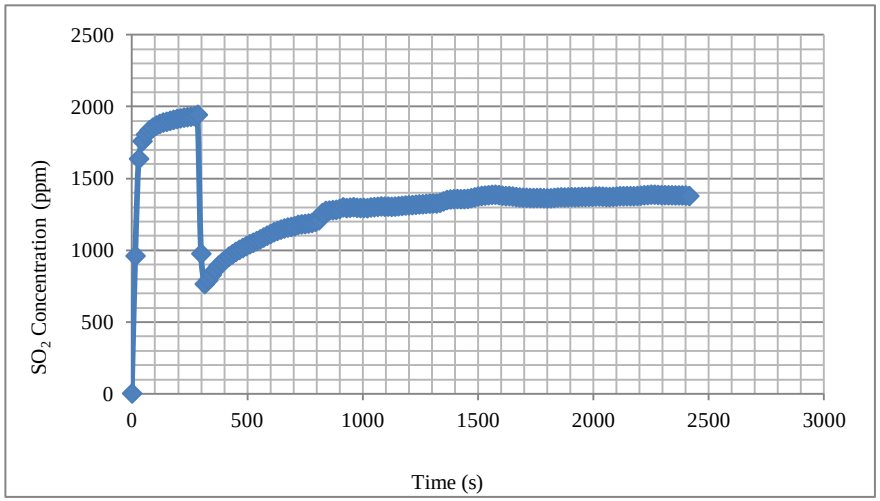

Figure F-21: Sorbent B, 850-1000 µm

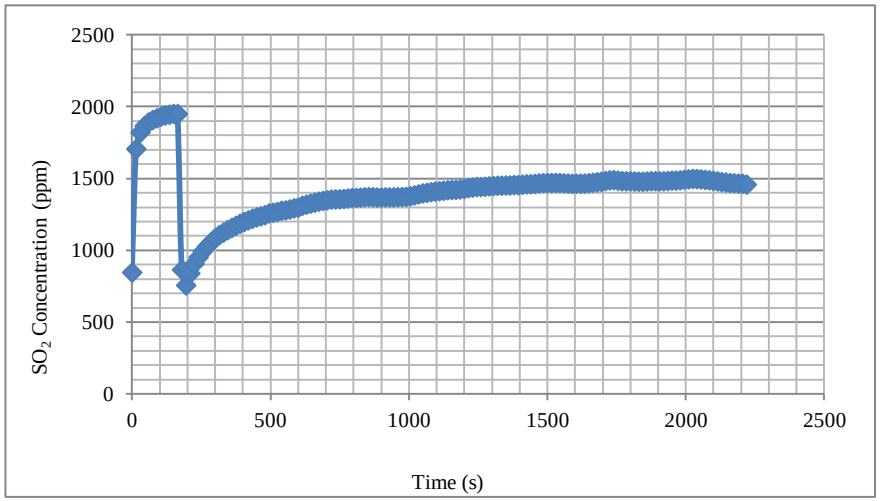

Figure F-22: Sorbent B, 710-850 µm

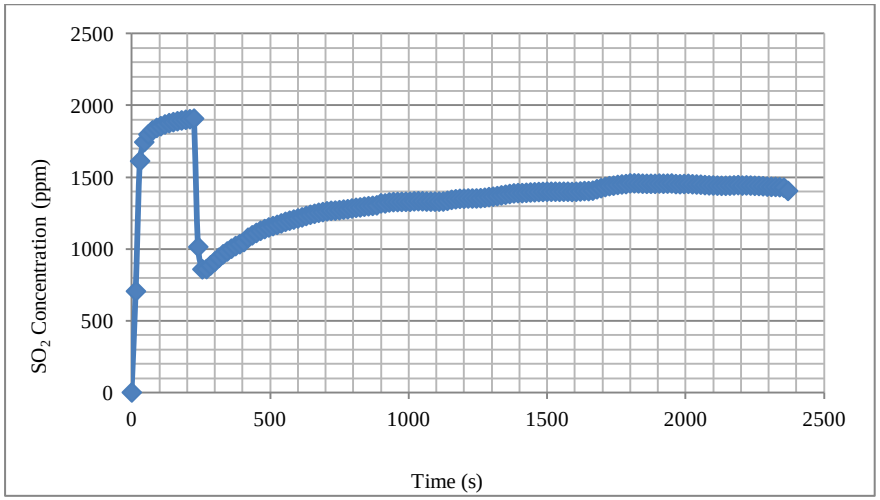

Figure F-23: Sorbent B, 500-710 µm

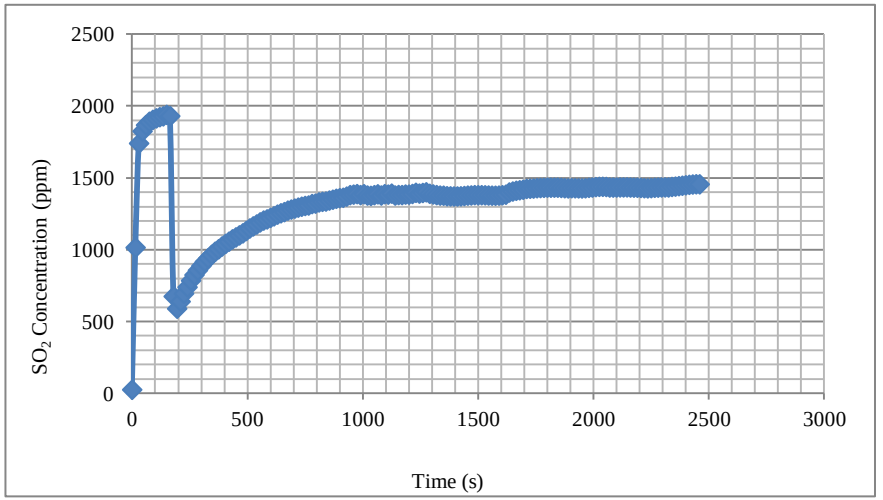

Figure F-24: Sorbent B, 250-500 µm

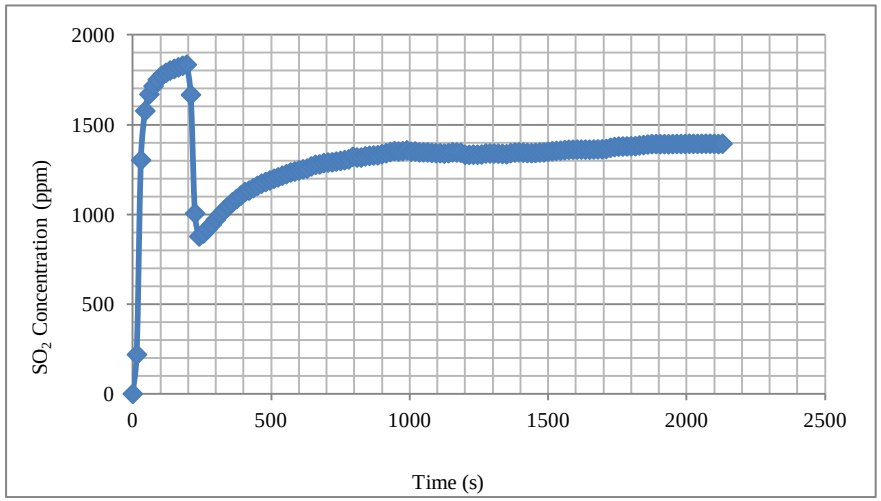

Figure F-25: Sorbent C, 850-1000 µm

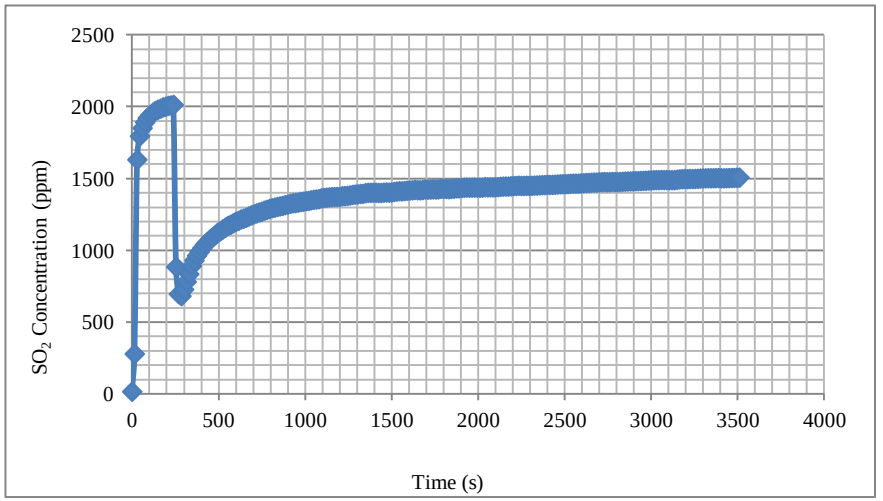

Figure F-26: Sorbent C, 710-850 µm

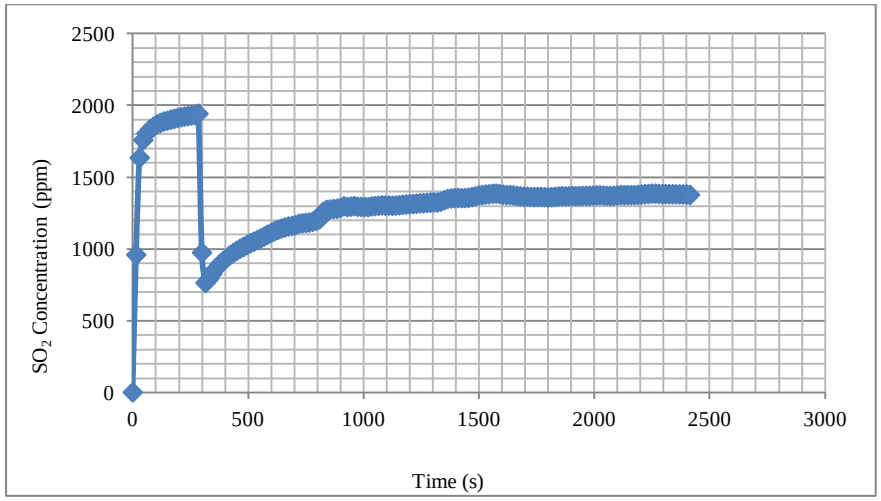

Figure F-27: Sorbent C, 500-710 µm

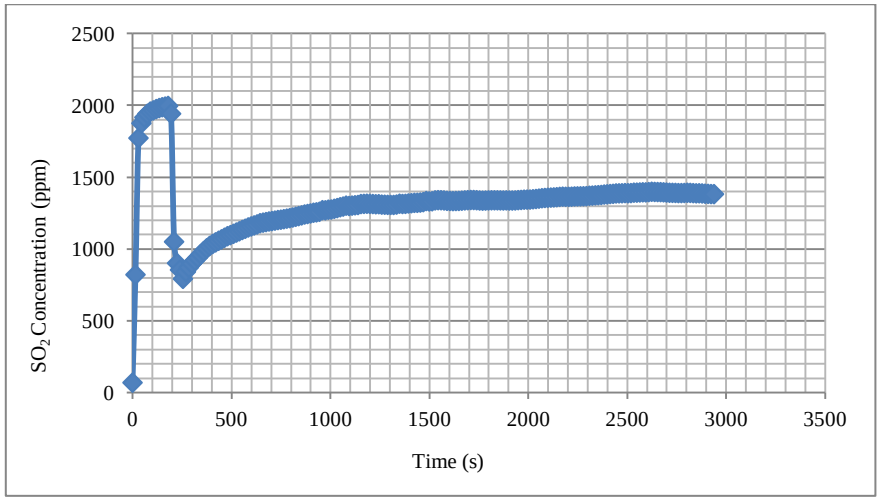

Figure F-28: Sorbent C, 250-500 µm

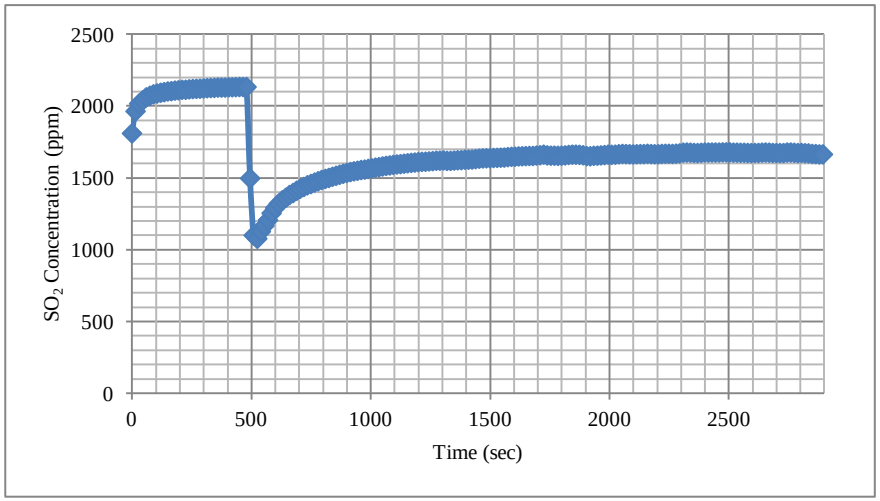

Figure F-29: Sorbent D, 850-1000 µm

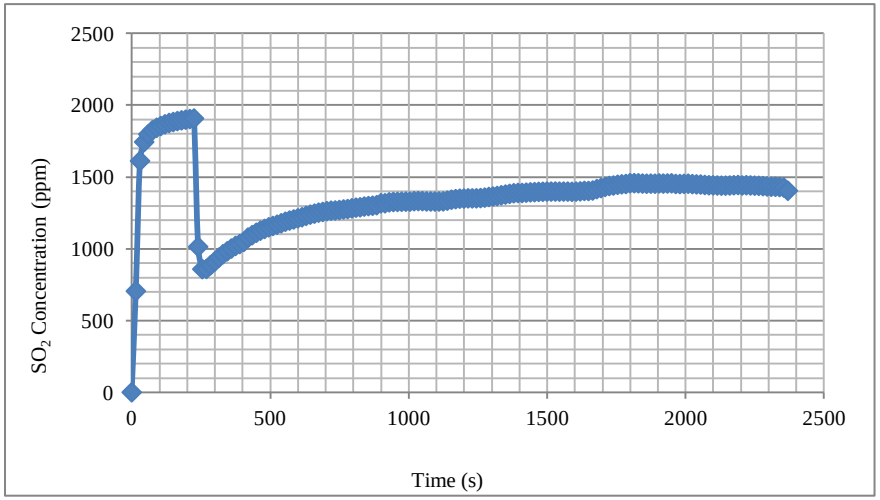

Figure F-30: Sorbent D, 710-850 µm

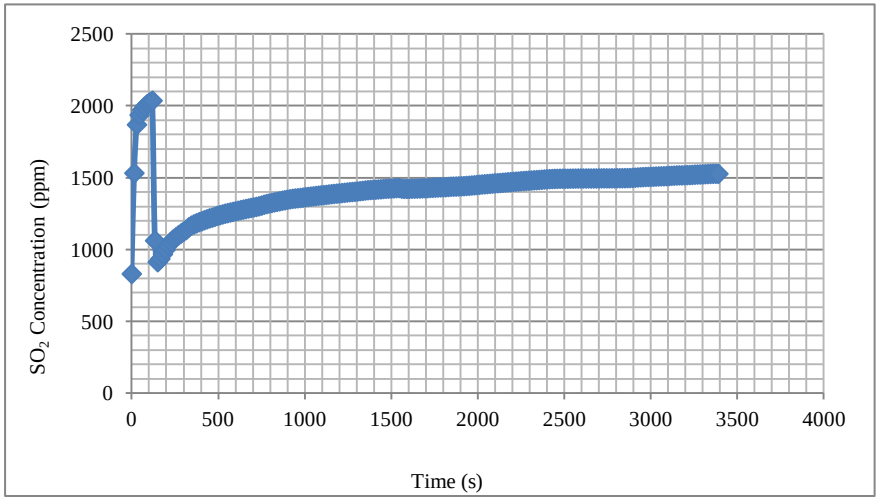

Figure F-31: Sorbent D, 500-710 µm

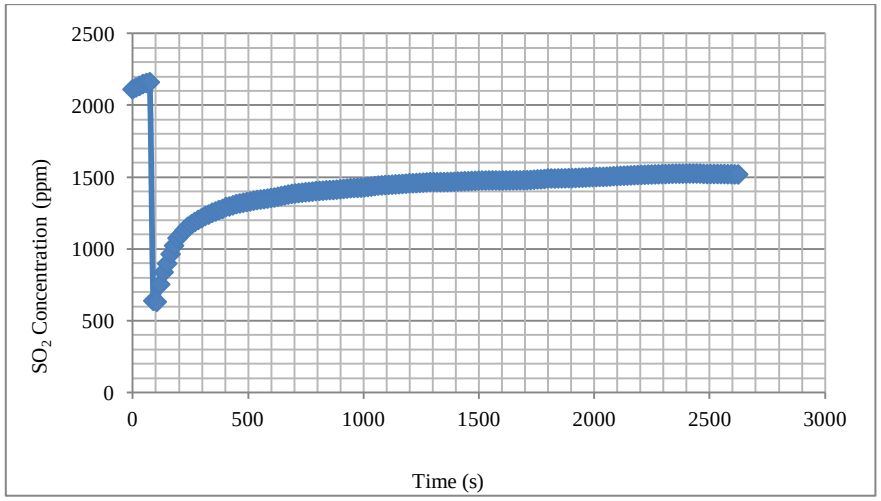

Figure F-32: Sorbent D, 250-500 µm

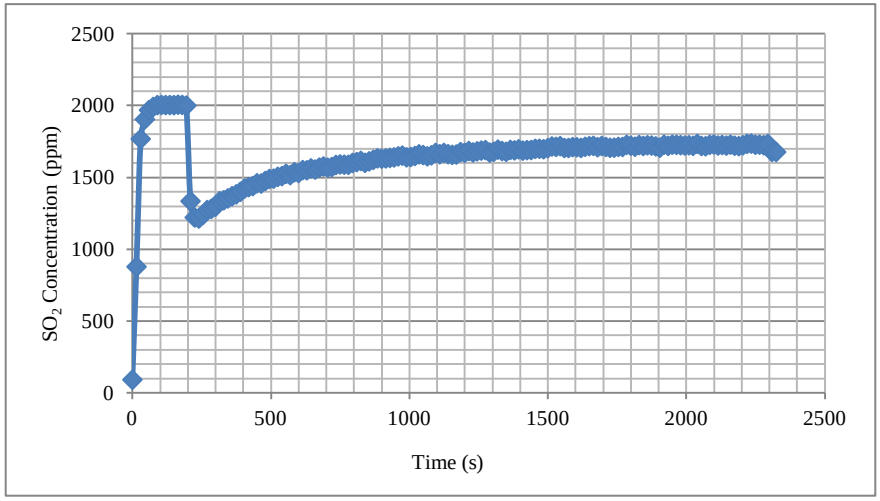

Figure F-17: Sorbent A, 850-1000 µm

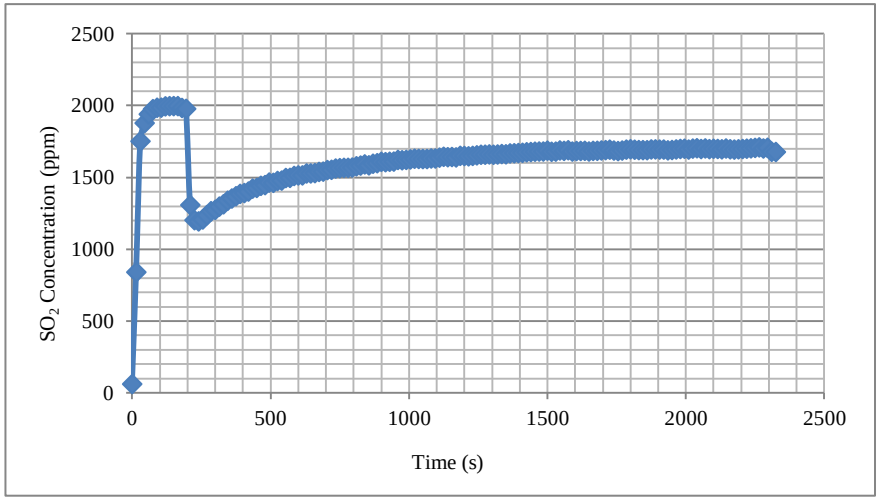

Figure F-18: Sorbent A, 710-850 µm

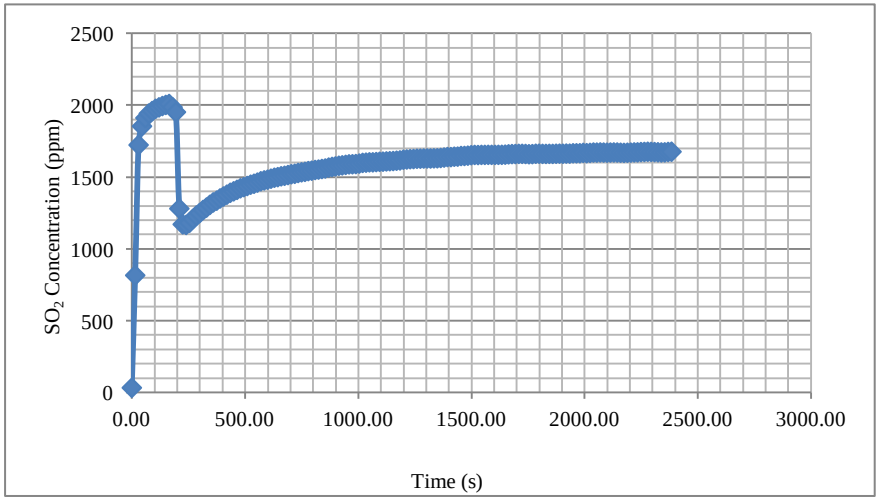

Figure F-35: Sorbent A, 500-710 µm

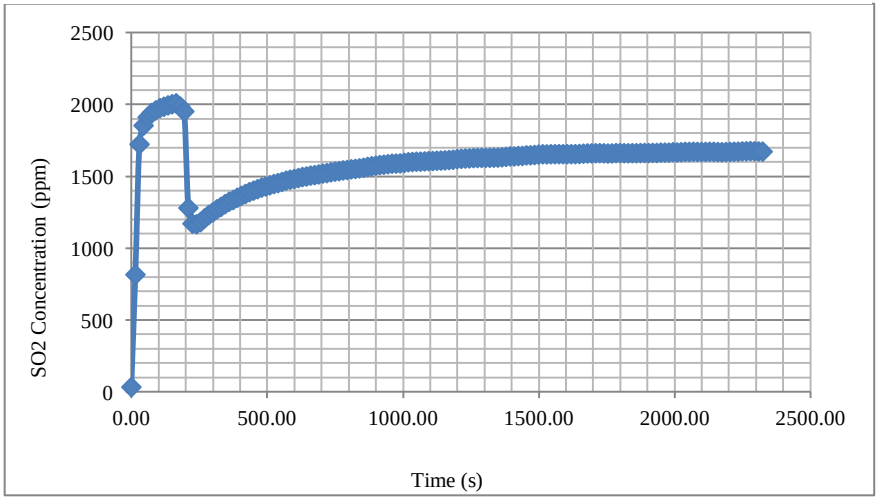

Figure F-36: Sorbent A, 250-500 µm

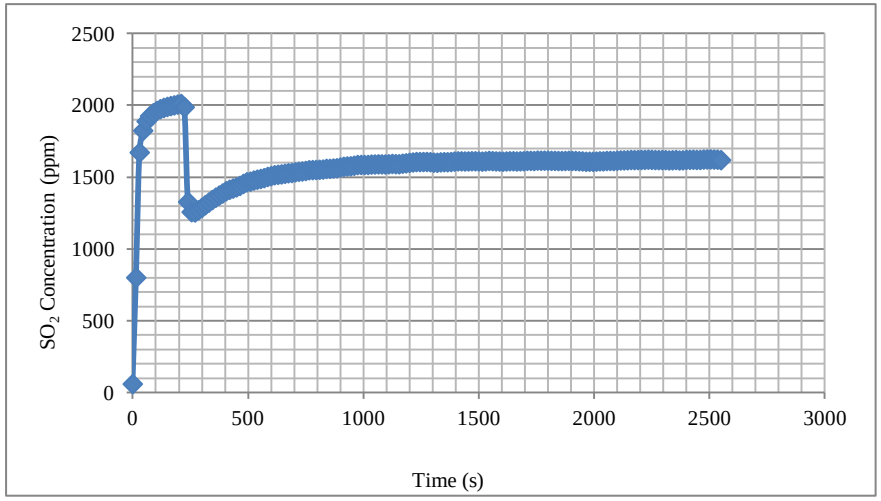

Figure F-37: Sorbent B, 850-1000 µm

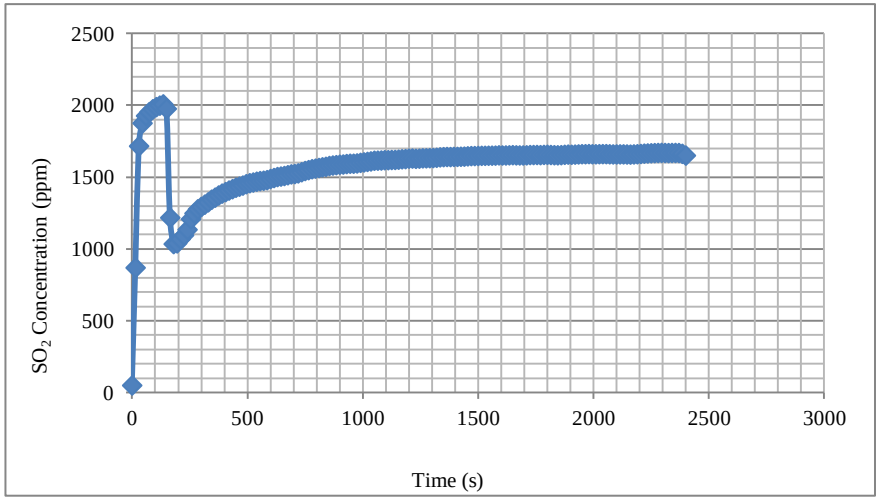

Figure F-38: Sorbent B, 710-850 µm

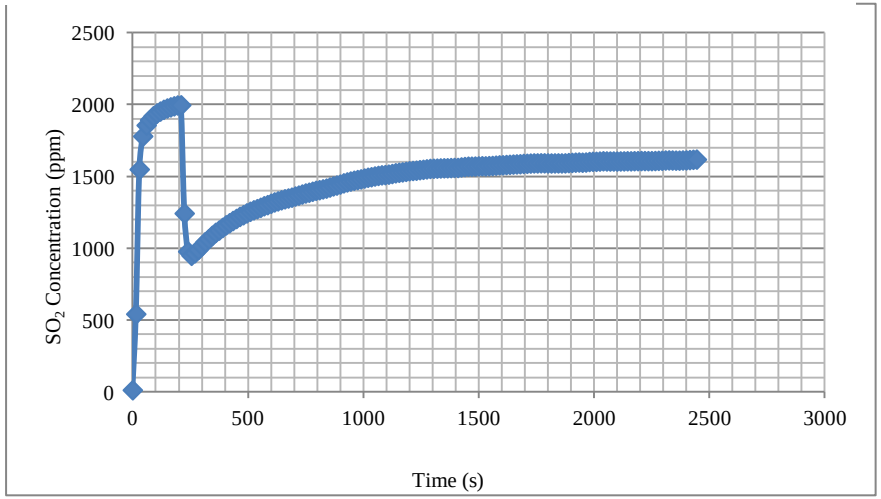

Figure F-39: Sorbent B, 500-710 µm

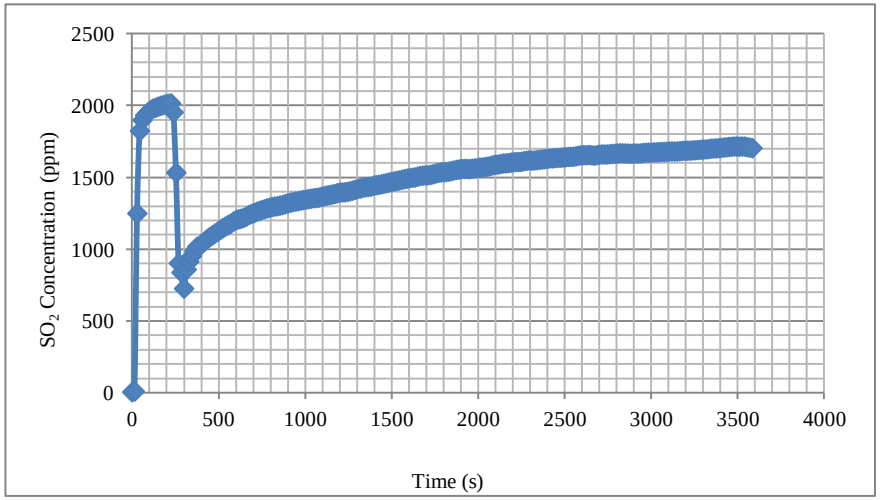

Figure F-40: Sorbent B, 250-500 µm

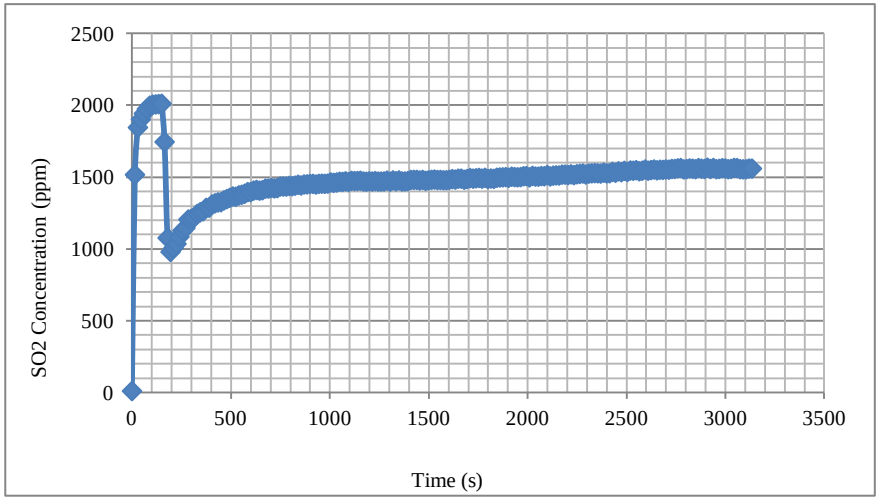

Figure F-41: Sorbent C, 850-1000 µm

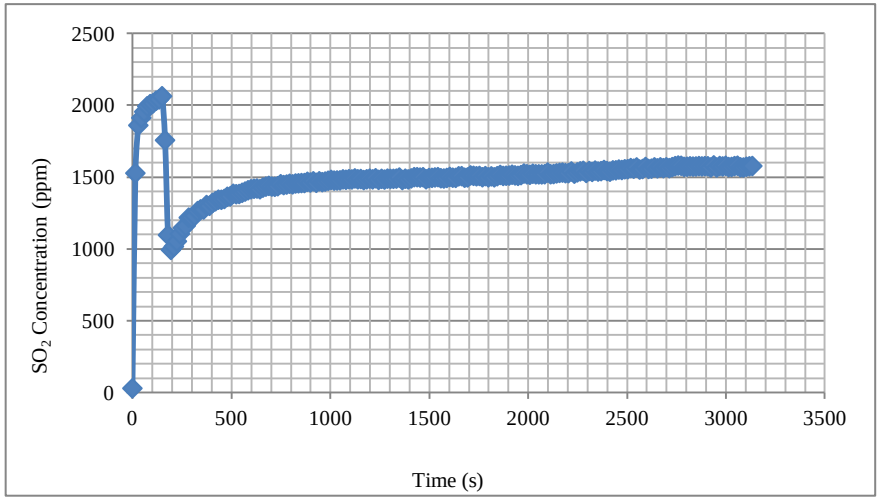

Figure F-42: Sorbent C, 710-850 µm

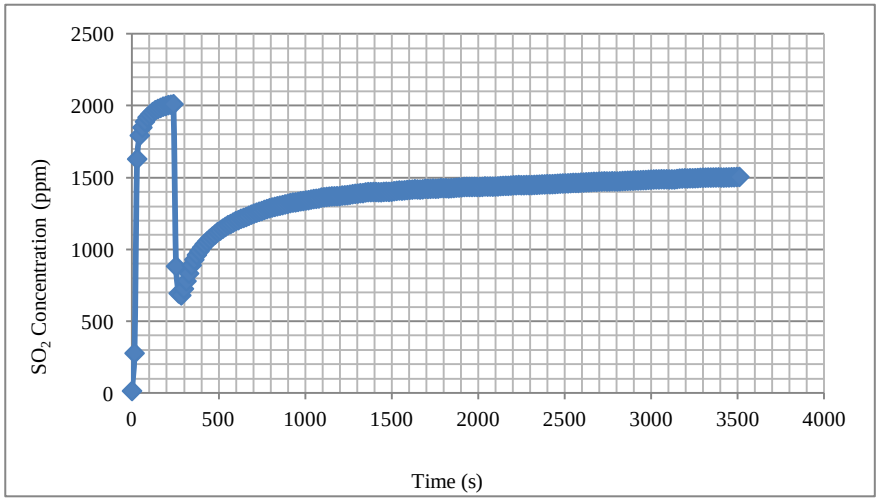

Figure F-43: Sorbent C, 500-710 µm

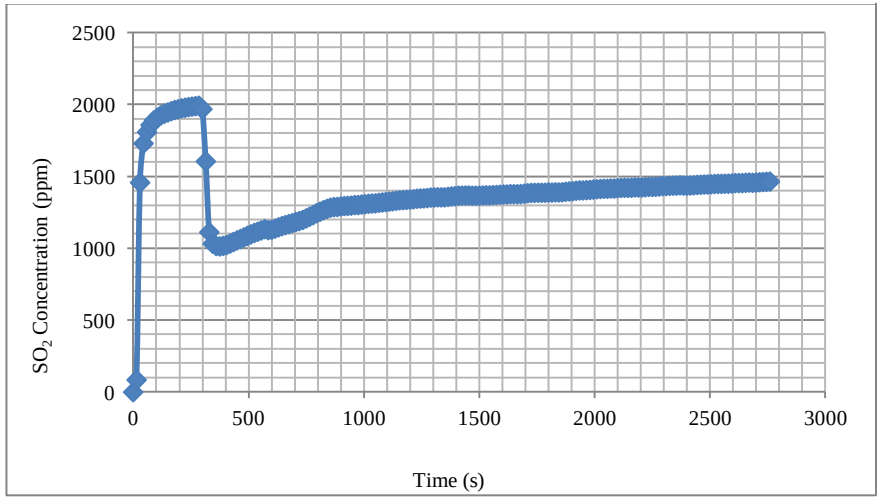

Figure F-44: Sorbent C, 250-500 µm

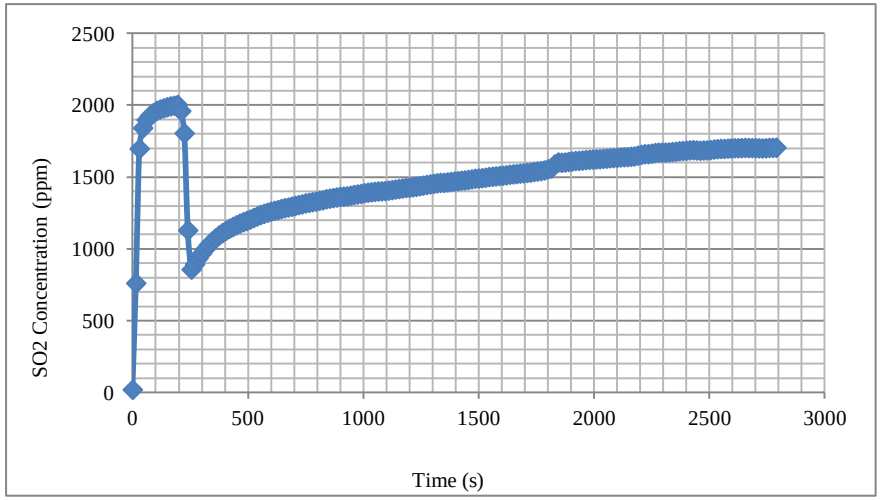

Figure F-45: Sorbent D, 850-1000 µm

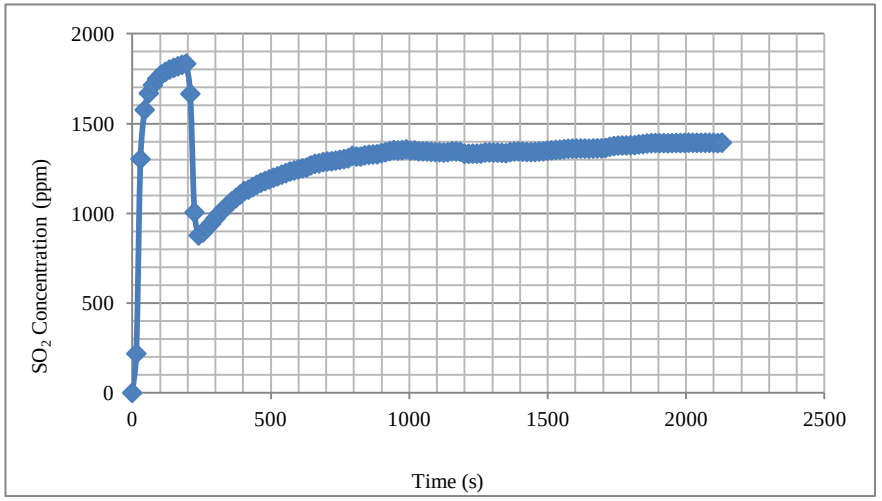

Figure F-46: Sorbent D, 710-850 µm

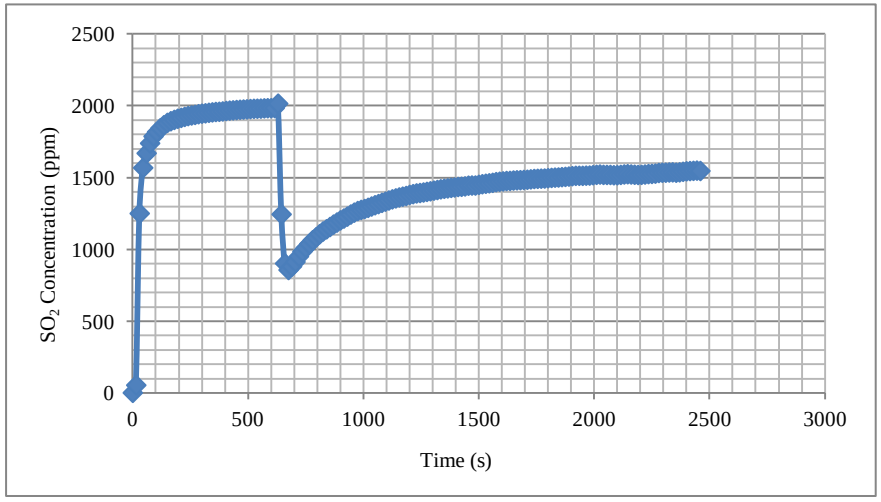

Figure F-47: Sorbent D, 500-710 µm

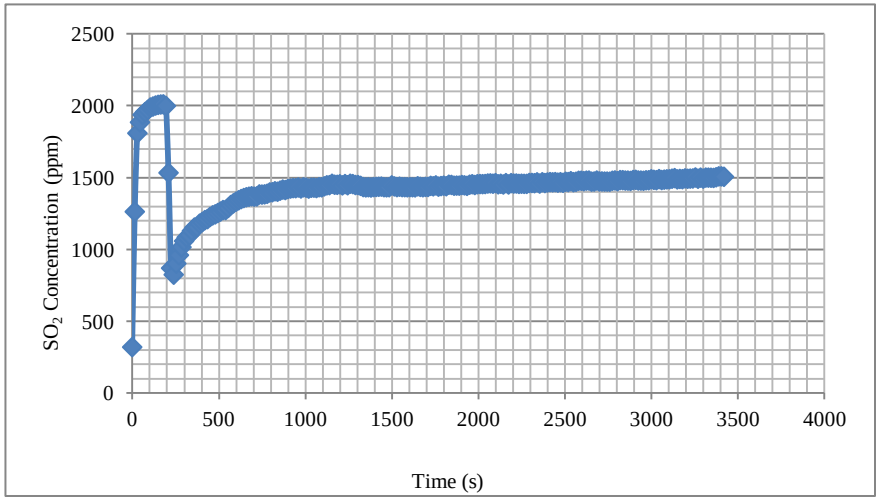

Figure F-48: Sorbent D, 250-500 µm